

Supramolecular chirality : from molecules to helical assemblies in polar media

Citation for published version (APA):

Brunsveld, L. (2001). *Supramolecular chirality : from molecules to helical assemblies in polar media*. [Phd Thesis 1 (Research TU/e / Graduation TU/e), Chemical Engineering and Chemistry]. Technische Universiteit Eindhoven. <https://doi.org/10.6100/IR545491>

DOI:

[10.6100/IR545491](https://doi.org/10.6100/IR545491)

Document status and date:

Published: 01/01/2001

Document Version:

Publisher's PDF, also known as Version of Record (includes final page, issue and volume numbers)

Please check the document version of this publication:

- A submitted manuscript is the version of the article upon submission and before peer-review. There can be important differences between the submitted version and the official published version of record. People interested in the research are advised to contact the author for the final version of the publication, or visit the DOI to the publisher's website.
- The final author version and the galley proof are versions of the publication after peer review.
- The final published version features the final layout of the paper including the volume, issue and page numbers.

[Link to publication](#)

General rights

Copyright and moral rights for the publications made accessible in the public portal are retained by the authors and/or other copyright owners and it is a condition of accessing publications that users recognise and abide by the legal requirements associated with these rights.

- Users may download and print one copy of any publication from the public portal for the purpose of private study or research.
- You may not further distribute the material or use it for any profit-making activity or commercial gain
- You may freely distribute the URL identifying the publication in the public portal.

If the publication is distributed under the terms of Article 25fa of the Dutch Copyright Act, indicated by the "Taverne" license above, please follow below link for the End User Agreement:

www.tue.nl/taverne

Take down policy

If you believe that this document breaches copyright please contact us at:

openaccess@tue.nl

providing details and we will investigate your claim.

Supramolecular Chirality

From Molecules to Helical Assemblies in Polar Media

Supramolecular Chirality

From Molecules to Helical Assemblies in Polar Media

PROEFSCHRIFT

ter verkrijging van de graad van doctor aan de Technische
Universiteit Eindhoven, op gezag van de Rector Magnificus,
prof.dr. M. Rem, voor een commissie aangewezen door het
College voor Promoties in het openbaar te verdedigen op
woensdag 4 juli 2001 om 14.00 uur

door

Lucas Brunsveld

geboren te Culemborg

Dit proefschrift is goedgekeurd door de promotoren:

prof.dr. E.W. Meijer

en

prof. dr. J.S. Moore

Copromotor:

dr. J.A.J.M. Vekemans

This research has been financially supported by the National Research School Combination-Catalysis (NRSC-Catalysis).

Druk: Universiteitsdrukkerij, Technische Universiteit Eindhoven.

CIP-DATA LIBRARY TECHNISCHE UNIVERSITEIT EINDHOVEN

Brunsveld, Lucas

Supramolecular chirality : from molecules to helical assemblies in polar media / by Lucas Brunsveld. - Eindhoven : Technische Universiteit Eindhoven, 2001.

Proefschrift. - ISBN 90-386-2852-8

NUGI 813

Trefwoorden: supramoleculaire chemie / chiraliteit / vloeibare kristallen ; discoten / coöperativiteit ; helixovergang

Subject headings: supramolecular chemistry / chirality / liquid crystals ; discotics / cooperative phenomena ; helical transition

Hetgeen er geweest is, hetzelfde zal er zijn, en hetgeen er gedaan is, hetzelfde zal er gedaan worden; zodat er niets nieuws is onder de zon. Is er enig ding, waarvan men zou kunnen zeggen: Ziet dat, het is nieuw? Het is alreeds geweest in de eeuwen, die voor ons geweest zijn.

Prediker 1 Vers 9, 10

En ik begaf mijn hart om wijsheid en wetenschap te weten, onzinnigheden en dwaasheid; ik ben gewaar geworden, dat ook dit een kwelling des geestes is. Want in veel wijsheid is veel verdriet; en die wetenschap vermeerdert, vermeerdert smart.

Prediker 1 Vers 17, 18

Ik heb gemerkt, dat er niets beters voor henlieden is, dan zich te verblijden, en goed te doen in zijn leven. Ja ook, dat ieder mens ete en drinke, en het goede geniete van al zijn arbeid, Dit is een gave Gods.

Prediker 3 Vers 12, 13

Contents

Chapter 1: Conformational uniqueness of supramolecular architectures; chirality as a muse	1
1.1 Conformational uniqueness of (bio)macromolecules	2
1.1.1 Folding of biomacromolecules	3
1.1.2 Folding of synthetic macromolecules	4
1.2 Conformational uniqueness of supramolecular architectures	5
1.2.1 Supramolecular architectures in water	7
1.3 Chirality	8
1.3.1 Supramolecular chirality	9
1.3.2 Amplification of chirality	10
1.4 Aim of the thesis	12
1.5 Outline of the thesis	12
1.6 References	14
Chapter 2: Helical columns of discotic molecules via assembly by threefold intermolecular hydrogen bonding	17
2.1 Introduction	18
2.2 Helical columns using threefold hydrogen bonding in hexane	19
2.2.1 Synthesis and characterization	19
2.2.2 Aggregation in solution	20
2.2.3 Amplification of chirality	21
2.3 Helical columns using threefold hydrogen bonding in water	22
2.3.1 Introduction	22
2.3.2 Synthesis and characterization	23
2.3.3 Aggregation in solution	26
2.3.4 Chirality at the supramolecular level	28
2.4 Conclusions	29
2.5 Experimental section	31
2.6 References and notes	35
Chapter 3: Hierarchical growth of helical columns in alcohols and water	37
3.1 Introduction	38
3.2 Hierarchical self-assembly in <i>n</i> -butanol	40

3.2.1. Synthesis and characterization	40
3.2.2 Self-assembly in solution	41
3.2.3 The hierarchical growth	47
3.2.4 Concluding remarks	50
3.3 Amplification of chirality and determination of the column length in <i>n</i> -butanol	50
3.3.1 Amplification of chirality	51
3.3.2 Determination of column length – An experimental and theoretical approach	52
3.3.3 Concluding remarks	55
3.4 Self-assembly and amplification of chirality in water	55
3.4.1 Hierarchical self-assembly	55
3.4.2 Amplification of chirality	56
3.4.3 Concluding remarks	58
3.5 Towards multi-columnar architectures	58
3.6 Overall conclusions	59
3.7 Experimental section	60
3.8 References and notes	62

Chapter 4: Solid-state organization and ion conduction

of oligo(ethylene oxide) modified extended core discotics	65
4.1 Introduction	66
4.2 Synthesis and characterization	67
4.3 Solid-state organization	71
4.3.1 Thermogravimetric analysis (TGA) and differential scanning calorimetry (DSC)	71
4.3.2 Polarization microscopy	72
4.3.3 X-ray diffraction	74
4.3.4 Solid-state NMR	76
4.4 Ion conduction	77
4.5 Conclusions	79
4.6 Experimental section	81
4.7 References	84

Chapter 5: Helical self-assembled polymers

via cooperative stacking of hydrogen bonded pairs in water	87
5.1 Introduction	88
5.2 Helical columns in water	89
5.2.1 Synthesis and characterization	89

5.2.2 Self-assembly in solution	90
5.2.3 Self-assembly in chiral columns in water via stacking of hydrogen bonded pairs	94
5.2.4 Cooperativity within the columns	97
5.3 Conclusions	99
5.4 Towards water-soluble random coil supramolecular polymers	99
5.5 Experimental section	101
5.6 References and notes	103

Chapter 6: Cooperative and hierarchical folding of chiral

***m*-phenylene ethynylene oligomers and their self-assembly in columns 105**

6.1 Introduction	106
6.2 Conformational ordering of polar, chiral <i>m</i> -phenylene ethynylene oligomers	107
6.2.1 Synthesis	107
6.2.2 Hierarchical folding from random coils into chiral helices	110
6.3 Cooperativity in the folding of helical <i>m</i> -phenylene ethynylene oligomers based upon the 'Sergeant and Soldiers' principle	113
6.3.1 Synthesis	113
6.3.2 Cooperative transfer of side chain chirality	114
6.4 Self-assembly of folded <i>m</i> -phenylene ethynylene oligomers into helical columns	116
6.4.1 Aggregation in aqueous acetonitrile	117
6.4.2 Intermolecular cooperative transfer of chirality	121
6.5 Conformational ordering of apolar, chiral <i>m</i> -phenylene ethynylene oligomers	124
6.5.1 Synthesis	124
6.5.2 Hierarchical folding from random coils into chiral helices	125
6.5.3 Time dependent folding	128
6.6 Conclusions	129
6.7 Experimental section	131
6.8 References and notes	146

Summary

Samenvatting

Curriculum Vitae

Dankwoord

Chapter 1

Conformational uniqueness of supramolecular architectures; chirality as a muse

Abstract: *In this chapter an introduction is given concerning the conformational uniqueness of macromolecules and the important interactions involved in their structural arrangement. This is then confronted with the positioning of molecules in supramolecular architectures in a conformationally unique fashion and the creation of such architectures in water. As a prominent tool to characterize these well-defined architectures, chirality is brought into the scene. These considerations served to formulate the aim and scope of this thesis.*

1.1 Conformational uniqueness of (bio)macromolecules

Macromolecules can adopt different conformations in solution and both for synthetic^{1,2} and natural^{3,4} macromolecules these conformations can be adjusted by external stimuli such as temperature and solvent type. A clear distinction between different kinds of conformations can be made. The majority of structures is characterized by a random walk situation in which the segments of the polymer hardly feel each other (the coil). Other structures are best described as a globule, a condensed state with low density fluctuations. Macromolecules are capable of reversibly interchanging between the different conformations by changes in their environment. Although most synthetic polymers feature a more or less collapsed state in their random coil conformation, a few distinct transformations are known. The folding into an ordered structure (a globule) out of a disordered coil is the most prominent one.

The folding of a macromolecule into different conformations is highly cooperative and generally induced by intramolecular interactions.⁵ This cooperativity is a feature characteristic for the conformational changes of macromolecules, both of biological and of synthetic nature. The covalent linkage between the interacting units creates a high local concentration and thus favors intramolecular interactions. Conformational changes imposed by specific sites on the polymer are as a result transferred in a cooperative manner. In addition, the generated intramolecular interactions are highly coupled because of the constraints imposed by the backbone.

The intramolecular interactions that arise as a result of the folding of macromolecules into globules are governed by non-specific solvophobic or –in the case of water– hydrophobic interactions⁶ and control the general structure of the macromolecules. However, not a unique native state, but a large number of different conformations of the macromolecules is generated with nearly equal energies. In contrast to most synthetic polymers, biomacromolecules feature additional specific design elements such as hydrogen bonds and arene-cation interactions, capable of generating ordered elements in the folded polymer backbone like the α -helix and β -sheet.⁷⁻⁹ These features account for the formation of one unique native state of biomacromolecules. Concomitantly, the absence of these specific elements results in the nonexistence of a native state for synthetic macromolecules.

The information for the folding of macromolecules is embedded in their sequence of monomers.¹⁰ Synthetic polymers are typically made from one to three monomers, which are, for copolymers, placed in a more or less random position within the chain,¹¹ although highly regular block copolymers have been prepared.¹² The chain length and composition are accordingly not well-controlled and as a result synthetic polymers consist of mixtures of macromolecules. Together with their polydisperse nature this results in ill-defined samples. In contrast, the chain length, composition and sequence of monomers in biomacromolecules are highly controlled.¹³ Biopolymers are often built up from different monomers that are placed in exact order within the main-chain and this allows for a vast body of information storage. DNA/RNA (4 different monomers)¹⁴ and proteins (20)¹⁵ are their

most famous examples. The ordered encoded information in biomacromolecules results in the formation of one unique native state, whereas the disordered information in synthetic macromolecules does not allow the formation of a unique conformation. To date, the generation of synthetic systems able of adopting one unique native conformation is possibly one of the greatest challenges for chemists; a study that complements the unraveling of the exact nature of protein folding as performed by biochemists, molecular biologists and polymer physicists.

In the following sections the folding of biomacromolecules and synthetic polymers will be shortly described in some more detail. An idea is given of the important features for designing novel supramolecular structures and the hurdles to be taken in these fields are summarized. In section 1.2 the aspect of conformationally unique supramolecular architectures is discussed, as well as their creation in water. Control of supramolecular architectures in water opens the way to bio-inspired functional architectures. In section 1.3 the issue of chirality is addressed. Being closely related to biological architectures, chirality is the tool "par excellence" for studying ordered supramolecular architectures, providing exclusive information about the order of the molecules in the supramolecular architectures in solution.

1.1.1 Folding of biomacromolecules

For the discussion concerning the unique native state of biomacromolecules the focus will be on proteins. The denaturation of a protein from its native state to a molten globule or random coil, *i.e.* the unfolding, was initially ascribed to hydrolysis of the peptide bond or dehydration.^{16,17} It was in the 1930's that denaturation was proposed to be an unfolding process, whereby the regular spatial arrangement of the protein is changed into a diffuse arrangement.¹⁸ The reversibility of protein folding was shown soon thereafter.^{19,20} The experiments performed by Anfinsen and coworkers proved that denatured proteins can be restored to their function upon return to their native state.³ The spontaneous, cooperative folding of a protein is actually amazing. It was Levinthal who indicated that there are too many possible conformations for a protein to achieve its native state purely by random searching.²¹ He stated that the folding of proteins must be directed by specific pathways. The current view is that the energy surface for folding is shaped like a funnel and the folding involves the parallel occurrence of numerous small steps.²² Protein folding is now more thought of as an ensemble of intermediates with multiple folding routes in contrast to specific structures and pathways. It is not the aim to discuss the folding of proteins in detail here and for that the reader is referred to review literature.²³⁻²⁷ Instead, the various interactions operative in proteins that give rise to their unique, highly ordered native state, are –shortly– discussed with emphasis on the hydrophobic effect and hydrogen bonding.

A globular, water-soluble protein consists of monomers with unequal polar character. In the native state in water, the protein looks like a drop of oil, with the nonpolar groups aggregated in the center and the polar groups at the periphery.²⁸ The hydrophobic effect (the clustering and desolvation

of apolar groups in water) plays the major role in establishing this globular conformation and is a consequence of the strong self-interaction of water, instead of a solute-solvent interaction.

A closer look at the interior of proteins reveals –in contrast to drops of oil– a high molecular order. The hydrophobic effect results in the burying of polar groups in the interior. In principle this order would induce a loss of entropy, since these groups coexist well with water. However, this effect is counteracted by the groups attaining ordered structures via additional intramolecular interactions, like those of the hydrogen-bonded type. The occurrence of additional interactions in the apolar core of proteins results in the formation of a lot of secondary structures (α -helices and β -sheets). In fact, around 90 % of all internal polar groups form hydrogen bonds, thus showing that almost all potential hydrogen bond energy is used for the stabilization of the native state.²⁹ The efficient activation of the specific secondary interactions guarantees a tight packing in the proteins as in good molecular crystals, except of course in the vicinity of the active center of enzymes, which needs to be flexible.⁹ It should be noted that apart from hydrogen bonding other electrostatic interactions and van der Waals forces may aid to the stabilization of the unique native conformation. In general, charged groups are primarily found at the periphery because there they constrain the conformation and thus direct the folding process and, importantly, as charged groups they account for solubility of the protein.⁹

Simplified, it might be stated that the hydrophobic effect accounts for the energetic requirements for collapse and the hydrogen bonds –although weak³⁰ are the single most important interactions determining the three-dimensional folding and unique native state of proteins. The weakness of individual hydrogen bonds is circumvented when the acceptor and donor are arranged in particular geometries, rendering the hydrogen bonds specific, with additive and cooperative strength.³¹

1.1.2 Folding of synthetic macromolecules

Alike biomacromolecules, synthetic homopolymers can be driven to fold cooperatively from a random coil in good solvents into a collapsed chain with compact conformations in poor solvents.^{1,2} The collapsed chains attain a globular shape and some examples resembling the molten-globule of proteins have been observed.³²⁻³⁴ However, these folded structures are not conformationally unique. As a result, the issue of folding of synthetic heteropolymers is highly complicated.³⁵ The difficulty of generating a conformationally unique arrangement from synthetic polymers is reflected in the fact that even when crystallized, they can be present in many conformations, also depending on the kinetics of annealing.³⁶ Nevertheless, synthetic homopolymers attaining a well-defined conformation, like a helix, are known.³⁷ In contrast to the folded polymers these helical polymers are poorly switchable and do not easily denaturate to a random coil due to the motional restrictions imposed by the backbone. Yet certain synthetic polymers have been shown to cooperatively fold from a coil into a helix. This feature has been mainly observed for homopolypeptides,^{38,39} but other systems are known as well.⁴⁰ In the early 50's in poly- γ -benzyl-L-glutamate the helix-coil transition was observed for the

first time⁴¹ and this inspired Zimm and Bragg to develop their theory for the transition between helix and random coil in polypeptide chains.⁴² Afterwards, this theory served as the basis for many others, describing different or more complicated transitions.⁴³

The difficulty in obtaining conformational uniqueness for folded synthetic copolymers is threefold.¹⁰ First of all the sequence design of a heteropolymer leading to a specific tertiary shape is complicated, keeping in mind that even for proteins this is not fully understood.¹⁵ Secondly, even if the necessary sequence could be predicted, the synthesis of such a designed polymer is highly complicated. Would the design imply the need for short repeating units only, even then the generally encountered polydispersity in conventional polymer chemistry would not allow the generation of unique polymers. Finally, the characterization of the polymers in solution is a problem not easily treated.

Recently, synthetic chemists have pursued non-biological, small oligomeric molecules that fold into unique conformations.^{10,44-46} These so-called 'foldamers'⁴⁵ are monodisperse and relatively small, allowing the incorporation of information encoded by design. Acquiring control over this process and knowledge of the structures formed should help in the elucidation of the conformational uniqueness of biomacromolecules. Secondly, control over the foldamer structure in solution will allow the creation of assemblies of these oligomers, presumably capable of exerting specific functions. The study of the required foldamer-foldamer interactions and their occurrence in different media is a field still to be pursued.

1.2 Conformational uniqueness of supramolecular architectures

Analogous to polymers, organic molecules can adopt several conformations in solution, albeit fewer due to their smaller sizes. The self-assembly of these smaller molecules into supramolecular architectures restricts the number of possible conformations. As such, supramolecular chemistry can be considered a structured confinement in conformations of molecules via secondary interactions. Yet the formation of self-assemblies generates new multi-molecular conformations. As an example the self-assembly of discotic molecules is considered. Discotics are molecules with a disc-shaped core provided with a periphery of side-chains.⁴⁷ The core generally consists of a planar aromatic system, while the side-chains are usually flexible alkyl chains. The conformation of the rigid core is fixed, unless the core consists of flexible units, but the side-chains are liquid-like in solution and can adopt many conformations. Discotics feature a strong interdisc stacking interaction which is several orders of magnitude stronger than the intercolumnar interactions, solely due to the phase separation induced by the side-chains, whose van der Waals interactions are much weaker.⁴⁸ As a result, the discotics tend to self-assemble and form columnar architectures in poor solvents for the cores. In the aggregates a conformational restriction is imposed on the individual molecules, but within the column the position of the discotics is not unique: they rotate constantly,⁴⁹ leading to a set of nearly energetically

equal conformations for the columnar polymer. At higher concentrations the columns can interact intercolumnarly. Again, generally these interactions result in disordered structures in which the position of the individual columns is less controlled. The discotic molecules in the solid phase possess liquid crystalline behavior with typically a columnar hexagonal ordered arrangement. An illustrative picture displaying the self-assembly of discotic molecules into supramolecular polymers is given in Figure 1.1.

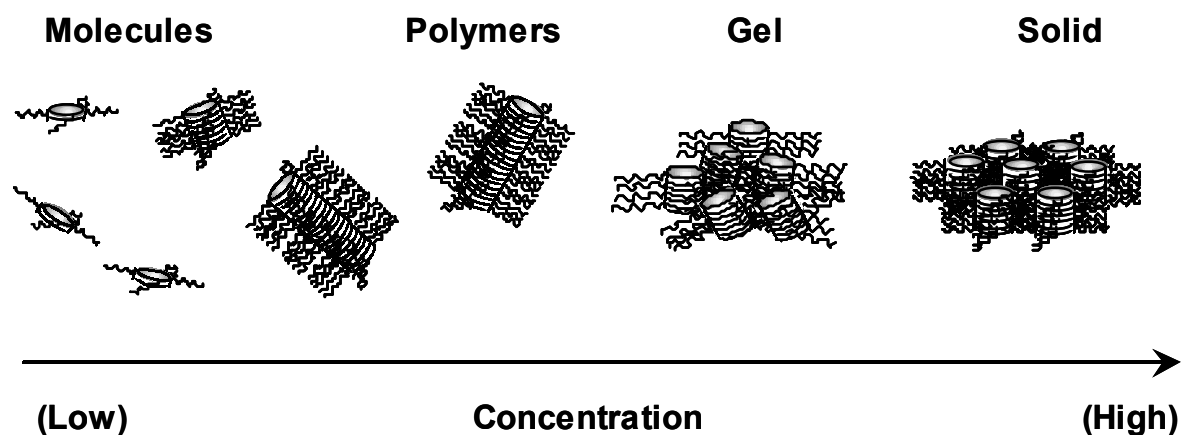


Figure 1.1: The self-assembly of discotics, with stacking interactions several orders of magnitude stronger than lateral interactions. The different stages of aggregation are given as function of concentration.

Analogous to the folding of synthetic polymers, the self-assembly of discotics generally does not result in the formation of architectures with a unique conformation. However, when these discotics possess additional specific intermolecular interactions on top of the stacking interactions, the formation of highly ordered supramolecular architectures becomes possible, in which the position of the individual molecules is better controlled. These specific interactions, comparable to the structuring effect of hydrogen bonds in proteins, can be *e.g.* a large and sterically demanding π - π stacking aromatic core,⁵⁰⁻⁵² intercalating side chains⁵³⁻⁵⁵ or specific intermolecular interactions such as hydrogen bonding (Figure 1.2).⁵⁶⁻⁶¹ The combination of two or more interactions often accounts for the formation of highly ordered columnar architectures. Apart from discotics, the combination of generic and specific interactions also results in conformationally unique supramolecular architectures with other types of molecules.⁶²⁻⁶⁵

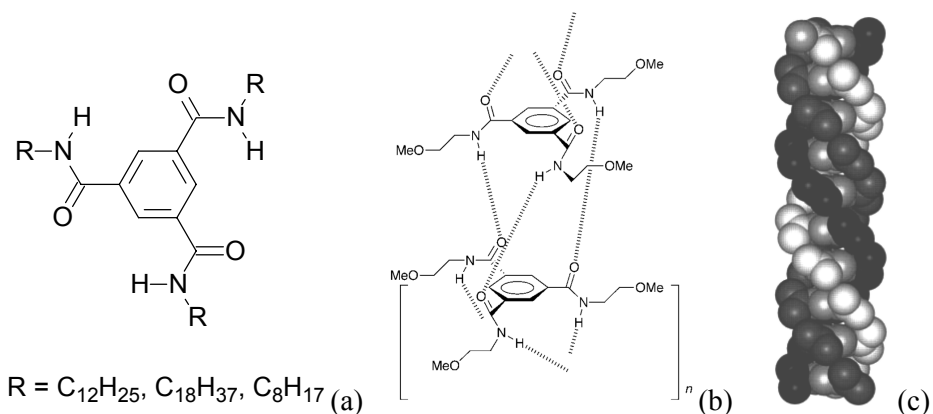


Figure 1.2: (a) 1,3,5-Benzene triscarboxamides that form columns in apolar solvents via threefold intermolecular hydrogen bonding;^{58,59} (b) Solid state X-ray structure of the helical columns; (c) Graphical representation of the conformationally unique hydrogen bonded helical columns.⁶⁰ The three shades of gray each represent one of the amides stacked on top of each other.

1.2.1 Supramolecular architectures in water

A high degree of control is currently possible over the formation of multimolecular supramolecular architectures in organic solvents.⁶⁶ However, the realization of artificial structures with a similar control in water is still a challenge, especially since the reliable use of specific polar interactions in this solvent is difficult. Supramolecular architectures in water are well known and have been intensely studied.^{67,68} In fact, systems such as micelles^{69,70} and chromonics⁷¹ actually belong to the most applied supramolecular architectures. Amphiphiles, either small organic molecules or polymers,⁷² self-assemble in micelles or vesicles in water and allow for the creation of emulsions and inclusion complexes. Drugs and dyes are members of the so-called class of chromonics and self-assemble in stacked architectures by virtue of their aromatic core and ionic side groups. More exotic examples of water-soluble supramolecular architectures can be found in recent literature, *e.g.* the (poly)rotaxanes,⁷³ for which a molecule⁷⁴ or polymer⁷⁵ is treaded through water-soluble molecules. Schematic representations of these architectures are given in Figure 1.3.

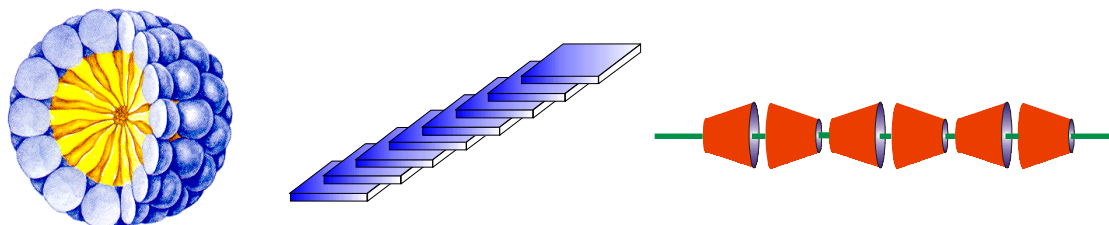


Figure 1.3: Graphical representation of a micelle, stacked chromonics and a polyrotaxane.

The driving force for the formation of these supramolecular architectures in water is the hydrophobic effect.⁷⁶ Due to the lack of directionality of hydrophobic interactions, the formed architectures are disordered and numerous different 'conformations' are possible. The inner part of the micelles as an example might be best compared to the globules formed by collapsed polymers and in the stacked chromonics and polyrotaxanes the molecules are continuously moving within the self-assembly.

Higher ordered structures like vesicles have been formed in water and even chiral architectures have been obtained.^{77,78} However, the positional order of the molecules within these architectures is also not well controlled, despite the fact that transition between different phases are observed. An exception to these disordered structures in water are biological related oligomers as studied by Gottarelli and coworkers.⁷⁹ These guanosine derivatives aggregate and form well-defined chiral columns in water. The oligomeric deoxyguanosines depicted in Figure 1.4 all assemble into columns in water.⁸⁰ At higher concentrations, lyotropic mesophases are formed.⁸¹ The self-assembly involves a delicate interplay between hydrophobic, hydrogen bonding and ion-dipole interactions. Using melting experiments it was found that self-assembly is a hierarchical process for which a well-defined "barrel" is first formed by the assembly of four oligodeoxyguanosine derivatives and then these "barrels" stack on top of each other to give the columns (Figure 1.4 (b)).

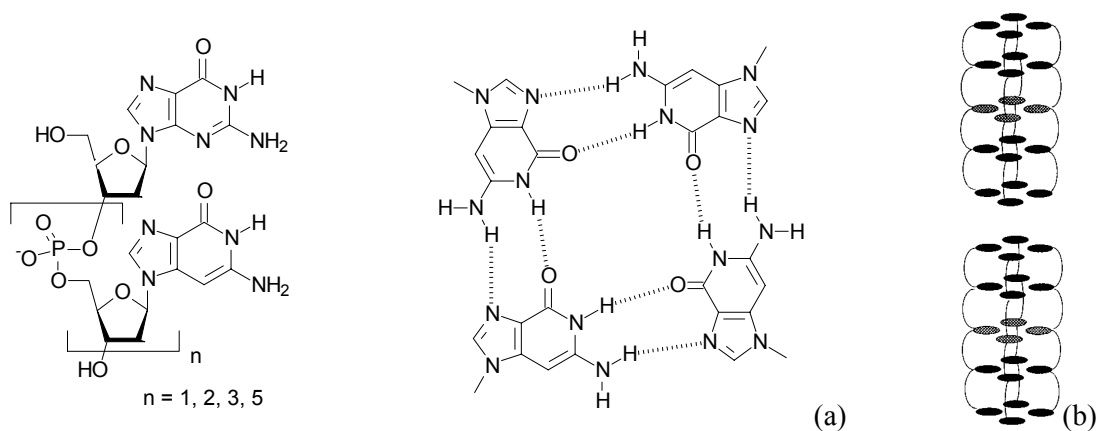


Figure 1.4: (a) Deoxyguanosine oligomers and their mode of self-assembly in a tetramer, (b) The mode of aggregation of eight *d*(GpGpApGpG) molecules. First self-assembly in 'barrels' occurs, followed by stacking of these 'barrels' in columns.⁸²

1.3 Chirality

When large molecular architectures are studied, either mono- or multimolecular, chirality is a feature that quickly comes to mind, especially when biomacromolecules are considered. In the following section a short overview of the history of chirality is given. Subsequently, it will be discussed how chirality can be used as an unequivocal tool for the recognition of order in

supramolecular architectures. Finally the amplification of chirality in supramolecular architectures is discussed and related to the amplification of chirality in synthetic polymers. This feature is a clear measure for order and cooperativity within supramolecular architectures.

Around 1820 it was discovered that certain sets of crystals rotate plane polarized light either levorotatory or dextrorotatory (that is anti-clockwise or clockwise, respectively, as viewed from the end of the polarimeter).⁸³ In the middle of the nineteenth century it was Louis Pasteur who showed that the two different crystals obtained from racemic sodium ammonium tartrate are chiroptical, with opposite signs.^{84,85} It was, however, not until the 1870's that van 't Hoff proposed the tetrahedral carbon atom, the three-dimensional structure rationalizing the occurrence of non-superimposable mirror images.⁸⁶ The studies concerning chiroptical properties of materials had until then always been performed using ORD (optical rotatory dispersion) following the work by Biot in the 1820's.⁸⁷ The description by Curie of circularly polarized light being the oscillation of its rotary and linear components,⁸⁸ was given a physical basis by the discovery of CD (circular dichroism) by Cotton in 1895.⁸⁹ A CD effect and its corresponding ORD effect are accordingly termed a "Cotton effect" where CD is the absorption counterpart of ORD. From the second part of the nineteenth century until the middle of the twentieth century CD/ORD was a less used tool,⁹⁰ but in the 1950's it had experienced an increase of attention because of the use by organic chemists for the structural study of organic compounds⁹¹ and by the use of biochemists for the study of the conformation of polypeptides and proteins.⁸⁷ Nowadays CD is used much more frequently for the characterization of molecules and especially of biomacromolecules. CD has the advantage that it provides the direct observation of the absorption of the chromophores of specific elements in the molecules, whereas ORD is an overall signal resulting from contributions of all CD bands.⁹²

1.3.1 Supramolecular chirality

Organic chemistry deals with the conformation and configuration of individual molecules and, as such, molecular chirality relates to the stereochemistry of these individual molecules. Biochemistry deals with the supramolecular conformation and configuration of natural molecules or polymers. For these large structures chirality not only relates to the stereochemistry of the building blocks, but also to the different levels of supramolecular organization, *e.g.* the secondary and tertiary structure of proteins.¹⁵ This self-assembly of molecules or polymers into an overall chiral architecture is referred to as supramolecular chirality. The stereochemistry of individual molecules generally results in a small local ordering, but in a well-defined self-assembled architecture it can bias long-range overall order to one supramolecular chirality preferably. As such, supramolecular chirality has become a tool to recognize (chiral) order in self-assembled architectures, since it only arises when the individual molecules within the architecture are collectively present in a conformationally ordered fashion.

A chiral, but isolated, chromophore shows a typical Cotton effect due to the preferential absorption of one of the helical components of light. In contrast, an isolated UV active chromophore provided with a distant chiral unit, *e.g.* in a UV inactive side chain, does not feature a Cotton effect. The remote chirality does not influence the absorption of the two helical components of light by the chromophore. When molecules with remote chirality self-assemble in disordered architectures –not featuring a preferred orientation of the molecules–, a Cotton effect is observed neither. However, when the self-assembled architecture is ordered with an intrinsic overall chiral / helical conformation, the chiral side-chains can induce a bias of one of the supramolecular diastereomers expressing chirality in the distant chromophore; supramolecular chirality is said to be expressed.

1.3.2 Amplification of chirality

Strong amplification of chirality for the generation of homochiral molecules or architectures is a fascinating aspect of life that has inspired chemists repeatedly.^{93,94} One approach to investigate this feature is taking advantage of the cooperativity in polymers.⁵ Many polymers have an intrinsically chiral backbone and polymer stereochemistry has received considerable attention for several decades.^{11,95} Apart from tacticity or backbone chirality, it has now been frequently shown for a variety of polymers that side chain chirality can be brought to express conformational bias within the backbone. Approximately 30 years ago Ciardelli and co-workers demonstrated the positive non-linear dependence of the specific rotation of synthetic copolymers made from chiral and achiral monomers.^{96,97} It was concluded that the achiral units in the copolymer are included in sections of the chain having a preferred helical conformation because of the chiral units. Around that time, similar phenomena were observed for copolymers of D- and L-peptides.^{98,99} The handedness of the stable α -helices formed by the polypeptides was governed by the chiral amino acid that was present in majority. Recently, more examples of this non-linear behavior have been disclosed.¹⁰⁰ The most influential work in this field has been performed by Green and coworkers, who demonstrated with a variety of experiments the high cooperativity in poly(isocyanates).^{101,102} Among those the ‘majority rules’ and the ‘sergeant and soldiers’ experiments are most illustrative. It was shown, for example, that the replacement of a hydrogen for a methyl or even a deuterium in only ~ 10% of the side-chains is sufficient to induce the same optical rotation as for the pure chiral homopolymers (Figure 1.5). Green and coworkers furthermore showed the ability to bias the helicity of the polyisocyanates with chiral solvents. It was concluded that the high cooperativity within polyisocyanates was due to the extended helical conformation of the polymers in solution. Likewise, the cooperativity for more flexible polymers is lower.

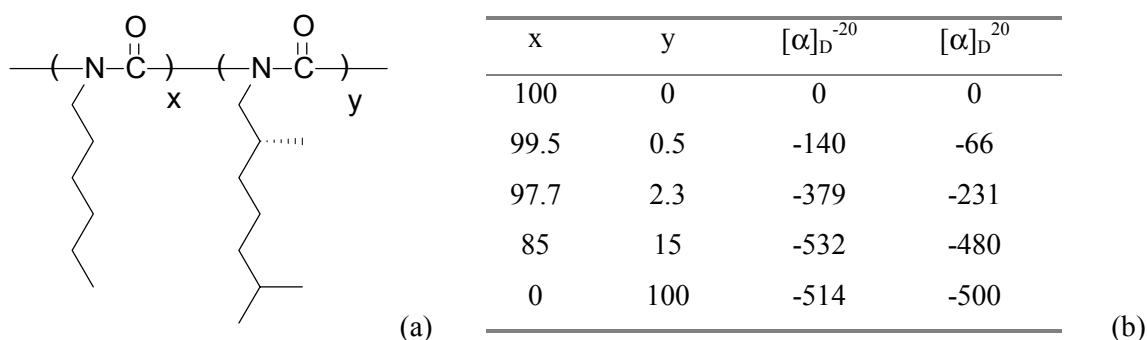


Figure 1.5: (a) Random polyisocyanate copolymer of achiral x and chiral y . (b) Table showing the non-linear optical activity of these copolymers measured in CHCl_3 ($0.5 \text{ mg}\cdot\text{mL}^{-1}$) at -20 and 20 °C.¹⁰¹

For small molecules, molecularly dispersed, the lack of bonding keeping them together dramatically lowers the interactions between them. Therefore, small molecularly dispersed compounds generally feature no cooperative intermolecular interaction. However, once the molecules form well-defined supramolecular aggregates, cooperativity may arise. As an example the discotic molecules depicted in Figure 1.6 are discussed. These discotics form polymeric structures with a rigid-rod character in very dilute solution (10^{-6} M in hexane), due to their large (10^8 l/mol) association constant.¹⁰³ In chloroform the association constant is low and the discs are molecularly dispersed. The aggregation of the discs in hexane is a cooperative process; the molecules attain a chiral, propeller-like conformation (Figure 1.6 (b)) and the conformation of neighboring discs is biased towards a propeller with the same handedness. The optimal stacking interactions result in a conformationally unique helical column (Figure 1.6 (c)). With the presence of achiral side-chains racemic mixtures of both left- and right-handed helices are formed. In case of chiral side-chains diastereomers are formed. An energy difference exists between the two diastereomers, resulting in a bias of the helicity for one type of handedness preferentially. The chiral side chains thus account for homochiral columns. When chiral and achiral molecules are blended in solution, mixed columns are formed. Surprisingly, for these mixed supramolecular columns only one chiral disc at –on the average– every 80 achiral discs is sufficient to bias one helicity of a complete columnar polymer; a type of supramolecular 'Sergeant and Soldiers' effect.¹⁰¹ This result is rationalized by a strong intracolumnar cooperative effect in which, in addition to the solvophobic stacking interactions, directional intermolecular hydrogen bonding of the inner NH protons is used to orient the stacking of the discs, leading to a homochiral superstructure. The strong effect as observed, is due to the conformationally unique supramolecular helicity of the columns, in which the molecules are all aligned in one direction due to specific intermolecular interactions. In conclusion, it might be stated that cooperativity is a mechanism to generate order in supramolecular assemblies, counterbalancing the loss of entropy.

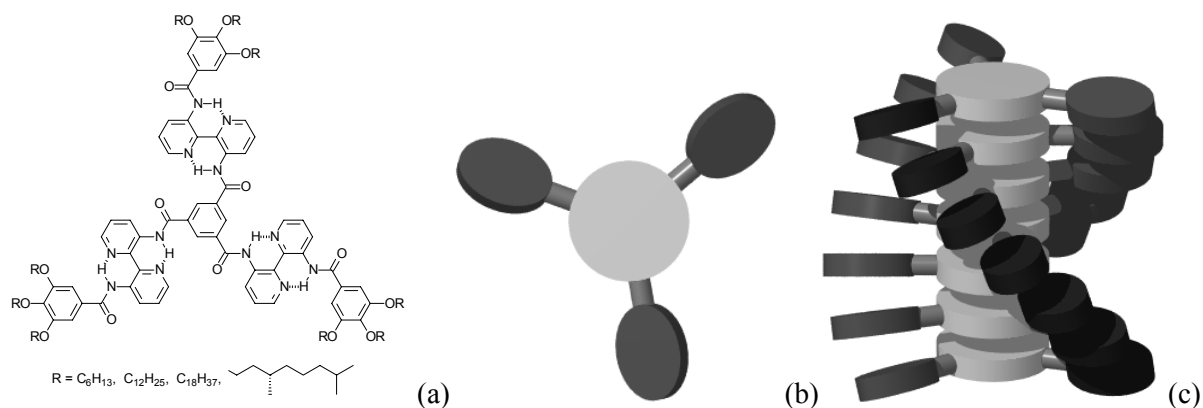


Figure 1.6: (a) C_3 -symmetrical disc-shaped molecules provided with achiral and chiral side chains;¹⁰³ (b) A cartoon representation of the propeller-like conformation attained by the C_3 -symmetrical molecule; (c) Cartoon representation of the conformationally unique helical columns formed by the discotics.

1.4 Aim of the thesis

Biomacromolecules rely heavily on the cooperative use of generic interactions, such as van der Waals and solvophobic interactions, and on specific interactions, like hydrogen bonding and ion-dipole interactions, for the control over their structure in solution. Thus artificial, conformationally unique architectures in polar solvents should also feature these characteristics. This thesis discusses the design requirements for such molecules, their synthesis and the self-assembly of the molecules into ordered chiral supramolecular architectures in polar protic media (amongst others water). The understanding of the design elements and of the self-assembly process itself should aid in obtaining control over conformationally unique architectures in polar solvents.

As a general type of building block for the construction of conformationally unique architectures discotics are used. These molecules, with their ease of design and synthesis, allow for incorporation of functional units at wish, enabling a selective investigation of the important processes at hand. By using additional structuring or specific interactions on top of the solvophobic stacking of the cores, order can be introduced in the self-assemblies. Side chain chirality has been used as an explicit instrument to detect supramolecular chirality in the self-assemblies.

1.5 Outline of the thesis

The use of cooperative threefold intermolecular hydrogen bonding as the tool for both the association into columns and the induction of helicity by discotics is discussed in Chapter 2. In apolar solvents the strong unidirectional hydrogen bonding allows for a strong cooperativity in the columns, for which a 200-fold amplification of chirality has been observed via hydrogen bonding interactions only.¹⁰⁴ In water, the solvent interferes with the threefold intermolecular hydrogen bonding, the latter only arises at very high concentrations, stimulated by additional hydrophobic interactions of the

aromatic core of the discotics. The results show that hydrogen bonding alone does not suffice for the creation of well-defined self-assemblies in polar protic media.

In Chapter 3, strong hydrophobic interactions are used, additional to the threefold intermolecular hydrogen bonding, allowing for self-assembly into long helical columns in polar protic solvents.^{105,106} The self-assembly is a reversible process that occurs in a hierarchical fashion, where the created hydrophobic microenvironment by the stacking allows specific structuring interactions to occur, generating a unique helical motif. The presence or absence of chirality at the supramolecular level can be controlled by temperature and solvent type. Amplification of chirality is highly favored in columns formed in alcohols,¹⁰⁷ whereas in water the chiral order is lower. The self-assembly is discussed in detail and correlated to a two-step model.¹⁰⁸ The solid state organization of these discotics and their ion conduction upon charging with lithium salts is discussed in Chapter 4.¹⁰⁹

The combination of cooperative four-fold intermolecular hydrogen bonding and arene-arene stacking is discussed in Chapter 5. The combination of hydrophobic groups and hydrogen bonding as design elements in one type of molecules has allowed the creation of helical columns of stacked hydrogen bonded pairs in water.¹¹⁰ The design implies the molecules polymerize via intermolecular four-fold hydrogen bonding, which are shielded from the water by the self-assembly of the hydrophobic units. The chiral side-chains direct the twist sense bias of the columns. The presence of a supramolecular backbone in the self-assembly was shown to be important, both for the stability of the columns in dilute solution and for the control over positional order of the discs in the columns.

The final chapter deals with the hierarchical folding and assembly in columns of chiral *m*-phenylene ethynylene oligomers. For these oligomers, only solvophobic and steric interactions have been used for the creation of well defined supramolecular architectures in polar media. The use of chirality has elucidated the stepwise process of folding of the oligomers from a random coil, via intermediate helical states, into a conformationally unique chiral helix.¹¹¹⁻¹¹³ Subsequently, these helices can be brought to stack in helical columns in which chirality can be amplified from one helix to the other.¹¹⁴

1.6 References and notes

- ¹ Flory, P. *Principles of polymer chemistry*; Cornell Univ. Press: Ithaca, **1953**.
- ² Williams, C.; Brochard, F.; Frisch, H.L. *Ann. Rev. Phys. Chem.* **1981**, *32*, 433-451.
- ³ Anfinsen, C.B. *Science* **1973**, *181*, 223-230.
- ⁴ *Advances in protein chemistry Vol. 53 Protein Folding Mechanisms*; Ed. Matthews, C.R.; Academic Press: San Diego, **2000**.
- ⁵ Chan, H.S.; Bromberg, S.; Dill, K.A. *Phil. Trans, R. Soc. Lond. B* **1995**, *348*, 61-70.
- ⁶ Vendruscolo, M. *Eur. Phys. J. B.* **1999**, *8*, 323-326.
- ⁷ Creighton, T.E. *Proteins, structures and molecular properties*; W.H. Freeman and Company: New York, **1984**.
- ⁸ *Prediction of protein structure and the principles of protein conformation*; Ed. Fasman, G.D.; Plenum Press: New York, **1990**.
- ⁹ Schulz, G.E.; Schirmer, R.H. *Principles of protein structure*; Springer-Verlag: New York, **1979**.
- ¹⁰ Moore, J.S.; Nelson, J.C.; Prince, R.B. *Conjugated Oligomers, Polymers, and Dendrimers: From Phenylacetylene to DNA*; Ed. Bredas, J.-L.; Deboeck Université: Paris, **1999**; pp. 263-290 *Conformational order of nonbiological oligomers in solution: molecular design principles*.
- ¹¹ *Encyclopedia of polymer science and engineering*; Eds. Mark, H.F.; Bikales, N.M.; Overberger, C.G.; Wiley-Interscience: New York, **1985**-.
- ¹² Noshay, A.; McGrath, J.E.; *Block copolymers: overview and critical survey*; Academic Press: London, **1977**.
- ¹³ Stryer, L. *Biochemistry*; Freeman: New York, 4th ed. **1995**.
- ¹⁴ *Bioorganic chemistry: nucleic acids*; Ed. Hecht, S.M.; Oxford University Press: New York, **1996**.
- ¹⁵ *Bioorganic chemistry: peptides and proteins*; Ed. Hecht, S.M.; Oxford University Press: New York, **1996**.
- ¹⁶ Robertson, T.B. *The physical chemistry of the proteins*; Longmans, Green and Co.: New York, **1918**.
- ¹⁷ Anson, M.L.; Mirsky, A.E. *J. Gen. Physiol.* **1925**, *9*, 169.
- ¹⁸ Wu, H. *Am. J. Physiol.* **1929**, *90*, 562.
- ¹⁹ Neurath, H. *Chem. Rev.* **1944**, *34*, 157.
- ²⁰ Anson, M.L. *Adv. Protein Chem.* **1945**, *2*, 361.
- ²¹ Levinthal, C. *J. Chim. Phys.* **1968**, *65*, 44-45.
- ²² Dill, K.A.; Chan, H.S. *Nature Structural Biology* **1997**, *4*, 10-19.
- ²³ Dill, K.A. *Biochemistry* **1990**, *29*, 7133-7155.
- ²⁴ Bryngelson, J.D.; Onuchic, J.N.; Socci, N.D.; Wolynes, P.G. *Proteins: Struct. Funct. Genet.* **1995**, *21*, 167-195.
- ²⁵ Shakhovich, E.I. *Curr. Opin. Struct. Biol.* **1997**, *4*, 29-40.
- ²⁶ Dobson, C.M.; Šali, A.; Karplus, M. *Angew. Chem. Int. Ed.* **1998**, *37*, 868-893.
- ²⁷ Pande, V.S.; Grosberg, A.Y.; Tanaka, T. *Rev. Mod. Phys.* **2000**, *72*, 259-314.
- ²⁸ Kauzmann, W. *Adv. Prot. Chem.* **1959**, *14*, 1-63.
- ²⁹ Chothia, C. *Nature* **1975**, *254*, 304-308.
- ³⁰ Watson, J.D.; Hopkins, N.H.; Roberts, J.W.; Steitz, J.A.; Weiner, A.M. *Molecular biology of the gene*; Benjamin/Cummings: Menlo Park, 4th ed., **1987**; pp. 126-163, *The importance of weak chemical interactions*.
- ³¹ Jeffrey, G.A.; Saenger, W. *Hydrogen bonding in biological structures*; Springer-Verlag: Berlin, **1994**.
- ³² Park, I. H.; Kim, J.-H.; Chang, T. *Macromolecules* **1992**, *25*, 7300-7305.
- ³³ Tiktopulo, E.I.; Uversky, V.N.; Lushchik, V.B.; Klenin, S.I.; Bychkova, V.E.; Ptitsyn, O.B. *Macromolecules* **1995**, *28*, 7519-7524.
- ³⁴ Liang, H. *J. Chem. Phys.* **1999**, *110*, 10212-10215.
- ³⁵ Ganazzoli, F. *J. Chem. Phys.* **1998**, *108*, 9924-9932.
- ³⁶ Mandelkern, L. *Crystallization of polymers*; McGraw-Hill: New York, **1964**.
- ³⁷ Cornelissen, J.J.L.M.; Rowan, A.E.; Nolte, R.J.M.; Sommerdijk N.A.J.M. *Chem. Rev.* in preparation.
- ³⁸ *Encyclopedia of polymer science and engineering*; Wiley: New York, **1985**, Vol. 7, pp. 685-698.
- ³⁹ Kallenbach, N.R.; Lyu, P.; Zhou, H. *Circular dichroism and the conformational analysis of biomolecules*; Ed. Fasman, G.D.; Plenum Press: New York, **1996**, pp. 201-261.
- ⁴⁰ *The polysaccharides*; Ed. Aspinall, G.O.; Academic Press: New York, Vol 1-3 **1982-1985**.
- ⁴¹ Doty, P.; Holtzer, A.M.; Bradbury, J.H.; Blout, E.R. *J. Am. Chem. Soc.* **1954**, *76*, 4493-4494.
- ⁴² Zimm, B.H.; Bragg, J.K. *J. Chem. Phys.* **1959**, *31*, 526-535.

- 43 As an example see: Luthey-Schulten, Z.; Ramirez, B.E.; Wolynes, P.G. *Phys. Chem.* **1995**, *99*, 2177-2185.
- 44 Seebach, D.; Matthews, J.L. *Chem. Commun.* **1997**, 2015-2022.
- 45 Gellman, S. H. *Acc. Chem. Res.* **1998**, *31*, 173-180.
- 46 Kirshenbaum, K.; Zuckermann, R.N.; Dill, K.A. *Curr. Opin. Struct. Biol.* **1999**, *9*, 530-535.
- 47 *Handbook of liquid crystals*; Eds. Demus, D.; Goodby, J.; Gray, G.W.; Spiess, H.W.; Vill, V.; Wiley-VCH Verlag: Weinheim, Vol 2B **1998**.
- 48 Brunsveld, L.; Folmer, B.J.B.; Meijer, E.W. *MRS Bulletin* **2000**, *25*, 49-53.
- 49 Vallerien, S.U.; Werth, M.; Kremer, F.; Spiess, H.W. *Liq. Cryst.* **1990**, *8*, 889-893.
- 50 Fox, J.M.; Katz, T.J.; van Elshocht, S.; Verbiest, T.; Kauranen, M.; Persoons, A.; Thongpanchang, T.; Krauss, T.; Brus, L. *J. Am. Chem. Soc.* **1999**, *121*, 3453-3459.
- 51 Nuckolls, C.; Katz, T.J. *J. Am. Chem. Soc.* **1998**, *120*, 9541-9544.
- 52 Cuccia, L.A.; Lehn, J.-M.; Homo, J.-C.; Schmutz, M. *Angew. Chem. Int. Ed.* **2000**, *39*, 233-237.
- 53 Gallivan, J.P.; Schuster, G.B. *J. Org. Chem.* **1995**, *60*, 2423-2429.
- 54 Engelkamp, H.; Middelbeek, S.; Nolte, R.J.M. *Science* **1999**, *284*, 785-788.
- 55 Kraft, A.; Osterod, F.; Fröhlich, R. *J. Org. Chem.* **1999**, *64*, 6425-6433.
- 56 Kimura, M.; Muto, T.; Takimoto, H.; Wada, K.; Ohta, K.; Hanabusa, K.; Shirai, H.; Kobayashi, N. *Langmuir* **2000**, *16*, 2078-2082.
- 57 Fuhrhop, J.-H.; Demoulin, C.; Boettcher, C.; Köning, J.; Siggel, U. *J. Am. Chem. Soc.* **1992**, *114*, 4159-4165.
- 58 Yasuda, Y.; Iishi, E.; Inada, H.; Shirota, Y. *Chem. Lett.* **1996**, 575-576.
- 59 Hanabusa, K.; Koto, C.; Kimura, M.; Shirai, H.; Kakehi, A. *Chem. Lett.* **1997**, 429-430.
- 60 Lightfoot, M.P.; Mair, F.S.; Pritchard, R.G.; Warren, J.E. *Chem. Commun.* **1999**, 1945-1946.
- 61 Mezzina, E.; Mariani, P.; Itri, R.; Masiero, S.; Pieraccini, S.; Spada, G.P.; Spinozzi, F.; Davis, J.T.; Gottarelli, G. *Chem. Eur. J.* **2001**, *7*, 388-395.
- 62 Whitesides, G.M.; Mathias, J.P.; Seto, C.T. *Science* **1991**, *254*, 1312-1319.
- 63 G.-Krzywicki, F.; Fouguey, C.; Lehn, J.-M. *Proc. Natl. Acad. Sci. USA* **1993**, *90*, 163-167.
- 64 Castellano, R.K.; Rudkevich, D.M.; Rebek, J. *Proc. Natl. Acad. Sci. USA* **1997**, *94*, 7132-7137.
- 65 Prins, L.J.; Huskens, J.; de Jong, F.; Timmerman, P.; Reinhoudt, D.N. *Nature* **1999**, *398*, 498-502.
- 66 *Comprehensive supramolecular chemistry*; Ed. J.-M. Lehn.; Pergamon: Oxford, UK, 11 issues **1996**.
- 67 Engberts, J.B.F.N.; Kevelam, J. *Curr. Opin. Colloid Interface Sci.* **1996**, *1*, 779-789.
- 68 Feiters, M.C.; Nolte, R.J.M. *Adv. Supramol. Chem.* **2000**, *6*, 41-156.
- 69 Tanford, C. *The hydrophobic effect: formation of micelles and biological membranes*; Wiley: New York, 2nd ed. **1980**.
- 70 *Micelles, membranes, microemulsions and monolayers*; Eds. Gelbart, W.M.; Ben-Shaul, A.; Roux, D.; Springer: New York, **1994**.
- 71 Lydon, J. *Curr. Opin. Colloid Interface Sci.* **1998**, *3*, 458-466.
- 72 Gast, A.P. *Curr. Opin. Colloid Interface Sci.* **1997**, *2*, 258-263.
- 73 Harada, A. *Acta Polym.* **1998**, *49*, 3-17.
- 74 Anderson, S.; Anderson, H.L. *Angew. Chem., Int. Ed. Engl.* **1996**, *35*, 1956-1958.
- 75 Harada, A.; Li, J.; Kamachi, M. *Nature* **1992**, *356*, 325-327.
- 76 Blokzijl, W.; Engberts, J.B.F.N. *Angew. Chem. Int. Ed. Engl.* **1993**, *32*, 1545-1579.
- 77 Kunitake, T. *Angew. Chem. Int. Ed. Engl.* **1992**, *31*, 709-726.
- 78 Fuhrhop, J.-H. *Compr. Supramol. Chem.* **1996**, *9*, 407-450.
- 79 For a review on guanosine and pterine self-assembly until 1996 see: Gottarelli, G.; Spada, G.P.; Garbesi, A. in *Comprehensive Supramolecular Chemistry*, ed. Lehn, J.-M. Pergamon Press, Oxford, UK, **1996**, *9*, 483-506.
- 80 Bonazzi, S.; Capobianco, M.; DeMoraes, M.M.; Garbesi, A.; Gottarelli, G.; Mariani, P.; Ponzi Bossi, M.G.; Spada, G.P.; Tondelli, L. *J. Am. Chem. Soc.* **1991**, *113*, 5809-5816.
- 81 Mariani, P.; Mazabard, C.; Garbesi, A.; Spada, G.P. *J. Am. Chem. Soc.* **1989**, *111*, 6369-6373.
- 82 Gottarelli, G.; Proni, G.; Spada, G.P.; Bonazzi, S.; Garbesi, A.; Ciuchi, F.; Mariani, P. *Biopolymers* **1997**, *42*, 561-574.
- 83 Herschel, J.W.F. *Trans. Cambridge Phil. Soc.* **1822**, *1*, 43-50.
- 84 Pasteur, L. *C. R. Acad. Sci. Paris* **1848**, *26*, 535-538.
- 85 Intriguingly, the two types of sodium ammonium tartrate crystals form a racemate at temperatures above 26 °C.
- 86 van 't Hoff, J.H. *Arch. Neerl. Sci. Exactes Nat.* **1874**, *9*, 445-454.

- ⁸⁷ Yang, J.T. *Circular dichroism and the conformational analysis of biomolecules*; Ed. Fasman, G.D.; Plenum Press: New York, **1996**, pp. 1-24 *Remembrance of things past: a career in chiroptical research*.
- ⁸⁸ Curie, P. *J. Phys.* **1893**, *3*, 393.
- ⁸⁹ Cotton, A. C. R. *Acad. Sci. Paris* **1895**, *120*, 337-347.
- ⁹⁰ The decline in attention for ORD is related to the invention of the Bunsen burner in 1866. This apparatus allowed for the facile use of the monochromatic light of the sodium flame, thus inhibiting the highly laborious study of rotatory dispersion, generally using sunlight.
- ⁹¹ Djerassi, C. *Optical rotatory dispersion*; McGraw-Hill: New York, **1960**.
- ⁹² *Circular dichroism*; Eds. Berova, N.; Nakanishi, K.; Woody, R.W.; Wiley-VCH: New York, 2nd ed. **2000**.
- ⁹³ Feringa, B.L.; van Delden, R.A.; *Angew. Chem. Int. Ed.* **1999**, *38*, 3419-3438.
- ⁹⁴ Avalos, M.; Babiano, R.; Cintas, P.; Jimenez, J. L.; Palacios, J. C. *Tetrahedron: Asymmetry* **2000**, *11*, 2845-2874.
- ⁹⁵ Farina, M. *Top. Stereochem.* Eds. Eliel, E.L.; Wilen, S.H. New York: John Wiley & Sons, **1987**, *17*, pp. 1-111.
- ⁹⁶ Pino, P.; Ciardelli, F.; Montagnoli, G.; Pieroni, O. *Pol. Lett.* **1967**, *5*, 307-311.
- ⁹⁷ Carlini, C.; Ciardelli, F.; Pino, P. *Makromol. Chem.* **1968**, *119*, 244-248.
- ⁹⁸ Downie, A.R.; Elliot, A.; Hanby, W.E.; Malcolm, B.R. *Proc. R. Soc. London* **1957**, *A242*, 325-340.
- ⁹⁹ Heiz, F.; Spach, G. *Macromolecules* **1971**, *4*, 429-432.
- ¹⁰⁰ For a review: Okamoto, Y.; Nakano, T. *Chem. Rev.* **1994**, *94*, 349-372.
- ¹⁰¹ Green, M.M.; Reidy, M.P.; Johnson, R.D.; Darling, G.; O'Leary, D.J.; Willson, G. *J. Am. Chem. Soc.* **1989**, *111*, 6452-6454.
- ¹⁰² For a review: Green, M.M.; Peterson, N.C.; Sato, T.; Teramoto, A.; Lifson, S. *Science* **1995**, *268*, 1860-1866.
- ¹⁰³ Palmans, A.R.A.; Vekemans, J.A.J.M.; Havinga, E.E.; Meijer, E.W. *Angew. Chem. Int. Ed. Engl.* **1997**, *36*, 2648-2651.
- ¹⁰⁴ Brunsveld, L.; Schenning, A.P.H.J.; Broeren, M.A.C.; Janssen, H.M.; Vekemans, J.A.J.M.; Meijer, E.W. *Chem. Lett.* **2000**, 292-293.
- ¹⁰⁵ Brunsveld, L.; Zhang, H.; Glasbeek, M.; Vekemans, J.A.J.M.; Meijer, E.W. *J. Am. Chem. Soc.* **2000**, *122*, 6175-6182.
- ¹⁰⁶ Brunsveld, L.; Lohmeijer, B.G.G.; Vekemans, J.A.J.M.; Meijer, E.W. *Chem. Commun.* **2000**, 2305-2306.
- ¹⁰⁷ Brunsveld, L.; Lohmeijer, B.G.G.; Vekemans, J.A.J.M.; Meijer, E.W. submitted.
- ¹⁰⁸ van der Schoot, P.; Michels, M.A.J.; Brunsveld, L.; Sijbesma, R.P.; Ramzi, A. *Langmuir* **2000**, *16*, 10076-10083.
- ¹⁰⁹ Brunsveld, L.; Vekemans, J.A.J.M.; Janssen, H.M.; Meijer, E.W. *Mol. Cryst. Liq. Cryst.* **1999**, *331*, 449-456.
- ¹¹⁰ Hirschberg, J.H.K.K.; Brunsveld, L.; Ramzi, A.; Vekemans, J.A.J.M.; Sijbesma, R.P.; Meijer, E.W. *Nature* **2000**, *407*, 167-170.
- ¹¹¹ Brunsveld, L.; Prince, R.B.; Meijer, E.W.; Moore, J.S. *Org. Lett.* **2000**, *2*, 1525-1528.
- ¹¹² Prince, R.B.; Brunsveld, L.; Meijer, E.W.; Moore, J.S. *Angew. Chem. Int. Ed.* **2000**, *39*, 228-230.
- ¹¹³ Brunsveld, L.; Meijer, E.W.; Prince, R.B.; Moore, J.S. submitted.
- ¹¹⁴ Brunsveld, L.; Meijer, E.W.; Prince, R.B.; Moore, J.S. submitted.

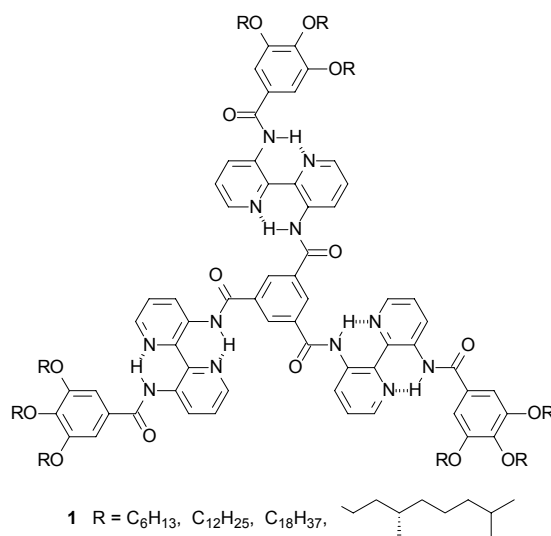
Chapter 2

Helical columns of discotic molecules via assembly by threefold intermolecular hydrogen bonding

Abstract: *Chiral trialkyl-1,3,5-benzenetricarboxamides self-assemble in dilute alkane solutions (10^{-6} M) into long columns via cooperative threefold intermolecular hydrogen bonding. The directionality of the intermolecular hydrogen bonding introduces an intrinsic helicity into the columns. The chiral side-chains account for a bias of the helicity and generate homochirality of the columns. Using "Sergeant and Soldiers" experiments with mixtures of chiral and achiral molecules it was shown that in a helical column, one chiral molecule can amplify its chirality to on average 200 achiral molecules. A chiral, water-soluble 1,3,5-benzenetricarboxamide derivative has been obtained by using chiral oligo(ethylene oxide) side chains. Directional self-assembly via threefold intermolecular hydrogen bonding in dilute aqueous media is prevented due to the interference of the water molecules with the hydrogen bonding. However, at high concentrations (10^{-2} M) in both water and chloroform aggregation occurs. In chloroform this aggregation is mainly mediated by the threefold intermolecular hydrogen bonding, whereas in water hydrophobic interactions dominate the aggregation. The difference in aggregate formation is expressed in an opposite Cotton effect for the self-assemblies in the two solvents.*

2.1 Introduction

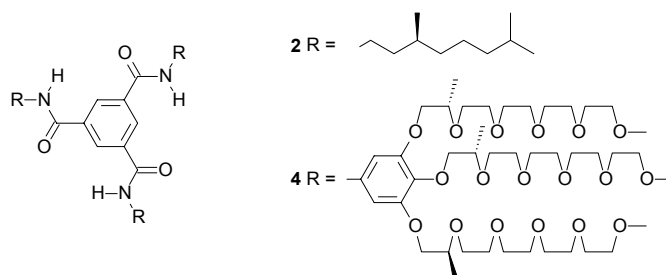
Discotic molecules (discotics) have been shown to self-assemble in a variety of solvents, ranging in polarity from hexane to water.¹ In general, the non-specific arene-arene, solvophobic or hydrophobic interactions of the cores have been utilized as the driving force for the assembly. These generic interactions create columnar aggregates in which the molecules typically lack positional order. Only through the use of additional specific interactions, positional order can be introduced in the column.²⁻¹² Cooperative helical structures have only been observed for a C_3 -symmetrical extended core discotic (**1**) that utilizes hydrogen bonding as a specific directional interaction, both for the planarization of the molecule and for inducing intermolecular positional order.⁵ Both the association constant and the cooperativity within the columns formed by **1** are very large; in dilute hexane solution (10^{-5} M) one chiral molecule is able to amplify its chirality to 80 achiral molecules when mixed in one column. Threefold intermolecular hydrogen bonding of the inner NH's and the adoption of a propeller-like conformation of all molecules within the column are responsible for this strong cooperative effect, whereas the extended aromatic core accounts for the strong aggregation.



From both an aesthetic and a practical point of view, C_3 -symmetrical molecules are highly attractive building blocks for the formation of supramolecular architectures. Especially those compounds that feature secondary amide bonds have extensively been utilized for the formation of organic gels by Shirota *et al.*^{13,14} and Hanabusa *et al.*^{15,16} It has convincingly been proven that the formation of such organogels is governed by intermolecular hydrogen bonding and intermolecular solvophobic interactions between the side chains. Recently, intermolecular hydrogen bonding in a single crystal of such a C_3 -symmetrical trimesic amide has been demonstrated to be responsible for the formation of helical columns.¹⁷

In order to investigate whether such highly cooperative and long columns as observed for **1** can also be obtained using primarily hydrogen bonding, compounds **2** and **4** were designed as target molecules for the creation of helical columns via intermolecular hydrogen bonding in both apolar (**2**)

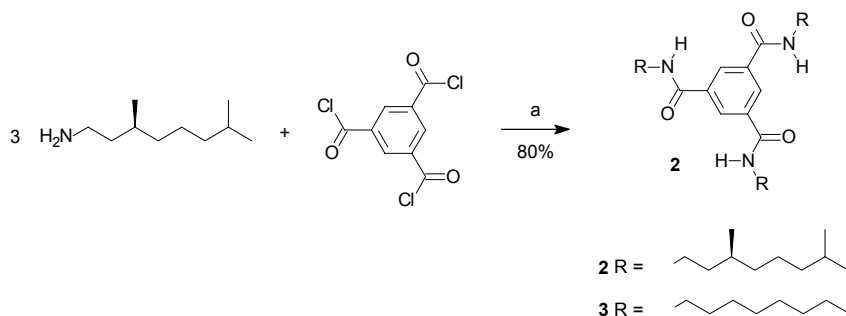
and in polar (**4**) media (water). Whether such cooperative helical columns based on intermolecular hydrogen bonding can also exist in water is an additional question. Obviously, hydrogen bonding interactions are generally much stronger in apolar media, not interfered by a competitive solvent, but presumably cooperative threefold hydrogen bonding, possibly aided by hydrophobicity, meets the requirements for their expression in water. In this chapter the formation of helical columns by **2** in alkanes will be discussed in section 2.2 and the self-assembly of **4** in water and chloroform in section 2.3.



2.2 Helical columns using threefold hydrogen bonding in hexane

2.2.1 Synthesis and characterization

N,N',N''-Tris((*S*)-3,7-dimethyloctyl)benzene-1,3,5-tricarboxamide (**2**) was synthesized by reacting 1,3,5-benzenetricarbonyl trichloride with three equivalents of (*S*)-3,7-dimethyloctylamine¹⁸ in methylene chloride, using triethylamine as a base (Scheme 2.1). The compound was identified by ¹H- and ¹³C-NMR spectroscopy, elemental analysis and MALDI-TOF mass spectrometry. Achiral **3** was synthesized in a similar fashion and has been reported previously.¹⁹ Compounds **2** and **3**¹⁹ both showed liquid crystalline behavior at elevated temperatures. Melting into the mesophase occurred for **2** at 119 °C ($\Delta H = 16$ kJ/mol) with evidence of a low enthalpy pre-transition at 105 °C, as compared to 102 °C for **3**. The mesophases of **2** and **3** extended until 236 °C ($\Delta H = 21$ kJ/mol) and 204 °C ($\Delta H = 17$ kJ/mol), respectively. Textures grown under the optical microscope show maltese crosses, pointing to the formation of a columnar mesophase.¹⁹ The large energy of the transition from liquid crystal to molten state is most probably due to melting of the three intermolecular hydrogen bonds.



Scheme 2.1: The synthesis of chiral apolar discotic **2** and the structure of its achiral octyl analogue **3**.
(a) Et_3N , CH_2Cl_2 , *r.t.*

2.2.2 Aggregation in solution

The formation of assemblies by **2** in dilute solution and the involvement of hydrogen-bonding was studied using infrared (IR) (Figure 2.1), UV-Vis and circular dichroism (CD) spectroscopy (Figure 2.2). In the solid state the N-H stretch vibration is present at 3223 cm^{-1} and in a hexane solution (10^{-4} M) this band remains at this position (3242 cm^{-1}). In a tetrachloromethane solution of 10^{-2} M this band was also prominent, but upon dilution to 10^{-4} M an upcoming vibration at 3458 cm^{-1} could be discerned. In chloroform only the vibration at 3450 cm^{-1} is present. The C=O stretch vibration shows similar characteristic shifts: in the solid state, in heptane and concentrated tetrachloromethane solutions this band can be found around 1640 cm^{-1} , whereas in dilute tetrachloromethane solution and chloroform this vibration is situated around 1665 cm^{-1} .

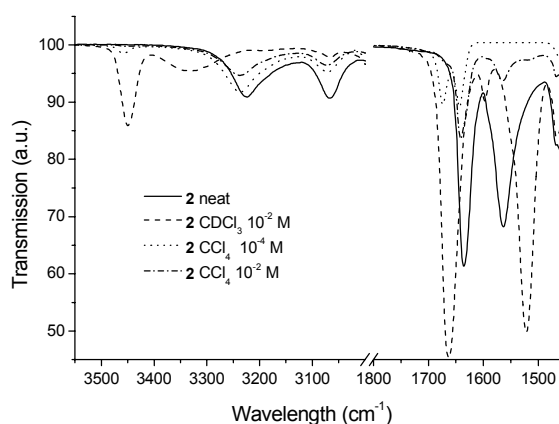


Figure 2.1: Infrared spectra of **2** under different conditions. Shown are the N-H stretch vibrations ($3500\text{-}3000\text{ cm}^{-1}$) and the C=O, C-N stretch vibrations and N-H deformations ($1800\text{-}1500\text{ cm}^{-1}$).

No detectable Cotton effect in the chromophore of the core was found in CD spectra of **2** recorded in chloroform. In heptane a negative Cotton effect appears for the chromophore of the core (Figure 2.2). The UV-Vis spectrum of **2** in heptane shows the absorption of the benzene and amide chromophores. Upon increasing the temperature the UV-Vis spectrum changes significantly and the Cotton effect disappears.

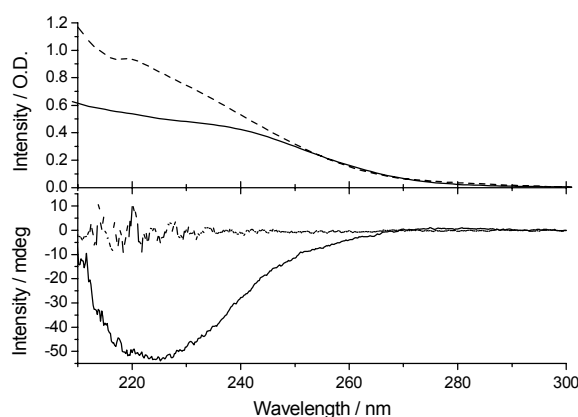


Figure 2.2: Absorption (top) and CD (bottom) spectra of **2** in heptane at 10 °C (—) and at 90 °C (---). Concentration = 6.5×10^{-5} M.

The N-H stretch vibration at 3223 cm^{-1} and the C=O stretch vibration at 1640 cm^{-1} result from intermolecular hydrogen bonding, whereas the vibrations at 3450 and 1665 cm^{-1} are indicative of absence of hydrogen bonding.^{14,16} It can thus be concluded that in the solid state and in heptane and tetrachloromethane solution aggregation occurs mediated by intermolecular hydrogen bonding. In chloroform, on the other hand, the molecules are molecularly dissolved and accordingly, no Cotton effect is observed with CD spectroscopy. The Cotton effect observed for heptane solutions indicates the formation of a chiral superstructure. For a close analog of **2** helical columns have been visualized with single crystal X-ray spectroscopy in the solid state.¹⁷ Within these columns, threefold intermolecular hydrogen bonding gives rise to the stacking of the molecules with a helical twist. In the self-assemblies of **2** in heptane solution the intermolecular hydrogen bonds apparently similarly lock the molecules on top of each other and give directionality to the stacking. The peripheral side-chains interact due to this self-assembly, enabling transfer of their chirality to the self-assembled helical columnar backbone.^{20,21} At higher temperatures the intermolecular hydrogen bonding disappears, resulting in the breaking up of the columns into single molecules with concomitant loss of supramolecular chirality.

2.2.3 Amplification of chirality

The cooperativity within the columns was illustrated by amplification of chirality in accordance with the ‘‘Sergeant and Soldiers’’ principle.²² For this, chiral **2** was used as the sergeant to bias the helicity of the intrinsic helical units formed by the soldiers: achiral discs **3**. The ‘Sergeant and Soldiers’ experiments on **2** / **3** mixtures in heptane were conducted at two different concentrations at 20 °C and the intensity of the Cotton effect divided by the absorption (g_{abs}) was monitored as a function of mole percent **2** added (Figure 2.3). Strong amplification of chirality was observed at a

concentration of 8×10^{-5} M, since the maximal g_{abs} was reached after addition of only 2.5 percent chiral **2**. The amplification of chirality at 6×10^{-6} M was considerably smaller, since then around 5 percent of sergeant was needed to achieve a full bias of helicity. The ‘Sergeant and Soldiers’ data were fitted to the model derived by Havinga⁵ in order to determine the association constant and the cooperativity length associated with chirality amplification, i.e. the number of soldiers in one helical unit in a column that respond to and follow the chirality of one sergeant. The cooperativity length over which one single chiral seed molecule can amplify its chirality was calculated to be around 200 molecules and the association constant K was determined to be approximately 5×10^8 L \times mol⁻¹ at 20 °C.

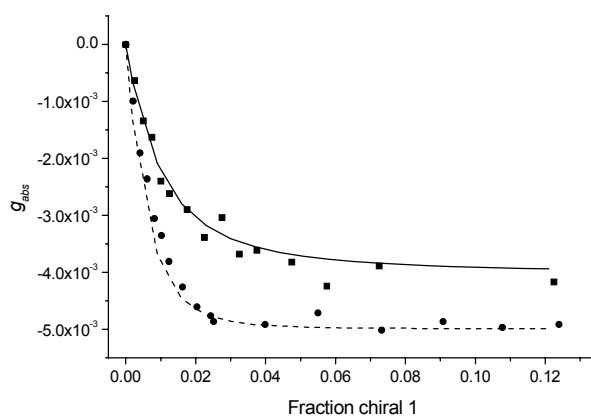


Figure 2.3: Dependence of the overall chirality on the mole fraction of chiral **2** in **2** / **3** mixtures in heptane at 20 °C, expressed in terms of the g -value measured at the maximum of the Cotton effect at 224 nm. Measurements were recorded in a 1 cm cell at 6×10^{-6} M (squares) and at 8×10^{-5} M (circles). The solid lines represent the best fit to the data using a cooperativity length of 200 molecules and a K of 5×10^8 L \times mol⁻¹.

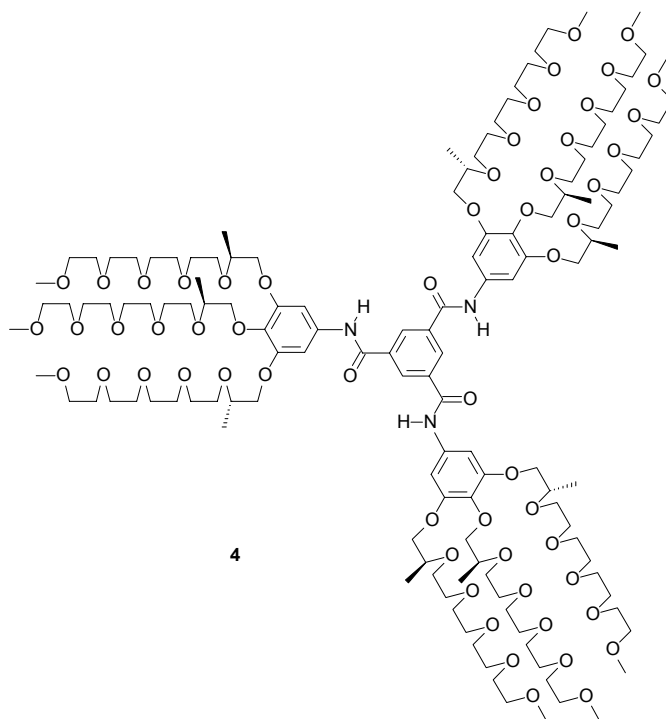
The cooperativity length of 200 molecules for amplification of chirality of **2** and **3** is even larger than that of the extended C₃-symmetrical molecule **1** previously reported.⁵ This feature and the high association constant K thus show that intermolecular hydrogen bonding within the self-assembled columns suffices for creation of long and highly ordered helical columns and no additional interactions are required. The side-chain interactions, occurring upon self-assembly, give rise to the bias of the supramolecular chirality.

2.3 Helical columns using threefold hydrogen bonding in water

2.3.1 Introduction

The formation of long helical columns by **2** in dilute alkane solutions on the basis of threefold intermolecular hydrogen bonding is possible because the apolar solvent supports intermolecular hydrogen bonding. In contrast, in chloroform the association does not arise at low concentrations,

because the chloroform molecules interfere with the intermolecular hydrogen bonding of the amides. It is, therefore, expected that polar solvents, like water, also will interfere with the intermolecular hydrogen bonding. As an example mononucleotides can be considered. These building blocks of DNA and RNA do not dimerize via hydrogen-bonded pairs in water ($K_{\text{dim}} \sim 1$),²³ but rather stack ($K'_{\text{dim}} \sim 20$) at higher concentrations.²⁴ Their modified analogs, soluble in organic solvents, on the other hand do dimerize substantially via hydrogen bonding.²⁵ It is generally known from biomacromolecules that hydrogen bonding can be induced in water by creation of a hydrophobic microenvironment.^{26,27} The expression of hydrogen bonds under aqueous conditions requires either the feature of a hydrophobic microenvironment or highly cooperative and strong intermolecular hydrogen bonding, not excluding the use of both. In order to explore the possibility of forming similar helical columns on the basis of cooperative intermolecular hydrogen bonding in water, chiral discotic **4** was synthesized and studied.

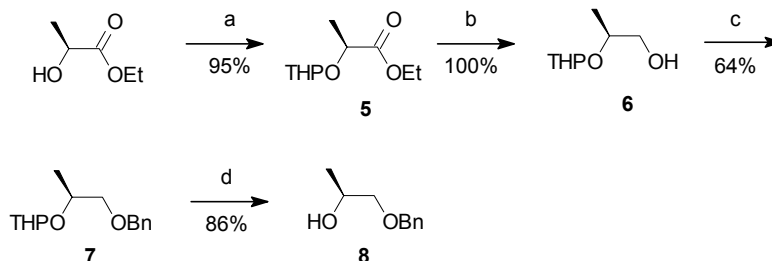


The creation of water-soluble columnar architectures demands the discotics to be functionalized with neutral water-soluble side chains, to avoid complexation from ionic groups. In the following sections first the synthesis of a variety of water-soluble side chains based on oligo(ethylene oxide) oligomers, both chiral and achiral will be discussed.²⁸ Subsequently, the synthesis of discotic **4** is shown and then the formation of aggregates by **4** in solution is discussed.

2.3.2 Synthesis and characterization

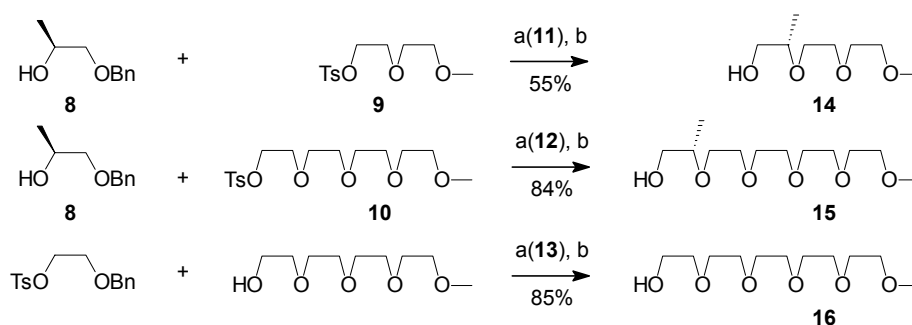
The incorporation of chirality in the water-soluble side-chains requires an easily accessible water-soluble chiral synthon. Benzyl protected (2*S*)-1,2-propanediol **8** was therefore designed and

synthesized (Scheme 2.2). Ethyl (*S*)-(-)-lactate was used as a cheap and enantiomerically pure chiral starting product. Using standard synthetic procedures,²⁹ the ethyl lactate was converted into (2*S*)-1-benzyloxy-propan-2-ol (**8**) in an overall yield of 52%. All products were characterized with ¹H- and ¹³C-NMR spectroscopy and GC-MS and had a purity > 98%.



Scheme 2.2: The synthesis of chiral synthon (2*S*)-1-benzyloxy-propan-2-ol **8**. (a) DHP, *p*-TsOH, Et₂O, *r.t.*; (b) (i) LiAlH₄, Et₂O, 0 °C; (ii) H₂O; (c) (i) *t*-BuOK, *t*-BuOH; (ii) Bu₄N⁺Cl, BnCl, 80 °C; (d) *p*-TsOH, MeOH, 0 °C.

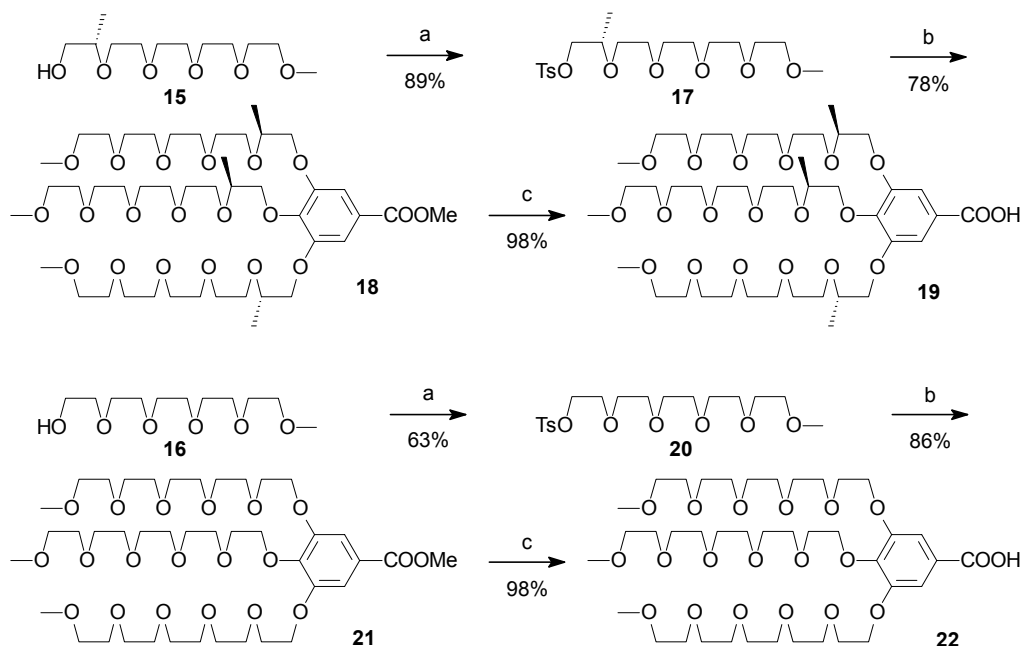
Chiral synthon **8** was employed for the synthesis of two chiral side-chains (**14** and **15**) via coupling with the tosylates of di and tetra(ethylene oxide) mono-methyl ether (**9** and **10**) and subsequent deprotection of the alcohol. In a similar fashion also an achiral penta(ethylene oxide) mono-methyl ether (**16**) was synthesized using tetra(ethylene oxide) mono-methyl ether. (Scheme 2.3). The alcohols were obtained pure (> 98 %, GC-MS) via Kugelrohr distillation. The chiral synthon **8** introduces a methyl group at the second carbon of each chiral side chain. This places the stereochemical information in reasonably close proximity to the core or backbone of the target molecules. Positioning of the methyl on the first carbon of the side chain was not pursued, in view of possible racemization of the chiral center in subsequent reactions.



Scheme 2.3: The synthesis of chiral (2*S*)-2-methyl-3,6,9-trioxadecan-1-ol, **14**, (2*S*)-2-methyl-3,6,9,12,15-pentaoxahexadecan-1-ol, **15**, and achiral 3,6,9,12,15-pentaoxahexadecan-1-ol, **16**; (a) KOH, THF, 65 °C; (b) Pd/C, EtOH, dil. HCl, *r.t.*

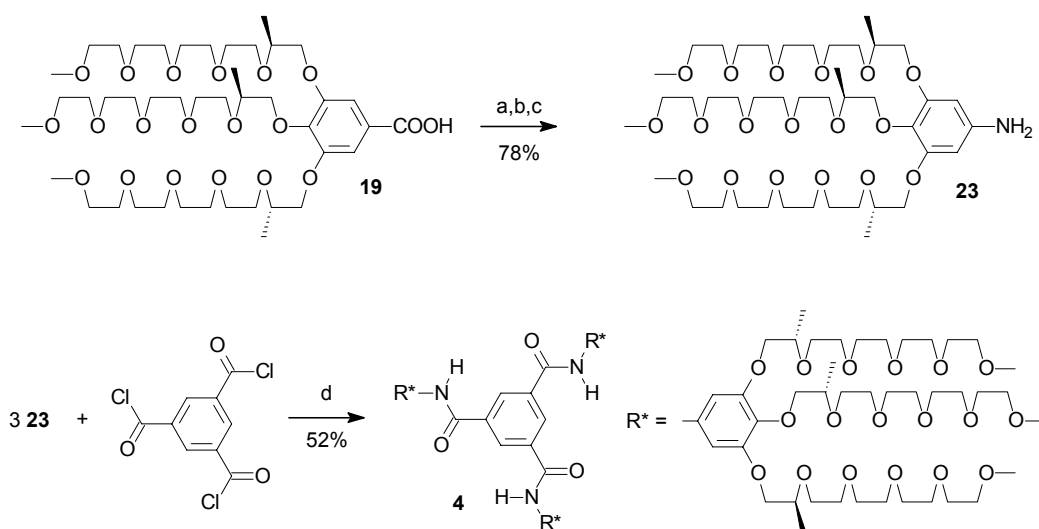
The chiral and achiral penta(ethylene oxide) mono-methyl ethers (**15** and **16**) were activated to their tosylates (**17** and **20**) and subsequent trialkylation of methyl 3,4,5-trihydroxybenzoate

generated mesogenic wedges **19** and **22**, in analogy with their apolar counterparts,³⁰ after saponification (Scheme 2.4). All compounds were obtained as colorless oils.



Scheme 2.4: Synthesis of mesogenic groups **19** and **22** (a) *p*-TsCl, NaOH, water /THF, 0 °C; (b) Methyl gallate (0.33 eq.), K₂CO₃, DMF, 70 °C; (c) (i) KOH, EtOH/water, 90 °C; (ii) H₃O⁺.

The synthesis of C₃-symmetrical discotic **4** with threefold amide bonds, requires the side-chain precursor to be present as an amine, to allow reaction with acid chlorides. The chiral acid **19** was converted into an amine using a four-step sequence via its acid chloride, acyl azide and isocyanate in a good yield.³¹ The obtained amine was then reacted three times with trimesic chloride to yield **4** as a light yellow oil after column chromatography (Scheme 2.5).



Scheme 2.5: Synthesis of amine **23** and water-soluble discotic **4** (a) oxalyl chloride, CH₂Cl₂, r.t.; (b) NaN₃, THF/water, 0 °C; (c) (i) dioxane, 101 °C; (ii) Bu₄NOH, dioxane, 90 °C; (d) Et₃N, CH₂Cl₂, r.t.

2.3.3 Aggregation in solution

Discotic molecule **4** dissolved readily in deuterated acetonitrile, acetone and methanol and featured clearly resolved and sharp ^1H -NMR spectra in these solvents, even at elevated concentrations (10^{-2} M). Due to exchange of the amide protons with the alcoholic deuterium proton of methanol, the signal around 10 ppm had disappeared in this solvent. The nature of the spectra indicates that **4** is molecularly dispersed in these solvents of moderate polarity. Dilute solutions of **4** in deuterated chloroform gave spectra with similar characteristics as for the polar solvents. However, highly concentrated solutions (~ 100 mg/ml) gave rise to broadening of all signals and particularly the signals corresponding to the amide and aromatic protons. Figure 2.4 displays the proton NMR spectra of **4** (100 mg/ml) in chloroform at five different temperatures. At 60 °C a spectrum featuring relatively sharp signals is obtained, but lowering the temperature resulted in a gradual broadening and shift of the signals. These spectral features are indicative for aggregation of the molecules. The considerable change in the signal of the amide protons suggests intermolecular hydrogen bonding to be the driving force for the aggregation in chloroform. Presumably, the large aromatic core of **4**, compared to compound **2**, contributes favorably to the aggregation via enhanced π - π stacking, as indicated by the broadening of its aromatic signals. The combination of these two effects induces aggregation via intermolecular amide-amide hydrogen bonding at around 10^{-2} M in chloroform.

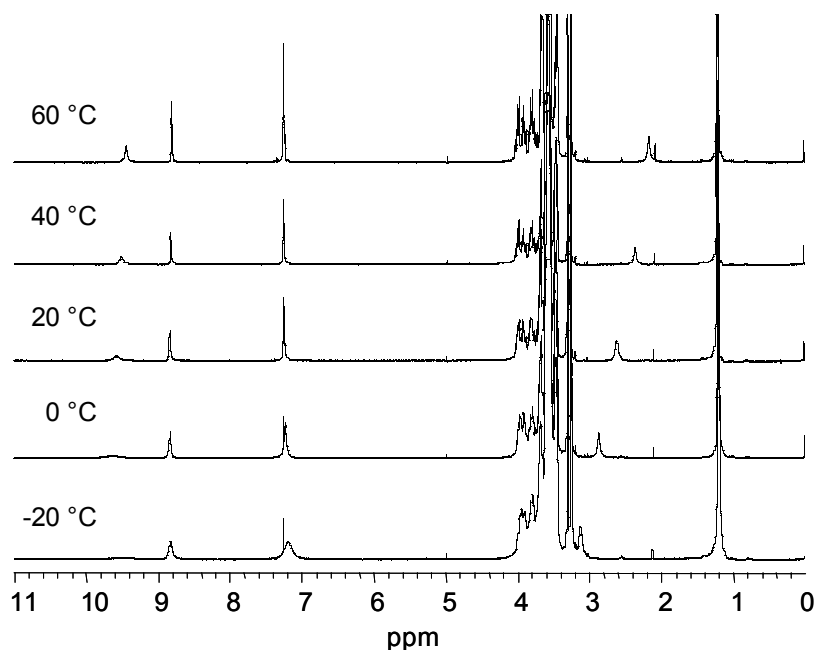


Figure 2.4: ^1H -NMR spectra of **4** in CDCl_3 (~ 100 mg/ml; 35 mM) at different temperatures. A broadening of the signals, especially of the amide protons around 9.5 ppm, can be observed upon cooling. The signal shifting from 2 to 3 ppm is attributed to residual water.

Compound **4** dissolves in water by virtue of its polar side-chains. In order to investigate the occurrence of self-assembly of **4** in water, either by intermolecular hydrogen bonding or by arene-

arene interactions, variable temperature $^1\text{H-NMR}$ spectra were recorded. The spectrum of **4** in water at 50 °C at high concentrations featured relatively sharp signals (Figure 2.5).³² The ability to detect the amide proton indicates that exchange of this proton with water is slow on the NMR time-scale. Lowering the temperature to 0 °C induces broadening of all signals while small shifts are observed. In contrast to the chloroform spectra, the broadening of the aromatic signals (especially the signal attributed to the central benzene at 8.5 ppm) precedes the broadening of the amide protons. Intriguingly, and in contrast to the chloroform spectra, two signals in a 2:1 ratio are present for the methyl protons at the stereocenter. This chemical shift difference has to originate from a more ordered arrangement of the side chains in water compared to the situation in chloroform. Most probably, the water molecules are coordinating to the oligo(ethylene oxide) side-chains thus inducing an ordered conformation. Lowering of the temperature also gives rise to broadening of the side chain protons, indicating a decrease in freedom for motion.

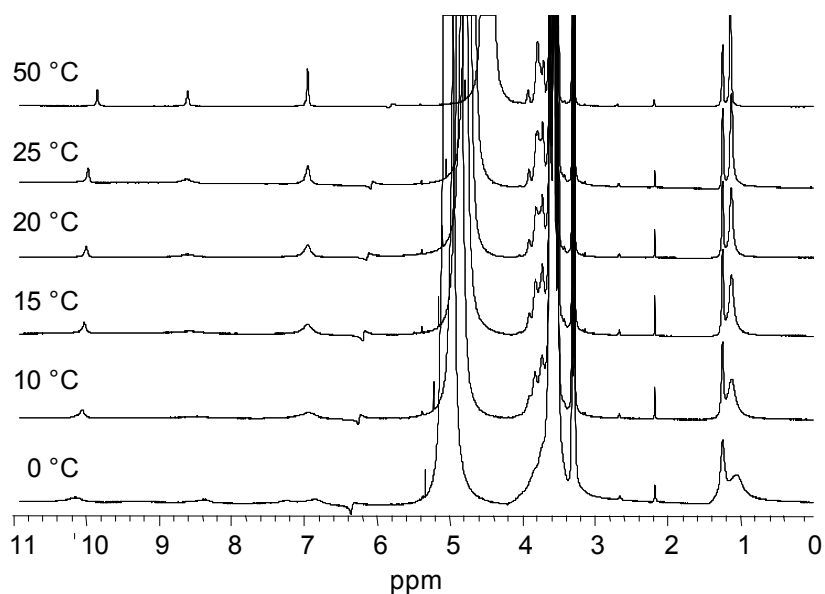


Figure 2.5: $^1\text{H-NMR}$ spectra of **4** in water (~ 100 mg/ml; 35 mM in 90% H_2O , 10% D_2O) at different temperatures. A broadening of the signals, especially of the inner aromatic proton around 8.5 ppm, can be observed upon cooling. The water signal is not suppressed in these measurements, because the high concentration of **4** allows for a facile detection.

In order to investigate the contribution of the intermolecular hydrogen bonding to the association in solution, infrared studies were performed. To allow a more facile detection of the carbonyl stretching vibration, the experiments in water were performed using D_2O . This implies an exchange of the N-H for an N-D and, therefore, all other measurements were also performed on the threefold deuterated compound. The spectra in Figure 2.6 show the carbonyl stretching vibration (amide I band) of **4** in the liquid state, in concentrated deuterium oxide solution and in chloroform solutions of different concentrations. The position of the signals from the neat sample and the

concentrated chloroform sample are similar at 1668 cm^{-1} . Dilution of the chloroform solution results in a shift of the vibration towards 1679 cm^{-1} . This shows that in concentrated chloroform solutions intermolecular hydrogen bonding occurs, similar as in the oil. Upon dilution the hydrogen bonding is destroyed, just as was found upon an increase of the temperature with proton NMR (Figure 2.4). The carbonyl stretching band in deuterium oxide solution is found at a wavelength of 1657 cm^{-1} . This red-shift of the band is somewhat unexpected, because it would in principle indicate stronger hydrogen bonding than in the neat oil. It possibly results, however, from the subtraction of the deuterium oxide signal, giving rise to lowering of the intensity of the signal at the left side.³³ In general, the infrared spectra indicate that in concentrated aqueous and chloroform solution hydrogen bonding exists.

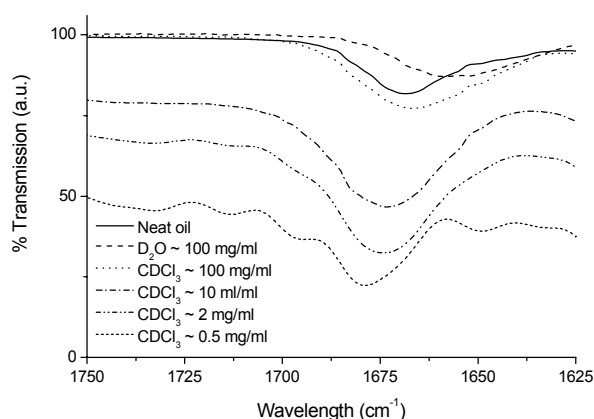


Figure 2.6: IR spectra of **4** as oil and in solution. A change of the carbonyl stretching band upon dilution in chloroform can be observed, indicating loss of intermolecular hydrogen bonding.

2.3.4 Chirality at the supramolecular level

CD spectroscopy measurements on dilute solutions of **4** ($<10^{-3}\text{ M}$) did not reveal any Cotton effect neither in chloroform nor in water for the amide or benzene chromophores, revealing that without the formation of aggregates, no preferred chiral conformation exists for the core of the molecule. The concentrated solutions in both water and chloroform, however, did feature a Cotton effect in the chromophore of the core. A small, but significant effect of $\sim 2\text{ mdeg}$ was found for the aqueous sample and the effect was found to disappear upon heating to $60\text{ }^{\circ}\text{C}$ (Figure 2.7, left), in accordance with the sharpening of the NMR signals upon increasing the temperature. The Cotton effect in chloroform is somewhat stronger ($\sim 10\text{ mdeg}$) and surprisingly, has an opposite sign. Also for this solution the intensity of the Cotton effect decreases upon heating, but an effect remains present up to $60\text{ }^{\circ}\text{C}$ (Figure 2.7, right). Apparently, at high temperatures still some aggregation occurs for this chloroform sample, in line with the NMR signals at $60\text{ }^{\circ}\text{C}$ that are not as sharp as in the molecularly dissolved samples in acetonitrile, methanol or acetone.

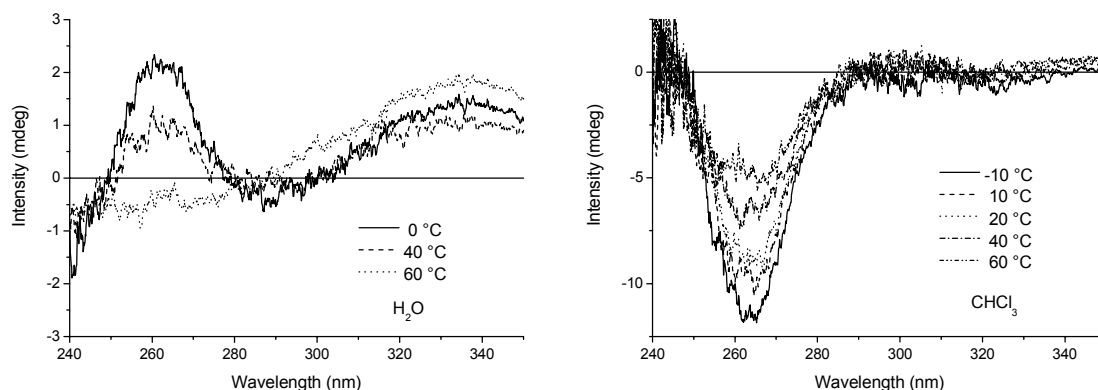


Figure 2.7: CD spectra of **4** in water (left) and chloroform (right) at a concentration of ~ 100 mg/ml (35 mM). The CD band occurs at the same position in both solvents, but has opposite sign.

The inversion of the Cotton effect suggests different processes to be responsible for the formation of the aggregates in water and chloroform.³⁴ The differences observed in the NMR and IR spectra support this idea. In water the aggregation seems to be partly dominated by the non-directional hydrophobic interactions as evidenced by a very small Cotton effect and stronger broadening of the aromatic signals in the NMR spectra. In chloroform hydrogen bonding seems to account for the self-assembly. Sharpening of the amide signal in the proton spectra upon increase of the temperature and loss of hydrogen bonding upon dilution as observed with IR spectroscopy coincide with the loss of the Cotton effect as observed with CD spectroscopy.

2.4 Conclusions

In an apolar solvent threefold intermolecular hydrogen bonding in **2** gives rise to long and stable helical columnar self-assemblies and together with chiral side-chains accounts for a remarkable control of chirality within the column, as one chiral molecule **2** on every 200 molecules **3** suffices to render all columns homochiral. The combination of IR and CD spectroscopy clarified that intermolecular hydrogen bonding is the driving force for both the self-assembly and for the expression of chirality. The results gathered for **2** show that in apolar solvents hydrogen bonding suffices for the creation of helical columns and no additional solvophobic interactions are required.

The aggregation via hydrogen bonding in polar media was studied using compound **4**. However, in polar solvents the solvent interferes with the hydrogen bonding and self-assembly does not longer occur in dilute solution. In chloroform high concentrations are required to allow intermolecular hydrogen bonding of **4** to generate helical columns. At high concentration in water, the aromatic rings of the core self-assemble by hydrophobic interactions, thus allowing intermolecular hydrogen bonding. This difference in superstructure formation between chloroform and water is translated in different CD spectra. On the basis of the results found it can be expected that the

incorporation of additional strong hydrophobic or solvophobic interactions, not unlike those operative in biopolymers, will account for superstructure formation in dilute aqueous solutions. Specific interactions, like hydrogen bonding, then can be expressed in the created hydrophobic environment for the generation of helical structures.

2.5 Experimental section

General. All starting materials were obtained from commercial suppliers and used as received. All moisture-sensitive reactions were performed under an atmosphere of dry argon. Dry and ethanol-free dichloromethane was obtained by distillation from P₂O₅; dry tetrahydrofuran was obtained by distillation from Na/K/benzophenone; dimethylformamide was dried over BaO and triethylamine was dried over potassium hydroxide. Analytical thin layer chromatography was performed on Kieselgel F-254 precoated silica plates. Visualization was accomplished with UV light. Column chromatography was carried out on Merck silica gel 60 (70-230 mesh) or on Merck aluminum oxide 90 (70-230 mesh, activity II-III). Preparative size exclusion chromatography was performed on BIO RAD Bio Beads S-X1 (200-400 mesh) swollen in methylene chloride. ¹H-NMR and ¹³C-NMR spectra were recorded on a 500 MHz NMR (Varian Inova, 500 MHz for ¹H-NMR), on a 400 MHz NMR (Varian Mercury, 400 MHz for ¹H-NMR and 100 MHz for ¹³C-NMR), or on a 300 MHz NMR (Varian Gemini, 300 MHz for ¹H-NMR and 75 MHz for ¹³C-NMR). Proton chemical shifts are reported in ppm downfield from tetramethylsilane (TMS) and carbon chemical shifts in ppm downfield of TMS using the resonance of the deuterated solvent as internal standard. Splitting patterns are designated as s, singlet; bs, broad singlet; d, doublet; t, triplet; q, quartet; dd, double doublet; ddd, double double doublet; dt, double triplet; m, multiplet; quin, quintet. Elemental analyses were carried out using a Perkin Elmer 2400. Matrix assisted laser desorption/ionization mass spectra were obtained using indole acrylic acid as the matrix on a PerSeptive Biosystems Voyager-DE PRO spectrometer. IR-spectra were measured on a Perkin Elmer 1600 FT-IR. Optical properties and melting points were determined using a Jeneval polarization microscope equipped with a Linkam THMS 600 heating device with crossed polarizers. DSC spectra were obtained on a Perkin Elmer Pyris 1 DSC. GC-MS measurements were performed on a Shimadzu GCMS QP5000. UV-Vis spectra were recorded on a Perkin Elmer Lambda 900 UV/VIS/NIR spectrometer. CD spectra were recorded on a Jasco J-600 spectropolarimeter. The syntheses of (2*S*)-ethyl-2-(tetrahydropyran-2-yl-oxy)-propionate (**5**) and (2*S*)-2-(tetrahydropyran-2-yl-oxy)-propan-1-ol (**6**) have been described previously.³⁵⁻³⁷

N,N',N''-Tris((*S*)-3,7-dimethyloctyl)benzene-1,3,5-tricarboxamide (2**).** A solution of (*S*)-3,7-dimethyloctyl amine¹⁸ (0.101 g, 0.64 mmol), benzene-1,3,5-tricarboxylic acid chloride (0.050 g, 0.20 mmol) and triethylamine (0.071 g, 0.70 mmol) in dry THF (20 mL) was stirred overnight at room temperature. After evaporation of the solvent, the compound was purified using column chromatography (silica; 2% ethanol in methylene chloride), to yield the pure product as off-white solid (0.10 g, 0.16 mmol, 80 %): ¹H NMR (CDCl₃) δ = 8.30 (s, 3H), 6.73 (t, *J* = 5.2 Hz, 3H), 3.45 (m, 6H), 1.62 (m, 3H), 1.51 (m, 6H), 1.42 (m, 3H), 1.28 (m, 9H), 1.15 (m, 9H), 0.93 (d, *J* = 6.4 Hz, 9H), 0.86 (d, *J* = 6.4 Hz, 18H); ¹³CNMR (CDCl₃) δ = 165.7, 135.3, 127.9, 39.2, 38.5, 37.1, 36.6, 30.7, 27.9, 24.6, 22.7, 22.6, 19.5; MALDI-TOF [M+Na]⁺ = Calcd. 650.5 Da. Obsd. 651.0 Da.; Anal. Calcd for C₃₉H₆₉N₃O₃ (Mw = 628.00 g/mol): C, 74.59; H, 11.07; N 6.69; Found: C, 74.19; H, 11.30; N, 6.69.

N,N',N''-Tris-{3,4,5-tris[(2*S*)-2-(2-{2-[2-(2-methoxyethoxy)-ethoxy]-ethoxy]-ethoxy)-propyloxy]-phenyl}benzene-1,3,5-tricarboxamide (4**).** A solution of **23** (0.38 g, 0.43 mmol), benzene-1,3,5-tricarboxyl trichloride (0.029 g, 0.11 mmol) and triethylamine (0.03 mL, 0.2 mmol) in dry CH₂Cl₂ (5 mL) was stirred overnight at room temperature. After evaporation of the solvent, the compound was purified using column chromatography (silica; 10 % methanol in chloroform) and preparative size exclusion chromatography (bio-beads S-X1, CH₂Cl₂), to yield the pure product as a colorless oil (0.16 g, 0.057 mmol, 52 %): ¹H NMR (CDCl₃) δ = 8.95 (bs, 3H), 7.38 (bs, 6H), 5.94 (bs, 3H), 4.05 (m, 9H), 3.95-3.49 (m, 162H), 3.37 (s, 18H), 3.32 (s, 9H), 1.31 (d, 27H).

(2*S*)-1-Benzyloxy-2-(tetrahydropyran-2-yl-oxy)-propane (7**).** A solution of *t*-BuOK (78.5 g, 0.70 mol) in *t*-butanol (570 g) was added dropwise to **6**. The solution was stirred for 2 h, concentrated and subsequently diluted with dioxane (400 mL). A catalytic amount of tetrabutylammonium chloride (2 g) was added after which benzyl chloride (88.6 g, 0.70 mol) was added dropwise at room temperature. The mixture was heated at 80°C overnight. After reaction, water was added and the mixture was extracted with diethylether (3 times). The organic layers were combined and back-washed with water and brine, subsequently dried over magnesium sulfate and concentrated *in vacuo* leaving a yellow oil. Distillation (118°C, 5·10⁻² mbar) gave the pure title compound as a colorless oil (99.3 g, 0.40 mol, 64%): ¹H NMR (CDCl₃) δ = 7.40-7.20 (m, 5H), 4.78 (dd, 1H), 4.56 (d, 2H), 4.07-3.90 (m, 2H), 3.62-3.42 (m, 3H), 1.90-1.80 (m, 1H), 1.80-1.68 (m, 1H), 1.65-1.50 (m, 4H), 1.27-1.15 (m, 3H); ¹³C NMR (CDCl₃) δ = 138.5, 138.4, 128.3, 128.2, 127.5, 127.4, 127.4, 98.8, 96.1, 74.3, 74.2, 73.2, 73.1, 71.9, 70.4, 62.7, 62.2, 31.0, 31.0, 25.5, 19.9, 19.5, 18.6, 16.6.

(2*S*)-1-Benzyloxy-propan-2-ol (8**).** To an ice cooled solution of **7** (98 g, 0.39 mol) in methanol (500 mL) was added *p*-TsOH·H₂O (3 g, 18 mmol). The solution was subsequently stirred at room temperature overnight.

Excess NaHCO₃ was added to quench the reaction. The methanol was evaporated and additional coevaporation with methanol was performed to remove all THP products. Water/diethylether extraction, drying of the collected organic layers with magnesium sulfate and evaporation of the solvent gave the crude yellow product. Distillation (91°C, 8·10⁻¹ mbar) gave pure **8** as a colorless oil (56.0 g, 0.34 mol, 86%): ¹H NMR (CDCl₃) δ = 7.37-7.24 (m, 5H), 4.54 (s, 2H), 4.00-3.95 (m, 1H), 3.46-3.25 (m, 2H), 1.13 (d, 3H); ¹³C NMR (100 MHz, CDCl₃) δ = 137.9, 128.4, 127.7 (2x), 75.8, 73.2, 66.4, 18.6.

2-(2-Methoxyethoxy)-ethyl *p*-tosylate (9). NaOH (48.0 g, 1.20 mol) and 2-(2-methoxy-ethoxy)-ethanol (100 g, 0.83 mol), in a two-phase system of water (230 mL) and THF (120 mL) were cooled via an ice-bath with magnetic stirring. *p*-Toluenesulfonyl chloride (174 g, 0.91 mol) dissolved in THF (240 mL) was added dropwise to the mixture, while maintaining the temperature below 5°C. The solution was stirred at 0°C for another 3 h and then poured into ice-water (500 mL). The mixture was extracted with CH₂Cl₂ (3 x 500 ml) and the combined organic layers were washed with water (pH = 1) (2x) and with brine (1x). After drying over MgSO₄, the solvent was evaporated *in vacuo* to yield pure **9** as a colorless oil (214 g, 0.78 mol, 94%): ¹H NMR (CDCl₃) δ 7.79 (d, 2H), 7.35 (d, 2H), 4.15 (t, 2H), 3.68 (t, 2H), 3.54 (t, 2H), 3.46 (t, 2H), 3.33 (s, 3H), 2.44 (s, 3H); ¹³C NMR (CDCl₃) δ 144.6, 132.7, 129.5, 128.0, 71.6, 70.4, 69.1, 68.4, 58.8, 21.4.

2-{2-[2-(2-Methoxyethoxy)-ethoxy]-ethoxy}-ethyl *p*-tosylate (10). A mixture of NaOH (9.9 g, 0.25 mol) and 2-{2-[2-(2-methoxy-ethoxy)-ethoxy]-ethoxy}-ethanol (36.0 g, 0.173 mol), in a two-phase system of water (50 mL) and THF (400 mL) was cooled via an ice-bath with magnetic stirring. *p*-Toluenesulfonyl chloride (36.2 g, 0.190 mol) in tetrahydrofuran (50 mL) was added dropwise to the mixture, while maintaining the temperature below 5°C. The solution was stirred at 0°C for another 3 h and then poured into ice-water (100 mL). The mixture was extracted with methylene chloride (3 x 100 mL) and the combined organic layers were washed with water (pH = 1) (2x) and with brine (1x). After drying over magnesium sulfate, the solvent was evaporated *in vacuo* to yield the pure compound as a colorless oil (60.7 g, 0.167 mol, 97%): ¹H NMR (CDCl₃) δ = 7.79 (d, 2H), 7.35 (d, 2H), 4.15 (t, 2H), 3.68 (t, 2H), 3.67-3.58 (m, 10H), 3.54 (t, 2H), 3.36 (s, 3H), 2.44 (s, 3H); ¹³C NMR (CDCl₃) δ = 144.6, 132.7, 129.5, 128.0, 71.8, 70.6 (2x), 70.4 (2x), 70.3, 69.1, 68.5, 58.8, 21.4.

(2S)-1-Benzyloxy-2-[2-(2-methoxyethoxy)-ethoxy]-propane (11). A solution of **8** (30.0 g, 0.180 mol), **9** (70.0 g, 0.255 mol) and KOH (40.0 g, 0.606 mol) in THF (400 mL) was stirred under reflux for 12 h under an argon atmosphere. Subsequently water (50 mL) was added to hydrolyze excess **9** to the corresponding alcohol. H₂O/CH₂Cl₂ extraction, drying of the collected CH₂Cl₂ layers with magnesium sulfate and evaporation of the solvent gave the crude yellow product. Distillation (120°C, 8 x 10⁻² mbar) gave pure **11** as a colorless oil (27.1 g, 0.101 mol, 56%): ¹H NMR (CDCl₃) δ 7.35-7.20 (m, 5H), 4.53 (d, 2H), 3.72-3.65 (m, 3H), 3.65-3.48 (m, 4H), 3.54-3.38 (m, 4H), 3.35 (s, 3H), 1.15 (d, 3H); ¹³C NMR (CDCl₃) δ 138.3, 128.3, 127.9, 127.5, 75.0, 73.9, 73.1, 71.8, 70.7, 68.4, 58.9, 17.1.

(2S)-1-Benzyloxy-2-(2-{2-[2-(2-methoxyethoxy)-ethoxy]-ethoxy}-ethoxy)-propane (12). A solution of **8** (19.9 g, 0.120 mol), **10** (50.0 g, 0.138 mol) and KOH (26.6 g, 0.404 mol) in tetrahydrofuran (350 mL) was stirred under reflux for 12 h under an argon atmosphere. Subsequently water (50 mL) was added to hydrolyze the excess of **10** to the corresponding alcohol. Water/diethylether extraction, drying of the collected organic layers with magnesium sulfate and evaporation of the solvent gave the crude yellow product. Distillation with kugelrohr (225°C, 5×10⁻² mbar) gave the pure title compound as a colorless oil (37.6 g, 0.105 mol, 88%): ¹H NMR (CDCl₃) δ = 7.35-7.22 (m, 5H), 4.53 (d, 2H), 3.71-3.37 (m, 19H), 3.35 (s, 3H), 1.15 (d, 3H); ¹³C NMR (CDCl₃) δ = 138.3, 128.3, 127.5, 127.4, 75.0, 74.0, 73.2, 71.8, 70.8, 70.5 (4x), 70.4, 68.5, 59.0, 17.2.

1-Benzyloxy-2-(2-{2-[2-(2-methoxyethoxy)-ethoxy]-ethoxy}-ethoxy)-ethane (13). Tetraethylene glycol monomethyl ether (15.00 g, 72 mmol), 2-benzyloxy-ethane-1-*p*-tosylate (27.68 g, 86 mmol) and KOH (18.37 g, 287 mmol) were heated under reflux in THF (200 mL). After 4 h the reaction mixture was poured in ice water and extracted with CH₂Cl₂ (3 x 75 mL). The combined organic layers were washed with brine (1x), dried over MgSO₄ and evaporated *in vacuo*. The crude product was purified by column chromatography (flash silica, starting with 100% chloroform and gradually increasing the polarity to 5% methanol in chloroform) to yield the pure compound as a colourless oil (22.59 g, 68 mmol, 94%): ¹H NMR (CDCl₃) δ = 7.34 (m, 5H), 4.57 (s, 2H), 3.70-3.62 (m, 20H), 3.37 (s, 3H); ¹³C NMR (CDCl₃) δ = 138.2, 128.3, 128.1, 127.5, 73.2, 70.6-69.4, 58.9. Anal. Calcd for C₁₈H₃₀O₆ (Mw = 342.43 g/mol): C, 63.14; H, 8.83; Found: C, 63.51; H, 8.99.

(2S)-2-[2-(2-Methoxyethoxy)-ethoxy]-propan-1-ol (14). The benzyl protected precursor **11** (26.0 g, 0.097 mol) was dissolved in ethanol (100 mL) and acidified with conc. HCl (0.1 mL). A catalytic amount of Pd/C

(10%) was added to the solution and hydrogenation at 50 psi H₂-overpressure was carried out during 4 h. Filtration and evaporation of the solvents gave pure **14** as a colorless oil (17.0 g, 0.095 mol, 98%): ¹H NMR (CDCl₃) δ 3.85-3.78 (m, 1H), 3.69-3.62 (m, 4H), 3.61-3.52 (m, 5H), 3.49-3.43 (m, 1H), 3.36 (s, 3H), 1.12 (d, 3H); ¹³C NMR (CDCl₃) δ 76.7, 71.7, 70.6, 70.2, 67.9, 66.0, 58.8, 16.0; [α]_D²⁰ +13.3 ° (neat).

(2S)-2-(2-{2-[2-(2-Methoxyethoxy)-ethoxy]-ethoxy}-ethoxy)-propan-1-ol (15). The benzyl protected precursor **12** (37.0 g, 0.104 mol) was dissolved in ethanol (96%) (100 mL) and acidified with hydrochloric acid (0.1 mL, 37%). A catalytic amount of Pd/C (10%) was added to the solution and hydrogenation at 50 psi H₂-pressure was carried out during 4 h. Filtration, evaporation of the solvents and distillation with kugelrohr (175°C, 5·10⁻² mbar) gave the pure title compound as a colorless oil (26.4 g, 0.099 mol, 95%): ¹H NMR (CDCl₃) δ = 3.85-3.78 (m, 1H), 3.69-3.43 (m, 18H), 3.36 (s, 3H), 2.99 (bs, 1H) 1.12 (d, 3H); ¹³C NMR (CDCl₃) δ = 76.7, 71.8, 70.7, 70.5 (4x), 70.4, 68.0, 66.2, 58.9, 16.2. [α]_D²⁰ (c = 0.88; chloroform) = + 13.3°.

2-(2-{2-[2-(2-Methoxyethoxy)-ethoxy]-ethoxy}-ethoxy)-ethan-1-ol (16). To a solution of **13** (21.72 g, 63 mmol) in ethanol (25 mL) and a trace of acetic acid a catalytic amount of Pd/C (10%) was added. The suspension was shaken mechanically for 3 h under an H₂-atmosphere of 50 psi and then filtered off. The filtrate was evaporated *in vacuo* to yield the product as a colourless oil (14.41 g, 57 mmol, 90%): ¹H NMR (CDCl₃) δ = 3.75-3.55 (m, 20H), 3.37 (s, 3H), 2.53 (s, 1H); ¹³C NMR (CDCl₃) 70.9-69.3, 58.7.

(2S)-2-(2-{2-[2-(2-Methoxyethoxy)-ethoxy]-ethoxy}-ethoxy)-propyl-1-*p*-tosylate (17). NaOH (0.92 g, 0.023 mol) and **15** (4.0 g, 0.015 mol), in a two-phase system of water (4 mL) and tetrahydrofuran (4 mL) were cooled via an ice-bath with magnetic stirring. *p*-Toluenesulfonyl chloride (3.3 g, 0.017 mol) in tetrahydrofuran (4 mL) was added dropwise to the mixture, while maintaining the temperature below 5°C. The solution was stirred at 0°C for another 3 h and then poured into ice-water (25 mL). The mixture was extracted with methylene chloride (3 x 25 mL) and the combined organic layers were washed with water (pH = 1) (2x) and with brine (1x). After drying over magnesium sulfate, the solvent was evaporated *in vacuo* to yield the pure compound as a colorless oil (5.7 g, 0.013 mol, 89%): ¹H NMR (CDCl₃) δ = 7.81 (d, 2H), 7.36 (d, 2H), 4.00-3.88 (m, 2H), 3.70-3.50 (m, 17H), 3.36 (s, 3H), 2.45 (s, 3H), 1.14 (d, 3H); ¹³C NMR (CDCl₃) δ = 144.5, 132.7, 129.6, 127.7, 73.4, 72.5, 71.8, 70.6, 70.5 (2x), 70.4 (3x), 68.8, 58.9, 21.6, 16.7.

Methyl 3,4,5-tris[(2S)-2-(2-{2-[2-(2-methoxyethoxy)-ethoxy]-ethoxy}-ethoxy)-propoxy]-benzoate (18). A mixture of **17** (5.60 g, 13.3 mmol), methyl 3,4,5-trihydroxybenzoate (0.73 g, 4.0 mmol) and K₂CO₃ (5.5 g, 40 mmol) in dimethyl formamide (40 mL) was stirred overnight at 70°C. After cooling, the mixture was poured into water (200 mL, pH = 2) and extracted with methylene chloride. The organic layer was washed with water (3x) and brine (1x), dried over magnesium sulfate and the solvent was evaporated *in vacuo*. The crude product was purified by column chromatography (alumina; 1% ethanol in methylene chloride) to yield pure **18** as a viscous colorless oil (2.9 g, 3.1 mmol, 78%): ¹H NMR (CDCl₃) δ = 7.30 (s, 2H), 4.12-4.05 (m, 3H), 3.98-3.85 (m, 6H), 3.89 (s, 3H), 3.84-3.50 (m, 48H), 3.37 (s, 3H), 3.36 (s, 6H), 1.32 (m, 9H); ¹³C NMR (CDCl₃): δ= 166.6, 152.2, 142.0, 124.9, 108.2, 76.3, 75.0, 74.3, 72.6, 71.9, 70.8, 70.5, 70.4, 68.8, 68.5, 59.0, 52.2, 17.5.

3,4,5-Tris[(2S)-2-(2-{2-[2-(2-methoxyethoxy)-ethoxy]-ethoxy}-ethoxy)-propoxy]-benzoic acid (19). A solution of **18** (2.80 g, 3.0 mmol) and KOH (85%) (0.53 g, 9.0 mmol) in ethanol (20 mL) and water (20 mL) was heated under reflux overnight. Subsequently, the solution was acidified to pH = 2 with conc. hydrochloric acid under reflux and then the solution was poured onto an water/ice mixture. The aqueous layer was extracted with methylene chloride (2x). The combined organic layers were washed with brine (pH = 2), dried over magnesium sulfate and evaporation of the solvent *in vacuo*, afforded pure **19** as a colorless oil (2.7 g, 2.95 mmol, 98%): ¹H NMR (CDCl₃) δ = 7.33 (s, 2H), 4.12-4.05 (m, 3H), 3.98-3.88 (m, 9H), 3.86-3.53 (m, 45H), 3.38 (s, 3H), 3.37 (s, 6H), 1.32 (m, 9H); ¹³C NMR (CDCl₃) δ = 168.9, 152.0, 142.3, 124.5, 108.6, 76.0, 74.9, 74.2, 72.5, 71.7, 70.7, 70.6, 70.4, 70.3, 70.2, 68.7, 68.4, 58.8, 17.3.

2-(2-{2-[2-(2-Methoxyethoxy)-ethoxy]-ethoxy}-ethoxy)-ethyl-1-*p*-tosylate (20). A solution of *p*-toluenesulfonyl chloride (13.07 g, 69 mmol) in THF (25 mL) was added dropwise to a stirred 2-phase system of NaOH (2.28 g, 57 mmol) in water (25 mL) and **16** (14.41 g, 57 mmol) in THF (25 mL), while the temperature was kept below 5°C. Subsequently the temperature was kept at 0°C and stirring was continued for another 3 h after which the reaction mixture was poured into ice water. The mixture was extracted with CH₂Cl₂ (3 x 50 mL) and the combined organic layers were washed with 1 M HCl (2 x 50 mL) and brine (75 mL). Drying over MgSO₄ and evaporating the solvent *in vacuo* yielded the crude product. Purification by column chromatography (flash-silica, starting with 100% chloroform and increasing the polarity to 5% methanol in chloroform) yielded

the pure compound as a colourless oil (14.58 g, 36 mmol, 63%): ^1H NMR (CDCl_3) δ = 7.81 (d, 2H), 7.34 (d, 2H), 4.13 (t, 2H), 3.70-3.53 (m, 18H), 3.38 (s, 3H), 2.45 (s, 3H); ^{13}C NMR (CDCl_3) δ = 144.3, 133.4, 129.7, 128.2, 72.3-69.4, 58.6, 22.5; IR (ATR): ν = 2872, 1598, 1452, 1176, 1096, 1018, 920, 817; Anal. Calcd for $\text{C}_{18}\text{H}_{30}\text{O}_8\text{S}$ (Mw = 406.57 g/mol): C, 53.18; H, 7.43; Found: C, 52.78; H, 7.39.

Methyl 3,4,5-tris[2-(2-{2-[2-(2-methoxyethoxy)-ethoxy]-ethoxy}-ethoxy)-ethoxy]-benzoate (21). A mixture of **20** (10.0 g, 20.5 mmol), methyl 3,4,5-trihydroxybenzoate (1.25 g, 6 mmol) and K_2CO_3 (10.2 g, 74 mmol) was stirred for 6 h at 70 °C in dry DMF (50 mL). The reaction mixture was poured in water (120 mL) and extracted with CH_2Cl_2 (3 x 75 mL). The combined organic layers were washed with brine (1 x 75 mL), dried over MgSO_4 and evaporated *in vacuo*. The crude product was purified by column chromatography (alumina, 1% ethanol in chloroform) affording the pure compound (4.76 g, 5.4 mmol, 86%): ^1H NMR (CDCl_3) δ = 7.30 (s, 2H), 4.21 (t, 4H), 4.19 (t, 2H), 3.89 (s, 3H), 3.86 (t, 4H), 3.79 (t, 2H), 3.73-3.52 (m, 48H), 3.38 (s, 9H); ^{13}C NMR (CDCl_3) δ = 166.5, 152.2, 142.5, 124.9, 108.9, 72.3-68.8, 58.9, 52.1; IR (ATR): ν = 2869, 1717, 1586, 1333, 1214, 1100, 852.

3,4,5-Tris[2-(2-{2-[2-(2-methoxyethoxy)-ethoxy]-ethoxy}-ethoxy)-ethoxy]-benzoic acid (22). A solution of **21** (2.93 g, 3.3 mmol) and KOH (0.56 g, 10 mmol) in ethanol (20 mL) and water (20 mL) was heated under reflux overnight. Subsequently, the solution was acidified to pH=2, cooled and extracted with CH_2Cl_2 (3 x 25 mL). The CH_2Cl_2 layer was washed with brine. Drying over MgSO_4 , evaporating *in vacuo* and drying over P_2O_5 afforded the pure compound (2.80 g, 3.2 mmol, 97%): ^1H NMR (CDCl_3) δ = 7.38 (s, 2H), 4.22 (t, 4H), 4.20 (t, 2H), 3.86 (t, 4H), 3.80 (t, 2H), 3.77-3.54 (m, 48H), 3.38 (s, 9H); ^{13}C NMR (CDCl_3) δ = 168.2, 152.0, 142.5, 124.7, 109.3, 72.3-68.8, 58.9; IR (ATR): 3507, 2870, 1713, 1586, 1429, 1324, 1201, 1099, 851.

3,4,5-Tris[(2S)-2-(2-{2-[2-(2-methoxyethoxy)-ethoxy]-ethoxy}-ethoxy)-propyloxy]-aniline (23). To a solution of **19** (0.50 g, 0.55 mmol) and two drops of dry DMF in CH_2Cl_2 (5 mL) oxalyl chloride (0.06 mL, 0.66 mmol) was added. The mixture was stirred overnight at room temperature in the absence of light and subsequently, the solvent was removed by evaporation *in vacuo* and the compound was dried under vacuum (1 mbar) for 2 h. The oil was dissolved in THF (3 mL) and added dropwise to a solution of sodium azide (0.40 g, 6.2 mmol) in water (3 mL) at 0 °C. After stirring for another 0.5 h at room temperature, the solution was extracted with CH_2Cl_2 . The organic layer was dried over MgSO_4 and filtered. Subsequent evaporation of the solvent *in vacuo* yielded a colored oil which was dissolved in dioxane (15 mL) and heated under reflux for 30 min. After cooling to 80 °C, the solution was added dropwise to a solution of Bu_4NOH (40 wt.% in water, 0.8 mL) in dioxane (15 mL) at 90 °C. After stirring for 15 min at 90 °C the solution was cooled and extracted with CH_2Cl_2 . The solution was dried using Na_2SO_4 and after filtration the solvent was evaporated *in vacuo*. The crude product was purified using column chromatography (silica, 5% methanol in CH_2Cl_2) to yield X as a light yellow oil (0.38 g, 0.43 mmol, 78%): ^1H NMR (CDCl_3) δ = 5.92 (s, 2H), 3.95 (m, 3H), 3.85-3.52 (m, 54H), 3.36 (s, 9H), 1.26 (d, 9H); ^{13}C NMR (CDCl_3) δ = 153.0, 142.8, 130.4, 94.5, 76.6, 74.9, 72.6, 72.4, 72.3, 71.8, 70.7 (2x), 70.5 (2x), 70.4, 68.7, 68.4, 58.9, 17.7, 17.5.

2.6 References and notes

- ¹ Brunsveld, L.; Folmer, B.J.B.; Meijer, E.W.; Sijbesma, R.P. *Chem. Rev.* in preparation.
- ² Fuhrhop, J.-H.; Demoulin, C.; Boettcher, C.; Köning, J.; Siggel, U. *J. Am. Chem. Soc.* **1992**, *114*, 4159-4165.
- ³ Gallivan, J.P.; Schuster, G.B. *J. Org. Chem.* **1995**, *60*, 2423-2429.
- ⁴ Gottarelli, G.; Spada, G.P.; Garbesi, A. in *Comprehensive Supramolecular Chemistry*, ed. Lehn, J.-M. Pergamon Press, Oxford, UK, **1996**, *9*, 483-506.
- ⁵ Palmans, A.R.A.; Vekemans, J.A.J.M.; Havinga, E.E.; Meijer, E.W. *Angew. Chem. Int. Ed. Engl.* **1997**, *36*, 2648-2651.
- ⁶ Nuckolls, C.; Katz, T.J. *J. Am. Chem. Soc.* **1998**, *120*, 9541-9544.
- ⁷ Engelkamp, H.; Middelbeek, S.; Nolte, R.J.M. *Science* **1999**, *284*, 785-788.
- ⁸ Fox, J.M.; Katz, T.J.; van Elshocht, S.; Verbiest, T.; Kauranen, M.; Persoons, A.; Thongpanchang, T.; Krauss, T.; Brus, L. *J. Am. Chem. Soc.* **1999**, *121*, 3453-3459.
- ⁹ Hirschberg, J.H.K.K.; Brunsveld, L.; Ramzi, A.; Vekemans, J.A.J.M.; Sijbesma, R.P.; Meijer, E.W. *Nature* **2000**, *407*, 167-170.
- ¹⁰ Brunsveld, L.; Zhang, H.; Glasbeek, M.; Vekemans, J.A.J.M.; Meijer, E.W. *J. Am. Chem. Soc.* **2000**, *122*, 6175-6182.
- ¹¹ Brunsveld, L.; Schenning, A.P.H.J.; Broeren, M.A.C.; Janssen, H.M.; Vekemans, J.A.J.M.; Meijer, E.W. *Chem. Lett.* **2000**, 292-293.
- ¹² Kimura, M.; Muto, T.; Takimoto, H.; Wada, K.; Ohta, K.; Hanabusa, K.; Shirai, H.; Kobayashi, N. *Langmuir* **2000**, *16*, 2078-2082.
- ¹³ Yasuda, Y.; Takebe, Y.; Fukumoto, M.; Inada, H.; Shirota, Y. *Adv. Mater.* **1996**, *8*, 740-741.
- ¹⁴ Yasuda, Y.; Iishi, E.; Inada, H.; Shirota, Y. *Chem. Lett.* **1996**, 575-576.
- ¹⁵ Hanabusa, K.; Kawakami, A.; Kimura, M.; Shirai, H. *Chem. Lett.* **1997**, 191-192.
- ¹⁶ Hanabusa, K.; Koto, C.; Kimura, M.; Shirai, H.; Kakehi, A. *Chem. Lett.* **1997**, 429-430.
- ¹⁷ Lightfoot, M.P.; Mair, F.S.; Pritchard, R.G.; Warren J.E. *Chem. Commun.* **1999**, 1945-1946.
- ¹⁸ For the synthesis of (S)-3,7-dimethyloctylamine: Schenning, A.P.H.J. *manuscript in preparation*.
- ¹⁹ Matsunaga, Y.; Miyajima, N.; Nakayasu, Y.; Sakai, S.; Yonenaga, M. *Bull. Chem. Soc. Jpn.* **1988**, *61*, 207-210.
- ²⁰ Moore, J.S.; Gorman, C.B.; Grubbs, R.H. *J. Am. Chem. Soc.* **1991**, *113*, 1704-1712.
- ²¹ Schlitzer, D.S.; Novak, B.M. *J. Am. Chem. Soc.* **1998**, *120*, 2196-2197.
- ²² Green, M.M.; Reidy, M.P.; Johnson, R.D.; Darling, G.; O'Leary, D.J.; Wilson, G. *J. Am. Chem. Soc.* **1989**, *111*, 6452-6454.
- ²³ Raszka, M.; Kaplan, N.O. *Proc. Nat. Acad. Sci. USA*, **1972**, *69*, 2025-2029.
- ²⁴ Nakano, N.I.; Igarashi, S.J. *Biochemistry*, **1970**, *9*, 577-583.
- ²⁵ Beijer, F.H. *Ph.D. thesis*, Eindhoven University of Technology **1998**.
- ²⁶ Creighton, T.E. *Proteins, structures and molecular properties*; W.H. Freeman and Company: New York, **1984**.
- ²⁷ *Prediction of protein structure and the principles of protein conformation*; Fasman, G.D. Eds.; Plenum Press: New York, **1990**.
- ²⁸ Part of the side groups discussed here are used for the synthesis of other structures, see chapters 3, 5 and 6.
- ²⁹ Janssen, H.M. *Ph.D. thesis*, Eindhoven University of Technology **1997**.
- ³⁰ Palmans, A.R.A.; Vekemans, J.A.J.M.; Fischer, H.; Hikmet, R.A.; Meijer, E.W.; *Chem. Eur. J.* **1997**, *3*, 300-307.
- ³¹ For details concerning the synthetic approach to transform a benzoic acid into a benzamine see: Pieterse, K. *Ph.D. thesis*, Eindhoven University of Technology *in preparation*.
- ³² An increase of the temperature to 75 °C accounts for a phase separation of **4** with the solvent. This feature is due to the LCST of PEO in water: Bailey, F. Jr.; Koleske, J. *Poly (Ethylene Oxide)* Academic Press Inc., New York, **1976**.
- ³³ Another indication for this comes from the lower relative intensity when compared with other bands, such as the amide II band.
- ³⁴ It should be noted that inversion of the Cotton effect upon changes in solvent polarity has been observed before, see for example: Peeters, E. *Ph.D. thesis*, chapter 5, Eindhoven University of Technology **2000** and references therein. Such behavior may result from a difference in how the side chains are solvated in different solvents.
- ³⁵ Perkins, M.V.; Kitching, W.; König, W.A.; Drew, R.A.I. *J. Chem. Soc. Perkin Trans. 1* **1990**, 2501-2506.

- ³⁶ Cowie, J.M.G.; Hunter, H.W. *Makromol. Chem.* **1990**, *191*, 1393-1401.
- ³⁷ Chiellini, E.; Galli, G.; Carrozzino, S. *Macromolecules* **1990**, *23*, 2106-2112.

Chapter 3

Hierarchical growth of helical columns in alcohols and water

Abstract: *An extended core C_3 -symmetrical hydrogen-bonded disc-shaped molecule having nine chiral peripheral penta(ethylene oxide) side chains assembles stepwise into helical columns in water and lower alcohols. This occurs in a reversible and hierarchical fashion. Specific and subtle solvent-molecule interactions within the created hydrophobic micro-environment account for an unprecedented stabilization of a preferred handedness of the helical stacks due to cooperative intermolecular interactions. The presence or absence of chirality at the supramolecular level can be tuned by temperature and solvent as judged from circular dichroism spectroscopy. In *n*-butanol, strong amplification of chirality occurs due to the existence of highly ordered, helical columns. One chiral seed molecule suffices to render a column of 400 molecules homochiral. In water, the positional order of the molecules is less pronounced, one chiral seed molecule rendering only 12 molecules homochiral. On the other hand, columns of stacked discs remain present in water also at elevated temperatures, whereas in alcohols a very strong temperature dependency exists, which allows for the creation of small oligomers as well as supramolecular polymers consisting of over 1000 molecules. The hierarchical nature of the formation of these columnar polymers in both water and *n*-butanol is discussed in depth.*

3.1 Introduction

Remarkable control of chirality in supramolecular architectures is achieved by cooperative hydrogen bonding^{1,2} often in combination with π - π stacking.³⁻⁵ It has been shown frequently that chirality present in the solubilizing side-chain of a (macro)molecule can be brought to expression at the next hierarchical level of organization by inducing a preference for one “supramolecular” conformation.^{4,6-15} Most of these studies to transfer chiral information through well-defined molecular assemblies are carried out in aprotic organic media, due to the difficulty of bringing the ensemble of secondary interactions to expression in protic media. As a result, multi-molecular architectures of synthetic, chiral structures in protic media are poorly controlled due to the undefined hydrophobic interactions and/or the weakness of cooperative interactions.¹⁶ This is primarily due to the lack of directional bonding patterns, like hydrogen bonding, in protic media.¹⁷ For natural proteins^{18,19} and (synthetic) foldamers²⁰⁻²² it is known that the stabilization of their supramolecular structure (i.e. their native fold) in polar solvents involves a variety of forces. Hydrophobicity has generally been considered the main driving force for the collapse of the random coil, whereas the well-defined 3-D structure is accounted for by specific interactions such as hydrogen bonding, arene-cation and dipole-dipole interactions. These specific interactions only arise after creation of a hydrophobic domain in the protein, while for the random coil conformation of a polypeptide solvation of hydrogen bond donors and acceptors by water occurs. Therefore, synthetic compounds large enough to create hydrophobic micro-domains, capable of shielding the more sensitive polar interactions from the protic solvent,²³⁻³² should allow the expression of all secondary interactions in a cooperative way and the study of their individual contributions to the formation of chiral superstructures. With this type of synthetic structures it should be feasible to bridge the gap between man-made “simple” architectures and biomacromolecules and to create new functional systems.³³ Moreover, their properties will serve to understand the distinct differences between superstructure formation in apolar and in polar media.

For multi-molecular assemblies in protic solvents, like chromonics in water, detailed information concerning the conformational uniqueness of the self-assembled state is scarce.³⁴ It has been shown, however, that chromonics aggregate in an isodesmic fashion, not forming chiral architectures by cooperative interactions. Recently it was shown that α,ω -di-substituted sexithiophenes possess one unique chiral self-assembled state in *n*-butanol that dissociates without passing an intermediate disordered state of aggregation.³⁵ It was, however, shown that for the folding of a series of oligo(*m*-phenylene ethynylene)s, a two-state process occurs, where first a folded non-chiral state appears before a unique helical conformation is obtained.⁷ The hierarchical folding is due to a stepwise occurrence of consecutive interactions; first a hydrophobic collapse of the backbone takes place followed by a structuring process in which the backbone becomes ordered together with the side-chains. Most probably the latter process results in a much smaller gain in energy than the hydrophobic collapse.

For C_3 -symmetrical disc-shaped molecule **1** (Figure 3.1) it has been shown previously that intramolecular hydrogen bonding favors planarity of the individual wedges and helps to create chiral columnar aggregates in dilute alkane solutions in a highly cooperative fashion.⁴ The homochiral side chains give preference to one helicity in the stacks of these columns, the cooperativity length of which is 80 molecules long as determined by “Sergeant-and-Soldiers” experiments.³⁶ The expression of supramolecular chirality is due to positional locking of the molecules that accompanies the self-assembly; such a process is generally observed for supramolecular architectures in apolar media. Here, it is demonstrated that chiral columnar aggregates can be formed in polar, protic media (water, alcohols) when (chiral) penta(ethylene oxide) side chains are present at the periphery of the hydrogen-bonded extended core. In addition, remarkable and pronounced hierarchical growth of the self-assembly is shown; first aggregation occurs, before fine-structuring interactions become operative. This sharply contrasts with the self-assembly of **1** in apolar solvents⁴ and with aggregation in apolar solvents in general. Thus, C_3 -symmetrical discs **2** and **3** are designed to ensure solubility in protic, polar solvents and enabling elucidation of the individual contributions of the secondary interactions (Figure 3.1). By locating the stereochemical information in the side-chains of **2** as close as possible to the core of the disc, the most favorable interactions of the side-chains were guaranteed. In this chapter first the hierarchical self-assembly in alcohols (section 3.2) will be discussed, followed by the amplification of chirality within the columnar stacks in *n*-butanol and the determination of their column length (section 3.3). The self-assembly and amplification of chirality in water will be discussed in section 3.4.

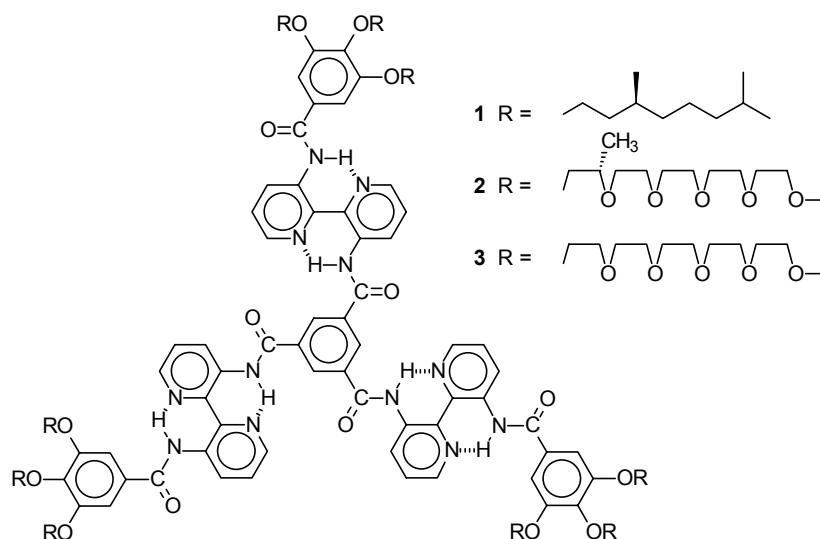
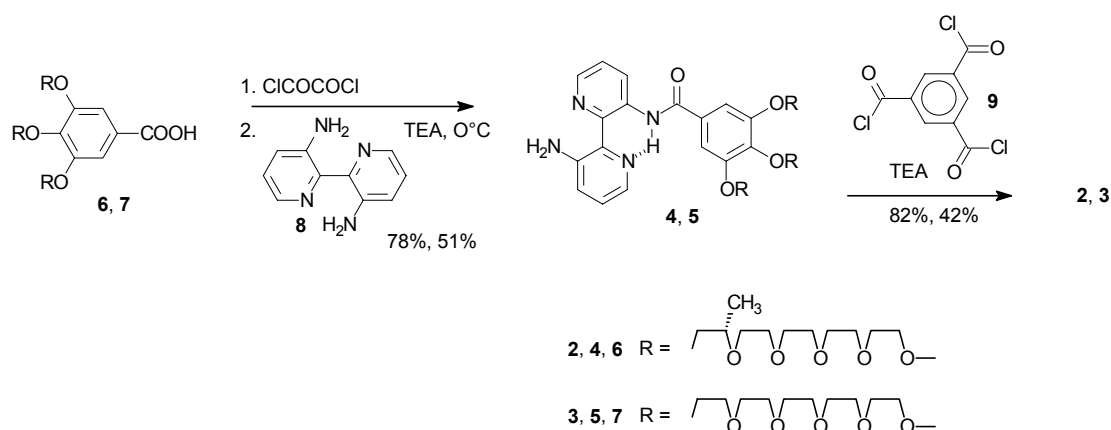


Figure 3.1: C_3 -symmetrical discotics **1**, **2** (chiral) and **3** (achiral).

3.2 Hierarchical self-assembly in *n*-butanol

3.2.1. Synthesis and characterization

The synthesis of **2** and **3** is based on the consecutive selective acylation of the two amino groups of 2,2'-bipyridine-3,3'-diamine (**8**).³⁷ Equimolar reaction of **8** with the acid chlorides of mesogen molecules **6** and **7** at 0 °C affords mono-*N*-acylated bipyridines **4** and **5** with a remarkable selectivity of 98%. Subsequent threefold reaction of **4** or **5** with trimesic chloride (**9**) gives target compounds **2** and **3** in an overall yield of 65% and 21% from **6** and **7**, respectively (Scheme 3.1). Extensive molecular characterization of all compounds is in full agreement with the structures assigned. The characteristic hydrogen-bonded N-H protons in **2** and **3** are observed at $\delta = 15.5$ (interior) and $\delta = 14.4$ ppm (exterior) in CDCl₃, indicative of the strong hydrogen-bonding within the bipyridine unit. As an illustration, the MALDI-TOF mass spectrum of **2** (Mw = 3405.7) as sodium adduct is depicted in Figure 3.2. Compounds **2** and **3** are thermotropic liquid crystalline and their mesomorphic properties are described in chapter 4, along with that of analogues displaying ion conduction upon charging with lithium salts.



Scheme 3.1: Synthesis of disc shaped molecules **2** and **3**.

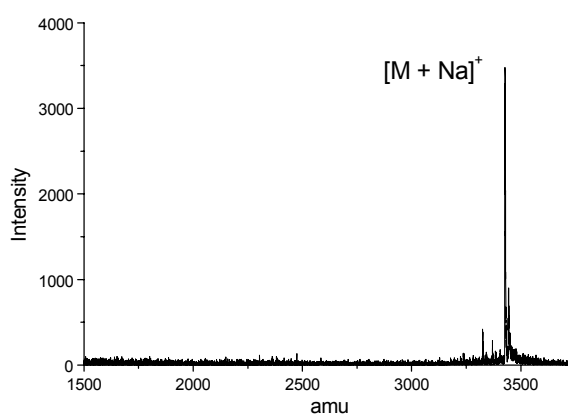


Figure 3.2: MALDI-TOF mass spectrum of **2**, showing its sodium adduct at $m/z = 3428.1$ (theoretical $m/z = 3428.7$) (Matrix = indole acrylic acid).

3.2.2 Self-assembly in solution

UV-Vis and NMR spectroscopy

In chloroform **2** is molecularly dispersed, as concluded from the shape of the UV spectrum.⁴ In polar solvents such as acetonitrile, methanol, ethanol and *n*-butanol these molecules aggregate as indicated by the red shift of about 10 nm in the UV spectrum. Raising the temperature of a solution of **2** (10^{-5} M) in *n*-butanol³⁸ from -10 °C to 100 °C resulted in two transitions as judged from the UV spectra (Figure 3.3). Whereas between -10 °C and 15 °C the UV spectrum is constant, a sharp transition (denaturation *vide infra*) takes place around 20 °C, resulting in a red-shifted spectrum. Further heating above 30 °C gives rise to the second transition as evidenced by a gradual blue shift of the spectra. At 100 °C a UV spectrum was obtained featuring the same bandshape as that of **2** in chloroform at room temperature. ¹H-NMR and ¹³C-NMR spectra of compound **2** in deuterated chloroform at room temperature showed clearly resolved spectra indicating the molecularly dispersed nature of **2**. A similarly resolved spectrum was obtained for a 1.5 wt.% solution of **2** in *n*-butanol-*d*₁₀ at 100 °C. However, cooling of the *n*-butanol-*d*₁₀ solution to 35 °C gave rise to a gradual broadening of the signals with a concomitant significant shielding of the aromatic protons (Figure 3.4). Both processes are indicative of aggregation via π - π stacking and also indicate that the assembly is not fully ordered yet. Lowering the temperature from 35 °C to 30 °C resulted in a sudden and complete loss of the signals attributed to the aromatic protons. Lowering the temperature even further did not change the spectrum anymore. This phenomenon is due to the total loss of freedom of movement within the self-assembly. This process seemed to be highly cooperative as indicated by the sharp S-curve observed with the temperature dependent UV-Vis spectroscopy and the sudden sharp transition observed with ¹H-NMR spectroscopy. Applying the Zimm-Bragg theory for the helical transition in conventional polymers to this transition proved that it is indeed highly cooperative ($\sigma \sim 0.01$).³⁹

The aggregation of achiral **3** in *n*-butanol shows similar characteristics as that of **2**. However, the two transition temperatures were at all times found a few degrees below that of **2**. This is most probably due to the difference in polarity between the two molecules, with chiral **2** being less polar because of the extra nine methyl groups close to the aromatic core.

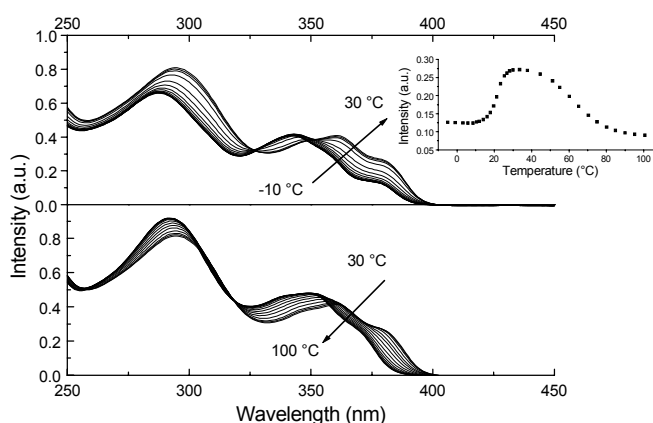


Figure 3.3: Temperature dependent UV-Vis spectra of **2** in *n*-butanol ($1.2 \cdot 10^{-5}$ M), showing the two transitions. Top, the increase of the temperature from -10 to 30 °C. Bottom, increase of the temperature from 30 to 100 °C. In the inset the absorbance at 385 nm at different temperatures is displayed.

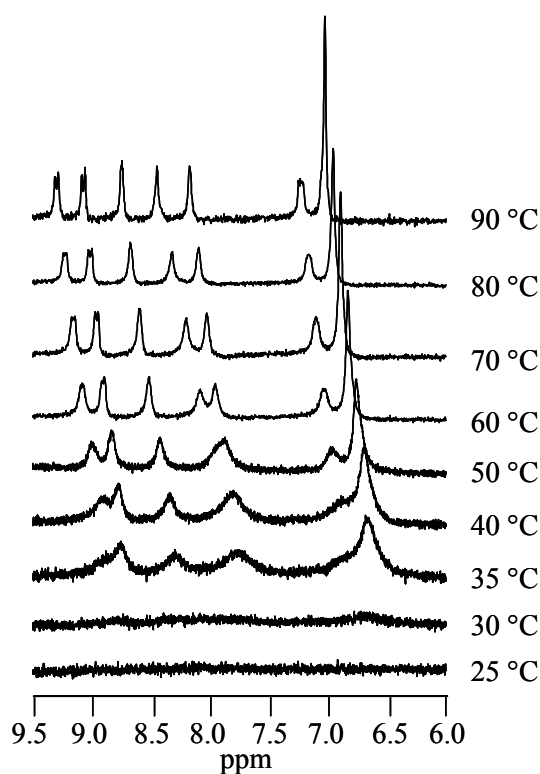
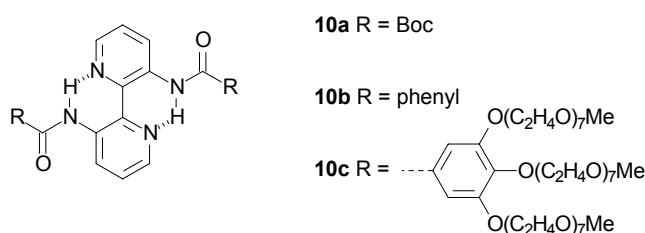


Figure 3.4: Aromatic region of the ^1H -NMR spectrum of **2** (*n*-butanol- d_{10} , $5 \cdot 10^{-3}$ M, 400 MHz) at different temperatures.

Time resolved fluorescence spectroscopy

In order to characterize the nature of the fluorescence, a comparative time-resolved fluorescence study of disc-shaped molecule **2** with model compounds **10a-c** (di-acylated 2,2'-bipyridine-3,3'-diamines) was performed (Scheme 3.2). Analogous to disc-shaped molecule **2**, all the

model compounds showed a large Stokes shift of the fluorescence emission ($\lambda_{max-fluor} \sim 513$ nm) under all experimental conditions. Measurements on **10c** in the molecularly dissolved state in chloroform with the femtosecond fluorescence upconversion technique⁴⁰ detecting emission at different wavelengths, showed a dynamic Stokes shift typical of intramolecular charge transfer; the characteristic time being approximately 3 ps (Figure 3.5). In analogy with the previously studied 2,2'-bipyridyl-3,3'-diol,⁴¹⁻⁴³ it is likely that its fluorescent state refers to a protonated form (obtained after intramolecular proton transfer from the amide to the nitrogen of the heterocycle upon excitation). The dynamic Stokes shift, in typically 3 ps, is representative of the solvation of the photoexcited protonated molecule dissolved in chloroform.⁴⁴



Scheme 3.2: Model compounds **10a-c**.

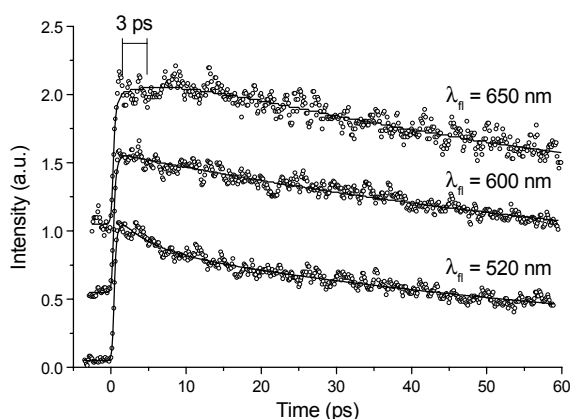


Figure 3.5: Fluorescence transients at room temperature of **10c** dissolved in chloroform at different detection wavelengths (open circles) with their fits (lines); concentration = 10^{-5} M.

The excited-state lifetime⁴⁵ of the molecularly dissolved compounds in chloroform was found to be dependent on the size of the amide substituents. The lifetime of the excited-state of compound **10a** is 10 ps, replacement of the Boc-group by a phenyl (**10b**) results in an increase of the lifetime to 50 ps. A further enlargement of the steric bulk by attachment of long oligo (ethylene oxide) chains (**10c**) increases the lifetime to 150 ps.⁴⁶ The results thus show that when rigidity is imposed onto the molecules, the non-radiative decay of the excited state is suppressed.

In analogy with the results for compounds **10a-c**, it was found that the lifetime of compound **2** had increased from 300 ps in chloroform (molecularly dissolved) to ~ 5 ns in the self-assembled state, i.e., an increase by more than one order of magnitude, due to the decreased motion of the molecules within the aggregate. Some typical fluorescence transients fitted to a biexponential function at various temperatures of **2** in chloroform and *n*-butanol (10^{-6} M) are displayed in Figure 3.6. One of the two characteristic time constants has a magnitude similar to the lifetime for **2** in the molecularly dissolved state in chloroform, whereas the second lifetime component is about one order of magnitude greater. This finding shows the simultaneous presence of two luminescent forms of **2** in solution, i.e., **2** in its molecularly dissolved state and in an aggregated form. It proved impossible to detect the dynamic Stokes shift in the aggregates of **2** in an accurate way. As a result, the time-resolved fluorescence data are focused on the equilibrium between the molecularly dissolved and aggregated forms only (the transition lies between 30 and 90 °C as was already established from UV-Vis and NMR spectroscopy, *vide supra*).

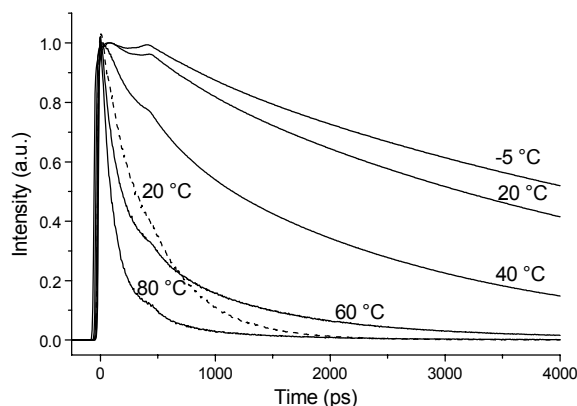


Figure 3.6: Fluorescence transients fitted to a biexponential decay function, of **2** in chloroform (----) and in *n*-butanol at different temperatures (—); $\lambda_{fl} = 520$ nm; concentration 10^{-6} M. The increase of the transients after ~ 600 ps is due to the system's response and is taken into account with the fitting.

Figure 3.7 displays the ratios of compounds being molecularly dissolved and self-assembled, respectively, at different temperatures as gathered from the fitted biexponential functions. The data reveal that above 80 °C all molecules **2** are molecularly dissolved. Lowering the temperature to 20 °C results in the formation of small aggregates and below 20 °C almost all molecules participate in aggregates. The lifetime of the aggregated species increases rapidly upon lowering the temperature to 20 °C (Figure 3.7). The increase of the lifetime is due to the formation of aggregates in which the flexibility of the molecules is decreased.

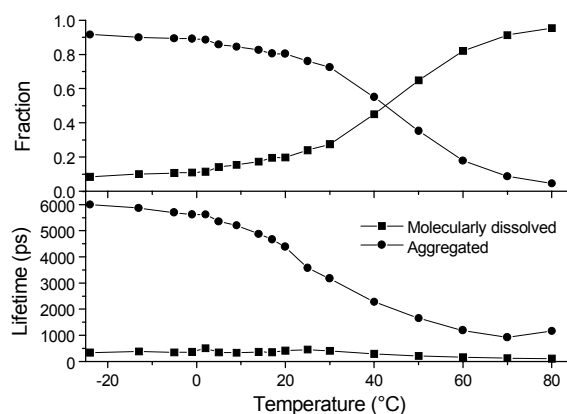


Figure 3.7: Top, fraction of aggregated molecules (circles) and molecularly dissolved molecules (squares) in a 10^{-6} M *n*-butanol solution of **2** at different temperatures. Bottom, lifetimes of the two species, aggregated (circles) and single molecules (squares), as a function of temperature in the same solution. The results follow from the biexponential fitting of the fluorescence spectra.

Circular dichroism and differential scanning calorimetry studies

Since **2** is molecularly dissolved in chloroform, no well-defined order exists and the side-chains cannot interact to transfer their chirality to the aromatic core; hence, no detectable CD effect is observed. In polar solvents, however, the cores of these molecules do aggregate, which in principle enables intermolecular side-chain interactions. Surprisingly, a significant Cotton effect in the $\pi-\pi^*$ transition is observed at temperatures below 20–30 °C. Apparently below room temperature the molecules are ordered within the self-assembly, together with the chiral side-chains this results in the formation of a chiral superstructure. In order to investigate the chirality of the aggregates during self-assembly, the CD effect of a solution of **2** in *n*-butanol was studied as a function of temperature (Figure 3.8). Raising the temperature from -10 °C to 90 °C in steps of 2 °C with ample time to equilibrate, resulted in a sharp transition at 20 °C, i.e., the same temperature as the low-temperature transition observed with UV-Vis and $^1\text{H-NMR}$ spectroscopy. At temperatures below the transition, the chirality within the self-assembly is constant, but during the transition the self-assembly totally loses its supramolecular chirality, as concluded from the rapid disappearance of the Cotton effect above 20 °C. These results indicate that in the self-assembly at low temperatures the molecules are locked in a particular position and nearly all molecules participate in the self-assembly. Consequently, the side-chains interact and transfer their chirality to the aromatic core of the discs. At temperatures above this transition, the molecules have lost their positional order, because the intermolecular interactions accounting for it are no longer operative. The temperature window over which the chirality is lost, is only slightly concentration dependent (Figure 3.9); over a concentration range from 10^{-6} M to 10^{-2} M the transition temperature changes by 10 °C only (around 20 °C at 10^{-6} M to 30 °C at 10^{-2} M), in

agreement with the transitions observed with UV-Vis and $^1\text{H-NMR}$ spectroscopy. This dependency most probably results from the larger aggregate size of the achiral assemblies at higher concentrations. The cooperativity of the transition is higher at increased concentrations as is deducible from the increase of the sharpness of the transition (Figure 3.9).³⁹

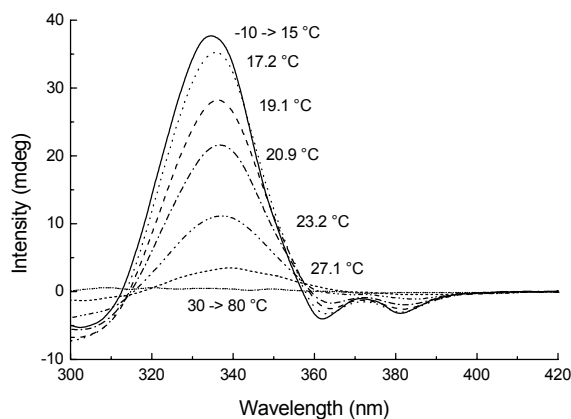


Figure 3.8: Temperature dependent CD spectra of **2** in *n*-butanol (10^{-5} M).

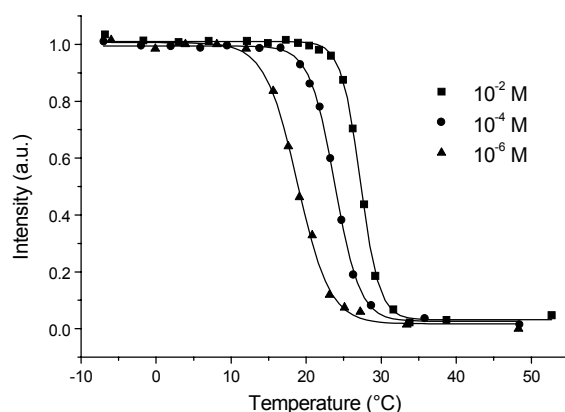


Figure 3.9: Normalized intensities of the CD-spectra of **2** in *n*-butanol at 337 nm at three different concentrations (10^{-6} , 10^{-4} and 10^{-2} M).

At 10^{-2} M in *n*-butanol a melting endotherm could be detected, using an ultra sensitive differential scanning calorimeter (DSC), corresponding to a melting point of 30 °C and a melting enthalpy of approximately 50 kJ/mol (Figure 3.10). The transition shifts to lower temperatures upon lowering the concentration (26.5 °C at $5 \cdot 10^{-4}$ M); the energy of the transition remains constant over the concentration range in which measurements could be performed (10^{-2} M – 10^{-4} M). The strong melting endotherm shows the high cooperativity of the transition ($\sigma \sim 0.03$ and ~ 0.01 at 10^{-6} M and 10^{-2} M respectively)³⁹ and reveals that very strong and specific interactions between the molecules are operative. The large energy of the transition also suggests that a significant growth of the aggregates

occurs during the transition, concomitant with the occurrence of the directional intermolecular interactions.

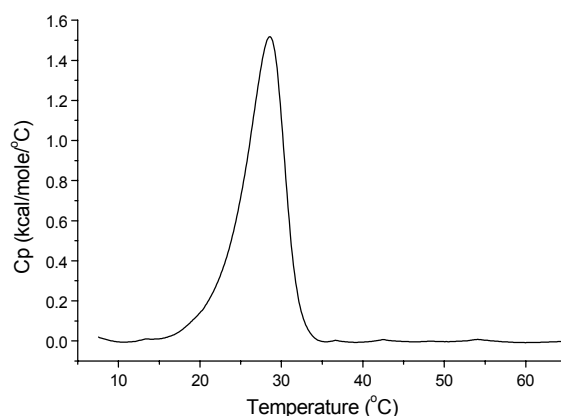


Figure 3.10: DSC thermodiagram of 3×10^{-3} M of **2** in *n*-butanol.

The UV-Vis and CD spectra near the transition midpoint around 20 °C can be modeled as a linear combination of the signals from the two limiting states (at 10 and 35 °C). Furthermore, the UV-Vis and CD data show coinciding sigmoidal transition curves. These results, together with the observation of a melting endotherm, indicate that the transition from chiral to achiral self-assembly has a two-state behavior.⁴⁷ The two limiting states –totally achiral columns and fully chiral columns– are both present and interconvert at the transition midpoint. The second UV-Vis transition at higher temperature, also detected with fluorescence spectroscopy, seems to follow isodesmic behavior, i.e. linear growth.³⁴

3.2.3 The hierarchical growth

The dynamic behavior of **2** in *n*-butanol with two different kinds of self-assemblies sharply contrasts with that of apolar analogue **1** in hexane and supramolecular architectures in apolar solvents in general. Upon heating a solution of **1** in hexane, optical activity and stacking are lost simultaneously over a broad temperature range (0 – 100 °C). Hence, aggregation and expression of chirality of the self-assembled stacks of **1** are strongly interrelated. The apolar solvent does not differentiate between ordering secondary interactions (like hydrogen bonding) and other interactions (like π – π stacking and solvophobic interactions) that account for the aggregation. In polar solvents, however, the solvent is capable of preferentially interfering with specific secondary interactions. Owing to its polar, protic nature *n*-butanol is capable of destroying the structuring secondary interactions between the molecules, essential for the positional order in the chiral supramolecular self-assembly. At the low temperatures where this interference starts to take place (~ 20 °C), the solubilizing power of *n*-butanol is not sufficient to overcome the solvophobic π – π interactions

between the aromatic cores. Therefore, the expression of chirality is lost prior to the loss of aggregation and two unique self-assembled states exist of which one expresses its chirality in the supramolecular assembly and the other does not. Based on the results presented here, it is proposed that the former is a rigid-rod extended stack, while the latter is a disordered aggregate of smaller dimensions. A cartoon visualizing the two-step self-assembly is given in Figure 3.11 and theoretical studies and small angle neutron scattering (SANS) measurements have confirmed the occurrence of this self-assembly process (see section 3.3.2). A tentative picture displaying the unique chiral columnar self-assembly is displayed in Figure 3.12.

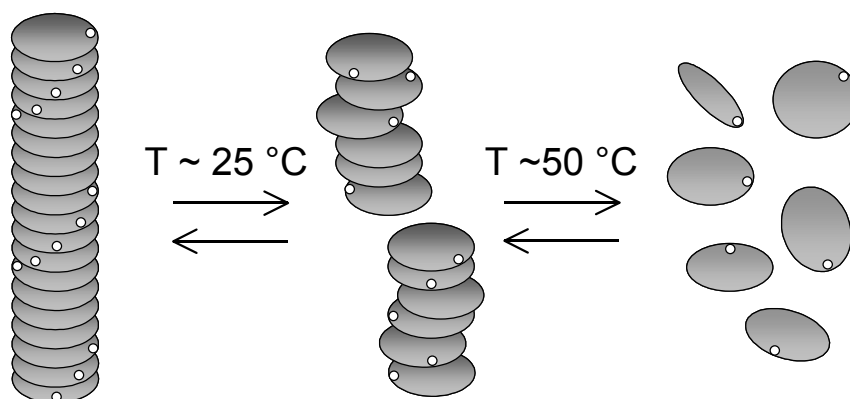


Figure 3.11: Cartoon showing the two-step self-assembly of chiral **2** from single molecules via short achiral columns to long homochiral helical columns.

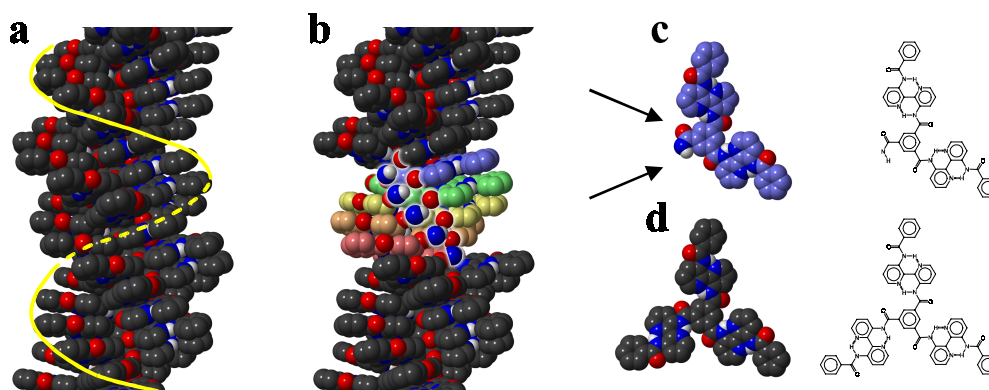


Figure 3.12: A tentative picture displaying the molecules packed in a chiral column with a pitch of nine molecules (**a**), the chiral side chains have been omitted for clarity. Structure **b** shows the same column, but for the middle molecules one of the outer benzene rings and one of the bipyridine groups have been omitted, enabling to look into the core of the column. Highlighted are the intermolecular hydrogen bonds that are proposed to regularly lock the molecules in the column. Structure **c** shows one of the molecules in which parts have been omitted, the arrows indicate the C=O and N-H involved in hydrogen bonding. Structure **d** is the aromatic core of **2** without chiral side-chains. The three bipyridine wedges are tilted, similar to the situation in columns **a** and **b**.

The hierarchical growth of the self-assembly of **2** in *n*-butanol contrasts with the behavior of the aforementioned α,ω -di-substituted sexithiophenes, showing one unique self-assembly, that is proposed to melt upon increasing the temperature.³⁵ This different behavior is due to the additional intermolecular interactions between molecules of type **2**, not present in the α,ω -di-substituted sexithiophene. The aggregation of the latter is basically the result of only hydrophobic interactions, whereas **2** has the possibility for extra, solvent dependent, interactions. A two-step process, however, was observed for a series of oligo(*m*-phenylene ethynylene)s.⁷ Similar as for **2**, two different types of interactions account for the hierarchical growth, of which one arises earlier than the other because of differences in sensitivity for solvophobicity.

The locking of the discs in a fixed chiral conformation is proposed to be governed by intra- and intermolecular hydrogen bonding with the consecutive molecules mutually twisted in such a way that self-assembled, highly regular chiral columnar stacks are formed. Column **a** in Figure 3.12 shows how these molecules can pack into chiral columns. The three wedges on the central core are twisted out of the plane due to steric hindrance thus providing a propeller-like scaffold for the efficient packing of the molecules. The second helix (**b**) in Figure 3.12, in which part of the outer groups are omitted, shows the possibility for the formation of intermolecular hydrogen bonds: due to the rotation of the subsequent molecules and the twist of the wedges linear intermolecular hydrogen bonding is possible, thus enabling positional locking of the molecules, reminiscent of the α -helix in peptides. As has been shown previously,^{4,48-50} intermolecular hydrogen bonding between similar C_3 -symmetrical discs is highly cooperative and directional and locks the subsequent molecules on top of each other. The creation of a hydrophobic microenvironment by π - π stacking of the aromatic cores allows for expression of these secondary interactions in polar media. This resembles the creation of the hydrophobic microenvironment in proteins, created by a hydrophobic collapse and allowing for the expression of hydrogen bonds.¹⁸ The molecularly dissolved molecules first aggregate into small self-assembled species via solvophobic interactions. When such self-assemblies are formed, the polar solvent cannot penetrate into the core anymore resulting in a hydrophobic microenvironment around the inner molecules. In this microenvironment, the native state of the helical structure can be created by intermolecular hydrogen bonding.

The self-assembly of **2** as depicted in Figure 3.11 shows great similarity to the assembly of proteins in the tobacco mosaic virus (TMV).⁵¹ The protein molecules self-assemble to form disc shaped structures.⁵² Lowering of the pH or increase of the ionic strength accounts for loose stacking of these discs into small oligomers. After a further lowering of the pH, a cooperative transition into highly stable and long helices takes place. The comparison between the two systems is striking, especially since also the size of the helical columns of **2** rapidly increases after the cooperative transition from loosely stacked discs into helices (see also section 3.3.2). These kind of molecules may prove simple models system for the self-assembly of viruses like the TMV.

3.2.4 Concluding remarks

In conclusion, the creation of well-defined chiral self-assembled structures from **2** in alcohols invoking a variety of secondary interactions has been demonstrated. These interactions occur in a hierarchical fashion, thus giving rise to a stepwise growth of the discotic molecules into chiral columns via intermediates lacking supramolecular chirality. The created hydrophobic micro-domain in the initially achiral aggregates allows the expression of the more sensitive polar interactions. The reversible chiral assemblage and its importance for the hierarchical growth resembles the folding and assembly of proteins and polynucleotides and together with the differences observed for superstructure formation between apolar and polar media, gives valuable information for a better understanding of supramolecular architecture formation in protic media.

3.3 Amplification of chirality and determination of the column length in *n*-butanol

Strong amplification of chirality for the generation of homochiral molecules or architectures, is a fascinating aspect of life that has inspired chemists repeatedly.^{53,54} Approaches to create such systems have ranged from crystallization-induced resolution to asymmetric synthesis. Copolymers made from chiral and achiral monomers have been shown to possess a positive, non-linear dependence of the specific rotation.⁵⁵ The work of Green and co-workers on polyisocyanates is seeding in this field and their ‘Sergeant and Soldiers’ and ‘Majority Rules’ principles have confirmed the importance of cooperativity for the amplification of chirality.^{13,36,56-58} Recently, it was shown that impressive amplification of chirality also occurs in well-defined aggregates of self-assembled molecules.^{4,48} The amplification of chirality in self-assembled architectures is increasingly gaining interest and the results obtained from the systems studied may aid in the elucidation of the self-assembly processes in Nature and, particularly, the chirality involved.^{3,4,7,26,48,59,60} The results show that cooperative interactions within the self-assembly are a prerequisite for strong amplification of chirality.

The discotics **2** and **3** in *n*-butanol feature a cooperative transition from achiral stacks to helical columns upon cooling, as described in section 3.2. The cooperative formation of the chiral architecture renders this system very attractive for generating a strong amplification of chirality. To investigate this, ‘Sergeant and Soldiers’³⁶ experiments were performed on mixtures of **2** and **3** containing equal amounts of chromophores. The results are correlated with a model describing the helicity and size of the columns as a function of temperature and with small angle neutron scattering (SANS) studies on **2** in deuterated *n*-butanol.³⁹ Finally, the transfer of chirality in *n*-butanol from one chiral seed molecule to 400 achiral molecules within a helical column will be discussed; an unprecedented amplification of chirality for self-assembled supramolecular architectures under reversible conditions.

3.3.1 Amplification of chirality

Obviously, achiral **3** does not show any optical activity in *n*-butanol, but the aggregation behavior is similar to that of **2** and hence equal amounts of *P* and *M* helices are formed. The ‘Sergeant and Soldiers’³⁶ experiments on **3** / **2** mixtures in *n*-butanol were conducted at two concentrations at 5 °C (Figure 3.13) and the intensity of the Cotton effect divided by the absorption (g_{abs}) was monitored as a function of mole percent sergeant added. A very strong amplification was observed at a concentration of 10^{-4} M; the maximal Cotton effect was reached already after addition of only one percent chiral **2**, implying an extremely large cooperativity within the helical columns. The amplification of chirality at 10^{-5} M appeared to be significantly smaller, since over five percent of sergeant was needed to achieve full bias of helicity. Apparently, at this tenfold lower concentration a substantial smaller number of achiral molecules undergoes amplification of chirality. The ‘Sergeant and Soldiers’ data were fitted to the model derived by Havinga⁴ to determine the association constant and the strength of the chirality amplification, i.e. the number of soldiers forming one unit of uniform helicity within one column. The length over which one single chiral seed molecule can amplify its chirality, the length of uniform helicity within one column, was calculated to slightly exceed 400 molecules and the association constant K was determined to be approximately $5 \times 10^8 \text{ L} \times \text{mol}^{-1}$ at 5 °C.

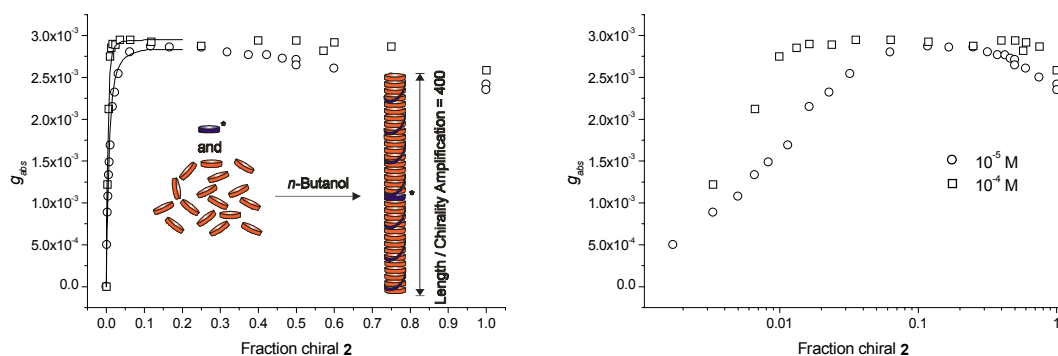


Figure 3.13: Dependence of the overall chirality on the mole fraction of chiral **2** in *n*-butanol at 5 °C, expressed in terms of the g -value measured at the maximum of the Cotton effect at 341 nm (left) and the representation of the data in a log-plot (right). Measurements were recorded at 10^{-5} M in a 1 cm cell (circles) and at 10^{-4} M in a 1 mm cell (squares). The solid lines in the left graph represent the best fit to the data using an uniform helicity length of 400 molecules and a K of $5 \times 10^8 \text{ L} \times \text{mol}^{-1}$.

In addition, these ‘Sergeant and Soldiers’ experiments were characterized by a strong time-dependence. After the addition of a small aliquot of chiral **2** to a solution of achiral **3** it took approximately 2 hours before full amplification of chirality was reached. This process was independent of the temperature at which the compounds were mixed, although at very high fractions of **2** (> 50%) the time became shorter. Apparently the high degree of order within the columns makes

them somewhat reluctant to dissociation. This stability on the other hand favors strong amplification of chirality in the thermodynamically favored aggregates.

Even though highly ordered columns are formed, the interactions accounting for the chirality transfer are subtle and involve an interplay between the supramolecular architecture and the solvent. Thus, achiral **3** was dissolved in the chiral solvent (*2S*)-(-)-methyl-1-butanol. UV-Vis and fluorescence spectroscopy measurements indicated that also in this solvent aggregation takes place upon cooling and the Cotton effect at temperatures below 10 °C indicated that the chirality of the solvent is transferred to the helical columns. Similar to solutions of chiral **2** in achiral alcohols, the achiral columns formed in *S*(-)-2-methyl-1-butanol become chiral at a defined temperature (~ 15 °C) (Figure 3.14). A Cotton effect comparable in shape and intensity ($g_{abs} = 2 \cdot 10^{-3}$) to that of **2** in *n*-butanol ($g_{abs} = 3 \cdot 10^{-3}$) can be observed. The transition from achiral to chiral columns is again relatively sharp.

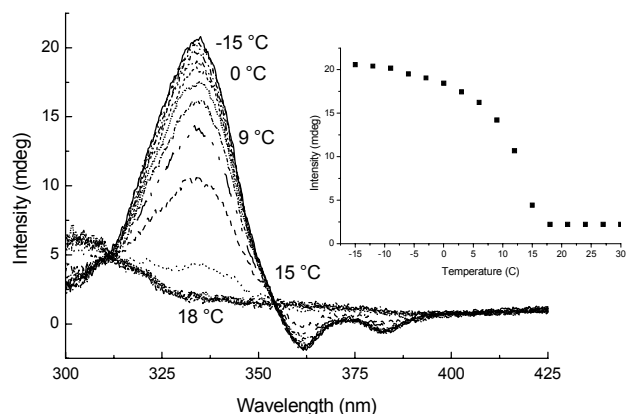


Figure 3.14: CD-spectra of **3** in (*2S*)-(-)-methyl-1-butanol at 10^{-5} M at different temperatures. The UV-Vis insensitive chiral solvent induces helicity in the columns built up from **3**, resulting in a Cotton effect in the chromophores of **3**. The inset shows the maxima of the Cotton effect as a function of temperature.

3.3.2 Determination of column length – An experimental and theoretical approach

The extent to which chirality can be amplified in the columns not only depends on the cooperativity length, but also on the size of the columns. In order to identify the length of the columns small angle neutron scattering (SANS) studies were performed on **2** in deuterated *n*-butanol at different temperatures and concentrations. The scattering curves obtained at low temperatures (< 30 °C) were typical for rigid rod columns and at high scattering angles the interdisc reflection ($\sim 3\text{-}4$ Å) could be identified. Concentration dependent measurements (0.05 – 2.0 wt.%) showed similar scattering patterns at all concentrations, thus verifying the concentration independent nature of the columns. A sample of 2.4×10^{-3} M was studied as a function of temperature. At high temperatures the

scattering patterns were in agreement with small particles until 35 °C. At lower temperatures the scattering intensity increased significantly, and the pattern was directly indicative for columnar particles. The shape of the scattering pattern did not change significantly when lowering the temperatures further, in contrast to the intensity that increased upon lowering the temperatures. In Figure 3.15 the intensities at zero angle are plotted as a function of temperature showing the strong growth of the architectures around the achiral-chiral transition at ~30 °C. Thus, the results indicate that at intermediate temperatures small aggregates are being formed lacking the well-defined columnar structure, present in the large structures formed at low temperatures.

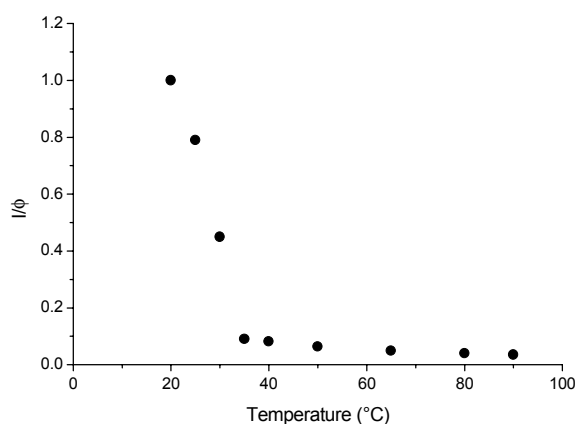


Figure 3.15: Results of SANS experiments on a sample of **2** in *n*-butanol-*d*₁₀ at a concentration of 2.4×10^{-3} M. Shown is the scattered intensity at zero-angle divided by the volume fraction of dissolved material, I/ϕ , as a function of the temperature for the columnar aggregates. The quantity I/ϕ , is given in arbitrary units.

The ‘Sergeant and Soldiers’ experiments on **3** / **2** mixtures have revealed a high association constant (5×10^8 L \times mol⁻¹ at 5 °C) and a cooperativity length of over 400 molecules. The assembly in columns yields supramolecular rod-like polymers with an average degree of polymerization (DP) depending on temperature and concentration, as also revealed by SANS studies. The association constant K allows for calculation of the number average degree of polymerization using the formula $DP = 2 \times \sqrt{(K \times \text{concentration})}$. At a concentration of 10^{-4} M the length of the columns is approximately 450 molecules and at 10^{-5} M 140 molecules (5 °C).⁶¹ These results thus reveal that at 10^{-5} M the column length (~140) is the limiting factor in the amplification of chirality. Even though the cooperativity / persistence length of uniform chiral domains is theoretically 400 molecules, the small ‘platoons’ of 140 soldiers limit the influence of the sergeants. At 10^{-4} M the two variables are comparable, both around 400. At this concentration the helical columns represent a (virtual) molecular weight as high as $1.4 \cdot 10^6$ Da and a length of ~140 nm (400×0.35 nm). Impressively, only one chiral seed molecule with a thickness of 3.5 Å is needed to render these long columns diastereomerically

pure. It should be noted, however, that due to a statistical location of the chiral seeds within the columns more than 0.25 % seed molecules are required. The experiments have shown that approximately 1% is necessary. Furthermore, the persistence length of the homochiral segments is constantly ‘moving’ over the columns, while thermal motion disconnects different segments.

Recently, van der Schoot *et al.* formulated a model rationalizing the experimentally observed self-assembly data described in section 3.2.2.³⁹ In this model, the standard theory of linear self-assembly was modified by adopting a two-state model for the molecules in the aggregates, to account for the cooperative transition. The theory allows for the calculation of the average number of molecules in the columns at any concentration and temperature. The theory predicted an average size of the aggregates at 5 °C of 160 molecules at 10^{-5} M and 440 at 10^{-4} M. These numbers are in excellent agreement with the ‘Sergeant and Soldiers’ experiments that yielded calculated column lengths at 5 °C of 140 and 450 molecules at 10^{-5} and 10^{-4} M, respectively. This is a remarkably close match, when one considers that the column lengths were obtained via totally different and independent experiments and calculations. Figure 3.16 shows the calculated column length, on the basis of the model by van der Schoot, as a function of temperature at three different concentrations. Clearly visible is the small aggregate size at high temperatures and the rapid increase of the size at temperatures below the achiral-chiral transition around 30 °C, in analogy with the stacked discs–helix transition in the TMV.⁵¹

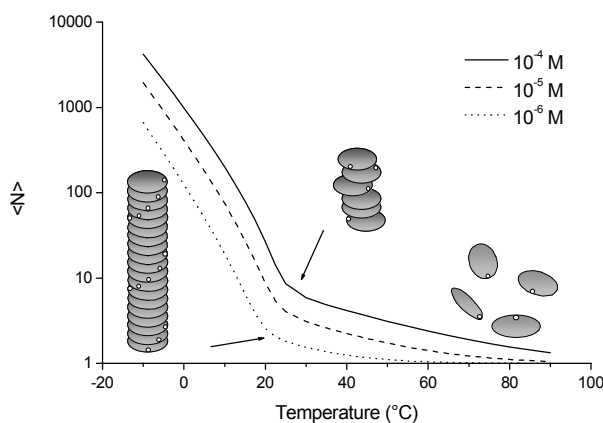


Figure 3.16: Prediction for the average number of molecules participating in one column, $\langle N \rangle$, at three different concentrations as a function of temperature. The arrows mark the transition from achiral to chiral aggregates. Please note the logarithmic Y-axis in contrast to the linear Y-axis of Figure 3.15.

3.3.3 Concluding remarks

Very strong amplification of chirality in *n*-butanol rationalizes why columns consisting of achiral molecules **3** can be made homochiral by only one chiral seed molecule **2** per 400 achiral molecules. The high cooperativity and the time-dependence for full expression of chirality demonstrate the high degree of order in the assembly. The calculated column lengths on the basis of the ‘Sergeant and Soldiers’ measurements nicely match with data obtained using a model for the two-step self-assembly in columns and data obtained via SANS. The results presented here show that for a strong amplification of chirality within self-assembled aggregates, cooperative interactions are essential, together with large aggregate sizes.

3.4 Self-assembly and amplification of chirality in water

3.4.1 Hierarchical self-assembly

Compounds **2** and **3** dissolve in water due to their hydrophilic side chains, but intriguingly, aggregation takes place as evidenced by broad signals in the ¹H-NMR spectra, a red shift in the UV-Vis spectra, and a strong intensity of the luminescence compared to solutions in chloroform. This aggregation in water resembles that of chromonics that are known to aggregate via hydrophobic interactions of their aromatic cores.³⁴ Remarkably and in contrast to chromonics, the architectures are chiral and well-defined as evidenced by the appearance of a Cotton effect for **2** at the wavelength corresponding to the aromatic core ($g_{abs} = 1.4 \cdot 10^{-3}$, 5 °C). Apparently, the arene-arene interactions of the aromatic cores not only account for aggregation, but also allow for structuring via the specific, solvent sensitive interactions, most probably by creation of a hydrophobic micro-environment. Furthermore, this implies that the peripheral chirality of the individual molecules can be transmitted to the center of the self-assemblies by side chain interactions in water.

In order to investigate the self-assembly in water, the solution of **2** in water was studied as a function of temperature. Raising the temperature from 0 to 90 °C resulted in gradual changes in the UV (Figure 3.17, top) and CD spectra (Figure 3.17, bottom) as well as the fluorescence characteristics. In contrast to the *n*-butanol solutions that were characterized by a highly cooperative loss of chirality around 20 °C,⁶² the Cotton effect of the aqueous solutions only decreased slowly from 0 to 60 °C. At temperatures as low as 0 °C the Cotton effect is still temperature-sensitive, suggesting that the individual molecules are not yet fully locked in one defined position, but still exhibit some motion within the columns. The bandshape characteristics of the UV-spectra and the high luminescence at all temperatures investigated (0 – 100 °C) suggest that the molecules are aggregated at all temperatures. The stacking at high temperatures contrasts with the behavior of **2** in *n*-butanol and to that of chromonics in general. This behavior is attributed to the combination of a large aromatic core, allowing for strong arene-arene interactions, especially in water, and the lower critical solution temperature (LCST) behavior of oligo(ethylene oxide)s in water.⁶³ Dilute solutions of **2** / **3** in water

become turbid around 70°C (Figure 3.17). The turbidity is ascribed to the formation of clusters of columns. However, already at 60°C another Cotton effect with opposite sign appears (Figure 3.17 bottom). Whether this ‘inversion’ results from the formation of clusters with super-helical structure, or is simply due to scattering of the large chiral particles is not clear yet.

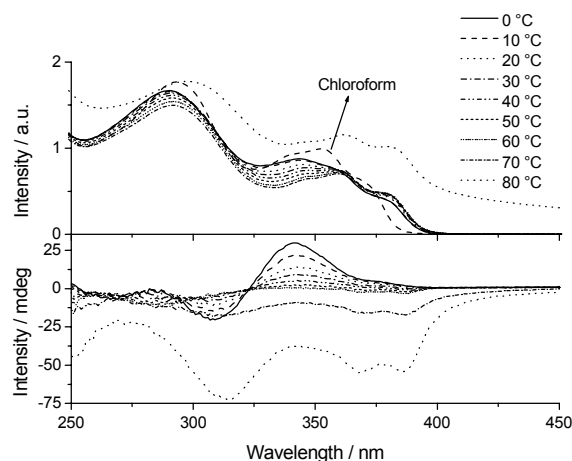


Figure 3.17: Temperature dependent UV-Vis (top) and CD (bottom) spectra of **2** in water ($2.6 \cdot 10^{-5}$ M). In addition, the UV-Vis spectrum of **2** in chloroform ($2.6 \cdot 10^{-5}$ M) is depicted.

SANS measurements performed on solutions of **2** in deuterated water have revealed the columnar nature of the aggregates. Surprisingly, temperature dependent measurements have shown the increase of the length of the columns upon increase of the temperature from 0 to 60 °C. At even higher temperatures the solutions become turbid and larger, non-columnar aggregates are formed. Apparently the strong arene-arene interactions and LCST behavior of the side-chains not only allow for stacking over the whole temperature regime from 0-100 °C, but even account for growth, both linear and lateral, of the columns at higher temperatures.⁶⁴

3.4.2 Amplification of chirality

‘Sergeant and Soldiers’ experiments³⁶ on **2** / **3** mixtures in water were conducted at two concentrations at 5 °C (Figure 3.18) and revealed that chirality is indeed amplified in the assembly in water; the maximal expression of chirality is reached after the addition of 25-30 % chiral compound. Adopting the model of Havinga,⁴ the association constant (K_{ass}) was calculated to be 1×10^8 L \times mol⁻¹, with a length of homochiral helicity of 12 molecules. This means that at 10^{-4} M columns with a degree of polymerization as high as 200 are being formed and that 15-20 chiral molecules are needed to achieve homochiral columns.

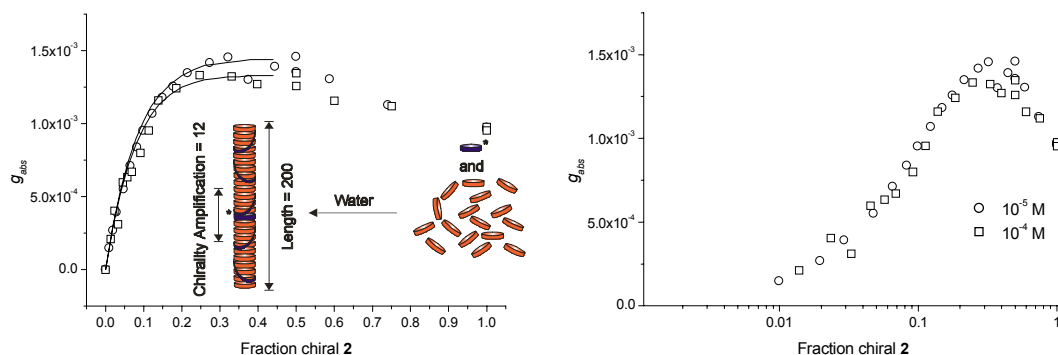


Figure 3.18: Dependence of the overall chirality on the mole fraction of chiral **2** in water at 5 °C, expressed in terms of the g -value and measured at the maximum of the Cotton effect at 336 - 341 nm (left) and the representation of the data in a log-plot (right). Measurements were recorded at 10^{-5} M in a 1 cm cell (circles) and at 10^{-4} M in a 1 mm cell (squares). The solid lines represent the best fit to the data using an uniform helicity length of 12 molecules and a K_{ass} of $1 \cdot 10^8$ L \cdot mol $^{-1}$.

The high stability and order of the columns, essential for amplification of chirality, is reflected in a strong time-dependence for the columns to become homochiral; after addition of a small aliquot of chiral **2** to a solution of achiral **3** it takes approximately 1.5 hours before full amplification of chirality is reached. This phenomenon either results from a diffusion-limited transport of molecules from one stack to the other, or, most likely, is due to an ordered and stable packing of the molecules, both **2** and **3**, in the columns.

Figure 3.18 clearly shows that in water the Cotton effect for particular mixtures is significantly stronger than for pure chiral **2**. In addition, it was established that in water the UV-Vis spectra of **2** and **3** differ and as a consequence the CD spectra, for which the maximum has been shifted from 342 nm for pure chiral **2** to 336 nm for the mixtures with low ‘seed’ content (Figure 3.19). These results demonstrate that the efficiency of packing in columns is different for **2** and **3**. The stronger Cotton effect of the mixtures, suggests the packing of the achiral molecules to be superior. The differences in packing might be attributed to the different hydrophobicity of **2** and **3** and the increased steric hindrance in stacks of **2** caused by the additional nine branching methyl groups.

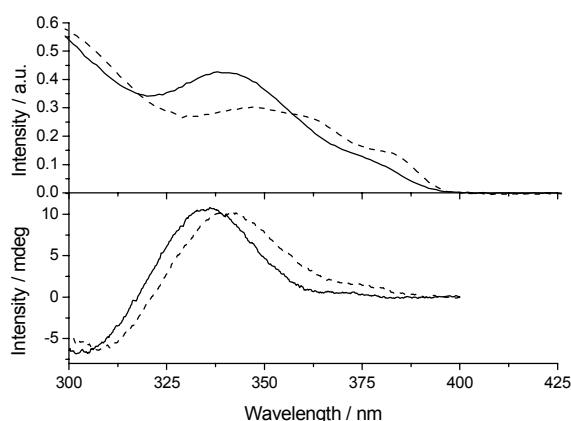


Figure 3.19: UV-Vis (top) and CD (bottom) spectra of **2** (----) and of a mixture containing 8% **2** and 92% **3** (—) in water at 5 °C at a total concentration of 10^{-5} M.

3.4.3 Concluding remarks

In conclusion, the creation of well-defined chiral self-assemblies in aqueous solutions has been demonstrated. Although the aggregation process of **2** in water has similarities with that in organic solvents,⁶² the special behavior in water and the interaction of water with ethylene oxide side chains is responsible for striking differences. Columnar aggregates in water remain present at all temperatures investigated (0 – 100 °C), whereas the chirality within the columns is governed by temperature. Even at temperatures as low as 0 °C a maximal chirality is not reached, showing that there is still rotational flexibility within the columns; the columns are not present in one unique conformation. This is also reflected in the modest cooperativity length for chirality amplification, with respect to **2** in *n*-butanol, being only 12.

3.5 Towards multi-columnar architectures

For the creation of active and enantiospecific functional architectures from the discussed chiral supramolecular columnar architectures, multi-columnar assemblies are required, reminiscent of the formation of a four-helix bundle by specific α -helical segments in polypeptides.⁶⁵ In order to create multi-columnar architectures, terpyridine functionalized discotic molecule **11** was designed and synthesized.⁶⁶ The incorporation of a terpyridine unit allows for the selective dimerization of two discotics **11** or the complexation of several discotics **11** with one multifunctional host, *e.g.* a catalytically active site. The addition of subsequent non-functionalized discotics **2** then allows for the formation of chiral columns around that center (Figure 3.20). Using optical techniques, it was established that **11** undergoes complexation with Fe^{2+} in water in a 1:2 ratio. Addition of Fe^{2+} to **11** results in the upcoming of a metal to ligand charge transfer band around 560 nm. Furthermore, a total quenching of the fluorescence upon addition of iron is observed, indicating that a fast energy transfer from the excited bipyridines to the metal complex takes place, followed by non-radiative decay processes of the metal complex. Chiral **11** was still capable of amplifying its chirality to achiral discotics **3** in water to a similar extent as the non-functionalized **2**.

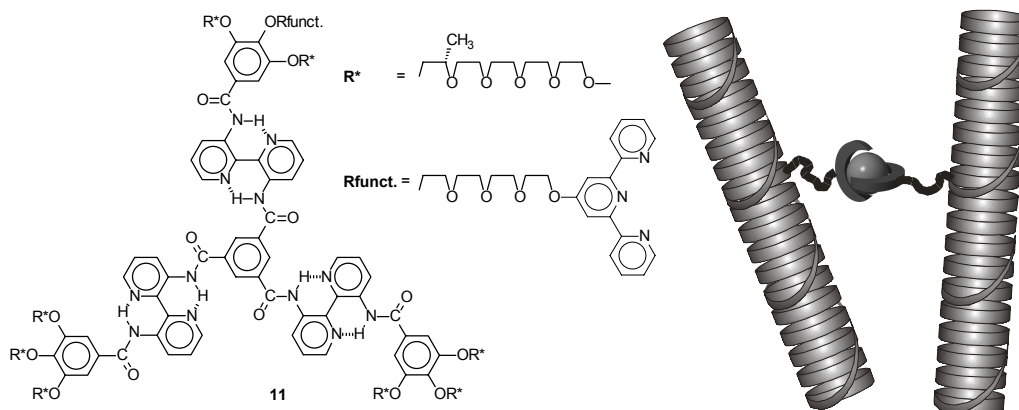


Figure 3.20: Terpyridine functionalized molecule **11** and its mode of association upon addition of Fe^{2+} and mixing with an excess of **2** or **3**.

3.6 Overall conclusions

The creation of well-defined chiral supramolecular architectures in water is a subject of increasing importance and one of the goals in bio-inspired supramolecular chemistry. The use of secondary interactions for the formation of well-defined self-assembled systems in apolar solutions is well known and studied. The utilization of these interactions to self-assemble relatively small molecules in water, however, is found to be very difficult, because of the competing solvent. Nevertheless, here it has been shown –using principles well known from biomacromolecules– that these interactions can also be operative in polar protic media. By the creation of hydrophobic micro-environments in supramolecular assemblies, secondary interactions are shielded from the competing solvent and allowed to express themselves. The polar solvents govern the hierarchical formation of assemblies due to specific, differentiating solvent-molecule interactions, that importantly differs from apolar solvents. Furthermore, the distinct influence of oligo(ethylene oxide) side chains on the supramolecular structure-formation of these chromonic-like structures affords highly stable structures even at elevated temperatures in water. As specific recognition tools to elucidate the positional order of the molecules, chirality transfer with the aid of chiral side-chains and amplification of chirality using mixtures of chiral and achiral discotics were successfully applied. Transfer of chirality to the aromatic core occurred when specific secondary intermolecular interactions are operative. Identification of supramolecular structures and recognition of the specific interactions that are operative in such structures will undoubtedly help to elucidate the complex matter of self-assembly and structure formation in aqueous media, both by simple organic molecules and by biomacromolecules.

3.7 Experimental section

General.⁶⁷ Optical properties and melting points were determined using a Jeneval polarization microscope equipped with a Linkam THMS 600 heating device with crossed polarizers. Ultrasensitive differential scanning microcalorimeter measurements were recorded on a VP-DSC from Heath Scientific. X-ray diffraction patterns were recorded using a multiwire area detector X-1000 coupled with a graphite monochromator. SEC measurements were done using a column with PL gel and chloroform as eluent and a flow rate of 1 mL min⁻¹, detection was done via an UV detector at a wavelength of 254 nm. Fluorescence emission spectra were recorded on a Perkin Elmer LS50B luminescence spectrometer. The femtosecond fluorescence upconversion transients were measured using the set-up (time resolution: ~ 150 fs) described previously.⁴⁰ Fluorescence transient measurements with picosecond time resolution were conducted using time-correlated single-photon-counting detection.⁴⁵ The syntheses of 2,2'-bipyridine-3,3'-diamine (**8**),⁶⁸ and compounds **10a-c**⁶⁹ have been described previously.

N,N',N''-Tris{3[3'-(3,4,5-tris{(2S)-2-(2-{2-[2-(2-methoxyethoxy)-ethoxy]-ethoxy}-ethoxy)-propyloxy]-benzoylamino]-2,2'-bipyridyl}benzene-1,3,5-tricarboxamide (2**).** To a solution of **4** (1.00 g, 0.92 mmol) and triethylamine (0.14 mL, 1.0 mmol) in dry methylene chloride (10 mL), a solution of trimesic chloride (**9**) (79 mg, 0.30 mmol) in dry methylene chloride (5 mL) was added dropwise at room temperature. The resulting mixture was stirred at room temperature overnight and the solvents were evaporated *in vacuo*. The crude product was purified by column chromatography (silica; 5% methanol in methylene chloride) and preparative size exclusion chromatography (methylene chloride) to give **2** as an off-white wax (0.87 g, 0.247 mmol, 82%). T_{cl} = 270°C. ¹H-NMR (CDCl₃): δ = 15.52 (s, 3H), 14.42 (s, 3H), 9.60 (dd, *J* = 8.5 and 1.2 Hz, 3H); 9.40 (dd, *J* = 8.5 and 1.4 Hz, 3H), 9.30 (s, 3H), 9.07 (dd, *J* = 4.6 and 1.4 Hz, 3H), 8.53 (dd, *J* = 4.4 and 1.3 Hz, 3H), 7.58 (m, 6H), 7.32 (s, 6H), 4.18-4.15 (m, 9H), 4.05-3.90 (m, 18H), 3.90-3.72 (m, 27H), 3.71-3.60 (m, 99H), 3.59-3.52 (m, 18H), 3.37 (m, 27H), 1.33 (m, 27H). ¹³C-NMR (CDCl₃): δ = 165.8 (CO'); 164.0 (CO); 152.6 (C-3 benzoyl); 142.2, 141.6 (C-2, C-2'); 141.5 (C-4 benzoyl); 140.6, 137.4, 137.3, 136.0 (C-6, C-6', C-3, C-3', C-1 trimesic); 130.4, 130.0, 129.8, 129.5 (C-4', C-1 benzoyl, C-4, C-2 trimesic); 124.6, 124.2 (C-5, C-5'); 107.5 (C-2 benzoyl); 76.3, 75.0, 74.3, 73.1, 71.8, 70.8, 70.7, 70.5 (3x), 70.4 (2x), 68.8, 68.5, 59.9, 17.5. MALDI-TOF [C₁₆₈H₂₅₈N₁₂O₆₀+Na⁺] = Calcd. 3428.7 Da. Obsd. 3428.1 Da.

N,N',N''-Tris{3[3'-(3,4,5-tris{2-(2-{2-[2-(2-methoxyethoxy)-ethoxy]-ethoxy}-ethoxy)-ethoxy)-benzoylamino]-2,2'-bipyridyl}benzene-1,3,5-tricarboxamide (3**).** To a solution of **5** (1.00 g, 0.96 mmol) and triethylamine (0.14 mL) in dry CH₂Cl₂ (10 mL), a solution of trimesic chloride (**9**) (80 mg, 0.3 mmol) in dry CH₂Cl₂ (5 mL) was added dropwise at room temperature. Stirring was continued overnight, after which the solution was diluted with CH₂Cl₂ and washed with water (2 x 25 mL). The combined water layers were extracted with CH₂Cl₂ (4 x 25 mL). The combined dichloromethane layers were washed with brine (1 x 75 mL), dried over MgSO₄ and evaporated *in vacuo*. The crude product was purified by column chromatography (silica, 10% methanol in CH₂Cl₂), size exclusion chromatography followed by column chromatography (silica, dimethoxyethane followed by 10% methanol in chloroform). Thoroughly drying over P₂O₅ afforded 0.41 g (0.12 mmol, 42%) of **3**. ¹H-NMR (CDCl₃): δ = 15.54 (s, 3H, NHCO); 14.50 (s, 3H, NH'CO); 9.61 (dd, *J* = 8.4 and 1.6 Hz, 3H, *H*-4); 9.40 (dd, *J* = 8.4 and 1.6 Hz, 3H, *H*-4'); 9.30 (s, 3H, *o*-H); 9.06 (dd, *J* = 4.4 and 1.6 Hz, 3H, *H*-6'); 8.53 (dd, *J* = 4.8 and 1.6 Hz, 1H, *H*-6); 7.58 (m, 6H, *H*-5 and *H*-5'); 7.36 (s, 6H, *H*-benzoyl); 4.29 (t, 12H, *m*-OCH₂CH₂O); 4.28 (t, 6H, *p*-OCH₂CH₂O) 3.91 (t, 12H, *m*-OCH₂CH₂); 3.84 (t, 6H, *p*-OCH₂CH₂); 3.77-3.52 (m, 144H, OCH₂CH₂O), 3.38 (s, 9H, *p*-OCH₃); 3.36 (s, 18H, *m*-OCH₃). ¹³C-NMR (CDCl₃): δ = 165.9 (CO'); 164.1 (CO); 152.8 (C-3 benzoyl); 142.4, 142.3 (C-2, C-2'); 141.6 (C-4 benzoyl); 140.8, 137.6, 137.5, 136.2 (C-6, C-6', C-3, C-3', C-1 trimesic); 130.6, 130.0, 129.6, 129.4 (C-4', C-1 benzoyl, C-4, C-2 trimesic); 124.7, 124.4 (C-5, C-5'); 108.6 (C-2 benzoyl); 72.5-69.4 (OCH₂CH₂O); 59.0 (OCH₃). IR (ATR): ν = 2871, 1670, 1568, 1515, 1493, 1371, 1297, 1241, 1094, 853, 800, 747, 665. Anal. Calcd for C₁₅₉H₂₄₀N₁₂O₆₀ (Mw = 3279.65 g/mol): C, 58.23; H, 7.38; N, 5.12; Found: C, 57.95; H, 7.53; N, 4.84.

3'-{3,4,5-Tris{(2S)-2-(2-{2-[2-(2-methoxyethoxy)-ethoxy]-ethoxy}-ethoxy)-propyloxy]-benzoylamino}-2,2'-bipyridine-3-amine (4**).** To a solution of **6** (2.6 g, 2.8 mmol) and two drops of dry dimethylformamide in dry methylene chloride (10 mL) a solution of oxalyl chloride (0.39 g, 3.1 mmol) in methylene chloride (5 mL) was added dropwise. The mixture was stirred overnight at room temperature in the absence of light and subsequently, the solvent was removed by evaporation *in vacuo* and the compound (**12**) was dried under vacuum (1 mbar) for 2 h. The product was dissolved in dry methylene chloride (20 mL) and added dropwise via a syringe to an ice-cooled, magnetically stirred solution of 2,2'-bipyridine-3,3'-diamine (**8**) (0.521 g, 2.8 mmol) and triethylamine (0.38 mL, 2.8 mmol) in dry methylene chloride (25 mL). Stirring was continued for another 2 h at 0°C and subsequently overnight at room temperature. The solution was diluted with methylene chloride and

washed with water (2x) and brine (1x), dried over sodium sulfate and the solvents were evaporated *in vacuo*. The crude product was purified by column chromatography (silica; 5% methanol in methylene chloride) and preparative size exclusion chromatography (methylene chloride) to yield the title compound as a yellow oil (2.2 g, 2.03 mmol, 78%). The product was thoroughly dried *in vacuo* over P₂O₅. ¹H-NMR (CDCl₃): δ = 14.40 (s, 1H), 9.21 (dd, *J* = 8.5 and 1.7 Hz, 1H), 8.33 (dd, *J* = 4.6 and 1.5 Hz, 1H), 8.03 (dd, *J* = 3.9 and 1.8 Hz, 1H), 7.33 (m, 3H), 7.15 (m, 2H), 6.57 (s, 2H), 4.12-4.05 (m, 3H), 3.98-3.53 (m, 54H), 3.38 (s, 3H), 3.37 (s, 6H), 1.32 (m, 9H). ¹³C-NMR (CDCl₃): δ = 165.7 (CO); 152.4 (C-3 benzoyl); 145.1 (C-3); 143.6 (C-4 benzoyl); 141.2 (C-2'); 140.8 (C-2); 138.4 (C-6'); 135.9 (C-3'); 134.8 (C-6); 130.7 (C-4'); 128.5 (C-1 benzoyl); 125.2 (C-5'); 124.2 (C-5); 122.7 (C-4); 106.7 (C-2 benzoyl); 76.3, 75.0, 74.3, 72.9, 71.8, 70.7, 70.4, 70.3, 68.8, 68.5, 58.9, 17.4 (CCH₃).

3'-{3,4,5-Tris[2-(2-{2-[2-(2-methoxyethoxy)-ethoxy]-ethoxy}-ethoxy)-ethoxy]-benzoylamino}-2,2'-bipyridine-3-amine (5). A solution of oxalyl chloride (0.40 g, 3.2 mmol) in dry CH₂Cl₂ (5 ml) containing a catalytic amount of DMF was added dropwise to a solution of **7** (2.53 g, 2.9 mmol, 0.28 ml) in dry CH₂Cl₂ (10 mL). The reaction mixture was stirred overnight at room temperature in the absence of light and evaporating the solvent *in vacuo* afforded the crude product **13** (2.50 g, 2.8 mmol, 95%). This product was dissolved in dry CH₂Cl₂ (25 mL) and added dropwise to a stirred solution of 2,2'-bipyridyl-3,3'-diamine (0.59 g, 3.2 mmol) and triethylamine (0.32 g, 3.2 mmol, 0.45 mL) in dry CH₂Cl₂ (25 mL), while the temperature was kept below 5 °C. After stirring for 1h the solution was diluted with CH₂Cl₂, washed with water (3 x 25 mL) and brine (1 x 25 mL) and dried over MgSO₄. After evaporation of the solvents *in vacuo* the crude product was purified by column chromatography (silica, EtOAc followed by 5% methanol in chloroform) and size exclusion chromatography. Drying over P₂O₅ gave compound **7** (1.57 g, 1.5 mmol, 54%). ¹H-NMR (CDCl₃): δ = 14.40 (s, 1H, NHCO); 9.21 (dd, *J* = 8.4 and 1.8 Hz, 1H, *H*-4'); 8.34 (dd, *J* = 4.5 and 1.5 Hz, 1H, *H*-6'); 8.04 (dd, *J* = 2.9 and 2.7 Hz, 1H, *H*-6); 7.33 (s, 2H, *H*-benzoyl); 7.31 (dd, *J* = 9.0 and 4.2 Hz, 1H, *H*-5'); 7.15 (m, 2H, *H*-4 and *H*-5); 6.59 (s, 2H, NH₂); 4.25 (m, 6H, benzoyl-OCH₂); 3.89 (t, 4H, *m*-OCH₂CH₂); 3.82 (t, 2H, *p*-OCH₂CH₂); 3.75-3.52 (m, 48H, OCH₂CH₂O), 3.37 (s, 6H, *m*-OCH₃); 3.36 (s, 3H, *p*-OCH₃). ¹³C-NMR (CDCl₃): δ = 165.7 (CO); 152.6 (C-3 benzoyl); 145.1 (C-3); 143.6 (C-4 benzoyl); 142.0 (C-2'); 140.8 (C-2); 138.5 (C-6'); 136.1 (C-3'); 135.0 (C-6); 130.8 (C-4'); 128.6 (C-1 benzoyl); 125.3 (C-5'); 124.3 (C-5); 122.7 (C-4); 107.8 (C-2 benzoyl); 72.4-69.2 (OCH₂CH₂O); 59.0 (OCH₃). IR (ATR): ν = 3416, 2870, 1665, 1574, 1493, 1329, 1205, 1102, 851. Anal. Calcd for C₅₀H₈₀N₄O₁₉ (Mw = 1041.19 g/mol): C, 57.68; H, 7.74; N, 5.38; Found: C, 57.07; H, 7.74; N, 5.45.

3.8 References and notes

- ¹ Rivera, J.M.; Martin, T.; Rebek Jr., J. *Science* **1998**, *279*, 1021-1023.
- ² Simanek, E.E.; Qiao, S.; Choi, I.S.; Whitesides, G.M. *J. Org. Chem.* **1997**, *62*, 2619-2621.
- ³ Prins, L.J.; Huskens, J.; de Jong, F.; Timmerman, P.; Reinhoudt, D.N. *Nature* **1999**, *398*, 498-502.
- ⁴ Russell, K. C.; Lehn, J.-M.; Kyritsakas, N.; DeCian, A.; Fischer, J. *New J. Chem.* **1998**, 123-128.
- ⁵ Palmans, A.R.A.; Vekemans, J.A.J.M.; Havinga, E.E.; Meijer, E.W. *Angew. Chem. Int. Ed. Engl.* **1997**, *36*, 2648-2651.
- ⁶ Yashima, E.; Maeda, K.; Okamoto, Y. *Nature* **1999**, *399*, 449-451.
- ⁷ Langeveld-Voss, B.M.W.; Waterval, R.J.M.; Janssen, R.A.J.; Meijer, E.W. *Macromolecules* **1999**, *32*, 227-230.
- ⁸ Mayer, S.; Maxein, G.; Zentel, R. *Macromolecules* **1998**, *31*, 8522-8525.
- ⁹ Gu, H.; Nakamura, Y.; Sato, T.; Teramoto, A.; Green, M.M.; Jha, S.K.; Andreola, C.; Reidy, M.P. *Macromolecules* **1998**, *31*, 6362-6368.
- ¹⁰ Schlitzer, D.S.; Novak, B.M. *J. Am. Chem. Soc.* **1998**, *120*, 2196-2197.
- ¹¹ Yashima, E.; Matsushima, T.; Okamoto, Y. *J. Am. Chem. Soc.* **1997**, *119*, 6345-6359.
- ¹² Gulik-Krzywicki, T.; Fouquey, C.; Lehn, J.-M. *Proc. Natl. Acad. Sci. U.S.A.* **1993**, *90*, 163-167.
- ¹³ Green M.M.; Peterson, N.C.; Sato, T.; Teramoto, A.; Cook, R.; Lifson, S. *Science* **1995**, *268*, 1860-1866.
- ¹⁴ Moore, J.S.; Gorman, C.B.; Grubbs, R.H. *J. Am. Chem. Soc.* **1991**, *113*, 1704-1712.
- ¹⁵ Prince, R.B.; Brunsveld, L.; Meijer, E.W.; Moore, J.S. *Angew. Chem. Int. Ed.* **2000**, *39*, 228-231. See also chapter 6 of this thesis.
- ¹⁶ Blokzijl, W.; Engberts, J.B.F.N. *Angew. Chem. Int. Ed. Engl.* **1993**, *32*, 1545-1579.
- ¹⁷ See for example chapter 2 for the difficulty for structures based on hydrogen bonding only, to form helical architectures in water.
- ¹⁸ Creighton, T.E. *Proteins, structures and molecular properties*; W.H. Freeman and Company: New York, **1984**.
- ¹⁹ *Prediction of protein structure and the principles of protein conformation*; Fasman, G.D. Eds.; Plenum Press: New York, **1990**.
- ²⁰ Seebach, D.; Matthews, J.L. *Chem. Commun.* **1997**, 2015-2022.
- ²¹ Gellman, S.H. *Acc. Chem. Res.* **1998**, *31*, 173-180.
- ²² Kirshenbaum, K.; Zuckermann, R.N.; Dill, K.A. *Curr. Opin. Struct. Biol.* **1999**, *9*, 530-535.
- ²³ Kunitake, T. *Angew. Chem. Int. Ed. Engl.* **1992**, *31*, 709-726.
- ²⁴ Rotello, V.M.; Viani, E.A.; Deslongchamps, G.; Murray, B.A.; Rebek, J., Jr. *J. Am. Chem. Soc.* **1993**, *115*, 797-798.
- ²⁵ Bonazzi, S.; De Morais, M.M.; Gottarelli, G.; Mariani, P.; Spada, G.P. *Angew. Chem. Int. Ed. Engl.* **1993**, *32*, 248-250.
- ²⁶ Carsughi, F.; Di Nicola, G.; Gottarelli, G.; Mariani, P.; Mezzina, E.; Sabatucci, A.; Spada, G.P.; Bonazzi, S. *Helv. Chim. Acta* **1996**, *79*, 220-234.
- ²⁷ Nowick, J.S.; Cao, T.; Noronha, G. *J. Am. Chem. Soc.* **1994**, *116*, 3285-3289.
- ²⁸ Torneiro, M.; Still, W.C. *J. Am. Chem. Soc.* **1995**, *117*, 5887-5888.
- ²⁹ Torneiro, M.; Still, W.C. *Tetrahedron* **1997**, *53*, 8739-8750.
- ³⁰ Bonar-Law, R.P. *J. Am. Chem. Soc.* **1995**, *117*, 12397-12407.
- ³¹ Appella, D.H.; Barchi Jr., J.J.; Durell, S.R.; Gellman, S.H. *J. Am. Chem. Soc.* **1999**, *121*, 2309-2310.
- ³² Hirschberg, J.H.K.K.; Brunsveld, L.; Ramzi, A.; Vekemans, J.A.J.M.; Sijbesma, R.P.; Meijer, E.W. *Nature* **2000**, *407*, 167-170.
- ³³ An interesting account on recognition at the air-water interface via hydrogen bonding has been given by Kunitake: Ariga, K.; Kunitake, T. *Acc. Chem. Res.* **1998**, *31*, 371-378.
- ³⁴ For a recent review on chromonics see: Lydon, J. *Curr. Opin. Colloid Interface Sci.* **1998**, *3*, 458-466.
- ³⁵ Kilbinger, A.F.M.; Schenning, A.P.H.J.; Goldoni, F.; Feast, W.J.; Meijer, E.W. *J. Am. Chem. Soc.* **2000**, *122*, 1820-1821.
- ³⁶ Green, M.M.; Reidy, M.P.; Johnson, R.D.; Darling, G.; O'leary, D.J.; Wilson, G. *J. Am. Chem. Soc.* **1989**, *111*, 6452-6454.
- ³⁷ Palmans, A.R.A.; Vekemans, J.A.J.M.; Fischer, H.; Hikmet, R.A.; Meijer, E.W. *Chem. Eur. J.* **1997**, *3*, 300-307.
- ³⁸ The higher boiling point of n-butanol, with respect to methanol and ethanol, enables the use of temperature as a tool to induce denaturation of the self-assemblies.

- ³⁹ van der Schoot, P.; Michels, T.; Brunsveld, L.; Sijbesma, R.P.; Ramzi, A. *Langmuir*, **2000**, *16*, 10076-10083.
- ⁴⁰ van der Meulen, P.; Zhang, H.; Jonkman, A.M.; Glasbeek, M. *J. Phys. Chem.* **1996**, *100*, 5367-5373.
- ⁴¹ Proposito, P.; Marks, D.; Zhang, H.; Glasbeek, M. *J. Phys. Chem. A* **1998**, *102*, 8894-8902.
- ⁴² Eyal, M.; Reisfeld, R.; Chernyak, V.; Kaczmarek, L.; Grabowska, A. *Chem. Phys. Lett.* **1991**, *176*, 531-535.
- ⁴³ Bulska, H. *Chem. Phys. Lett.* **1983**, *98*, 398-402.
- ⁴⁴ Horng, M.L.; Gardecki, J.A.; Papazyan, A.; Maroncelli, M. *J. Phys. Chem.* **1995**, *99*, 17311-17337.
- ⁴⁵ Lifetime measurements were performed using the picosecond fluorescence setup described previously: Middelhoek, E.R.; van der Meulen, P.; Verhoeven, J.W.; Glasbeek, M. *Chem. Phys.* **1995**, *198*, 373-380.
- ⁴⁶ Transients were found to be independent of the detection wavelength (520, 570 and 620 nm).
- ⁴⁷ Chan, H.S.; Bromberg, S.; Dill, K.A. *Phil. Trans. R. Soc. Lond. B* **1995**, *348*, 61-70.
- ⁴⁸ Brunsveld L.; Schenning, A.P.H.J.; Broeren, M.A.C.; Janssen, H.M.; Vekemans, J.A.J.M.; Meijer, E.W. *Chem. Lett.* **2000**, 292-293.
- ⁴⁹ Yasuda, Y.; Iishu, E.; Inada, H.; Shirota, Y. *Chem. Lett.* **1996**, 575-576.
- ⁵⁰ Yasuda, Y.; Takebe, Y.; Fukumoto, M.; Inada, H.; Shirota, Y. *Adv. Mater.* **1996**, *8*, 740-741.
- ⁵¹ Klug, A. *Angew. Chem.* **1983**, *95*, 579-596.
- ⁵² The discotics discussed here are not formed via self-assembly of smaller units, however it is possible to create such architectures and in chapter 5 such a system will be discussed.
- ⁵³ Feringa, B.L.; van Delden, R.A.; *Angew. Chem. Int. Ed.* **1999**, *38*, 3419-3438.
- ⁵⁴ Avalos, M.; Babiano, R.; Cintas, P.; Jiménez, J.L.; Palacios, J.C. *Chem. Commun.* **2000**, 887-892.
- ⁵⁵ Farina, M. *The stereochemistry of linear macromolecules*; In: Eliel, E.L.; Wilen, S.H. editors. Topics in stereochemistry. New York: John Wiley & Sons; **1987**. Iss17, p1-112.
- ⁵⁶ Green, M.M.; Garetz, B.A.; Munoz, B.; Chang, H.; Hoke, S.; Cooks, R.G. *J. Am. Chem. Soc.* **1995**, *117*, 4181-4182.
- ⁵⁷ Green, M.M.; Park, J.-W.; Sato, T.; Teramoto, A.; Lifson, S.; Selinger, R.L.B.; Selinger, J.V. *Angew. Chem. Int. Ed.* **1999**, *38*, 3138-3154.
- ⁵⁸ Li, J.; Schuster, G.B.; Cheon, K.-S.; Green, M.M.; Selinger, J.V. *J. Am. Chem. Soc.* **2000**, *122*, 2603-2612.
- ⁵⁹ Castellano, R.K.; Nuckolls, C.; Rebek Jr., J. *J. Am. Chem. Soc.* **1999**, *121*, 11156-11163.
- ⁶⁰ Brunsveld, L.; Lohmeijer, B.G.G.; Vekemans, J.A.J.M.; Meijer, E.W. *Chem. Commun.*, **2000**, 2305-2306.
- ⁶¹ The degree of polymerization calculated using the association constant K has an error of around 10 %.
- ⁶² Brunsveld, L.; Zhang, H.; Glasbeek, M.; Vekemans, J.A.J.M.; Meijer, E.W. *J. Am. Chem. Soc.* **2000**, *122*, 6175-6182. See also in this chapter paragraph 3.2
- ⁶³ Bailey, F. Jr.; Koleske, J. *Poly (Ethylene Oxide)* Academic Press Inc., New York, **1976**.
- ⁶⁴ This seems to be the first example of increasing stack length at increased temperatures. The comparison might be made however, to PEO-PPO-PEO copolymers that have been shown to form aggregates at high temperatures in water, while being molecular dispersed at low temperatures. Mortensen, K. *J. Phys.: Condes. Matter* **1996**, *8*, A103-A124.
- ⁶⁵ Stryer, L. *Biochemistry*, **1997**, 4th ed., W.H. Freeman and Company, New York.
- ⁶⁶ For a full account on the 20 step synthesis of **11** see: Lohmeijer, B.G.G. *Supramolecular architectures in polar media*, **2000**, graduation report Eindhoven University of Technology.
- ⁶⁷ For a description of the general procedures see also chapter 2, section 2.5 Experimental section.
- ⁶⁸ Kaczmarek, L.; Nantka-Namirski, P. *Acta. Polon. Pharm.* **1979**, *6*, 629-634.
- ⁶⁹ Palmans, A.R.A.; Vekemans, J.A.J.M.; Meijer, E.W. *Recl. Trav. Chim. Pays-Bas* **1995**, *114*, 277-284.

Chapter 4

Solid-state organization and ion conduction of oligo(ethylene oxide) modified extended core discotics

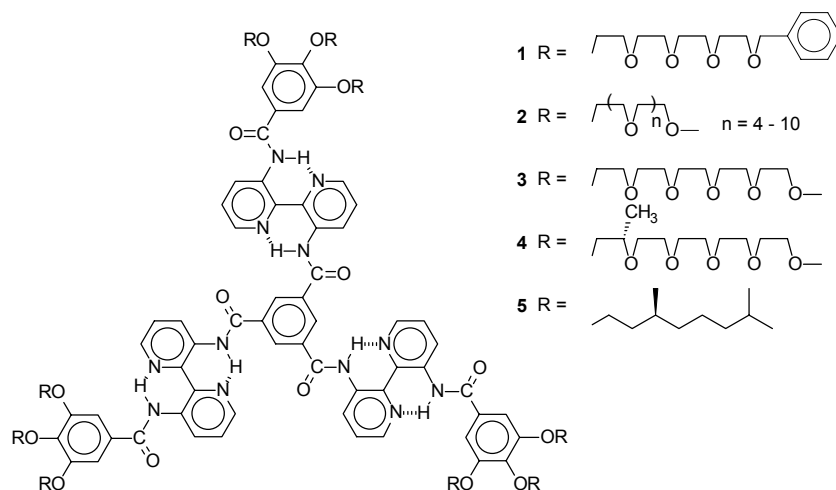
Abstract: *This chapter describes the solid-state organization of oligo(ethylene oxide) modified extended core discotic liquid crystals and the influence of added salt on the mesomorphic behavior and the accompanying ion conduction. The investigated discotic liquid crystalline compounds are C₃-symmetric trimesic amide derivatives bearing peripheral oligo(ethylene oxide) side chains (compounds 1 - 4). They show discotic mesomorphism in a broad temperature range due to the oligo(ethylene oxide) modified mesogenic groups, the strong arene-arene interactions and the hydrogen bonding interactions in the extended aromatic core ($T_g \sim -70^\circ\text{C}$; $T_{cl} \sim 280^\circ\text{C}$). Mixtures of compounds 1 or 2 and lithium perchlorate (LiClO_4) also exhibit liquid crystalline properties as shown by polarization microscopy, DSC and X-ray diffraction measurements. A significant increase of the T_g as well as a strong decrease of the clearing temperature are observed with increasing salt concentration. The salt induces disorder in the stacking between the molecules and is even capable of suppressing the liquid crystallinity. The ion conducting properties of the mixtures have been measured by complex impedance spectroscopy at different temperatures. Highly promising levels of conductivity, over 1×10^{-5} S/cm at room temperature and 6×10^{-4} S/cm at 100°C , have been recorded. Since these discotic liquid crystals are waxy solids not flowing without considerable stress, they may be of interest as electrolyte systems.*

4.1 Introduction

Since the discovery in 1977¹ of mesomorphism in disc-shaped molecules (discotic behavior), the synthesis and physical characterization of these molecules have been the subject of many profound and detailed studies.² Mesomorphism, or liquid crystallinity (LC), has been found in small disc-shaped molecules such as hexa-substituted benzenes and hexa-alkoxy-triphenylenes,³ and is also displayed by compounds with large aromatic cores such as hexa-peri-hexabenzocoronenes⁴ and *m*-phenylene ethynylene macrocycles.⁵ Disc-shaped molecules with extended cores experience strong π - π interactions between the rigid aromatic fragments and therefore, these compounds display mesophases in broad temperature windows.⁶⁻⁸ Also a high viscosity is obtained, the two being the main advantages of larger discotics over smaller discotics. Extended cores for discotic liquid crystals (LCs) can be built up *via* covalent bonds, but it is also possible to use secondary interactions such as metal-ion complexation,⁹⁻¹⁵ intermolecular H-bonds¹⁶⁻²⁴ and, less frequently used, intramolecular H-bonds.^{25,26} Recently, a new class of molecules, displaying discotic behavior, has been developed.²⁷ These compounds consist of a C_3 -symmetrical extended core with three intramolecularly hydrogen-bonded 3,3'-bis(acylamino)-2,2'-bipyridine units, each unit bearing three peripheral aliphatic chains (see for example structure **5**). The molecules associate into columns *via* π - π stacking and hydrogen bonding interactions. Columnar mesophases that are stable over broad temperature ranges have been observed for these systems ($\sim 20 - \sim 380$ °C).²⁷

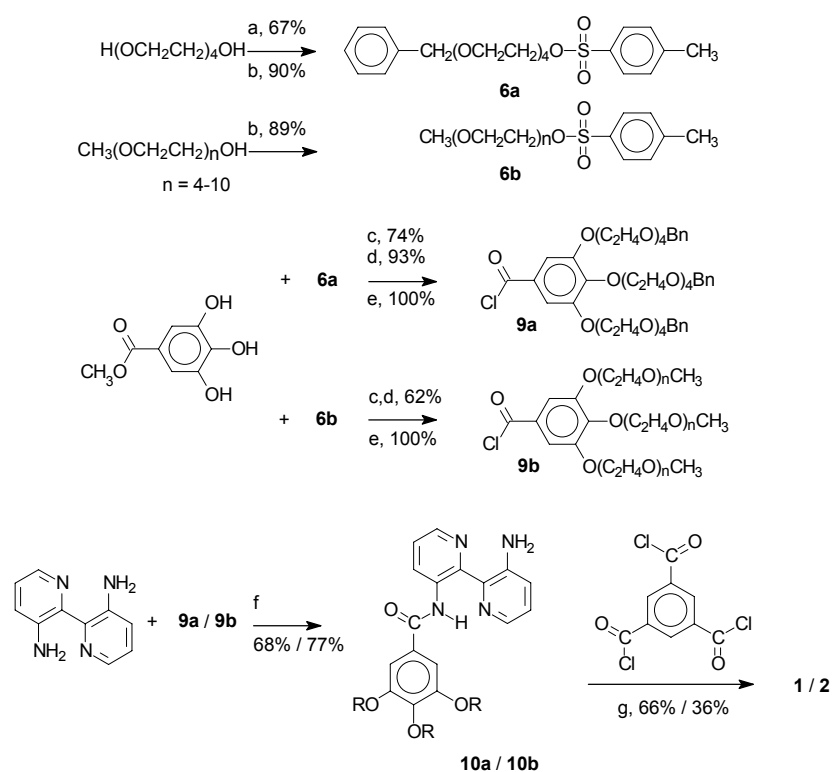
The peripheral side-chains in reported discotic LCs range from apolar aliphatics to polar oligo(ethylene oxide)s.² When oligo(ethylene oxide) side chains are used, it becomes possible to solvate salts in these side-chains, an interesting and attractive feature for a number of reasons. First, the added salt will exert a distinct influence on the mesophase properties. For calamitic LCs, the effect of added salt on the LC-characteristics has been investigated,²⁸ but a similar study has not been performed on disc-shaped LCs.²⁹ Secondly, LC-materials contain an amorphous, more or less liquid-like matrix –their flexible side-chains– and such a matrix is ideally suited to act as an ion transporting medium. The latter requires that (i) this matrix is capable of solvating ions (a trivial requirement) and (ii) the melting or glass transition temperature of the LC-material under investigation is well below room temperature, allowing the application of the material as an ion conductor at conventional temperatures.³⁰ Oligo(ethylene oxide) side chains fulfill these requirements and the ion conducting properties of a few salt-doped LCs have been investigated already.^{29,31-40} Recently, Kato and co-workers described a liquid crystalline ion-conductive material featuring a promising conductivity of *ca.* 10^{-5} (S/cm) at room temperature.^{41,42}

In this chapter, the synthesis of disc-shaped LC-compounds **1** and **2** is reported and their solid state characterization as well as that of previously described compounds **3** and **4**.⁴³ Furthermore, the influence of added salt on the liquid crystallinity of these materials (**1** and **2**) is discussed and the ion conducting properties of these salt mixtures have been investigated.⁴⁴



4.2 Synthesis and characterization

Disc-shaped molecules **1** and **2** were synthesized by a convergent approach, consisting of four parts: the synthesis of 2,2'-bipyridine-3,3'-diamine,⁴⁵ the synthesis of the activated mesogenic group – acid chlorides **9a** and **9b**– the mono-*N*-acylation of the 2,2'-bipyridine-3,3'-diamine with the acid chlorides and, finally, the coupling of three molecules of mono-acylated bipyridine to trimesic chloride, the central core (Scheme 4.1).



Scheme 4.1: Synthesis of discotics **1** and **2**. a) BnCl , NaOH , water, $100\text{ }^\circ\text{C}$; b) $p\text{-TsCl}$, NaOH , THF/water , $0\text{ }^\circ\text{C}$; c) K_2CO_3 , DMF , $70\text{ }^\circ\text{C}$; d) KOH , EtOH/water , $90\text{ }^\circ\text{C}$; e) oxalyl chloride, CH_2Cl_2 , *r.t.*; f) Et_3N , CH_2Cl_2 , $0\text{ }^\circ\text{C}$; g) Et_3N , CH_2Cl_2 , *r.t.*

The synthesis of acid chloride **9a** started with the monobenylation of tetra(ethylene oxide). As reported, a four-fold excess of tetra(ethylene oxide) was used.⁴⁶ Both mono-*O*-benzyl tetra(ethylene oxide) as well as mono-*O*-methyl oligo(ethylene oxide) ($n = 4-10$) were treated with *p*-tosyl chloride, using a two phase system of alkaline water and THF.⁴⁷ The *p*-tosylates thus obtained (**6a-b**) were used for the alkylation of methyl 3,4,5-trihydroxybenzoate. Next, the esters **7a-b** were saponified in an alkaline solution of water and ethanol to afford acids **8a** and **8b**. Finally, these acids were converted to their corresponding acid chlorides **9a-b** using oxalyl chloride in CH₂Cl₂.⁴⁸ The yields in the consecutive reaction steps towards the acid chlorides **9a** and **9b** were usually very good.

Previous studies have shown that the mono-*N*-acylation of 2,2'-bipyridine-3,3'-diamine can proceed with a high selectivity (85%).²⁷ This selectivity is caused by the decrease in nucleophilicity of the second amine as soon as the 2,2'-bipyridine-3,3'-diamine has been *N*-acylated once. Thus, acid chlorides experience a greater reactivity towards 2,2'-bipyridine-3,3'-diamine than towards a mono-acylated species of this diamine. To improve the observed selectivity to an even higher extent, the acylation was carried out in a somewhat dilute solution (~0.1 M), at a low temperature (0 °C), and—most importantly—the solution of the acid chloride in CH₂Cl₂ was added dropwise to the solution of the 2,2'-bipyridine-3,3'-diamine. The slow addition prevented the occurrence of high local concentrations of acid chloride which would favor undesired diacylation of the 2,2'-bipyridine-3,3'-diamine. ¹H-NMR of the crude reaction mixture indeed indicated that the desired compounds (**10a-b**) were formed in a very high selectivity of 98%. The selectivity greatly benefits to a high yield and easy purification. Nevertheless, column chromatography remained the only means to purify the products **10a-b**. The high polarity of both mono-acylated product and di-acylated contaminant (2%) made the column separation difficult, but eventually **10a** and **10b** could be obtained in good yields of 71% and 77%, respectively. Compounds **10a-b** are highly hygroscopic due to the pendant oligo(ethylene oxide) chains and the free amines. To ensure a complete reaction with the benzene-1,3,5-tricarbonyl trichloride in the next step, several methods were tested to remove traces of water from compounds **10a** and **10b** (MgSO₄, co-evaporation with toluene, molsieves, P₂O₅). The only successful and convenient method to remove the residual water was drying of the compounds in a vacuum desiccator over P₂O₅ for 24 hours. Disc-shaped molecules **1** and **2** were synthesized by reacting three equivalents of dried **10a-b** with benzene-1,3,5-tricarbonyl trichloride. Due to the polar character of the molecules, purification was extensive, but column chromatography could still be used to isolate the targeted materials. Substances **1-2** were obtained as light yellow, birefringent, waxy and sticky solids. Both substances are hygroscopic, but drying over P₂O₅ in a vacuum desiccator can remove all water. Attempts to debenzylate compound **1** failed. Catalytic debenzylation using H₂ / Pd/C in a variety of solvents (ethyl acetate, ethanol, aqueous acidic ethanol) was tried, but the catalyst seemed to be deactivated by complexation with the aromatic core of the molecules.

All new compounds were characterized by $^1\text{H-NMR}$, $^{13}\text{C-NMR}$ and IR spectroscopy. Compound **1**, with tetra(ethylene oxide) side chains, gave satisfactory elemental analyses and mass spectral data. Compound **2**, with the oligo(ethylene oxide) side chains, was not characterized using this technique, since these materials are not pure compounds but polydisperse mixtures. Size exclusion chromatography measurements confirmed the integrity of the discotics **1-2** with respect to higher and lower molecular weight substances.

Mixtures of lithium perchlorate (LiClO_4) with compounds **1** and **2** were made in various ratios by mixing the appropriate amounts in THF solutions followed by evaporation of the solvent (Table 4.1). Blends with increasing concentrations of salt (mixtures **1a-e** and **2a-e**) were thus obtained. In order to compare systems **1** and **2** adequately, the ratio of LiClO_4 molecules per ethylene oxide unit was kept constant for every pair of mixtures **1a-2a**, **1b-2b**, etc.

Table 4.1 Thermotropic behavior of compounds **1-4** and mixtures **1a-e** and **2a-e** with LiClO_4 .

Compound / Mixture	Li^+ per molecule	$\text{Li}^+:\text{EO}$ ratio	T_g	Mesophase	T_{cl}
1	0	0	-50	Col_{ho}	244
1a	1	1:36	-42	Col_{ho}	242
1b	2	1:18	-29	Col_{ho}	230
1c	3	1:12	-16	Col_{ho}	222
1d	6	1:6	3	Col_{hd}	182
1e	9	1:4	14	Col_{hd}	145
2	0	0	-73	Col_{ho}	214
2a	1.75	1:36	-61	Col_{ho}	194
2b	3.5	1:18	-50	Col_{ho}	181
2c	5.25	1:12	-41	Col_{hd}	168
2d	10.5	1:6	-28	Col_{hd}	134
2e	15.75	1:4	-26	-	-
3	0	0	-67	Col_{ho}	282
4	0	0	-74	Col_{ho}	270

$^1\text{H-NMR}$ spectra of substances **1** and **2** in deuterated chloroform showed sharp signals suggesting that the compounds are molecularly dissolved (as an example the spectrum of **1** is shown in Figure 4.1). The downfield NH absorptions at 14.5 and 15.5 ppm indicate the presence of intramolecular hydrogen bonds. The H-4 and H-4' protons at 9.60 and 9.38 ppm are deshielded as a result of the adjacent carbonyl functionalities. The strong hydrogen bonds as well as the distinct deshielding effect indicate the formation of a planar, transoid bipyridine system and, thus, the whole disc-shaped molecule must be strongly planarized, although rotation about the carbonyl benzene

bonds is still possible. In previous studies, the occurrence of intramolecular hydrogen bonding in *N*-acylated 2,2'-bipyridine-3,3'-diamine systems and the formation of planar, transoid bipyridines have been explored extensively.^{49,50} Strikingly, the difference in environment of the *meta* and *para* positions in the 3,4,5-trialkoxy benzamide could be discerned *via* ¹H NMR. For compound **1**, the Ar-OCH₂CH₂O signals of the *meta* and *para* ethylene oxide side chains were found at $\delta = 3.90$ and 3.84 ppm, respectively. Even the CH₂Ph signals (the benzylic protons) were located differently (at $\delta = 4.54$ and 4.56 ppm for the *meta* and *para* protons, respectively), showing the long range order within the architecture.

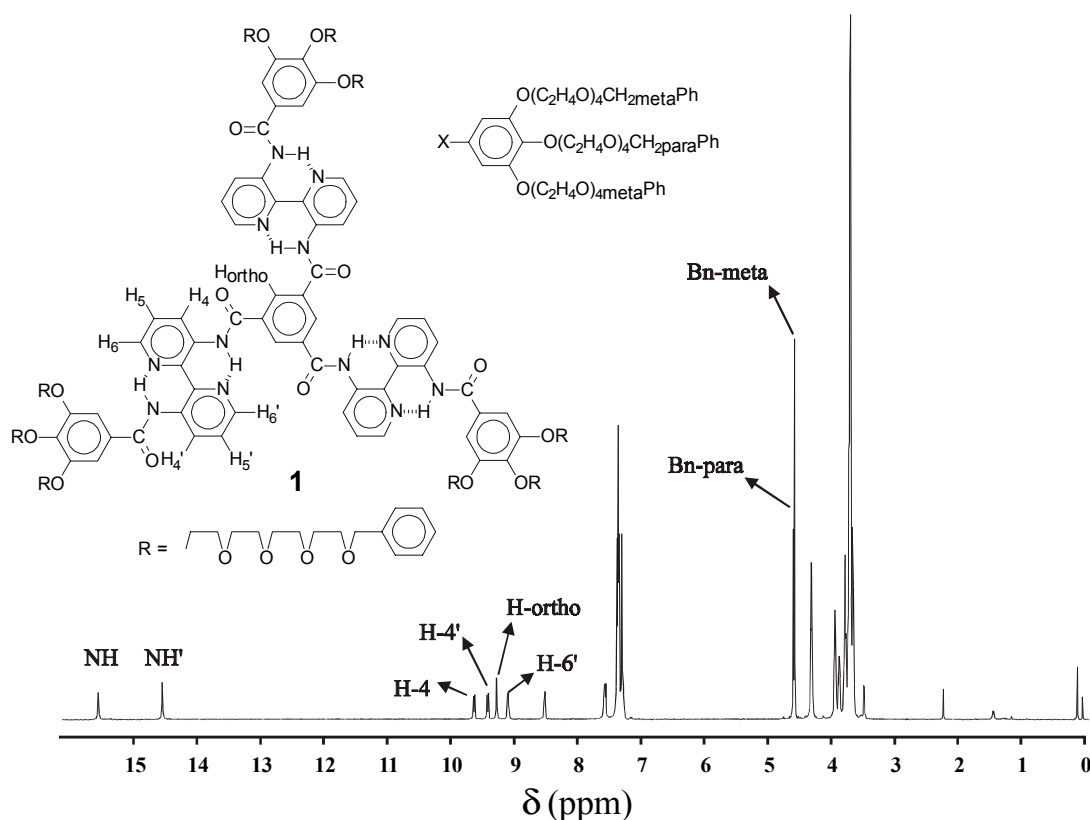


Figure 4.1: ¹H-NMR (400 MHz) spectrum of **1** in CDCl₃. The signals of the aromatic core are partially assigned and the difference between the benzylic *meta* and *para* protons is indicated.

The ¹H-NMR spectra of LiClO₄ mixtures **1a-e** or **2a-e** in deuterated chloroform showed broad signals as opposed to the sharp signals that were observed in the case of the salt-free compounds **1** and **2**. The broadening of the signals is certainly caused by the aggregation of the molecules.⁵¹ Presumably, the aggregation process is induced by the complexation of lithium cations with the pendant ethylene oxide chains (the cations will complex both intramolecularly as well as intermolecularly). The complexation in the side-chains causes subsequent π - π stacking between the large aromatic cores and, thus, the molecules aggregate. It should be noted that lithium perchlorate is not soluble in chloroform in the absence of compounds **1** and **2**.

4.3 Solid-state organization

4.3.1 Thermogravimetric analysis (TGA) and differential scanning calorimetry (DSC)

The thermal stability of the compounds **1** and **2** was investigated using TGA. Substances **1** and **2** showed *ca.* 5% weight loss under air at 240 °C and 200 °C, respectively. Presumably, the instability is the result of breakage of ether bonds. The temperature at which weight loss is observed is below the clearing temperature of the materials. Therefore, non-conventional peaks have been observed in DSC-runs for compounds **1-4** when several cycles were recorded around the initial clearing temperature (*i.e.* the clearing temperature observed in the first heating run, between 200 and 300 °C). The liquid crystal-salt mixtures **1a-e** and **2a-e** also displayed instability at higher temperatures (above 130 °C), due to degradation of the perchlorate anion. As a result determination of the melting enthalpies was not performed. All the clearing temperatures have been determined using polarization microscopy (*vide supra*, see Table 4.1), although the reported clearing temperatures were close to the clearing temperatures observed in the first runs of the DSC-experiments.

In Figure 4.2 the low-temperature regions of the DSC-scans are plotted. All transitions are reversible and the plotted heating runs have been obtained after several temperature cycles, during which the temperature did not exceed 100 °C. The plotted thermograms have been acquired using heating rates of 40 K/min, but the transitions found as such are not significantly different from those observed in measurements for which slower rates (10 K/min) have been used.

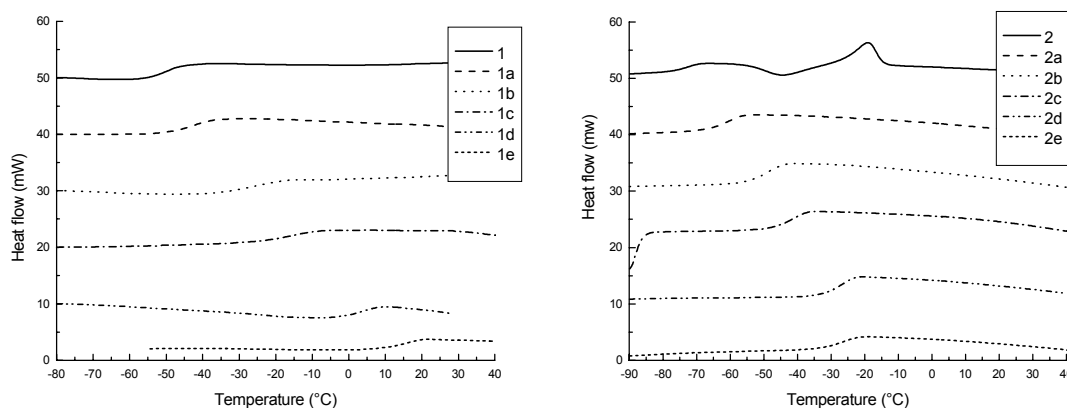


Figure 4.2: DSC thermodiagrams of compounds **1** and **2** and their mixtures with lithium perchlorate (**1a-e** and **2a-e**).

The low temperature phase transitions in substances **1-4** are not melting points but glass transitions (see Table 4.1 for all acquired T_g -values). The T_g of compound **1** was found at -50 °C, whereas substances **2-4** displayed a somewhat lower T_g around -70 °C. For substance **2**, additional side-chain recrystallization at -43 °C and subsequent melting at -18 °C were observed ($\Delta H = 75$ kJ/mol). Salt mixtures **1a-e** and **2a-e** showed a gradual increase in T_g upon increasing salt

concentration, resulting in a T_g for **1e** as high as 14 °C and a T_g for **2e** at -26 °C. At room temperature, mixture **1e** is a brittle solid material, whereas **2e** is still waxy like **2**, without added salt. The recrystallization and melting as observed for **2** disappeared in its salt mixtures **2a-e** (obviously, in these cases, the salt prohibits recrystallization of the side-chains).

The T_g 's of **1-4** are *ca.* 70 °C lower than the melting temperature of the previously reported LC-molecule provided with alkyl peripheral side-chains (compound **5**).²⁷ Apparently, the oligo(ethylene oxide) chains prevent crystallization and introduce an amorphous character to the material. The higher T_g 's of **1** as compared to the T_g of substances **2-4** can be rationalized by assuming a better packing of the benzyl groups in compound **1** relative to the packing of the methoxy moieties in **2-4**. Additionally, compound **1** has monodisperse short ethylene oxide side chains, whereas the side chains of **3** and **4** are somewhat longer, while the side chains of compound **2** even have an oligomeric character. The longer length of the side chains of compound **2** might be the cause for the occurrence of a recrystallization.

The increase of the T_g upon increasing salt concentration is a general phenomenon observed for polymers with hetero atoms.⁵² This increase is caused by ion-dipole solvation of the cations, which suppresses segmental motion of the ethylene oxide chains. When the difference in T_g of every couple of mixtures **1-2**, **1a-2a**, **1b-2b**, etc., is compared, a somewhat constant difference of 20–30 °C can be calculated. This observation indicates that the ratio of salt molecules per ethylene oxide unit (third column, Table 4.1) is an appropriate parameter to compare the T_g 's of the salt mixtures of **1** and **2**.

4.3.2 Polarization microscopy

All compounds and mixtures studied (except mixture **2e**) were highly viscous and birefringent at room temperature. The viscosity decreased upon increase of the temperature, resulting in low-viscosity samples at the clearing temperatures. The salt-LC mixtures did not display phase separation between liquid crystal and salt, indicating that all of the salt was completely dissolved in the ethylene oxide matrix. For all samples, the transition to the isotropic liquid state occurred rapidly within a temperature range of *ca.* 2 °C. Textures of the various mixtures were grown by slowly cooling the isotropic melt (1 K min⁻¹). The liquid crystalline phase reappeared only 1 or 2 degrees centigrade below T_{cl} , indicating a high degree of order, even in the isotropic state. The textures obtained showed large homeotropic monodomains with flower-like patterns, typical for discotic hexagonally ordered liquid crystalline systems (figure 4.3, left). The textures were similar to those of systems reported previously (such as LC-material **5**).²⁷

The salt-free materials **1** and **2** became isotropic at 244 °C and 214 °C, respectively. The T_{cl} 's gradually lower when **1** and **2** were charged with increasing amounts of LiClO₄ (see the T_{cl} 's of **1a-e** and **2a-e** in Table 4.1). Furthermore, it was observed that the salt influenced the size of the monodomains in the LC-textures: a higher salt concentration resulted in a considerable decrease in the

size of these domains. The flower-like texture, typical for Col_{ho} -phases, was also affected by the salt (Figure 4.3, right). At lower salt concentrations the flower-like texture could still be observed, but at increased salt levels the textures became less clear and, finally, became disordered (in these cases the mesophase is a Col_{hd} -phase, see also X-ray results). Mixture **2e** contained too much salt to retain birefringence. Only when shear was applied to this mixture, temporary birefringence could be observed as a result of short range alignment in the material.

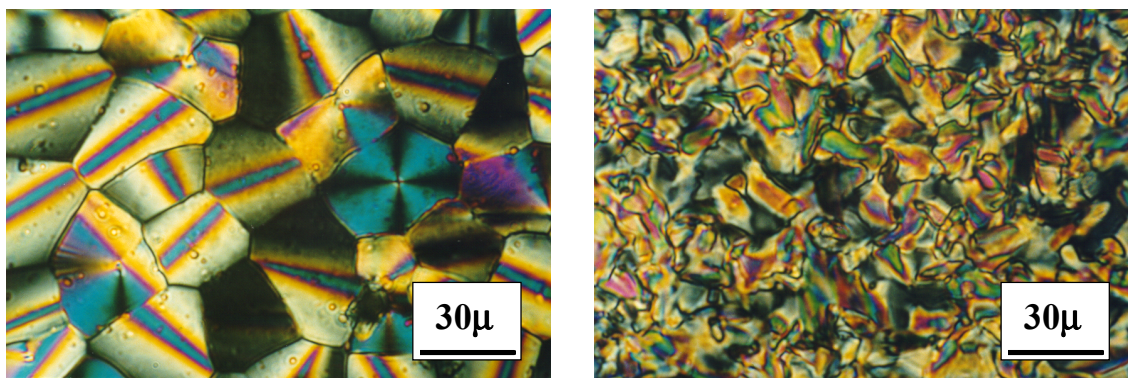


Figure 4.3: Optical microscopy photos of compound **1** (left) and mixture **1d** (right) after slow cooling from the melt to room temperature.

When the decrease of the clearing temperature of salt mixtures **1a-e** and **2a-e** is considered as a function of the salt concentration in salt-molecules per LC-molecule (second column, Table 4.1), a comparable decrease is observed. This indicates that the salt-concentration in salt-molecules per LC-molecule is an appropriate parameter to compare the T_{cl} 's of the salt mixtures **1a-e** and **2a-e**.

The decrease in clearing temperature can be explained considering the role of the salt more closely. On the one hand, the lithium cations act as a crosslinker between the different ethylene oxide side chains and, hence, these ions regulate the glass transition temperature (*vide supra*). On the other hand, the bulky perchlorate anions are important with respect to the packing in the LC-material. The anions are located in between the ethylene oxide side-chains, but are not bound to a specific unit of the molecule. The presence of the large anionic species, however, will influence the disc-to-disc distance and will render this distance less defined: disorder in the packing of the liquid crystal is introduced. Thus, the stacking between the aromatic cores is weakened and lower clearing temperatures are the result. In Figure 4.4 a cartoon is depicted visualizing the influence of the cations and anions on the packing of the molecules.

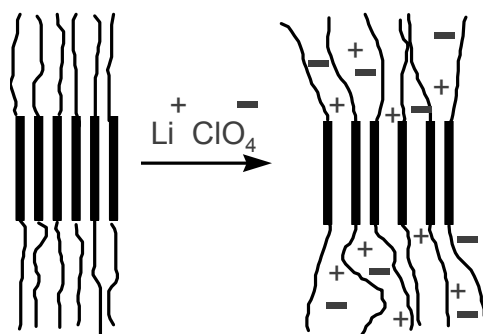


Figure 4.4: A cartoon representation of the influence of added salt on the self-assembly of discotics **1** and **2**. Without salt, the discotics are organized in ordered columns, with freely moving side-chains. Addition of salt accounts for lowering of the mobility of the side chains (increase of T_g), but at the same time for a less ordered packing of the aromatic core (decrease of T_c).

4.3.3 X-ray diffraction

Substances **1** and **2** and their mixtures with LiClO_4 were analyzed by X-ray diffraction measurements to investigate in detail the columnar mesophases observed *via* polarization microscopy. Materials **1** and **2** showed similar diffraction patterns and, as an illustration, the patterns of an unaligned and a shear-aligned⁵³ sample of **2** are displayed in Figure 4.5. The calculated diffraction spacings are summarized in Table 4.2. For compound **1**, four clear reflections are present in the small-angle area and two reflections in the wide-angle area. The reflections in the small-angle area are characteristic for a hexagonal arrangement of the columns. These reflections can be attributed to the 100, 110, 200 and 210 planes in the columnar packing of the molecules. The 100-reflection is very sharp and strong and from this reflection an intercolumnar distance of 42.5 Å can be calculated. At distances of $\sqrt{3}$, $\sqrt{4}$ and $\sqrt{7}$ the other three reflections are found. Upon shear alignment of the sample, the higher order reflections become splitted. This splitting of the reflections probably results from the helicity within the columns.^{27,54} By attaining a ship-screw conformation by the three wedges on the central core (Figure 4.7), these wedges are not in the plane of the 100 reflection anymore, which would give rise to a small inclination of the reflections. Because the helicity of the columns is random over the sample, this results in the occurrence of what looks like a splitting of the reflections. However, why this only effects the higher order reflections and not the 100 reflection is not clear yet. An alternative explanation is that the splitted reflections are independent reflections, not related to the hexagonal arrangement of the columns, and represent the helical pitch within the columns. This would also clarify why the 100 reflection is not splitted.

The two reflections in the wide-angle area feature d-spacings of 4.5 Å and 3.5 Å. The broad 4.5 Å reflection is the so-called halo-ring; it originates from the (weakly ordered) ethylene oxide side-chains. The 3.5 Å reflection is the typical 001 reflection that can be assigned to the disc-to-disc

distance between the aromatic cores. The 001 reflection is sharp, indicating that the molecules are stacked on top of each other in an ordered fashion. The diffraction pattern of the shear-aligned sample displays the 100 reflection perpendicular to the 001 reflection, proving the hexagonal arrangement of the columns. In conclusion, the diffraction data show that the mesophase of compound **1** is a columnar hexagonal ordered mesophase (Col_{ho}). Substance **2** shows identical features in the diffraction pattern, indicating a Col_{ho} mesophase for this material as well. In agreement with the larger size of the side chains in **2** as compared to those in **1**, a larger intercolumnar distance of 47.3 Å was calculated for **2**.

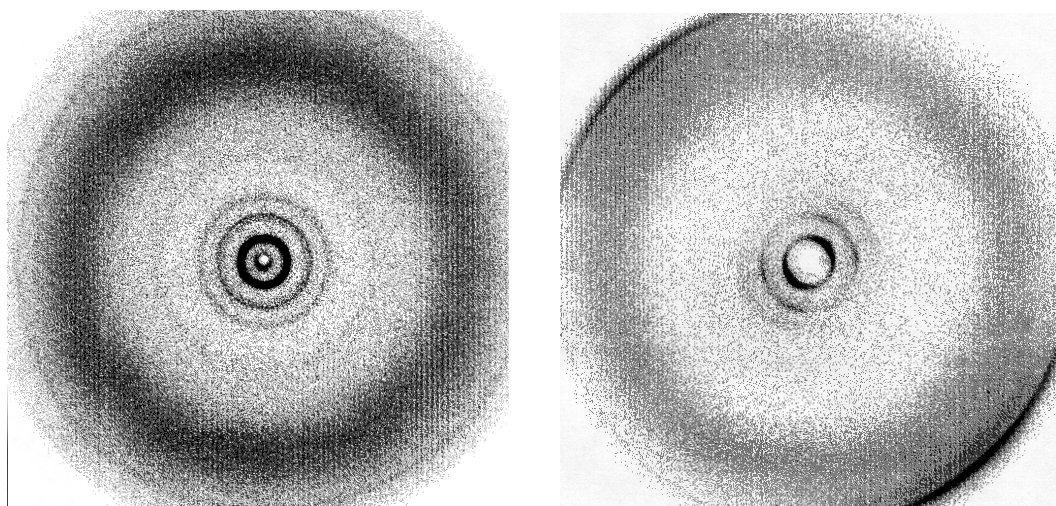


Figure 4.5: 2D X-ray diffraction patterns for non aligned (left) and shear aligned (right) **2**, measured at 20 °C.

Table 4.2 Diffraction spacings in Å obtained for compounds **1** and **2** at 20°C.

hkl	1	2
100	36.8	41.0
110 ⁺	21.0	-
200 ⁺	18.6	20.6
210 ⁺	13.8	15.2
splitted signal*	18.5	20.6
halo	4.5	4.2
001/interdisc	3.5	3.4
intercolumn	42.5	47.3

⁺these reflections were observed in the non aligned samples *this reflection was only observed in the shear aligned samples.

The influence of the lithium perchlorate on the X-ray diffraction pattern of the liquid crystals **1** and **2** is displayed in Figure 4.6. For both liquid crystalline systems, the intensity of the reflections decreases and the peaks broaden upon increasing salt concentration. The former phenomenon is due to the stronger X-ray absorption of the chloride in the perchlorate anion.⁵⁵ From mixtures **1c** and **2c** on, the reflections become significantly broader and for mixture **2e** the 001 reflection has disappeared totally. The broadening of the reflections is indicative for the introduction of disorder in the samples, implying a disorder in the packing of the molecules. Most strikingly, the disc-to-disc distance expressed in the 001-reflection becomes less well-defined at higher salt-ratios. Evidently, increasing salt concentrations cause the mesophase to change from a columnar hexagonal ordered mesophase (Col_{ho}) to a columnar hexagonal disordered mesophase (Col_{hd}). The absence of the 001 reflection in mixture **2e** shows that the packing of the aromatic cores is gone, suggesting the absence of long range order, in line with the loss of liquid crystallinity as observed with optical microscopy.

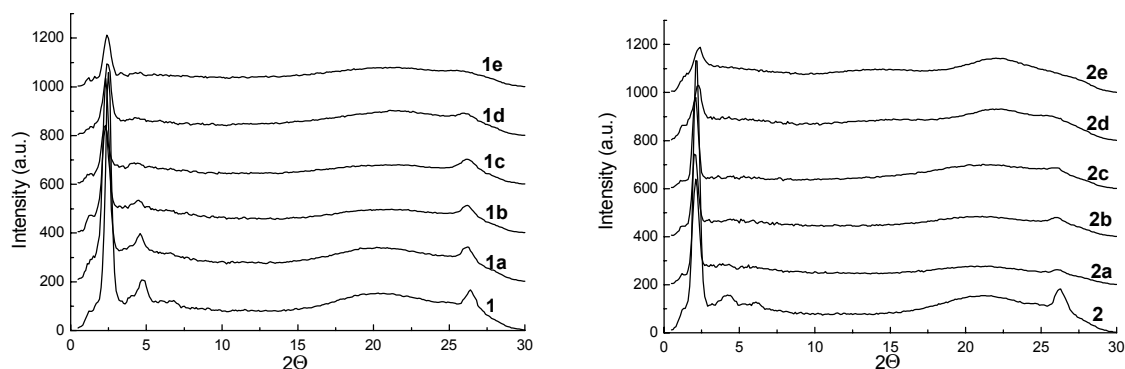


Figure 4.6: 1D X-ray diffraction patterns for **1** (left) and **2** (right) and their mixtures with lithium perchlorate (**1a-e** and **2a-e**).

4.3.4 Solid-state NMR

Solid state ^1H DQ MAS two dimensional NMR experiments have been performed on discotic **3** to obtain information about the order within the solid state. This technique provides information concerning the relative proximities of protons. As expected, the measurements revealed a significant mobility of the side-chains in the liquid crystalline state, a general phenomenon for liquid crystals. In contrast the mobility for the aromatic core was found to be restricted and indicates the absence of axial rotation. In other words, the discs do not rotate with respect to each other. This contrasts with the behavior of conventional discotic liquid crystals such as those with triphenylene or hexabenzocoronene as core.⁵⁶⁻⁵⁹ It is proposed that in the solid state molecules **1-4** attain a propeller-like conformation within the columns, like schematically shown in Figure 4.7. The stacking of subsequent propellers prevents axial rotation and the molecules thus are highly ordered within helical

columns. These results are in line with the absence of rotation in the self-assembled columns in solution as discussed in chapter 3.

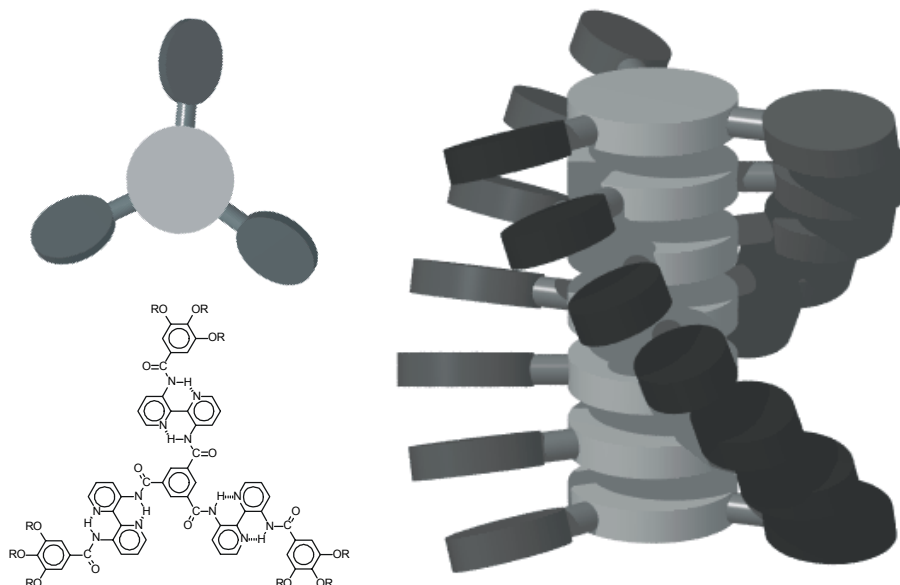


Figure 4.7: Mode of stacking of discotics **1-4** in helical columns in the solid state (right). The three wedges in the central core rotate cooperatively out of the plain, resulting in a propeller-like conformation of the molecule (left).

4.4 Ion conduction

The ionic conductivities of the mixtures **1a-e** and **2a-e** have been recorded as a function of temperature by using impedance spectroscopy. The conductivity values were collected from the cooling runs, but no significant discrepancies were found with respect to data acquired in the heating runs or values obtained for duplo samples (*i.e.* the values were reversible and reproducible). The conductivities of **1** and **2**, the materials without salt, remained well below 10^{-9} S/cm from 30 °C to 100 °C. In Figure 4.8 the measured conductivities are shown as a function of temperature in an Arrhenius plot. The data were fitted for every particular lithium perchlorate concentration using the Vogel-Tamman-Fulcher (VTF) equation, an empirical equation that is often used to describe the temperature dependence of ion conductivity.⁶⁰ The matching fits to the data points showed that for the ion conduction the free-volume model is applicable.³⁰ Furthermore, the maximal conductivity was found to relate to the lowest T_g . The conductivity of mixtures **2a-e** is generally about one order of magnitude higher than the conductivity of mixtures **1a-e**. At room temperature, mixtures **2a-c** have a favorable conductivity of around 10^{-5} S/cm, whereas mixtures **1a-c** show a room temperature conductivity of *ca.* 10^{-6} S/cm.

It is obvious that samples containing large salt concentrations (**1e** and **2e**) display the lowest conductivities. Not only the room temperature conductivities are low ($<10^{-9}$ S/cm), but also the conductivities at 100 °C do not exceed 10^{-5} S/cm considerably. Additionally, the conductivity in

samples **1e** and **2e** is highly temperature dependent ($\sigma [100^\circ\text{C}] / \sigma [30^\circ\text{C}] \sim 10^4$). The conductive properties improve extremely at decreased salt concentrations. Sample **2a** displays the maximal conductivity of all samples at room temperature ($\sigma > 10^{-5}$ S/cm), whereas mixture **2c** shows the maximal conduction at 100°C ($\sigma \approx 6 \cdot 10^{-4}$ S/cm). Also the ratio between the conductivities at 100°C and 30°C is considerably lower for mixtures containing less salt: for mixture **2a** this value amounts to 10 while for mixture **1a** this value is 40. Thus, the conductivities are rather constant over a broad temperature window when the materials are charged with small amounts of salt.

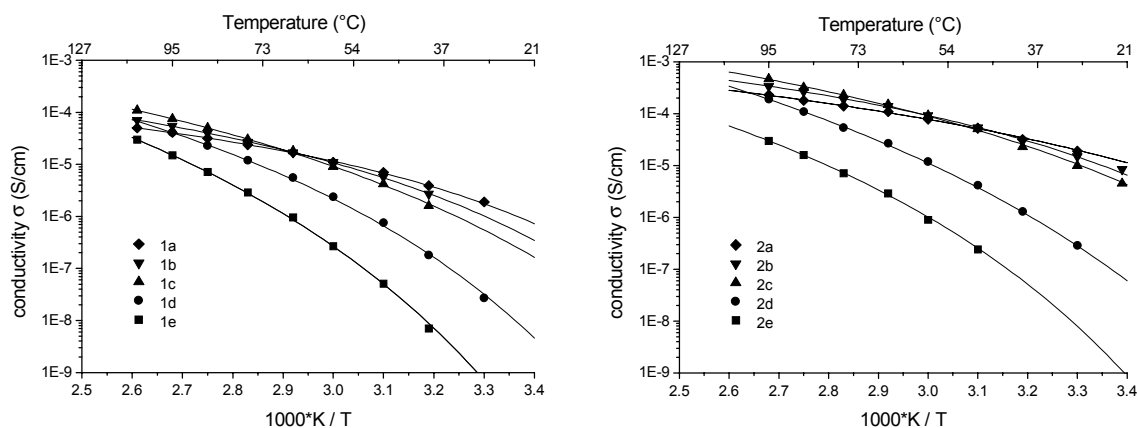


Figure 4.8: Conductivity of mixtures **1a-e** (left) and **2a-e** (right) as a function of temperature.

For every single temperature, the conductivities can be plotted as a function of salt concentration (Figure 4.9). The maximum conductivity shifts to samples with higher salt concentration when higher temperatures are considered. At 40°C the conductivity is highest for samples containing the smallest amount of salt (**1a**, **2a**), at 60°C the maximum has shifted to mixtures **1b** and **2b** and at 80°C and 100°C samples **1c** and **2c** display the highest conductivity.

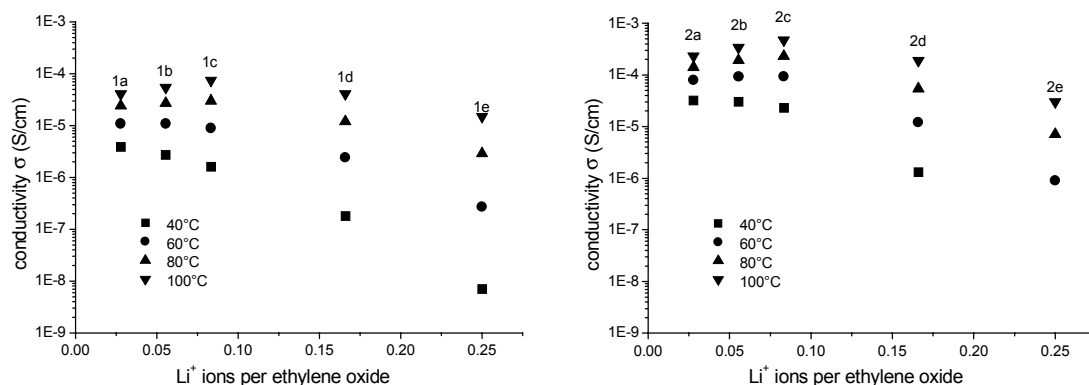


Figure 4.9: Conductivity of mixtures **1a-e** (left) and **2a-e** (right) as a function of salt concentration at four temperatures.

The observed phenomena can be rationalized by Equation 1 that shows the dependence of the conductivity $\sigma(T)$ on the different parameters.³⁰ In equation 1, n_i is the number of charge carriers of type i , q_i is the charge of those carriers and μ_i is their ionic mobility. The number of charge carriers n_i is related to the concentration of the ionic species and is thus related to the salt concentration in the conducting medium under investigation. The ionic mobility μ_i is related to the liquid character of the conducting matrix and thus is related to the T_g of the conducting medium that is considered.

Equation 1
$$\sigma(T) = \sum_i n_i q_i \mu_i$$

The higher conductivities of mixtures **2a-e** as compared to those displayed by mixtures **1a-e** are due to the lower T_g 's of mixtures **2a-e**, giving rise to higher mobilities, μ_i , of the ionic species in these samples. The low conductivity in the mixtures containing large amounts of salt (**1e** and **2e**) is due to the low mobility of the ions in these systems. Just above the T_g of the samples, the movement of the chains is highly constrained, thus limiting the transport of ions. At higher temperatures, however, the movement of the side-chains has increased strongly, resulting in higher mobilities of the ionic species and therefore, **1e** and **2e** show much higher conductivities at elevated temperatures. With this rationale, the high $\sigma [100 \text{ }^\circ\text{C}] / \sigma [30 \text{ }^\circ\text{C}]$ ratio can be explained. For the samples with lower salt concentrations the T_g of the samples is lower, favoring the mobility of the ionic species. The number of charge carriers is also lower, but overall a higher conductivity is measured. At the lowest salt concentrations, the number of charge carriers n_i becomes the limiting factor for the ion conduction. This is evident from *e.g.* mixture **2a**. This sample has very good room temperature conductivity, due to the low T_g of this mixture. The conductivity at 100 $^\circ\text{C}$, however, has not improved greatly, due to the limiting amount of charge carriers. This phenomenon has a positive effect on the $\sigma [100 \text{ }^\circ\text{C}] / \sigma [30 \text{ }^\circ\text{C}]$ ratio of mixture **2a** (this ratio is 10). The shift of the maximum in conductivity at different temperatures (Figure 4.9) can also be explained with Equation 1. At low temperatures, the conductivity is mainly determined by the T_g of the system and thus the samples with the lowest T_g 's display the highest conductivities. At higher temperatures the amount of charge carriers becomes more important and therefore the more salt containing samples show the maximum conductivities.⁶¹

4.5 Conclusions

Extended core discotic liquid crystals with oligo(ethylene oxide) side chains of different length and nature (**1-4**) have been prepared. The difference in mesomorphic behavior with respect to the nature of the side chains has been shown. The molecules organize into a liquid crystalline phase in which hexagonally packed helical columns are surrounded by an amorphous poly(ethylene oxide) matrix. The supramolecular structure remains intact until the clearing temperatures are reached, which are as high as 282 $^\circ\text{C}$. The glass transition temperatures of these systems rely on the nature of the side

chains and are as low as $-70\text{ }^{\circ}\text{C}$. Consequently, the liquid crystalline state in these materials is stable over a very broad and practical temperature range.

The addition of salt to the liquid crystalline materials leads to a considerable decrease of the mesophase temperature stability, but in general the mesophase remains intact over a useful temperature window. The salt also influences the packing of the molecules, resulting in less defined disordered structures at high salt concentrations.

The mechanical properties of the liquid crystalline compounds are not as good as those usually observed for regular amorphous solid polymer electrolytes; they are waxy solids. Still, these materials possess a considerable strength, due to the stiffening effect of the large aromatic core and they do not flow. The high flexibility of the side chains, that accounts for the low T_g , results in a high room temperature conductivity exceeding 10^{-5} S/cm . This value is well above those for previously reported liquid crystalline systems and is approaching the values obtained for the best non-plasticized ion conducting systems known so far ($\sim 10^{-4}\text{ S/cm}$).³⁰ Furthermore, improvement of the conductivity would be possible by optimization of the side-chain length and by tuning the counter anion.

Discotic liquid crystals are promising materials for ion conductivity studies since the extended aromatic core introduces order in the system and is accounting for the mechanical strength of the material while the flexible side-chains provide a liquid-like matrix, suitable for an efficient transport of ionic charge carriers. Additionally, in contrast to calamatic liquid crystals, extended core discotics feature mesophases in broad and useful temperature windows.

4.6 Experimental section

General.⁶² TGA measurements were performed with a Perkin Elmer TGA 7. Ion conductivity measurements were performed at Philips Research using a Hewlett Packard 4194A impedance/gain-phase analyzer and a Mettler FP82HT Hot Stage connected to a FP80 central processor. Samples of 140 μm thickness and 2 cm^2 round surface sandwiched between two stainless steel electrodes were prepared in a glove-box. The synthesis of 2,2'-bipyridine-3,3'-diamine was accomplished according to the previously described procedure.⁴⁵ Mono-O-benzyl tetra(ethylene oxide) was prepared according to a literature procedure⁴⁶ (28.7 g, 0.101 mmol, 67%). B.p.: 145°C (1·10⁻² mbar).

N,N',N''-Tris{3[3'-(3,4,5-tris{2-[2-(2-benzyloxyethoxy)-ethoxy]-ethoxy}-ethoxy)-benzoylamino]-2,2'-bipyridyl}benzene-1,3,5-tricarboxamide (1). To an ice-cooled solution of **10a** (4.00 g, 3.52 mmol) and TEA (0.80 mL, 5.7 mmol) in dry CH_2Cl_2 (40 mL), a solution of trimesic chloride (0.31 g, 1.2 mmol) in dry CH_2Cl_2 (12 mL) was added dropwise at room temperature. The resulting mixture was stirred at room temperature overnight and the solvents were evaporated *in vacuo*. The crude product was washed several times with MeOH and subsequently purified by column chromatography (silica; 5% EtOH in CHCl_3), the product was thoroughly dried *in vacuo* over P_2O_5 (2.70 g, 0.76 mmol, 66%). $T_{\text{cl}} = 244$ °C. ¹H-NMR (CDCl_3): $\delta = 15.53$ (s, 3H, inner NHCO); 14.52 (s, 3H, outer NHCO); 9.60 (dd, $J = 8.0$ and 1.1 Hz, 3H, H-4); 9.38 (dd, $J = 7.8$ and 1.0 Hz, 3H, H-4'); 9.22 (s, 3H, central H); 9.06 (dd, $J = 4.4$ and 1.2 Hz, 3H, H-6'); 8.48 (dd, $J = 4.4$ and 1.4 Hz, 3H, H-6); 7.55 (m, 6H, H-5 and H-5'); 7.34-7.24 (m, 51H, all gallic and benzyl ring protons); 4.56 (s, 6H, *para*- CH_2Ph); 4.54 (s, 12H, *meta*- CH_2Ph); 4.28 (t, 18H, ArOCH_2); 3.90 (t, 12H, *meta*- OCH_2CH_2); 3.84 (t, 6H, *para*- OCH_2CH_2); 3.77-3.61 (m, 108H, ethylene oxide protons). ¹³C-NMR (CDCl_3): $\delta = 165.6$; 163.8; 152.5; 142.1; 141.8; 141.2; 140.5; 138.0; 137.3; 137.2; 135.7; 130.3; 129.6; 128.0-127.4 (multiple signals); 124.6; 124.2; 107.8; 72.9; 72.3-69.2. IR (neat): $\nu = 3580$; 3514; 2865; 1669; 1571; 1495; 1446; 1372; 1299; 1241; 1104; 800; 742. MALDI-TOF Matrix: Sudan Orange; $[\text{M} + \text{Na}^+] = \text{Calcd. } 3590.7 \text{ Da. Obsd. } 3590.5 \text{ Da. Anal. Calcd for } \text{C}_{195}\text{H}_{240}\text{N}_{12}\text{O}_{51} \text{ (MW } 3568.14\text{): C } 65.64, \text{ H } 6.78, \text{ N } 4.71. \text{ Found: C } 65.39, \text{ H } 6.81, \text{ N } 4.62.$

N,N',N''-Tris{3[3'-(3,4,5-tris{methoxy-oligo[ethylenoxy]})-benzoylamino]-2,2'-bipyridyl}benzene-1,3,5-tricarboxamide (2). Starting from substance **10b**, compound **2** was prepared similar to **1**. The crude product was purified by column chromatography (3 times: 1 and 2. silica; CHCl_3 - 10% MeOH in CHCl_3 3. alumina; DME followed by 2% MeOH in CHCl_3). The product was thoroughly dried *in vacuo* over P_2O_5 (3.11 g, 0.76 mmol, 36%). $T_{\text{cl}} = 214$ °C. ¹H-NMR (CDCl_3): $\delta = 15.56$ (s, 3H, inner NHCO); 14.52 (s, 3H, outer NHCO); 9.60 (dd, $J = 7.4$ and 1.2 Hz, 3H, H-4); 9.40 (dd, $J = 7.5$ and 1.2 Hz, 3H, H-4'); 9.30 (s, 3H, central H); 9.07 (dd, $J = 4.3$ and 1.2 Hz, 3H, H-6'); 8.48 (dd, $J = 4.4$ and 1.4 Hz, 3H, H-6); 7.55 (m, 6H, H-5 and H-5'); 7.36 (s, 6H, peripheral aryl protons); 4.28 (m, 18H, ArOCH_2); 3.91 (t, 12H, *meta*- OCH_2CH_2); 3.84 (t, 6H, *para*- OCH_2CH_2); 3.77-3.52 (m, 216H, ethylene oxide protons); 3.37 (s, 27, OCH_3). ¹³C-NMR (CDCl_3): $\delta = 165.6$; 163.8; 152.5; 142.1; 142.0; 141.3; 140.5; 137.3; 137.3; 135.8; 130.4; 129.7; 129.7; 129.3; 124.5; 124.2; 107.8; 72.9; 72.3-69.2. IR (neat): $\nu = 3564$; 3519; 2870; 1671; 1571; 1497; 1373; 1300; 1244; 1107; 947; 853; 803; 747.

General procedure for preparing mono-O-tosyl oligo(ethylene oxide)s.⁴⁷ NaOH (8.0 g, 200 mmol) and a mono-protected oligo(ethylene oxide) derivative (140 mmol) in a two-phase system of water (40 mL) and THF (40 mL) was cooled via an ice-bath with magnetic stirring. *p*-Toluenesulfonyl chloride (27.0 g, 150 mmol) in THF (40 mL) was added dropwise to the mixture, while maintaining the temperature below 5°C. The solution was stirred at 0°C for another 3 h and then poured into ice-water (100 mL). The mixture was extracted with CH_2Cl_2 (3 x 200 mL) and the combined organic layers were washed with water (pH = 1) (2x) and with brine (1x). After drying over MgSO_4 , the solvent was evaporated *in vacuo* to yield the pure compound as a colorless oil.

Mono-O-benzyl tetra(ethylene oxide) monotosylate (6a). Yield is 55.40 g, 126 mmol, 90%. ¹H-NMR (CDCl_3): $\delta = 7.76$ (d, 2H, *ortho*-H tosyl); 7.34 (m, 7H, *CH*-phenyl and *meta*-H tosyl); 4.57 (s, 2H, CH_2 -benzyl); 4.12 (t, 2H, CH_2O -tosyl); 3.7-3.55 (m, 14H, $\text{OCH}_2\text{H}_2\text{O}$); 2.44 (s, 3H, CH_3 tosyl). ¹³C-NMR (CDCl_3): $\delta = 142.5$ (*para*-C tosyl); 138.1 (C-1 phenyl); 133.2 (C-1 tosyl); 129.7 (*meta*-C tosyl); 128.3-127.5 (C-Ph and *ortho*-C tosyl); 73.1 (CH_2 -benzyl); 70.6-68.6 ($\text{COCH}_2\text{CH}_2\text{OC}$); 21.5 (CH_3 tosyl).

Mono-O-methyl oligo(ethylene oxide) (n~7) monotosylate (6b).⁶³ Yield is 62.95 g, 125 mmol, 89%. ¹H-NMR (CDCl_3): $\delta = 7.79$ (d, 2H, *ortho*-H tosyl); 7.35 (d, 2H, *meta*-H tosyl); 4.15 (t, 2H, CH_2O -tosyl); 3.7-3.55 (m, 26H, OCH_2CH_2); 3.36 (s, 3H, OCH_3); 2.44 (s, 3H, CH_3 tosyl). ¹³C-NMR (CDCl_3): $\delta = 144.4$ (*para*-C tosyl);

132.7 (C-1 tosyl); 129.5 (*meta*-C tosyl); 127.5 (*ortho*-C tosyl); 71.5-68.3 (COCH₂CH₂OC); 58.6 (OCH₃) 21.2 (CH₃ tosyl).

Methyl 3,4,5-tris[2-{2-[2-(2-benzyloxyethoxy)-ethoxy]-ethoxy]-benzoate (7a). A mixture of **6a** (10.9 g, 25 mmol), methyl 3,4,5-trihydroxybenzoate (1.29 g, 7.0 mmol) and K₂CO₃ (10.4 g, 75 mmol) in DMF (50 mL) was stirred for 6 h at 80°C. After cooling, the mixture was poured into water (200 mL, pH = 2) and extracted with ether. The ether layer was washed with water (3x) and brine (1x), dried over MgSO₄ and the ether was evaporated *in vacuo*. The crude product was purified by column chromatography (silica; EtOAc followed by acetonitrile) to yield the pure compound as a viscous oil (5.11 g, 5.2 mmol, 74%). ¹H-NMR (CDCl₃): δ = 7.33-7.26 (m, 17H, all aromatic protons); 4.56 (s, 4H, *meta*-CH₂Ph); 4.55 (s, 2H, *para*-CH₂Ph); 4.22 (t, 2H, *para*-OCH₂); 4.17 (t, 4H, *meta*-OCH₂); 3.87 (s, 3H, OCH₃); 3.84 (t, 4H, *meta*-OCH₂CH₂); 3.78 (t, 2H, *para*-OCH₂CH₂); 3.66 (m, 36H, ethylene oxide protons). ¹³C-NMR (CDCl₃): δ = 166.5 (CO); 152.2 (C-3); 142.5 (C-4); 138.2 (C-1 benzyl); 128.3-127.5 (C-2 benzyl, C-3 benzyl, C-4 benzyl); 124.9 (C-1); 109.0 (C-2); 73.2 (CH₂ benzyl); 72.4-68.8 (ethylene oxide carbons); 52.1 (CH₃). IR (neat): ν = 2869; 1719; 1586; 1432; 1334; 1215; 1110; 738; 698.

Methyl 3,4,5-tris[methoxy-oligo(ethylenoxy)]-benzoate (7b). A mixture of **6b** (50.0 g, 100 mmol), methyl 3,4,5-trihydroxybenzoate (5.50 g, 30.0 mmol) and K₂CO₃ (41.5 g, 300 mmol) in dry acetone (300 mL) was stirred under reflux overnight. After cooling, the mixture was poured into water and extracted with CH₂Cl₂ (3x). The organic layer was washed with water (1x) and brine (1x), dried over MgSO₄ and the CH₂Cl₂ was evaporated *in vacuo*. The crude product was used as such for the preparation of **8b**.

3,4,5-Tris[2-{2-[2-(2-benzyloxyethoxy)-ethoxy]-ethoxy]-benzoic acid (8a). A solution of **7a** (14.5 g, 14.7 mmol) and KOH (85%) (2.39 g, 41.0 mmol) in ethanol (120 mL) and water (60 mL) was heated under reflux overnight. Subsequently, the solution was acidified to pH = 2 with conc. hydrochloric acid under reflux and then the solution was poured onto an water/ice mixture. The aqueous layer was extracted with ether (2x). The combined ether layers were washed with water (pH = 2) and brine (pH = 2). Drying over MgSO₄ and evaporation of the solvent *in vacuo*, afforded pure **8a** (13.3 g, 13.7 mmol, 93%). ¹H-NMR (CDCl₃): δ = 7.36-7.25 (m, 17H, all aromatic protons); 4.57 (s, 4H, *meta*-CH₂Ph); 4.56 (s, 2H, *para*-CH₂Ph); 4.23 (t, 2H, *para*-OCH₂); 4.18 (t, 4H, *meta*-OCH₂); 3.84 (t, 4H, *meta*-OCH₂CH₂); 3.79 (t, 2H, *para*-OCH₂CH₂); 3.66 (m, 36H, ethylene oxide protons). ¹³C-NMR (CDCl₃): δ = 170.5 (CO); 152.3 (C-3); 143.1 (C-4); 138.2 (C-1 benzyl); 128.3-127.6 (C-2 benzyl, C-3 benzyl, C-4 benzyl); 124.2 (C-1); 109.7 (C-2); 73.1 (CH₂ benzyl); 72.4-68.8 (ethylene oxide carbons). IR (neat): ν = 3029; 2870; 1713; 1586; 1497; 1430; 1325; 1208; 1108; 947; 740; 700. ESI-MS *m/z* (M - H)⁻ Calcd. 967.5 Da. Obsd. 968.0 Da. Anal. Calcd for C₅₂H₇₂O₁₇ (MW 969.14): C 64.45, H 7.49. Found: C 64.06, H 7.55.

3,4,5-Tris[methoxy-oligo(ethylenoxy)]-benzoic acid (8b). A solution of crude **7b** (32.5 g) and KOH (85%) (3.50 g, 62 mmol) in ethanol (200 mL) and water (200 mL) was heated under reflux overnight. Then, the solution was acidified to pH = 2 with conc. hydrochloric acid under reflux, subsequently the solution was poured onto an water/ice mixture. The aqueous layer was extracted with CH₂Cl₂ (3x). The combined organic layers were washed with brine (pH = 2) dried over MgSO₄ and the CH₂Cl₂ was evaporated *in vacuo*. The product was purified by column chromatography (silica; 5% ethanol in chloroform, followed by 5% formic acid in methanol) and subsequently dissolved in chloroform. The chloroform solution was washed with water (2x), dried over MgSO₄ and evaporated *in vacuo* to yield pure **8b** (21.1 g, 18.6 mmol, 62% after 2 reactions). ¹H-NMR (CDCl₃): δ = 7.35 (s, 2H, *H-ortho*); 4.23 (t, 2H, *para*-OCH₂); 4.19 (t, 4H, *meta*-OCH₂); 3.86 (t, 4H, *meta*-OCH₂CH₂); 3.79 (t, 2H, *para*-OCH₂CH₂); 3.66 (m, 72H, ethylene oxide protons); 3.38 (s, 9H, OCH₃). ¹³C-NMR (CDCl₃): δ = 168.4 (CO); 152.0 (C-3); 142.5 (C-4); 124.4 (C-1); 109.1 (C-2); 72.1-68.5 (ethylene oxide carbons); 58.7 (OMe). IR (neat): ν = 2873; 1714; 1586; 1431; 1351; 1324; 1204; 1111; 947; 853; 702.

3,4,5-Tris[2-{2-[2-(2-benzyloxyethoxy)-ethoxy]-ethoxy]-benzoyl chloride (9a). To a solution of **8a** (5.00 g, 5.16 mmol) and two drops of dry DMF in CH₂Cl₂ (15 mL) a solution of oxalyl chloride (0.72 g, 5.7 mmol) in CH₂Cl₂ (7 mL) was added dropwise. The mixture was stirred overnight at room temperature in the absence of light and subsequently, the solvent was removed by evaporation *in vacuo* and the compound was dried under vacuum (1 mbar) for 2 h (5.0 g, 5.16 mmol, 100%). ¹H-NMR (CDCl₃): δ = 7.37-7.25 (m, 17H, all aromatic protons); 4.57 (s, 6H, CH₂Ph); 4.26 (t, 2H, *para*-OCH₂); 4.18 (t, 4H, *meta*-OCH₂); 3.84 (t, 4H, *meta*-OCH₂CH₂); 3.79 (t, 2H, *para*-OCH₂CH₂); 3.66 (m, 36H, ethylene oxide protons). ¹³C-NMR (CDCl₃): δ = 167.3 (CO); 152.3 (C-3); 144.9 (C-4); 138.1 (C-1 benzyl); 128.3-127.3 (C-1, C-2 benzyl, C-3 benzyl, C-4 benzyl); 111.1 (C-2); 73.1 (CH₂ benzyl); 72.5-69.0 (ethylene oxide carbons).

3,4,5-Tris[methoxy-oligo(ethylenoxy)]-benzoyl chloride (9b). Acid chloride **9b** was prepared similar to **9a**. $^1\text{H-NMR}$ (CDCl_3): $\delta = 7.33$ (s, 2H, *H-ortho*); 4.23 (t, 2H, *para-OCH}_2*); 4.18 (t, 4H, *meta-OCH}_2*); 3.84 (t, 4H, *meta-OCH}_2\text{CH}_2*); 3.79 (t, 2H, *para-OCH}_2\text{CH}_2*); 3.66 (m, 72H, ethylene oxide protons); 3.38 (s, 9H, OCH_3). $^{13}\text{C-NMR}$ (CDCl_3): $\delta = 167.2$ (CO); 152.2 (C-3); 144.9 (C-4); 127.2 (C-1); 111.0 (C-2); 72.5-68.9 (ethylene oxide carbons); 58.8 (OMe).

3'-{3,4,5-Tris[2-{2-[2-(2-methoxyethoxy)-ethoxy]-ethoxy]-ethoxy}-benzoylamino}-2,2'-bipyridine-3-amine (10a). To an ice-cooled, magnetically stirred solution of 2,2'-bipyridine-3,3'-diamine (1.00 g, 5.4 mmol) and TEA (0.75 ml, 5.4 mmol) in dry CH_2Cl_2 (50 mL), **9a** (5.0 g, 5.2 mmol) in dry CH_2Cl_2 (40 mL) was added dropwise via a syringe. Stirring was continued for another h at 0°C and subsequently overnight at room temperature. The solution was diluted with CH_2Cl_2 and washed with water (2x) and brine (1x), dried over Na_2SO_4 and the solvents were evaporated *in vacuo*.⁶⁴ The crude product was purified by column chromatography (3 times: 1. silica; EtOAc followed by acetonitril 2. silica; acetonitril 3. flash silica; acetonitril) to yield the title compound (4.10 g, 3.60 mmol, 71%). The product was thoroughly dried *in vacuo* over P_2O_5 . $^1\text{H-NMR}$ (CDCl_3): $\delta = 14.40$ (s, 1H, NHCO); 9.21 (dd, $J = 8.5$ and 1.7 Hz, 1H, H-4'); 8.33 (dd, $J = 4.6$ and 1.5 Hz, 1H, H-6'); 8.03 (dd, $J = 3.9$ and 1.8 Hz, 1H, H-6); 7.33-7.25 (m, 18H, all phenyl protons and H-5'); 7.12 (m, 2H, H-4 and H-5); 6.57 (s, 2H, NH_2); 4.55 (s, 2H, *para-CH}_2\text{Ph}*); 4.54 (s, 4H, *meta-CH}_2\text{Ph}*); 4.24 (t, 6H, ArOCH_2); 3.87 (t, 4H, *meta-OCH}_2\text{CH}_2*); 3.78 (t, 2H, *para-OCH}_2\text{CH}_2*); 3.73-3.60 (m, 36H, ethylene oxide protons). $^{13}\text{C-NMR}$ (CDCl_3): $\delta = 165.6$ (CO); 152.5 (C-3 benzoyl); 145.0 (C-3); 143.5 (C-4 benzoyl); 141.8 (C-2'); 140.7 (C-2); 138.4 (C-6'); 138.2 (C-1 benzyl); 136.0 (C-3'); 134.8 (C-6); 130.7 (C-4'); 128.5 (C-1 benzoyl); 128.2, 127.6 and 127.5 (C-2 benzyl, C-3 benzyl, C-4 benzyl); 125.2 (C-5'); 124.2 (C-5); 122.6 (C-4); 107.7 (C-2 benzoyl); 73.1 (CH_2 benzyl); 72.3-69.1 (ethylene oxide carbons). IR (neat): $\nu = 3417$; 3280; 2870; 1663; 1576; 1521; 1494; 1454; 1330; 1208; 1109; 945; 805; 742; 699. ESI-MS m/z $[\text{M} + \text{H}]^+$ Calcd. 1137.6 Da. Obsd. 1138.1 Da.; $[\text{M} + \text{Na}]^+$ Calcd. 1159.6 Da. Obsd. 1159.8 Da. Anal. Calcd for $\text{C}_{62}\text{H}_{80}\text{N}_4\text{O}_{16}$ (MW 1137.35): C 65.48, H 7.09, N 4.93. Found: C 65.36, H 7.11, N 4.89.

3'-{3,4,5-Tris[methoxy-oligo(ethylenoxy)]-benzoylamino}-2,2'-bipyridine-3-amine (10b). Compound **10b** was prepared similar to **10a**.⁶⁴ The crude product was purified by column chromatography (2 times: 1. silica; EtOAc followed by 5% MeOH in CHCl_3 2. silica; 5% MeOH in CHCl_3) to yield the title compound (8.9 g, 6.8 mmol, 77%). The product was thoroughly dried *in vacuo* over P_2O_5 . $^1\text{H-NMR}$ (CDCl_3): $\delta = 14.39$ (s, 1H, NHCO); 9.21 (dd, $J = 7.0$ and 1.5 Hz, 1H, H-4'); 8.33 (dd, $J = 2.7$ and 1.6 Hz, 1H, H-6'); 8.04 (dd, $J = 3.0$ and 1.8 Hz, 1H, H-6); 7.33 (s, 2H, *ortho-H*); 7.30 (1H, H-5'); 7.15 (m, 2H, H-4 and H-5); 6.60 (s, 2H, NH_2); 4.25 (m, 6H, ArOCH_2); 3.87 (t, 4H, *meta-OCH}_2\text{CH}_2*); 3.80 (t, 2H, *para-OCH}_2\text{CH}_2*); 3.73-3.54 (m, 72H, ethylene oxide protons); 3.36 (s, 9H, OCH_3). $^{13}\text{C-NMR}$ (CDCl_3): $\delta = 165.6$ (CO); 152.5 (C-3 benzoyl); 145.1 (C-3); 143.6 (C-4 benzoyl); 141.9 (C-2'); 140.7 (C-2) 138.3 (C-6'); 136.0 (C-3'); 134.6 (C-6); 130.7 (C-4'); 128.5 (C-1 benzoyl); 125.3 (C-5'); 124.2 (C-5); 122.6 (C-4); 107.8 (C-2 benzoyl); 72.3-69.1 (ethylene oxide carbons); 58.9 (OMe). IR (neat): $\nu = 3417$; 3283; 2873; 1664; 1576; 1493; 1460; 1330; 1300; 1248; 1206; 1110; 947; 853; 807; 742.

Preparation of mixtures of 1 and 2 with lithium perchlorate (1a-e and 2a-e). For the preparation of the mixtures (**1a-e** and **2a-e**), first liquid crystalline compounds **1-2** were thoroughly dried *in vacuo* over P_2O_5 to remove all the water present in the systems. Stock solutions of **1** and **2** (approx. 7 mM) in dry THF as well as a stock solution of LiClO_4 (approx. 40 mM) in dry THF were prepared in a glove box. The mixtures were prepared by mixing the appropriate amounts of the stock solutions. The solvents were allowed to evaporate in the glove box and subsequently the samples were thoroughly dried *in vacuo* (1 mbar) at 70°C and stored *in vacuo* over P_2O_5 .

4.7 References

- ¹ Chandrasekhar, S.; Sadashiva, B.K.; Suresh, K.A. *Pramana* **1977**, *9*, 471-480.
- ² *Handbook of liquid crystals*, vol 2B, eds: Demus, D.; Goddby, J.; Gray, G.W.; Spiess, H.-W.; Vill, V., Wiley-VCH, Weinheim, **1998**.
- ³ Chandrasekhar, S. *Liq. Cryst.* **1993**, *14*, 3-14 and references cited herein.
- ⁴ Herwig, P.; Kayser, L.W.; Müllen, K.; Spiess, H.W. *Adv. Mater.*, **1996**, *8*, 510-513.
- ⁵ Zhang, J.; Moore, J.S. *J. Am. Chem. Soc.*, **1994**, *116*, 2655-2656.
- ⁶ Mohr, B.; Wegner, G.; Ohta, K. *J. Chem. Soc., Chem. Commun.* **1995**, 995-996.
- ⁷ Kretzschmann, H.; Müller, K.; Kolshorn, H.; Schollmeyer, D.; Meier, H. *Chem. Ber.* **1994**, *127*, 1735-1745.
- ⁸ van Nostrum, C.F.; Picken, S.J.; Schouten, A.-J.; Nolte, R.J.M. *J. Am. Chem. Soc.* **1995**, *117*, 9957-9965.
- ⁹ Barberá, J.; Cativiela, C.; Serrano, J.L.; Zurbano, M.M. *Adv. Mater.* **1991**, *3*, 602-605.
- ¹⁰ Serrette, A.G.; Swager, T.M. *Angew. Chem., Int. Ed. Engl.* **1994**, *33*, 2342.
- ¹¹ Fischer, H.; Plesnivý, T.; Ringsdorf, H.; Seitz, M. *J. Chem. Soc., Chem. Commun.* **1995**, 1615.
- ¹² Zheng, H.; Xu, B.; Swager, T.M. *Chem. Mater.* **1996**, *8*, 907.
- ¹³ Thompson, N.J.; Serrano, J.L.; Baena, M.J.; Espinet, P. *Chem. Eur. J.* **1996**, *2*, 214.
- ¹⁴ Kroczyński, A.; Pocięcha, D.; Szydłowska, J.; Przedmojski, J.; Gorecka, E. *Chem. Commun.* **1996**, 2731.
- ¹⁵ Barberá, J.; Iglesias, R.; Serrano, J.L.; Sierra, T.; de la Fuente, M.R.; Palacios, B.; Pérez-Jubindo, M.A.; Vázquez, J.T. *J. Am. Chem. Soc.* **1998**, *120*, 2908-2918.
- ¹⁶ Kleppinger, R.; Lillya, C.P.; Yang, C. *J. Am. Chem. Soc.* **1997**, *119*, 4097-4102.
- ¹⁷ Beginn, U.; Lattermann, G. *Mol. Cryst. Liq. Cryst.* **1994**, *241*, 215-219.
- ¹⁸ Latterman, G.; Staufer, G. *Mol. Cryst. Liq. Cryst.* **1990**, *191*, 199-203.
- ¹⁹ Koh, K.N.; Araki, K.; Komori, T.; Shinkai, S. *Tetrahedron Lett.* **1995**, *36*, 5191-5194.
- ²⁰ Ebert, M.; Kleppinger, R.; Soliman, M.; Wolf, M.; Wendorf, J.H.; Lattermann, G.; Staufer, G. *Liq. Cryst.* **1990**, *7*, 553-570.
- ²¹ Serrette, A.G.; Swager, T. *Angew. Chem., Int. Ed. Engl.* **1994**, *33*, 2342-2345.
- ²² Ungar, G.; Abramic, D.; Percec, V.; Heck, J.A. *Liq. Cryst.* **1996**, *21*, 73-86.
- ²³ Suarez, M.; Lehn, J.-M.; Zimmerman, S.C.; Skoulios, A.; Heinrich, B. *J. Am. Chem. Soc.* **1998**, *120*, 9526-9532.
- ²⁴ Hirschberg, J.H.K.K.; Brunsveld, L.; Ramzi, A.; Vekemans, J.A.J.M.; Sijbesma, R.P.; Meijer, E.W. *Nature* **2000**, *407*, 167-170.
- ²⁵ Paulus, W.; Ringsdorf, H.; Diele, S.; Pelzl, G. *Liq. Cryst.* **1991**, *9*, 807-819.
- ²⁶ Van der Auweraer, M.; Catry, C.; Feng Chi, L.; Karthaus, O.; Knoll, W.; Ringsdorf, H.; Sawodny, M.; Urban, U. *Thin Solid Films* **1992**, *210/211*, 39-41.
- ²⁷ Palmans, A.R.A.; Vekemans, J.A.J.M.; Fischer, H.; Hikmet, R.A.; Meijer, E.W. *Chem. Eur. J.* **1997**, *3*, 300-307.
- ²⁸ Lee, M.; Oh, N.-K. *J. Mater. Chem.* **1996**, *6*, 1079-1086.
- ²⁹ The influence of salt on a wedge-shaped molecule forming a columnar mesophase has been studied previously: Ungar, G.; Batty, S.V.; Percec, V.; Heck, J.; Johansson, G. *Adv. Mater. for Opt. and Electr.* **1994**, *4*, 303-313.
- ³⁰ For general information of ion conducting materials see: Gray, F.M. *Solid Polymer Electrolytes* **1991**, VCH Publishers, New York. Gray, F.M., *Polymer Electrolytes* **1997**, The Royal Society of Chemistry, Cambridge. Alamgir, M.; Abraham, K.M., *Lithium Batteries* **1994**, Elsevier, Amsterdam, Chapter 3.
- ³¹ Kimura, K.; Hirao, M.; Yokoyama, M. *J. Mater. Chem.* **1991**, *1*, 293-294.
- ³² Tokuhisa, H.; Yokoyama, M.; Kimura, K.; *J. Mater. Chem.* **1998**, *8*, 889-891.
- ³³ Lauter, U.; Meyer, W.H.; Wegner, G. *Macromolecules* **1997**, *30*, 2092-2101.
- ³⁴ Dias, F.B.; Batty, S.V.; Voss, J.P.; Ungar, G.; Wright, P.V. *Solid State Ionics* **1996**, *85*, 43-49.
- ³⁵ Dias, F.B.; Batty, S.V.; Gupta, A.; Ungar, G.; Voss, J.P.; Wright, P.V. *Electrochim. Acta* **1998**, *10-11*, 1217-1224.
- ³⁶ McHattie, G.S.; Imrie, C.T.; Ingram, M.D.; *Electrochim. Acta* **1998**, *10-11*, 1151-1154.
- ³⁷ Imrie, C.T.; Ingram, M.D.; McHattie, G.S. *Adv. Mater.* **1999**, *11*, 832-834.
- ³⁸ Hubbard, H.V.St.A.; Sills, S.A.; Davies, G.R.; McIntyre, J.E.; Ward I.M. *Electrochim. Acta* **1998**, *10-11*, 1239-1245.
- ³⁹ Hirose, T.; Tanaka, S.; Aoki, Y.; Nohira, H. *Chem. Lett.* **2000**, 1290-1291.
- ⁴⁰ Imrie, C.T.; Ingram, M.D. *Mol. Cryst. Liq. Cryst.* **2000**, *347*, 199-210.

- ⁴¹ Ohtake, T.; Ogasawara, M.; Ito-Akita, K.; Nishina, N.; Ujiie, S.; Ohna, H.; Kato T. *Chem. Mater.* **2000**, *12*, 782-789.
- ⁴² Ohtake, T.; Takamitsu, Y.; Ito-Akita, K.; Kanie, K.; Yoshizawa, M.; Mukai, T.; Ohno, H.; Kato, T. *Macromolecules* **2000**, *33*, 8109-8111.
- ⁴³ See chapter 3 for an account on the synthesis of compounds **3** and **4**.
- ⁴⁴ Parts of this work have been presented at 17th International Liquid Crystal Conference, Strasbourg, France, **1998**. Brunsveld, L.; Vekemans, J.A.J.M.; Janssen, H.M.; Meijer, E.W. *Mol. Cryst. Liq. Cryst.* **1999**, *331*, 449-456.
- ⁴⁵ Kaczmarek, L.; Nantka-Namirski, P. *Acta. Polon. Pharm.* **1979**, *6*, 629-634.
- ⁴⁶ Selve, C.; Achilefu, S.; Mansuy, L. *Synth. Commun.* **1990**, *20*, 799-807.
- ⁴⁷ Ouchi, M.; Inoue, Y.; Liu, Y.; Nagamune, S.; Nakamura, S.; Wada, K.; Hakushi, T. *Bull. Chem. Soc. Jpn.* **1990**, *63*, 1260-1262.
- ⁴⁸ It was found that when thionyl chloride was used, the *ortho*-carbon could be partially chlorinated.
- ⁴⁹ Palmans, A.R.A.; Vekemans, J.A.J.M.; Meijer, E.W. *Recl. Trav. Chim. Pays-Bas* **1995**, *114*, 277-284.
- ⁵⁰ Vekemans, J.A.J.M.; Groenendaal, L.; Palmans, A.R.A.; Delnoye, D.A.P.; van Mullekom H.A.M.; Meijer, E.W., *Bull. Soc. Chim. Belg.* **1996**, *105*, 659-674.
- ⁵¹ See chapter 3 of this thesis and: Brunsveld, L.; Zhang, H.; Glasbeek, M.; Vekemans, J.A.J.M.; Meijer, E.W. *J. Am. Chem. Soc.* **2000**, *122*, 6175-6182.
- ⁵² Armand, M., *Solid State Ionics* **1994**, *69*, 309-319.
- ⁵³ The alignment was confirmed by UV/Vis spectroscopy measurements using linear polarized (LP) light, showing a high absorption when the columns were shear-aligned perpendicular to the LP light and displaying a low absorption when the columns were aligned parallel to the LP light.
- ⁵⁴ Palmans, A.R.A.; Vekemans, J.A.J.M.; Havinga, E.E.; Meijer, E.W. *Angew. Chem.* **1997**, *109*, 2763-2766.
- ⁵⁵ Possibly, also the smaller size of the monodomains at higher salt concentrations decreases the sharpness of the signals.
- ⁵⁶ Vallerien, S.U.; Werth, M.; Kremer, F.; Spiess, H.W. *Liq. Cryst.* **1990**, *8*, 889-893.
- ⁵⁷ Werth, M.; Vallerien, S.U.; Spiess, H.W. *Liq. Cryst.* **1991**, *10*, 759-770.
- ⁵⁸ Möller, M.; Wendorff, J.H.; Werth, M.; Spiess, H.W. *J. Non-Cryst. Solids* **1994**, *170*, 295-299.
- ⁵⁹ Brown, S.P.; Schnell, I.; Brand, J.D.; Müllen, K.; Spiess, H.W. *J. Am. Chem. Soc.* **1999**, *121*, 6712-6178.
- ⁶⁰ Vogel, H. *Z. Phys* **1921**, *22*, 645. See also reference 30.
- ⁶¹ Using interdigitated electrodes the conductivity of oriented samples was determined. Even though anisotropy was observed in the conductivity, with the conductivity parallel to the columns higher than the conductivity perpendicular to the columns, the measurements were difficult to reproduce with a sufficient accuracy.
- ⁶² For a description of the general procedures see also chapter 2, section 2.5 Experimental section and chapter 3, section 3.7 Experimental section.
- ⁶³ Oligo(ethylene oxide) monomethyl ether was obtained as a mixture with Mw~350 from commercial suppliers.
- ⁶⁴ ¹H-NMR of the crude product showed a 98% selective monoacylation of the bipyridine.

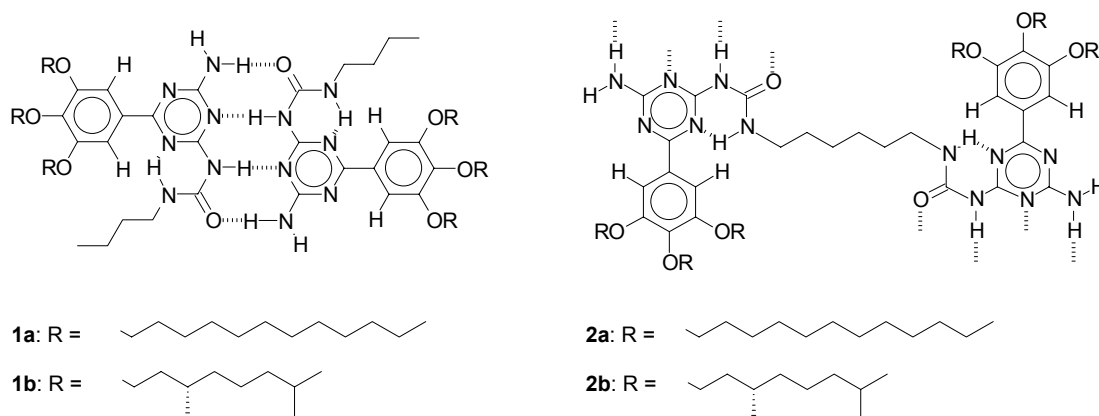
Chapter 5

Helical self-assembled polymers via cooperative stacking of hydrogen bonded pairs in water

Abstract: *Bifunctional ureido-s-triazines provided with chiral penta(ethylene oxide) side chains self-assemble in water into helical columns via cooperative stacking of the hydrogen bonded pairs (DADA). The presence of a hexamethylene spacer, covalently linking two units, is essential for the creation of these structures, since monofunctional ureido-s-triazines do not form such chiral architectures. The linker allows for a high local concentration of aromatic units, favorable for stacking interactions. The hydrophobic stacking of the aromatic units, induced by the linker, in turn allows intermolecular hydrogen bonding to occur because it shields the hydrogen bonds from the competitive water. The stacking of the hydrogen bonded pairs within the helical polymer is a cooperative phenomenon, as the chirality of an end group can be amplified into columns consisting of achiral bifunctional molecules.*

5.1 Introduction

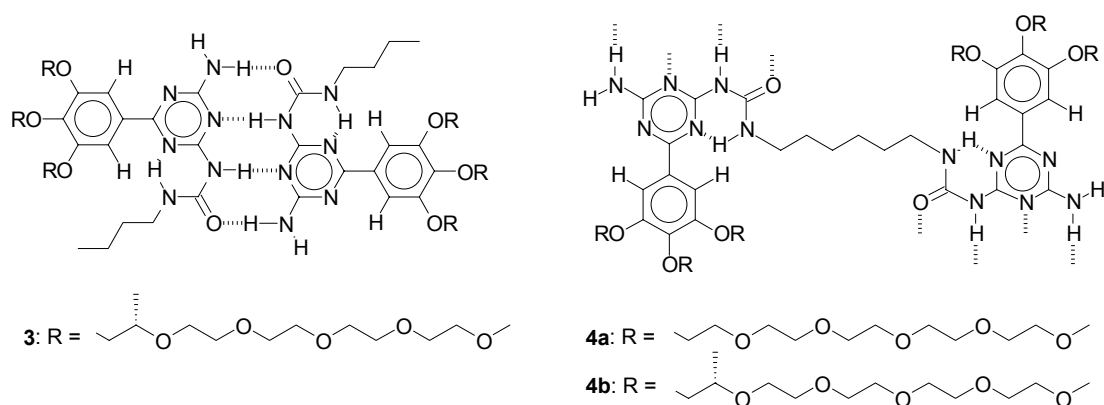
In Nature the well-known double helical motif originates from self-assembly and is stabilized by lateral hydrogen bonds between bases and by perpendicular solvophobic interactions between the covalently linked bases.¹ The bias of the helicity of the structure is induced by the peripheral chirality in the sugar-phosphate backbone. On the other hand, artificial non-covalently interacting molecules in organic solvents have been used to design systems that similarly form controlled architectures.²⁻⁷ Peripheral chiral centers in assemblies⁸⁻¹¹ and chiral side chains attached to a polymer backbone¹²⁻²⁰ have been shown to induce chirality at the supramolecular level. Highly ordered supramolecular structures stable in water are known.²¹⁻²⁴ However, it remains difficult to exploit directional non-covalent interactions in a cooperative way for the formation of multi-molecular assemblies stable in water. In water, the solvent molecules compete effectively with specific interactions such as hydrogen bonds, resulting in low association constants.



The formation of helical self-assembled polymers in alkane solvents by both stacking and hydrogen bonding has been demonstrated.^{25,26} Self-complementary apolar molecules **1** and **2** dimerize via strong cooperative four-fold hydrogen bonding (ADAD) in chloroform,²⁷ giving rise to the formation of a dimer by **1** and a random coil polymer by **2**, the latter featuring viscous solutions at higher concentrations. Additional to the hydrogen bonding, solvophobic interactions between the aromatic surfaces arise for **1** and **2** in alkanes. Association via hydrogen bonding of the ureidotriazine functional groups in **1** and **2** leads to the formation of dimers with a large and planar aromatic core surrounded by 6 flexible alkyl chains, a structure which is conducive to the formation of aggregates with a columnar architecture in environments, that are unable to solvate the core.²⁸ The concomitant occurrence of hydrogen bonding and solvophobic induced stacking of the aromatic cores results in the formation of columnar polymeric architectures for both **1** and **2**. In the columns built up by **1**, the discs are rotating freely, but in the columns formed by **2** this rotation is restricted by the hexamethylene spacer, linking two discs to each other. As a consequence helical columns are formed by **2**. The homochiral side chains in the case of **2b** act as a bias for the chirality of the helix. Cooperativity within the helix was shown by mixing chiral **1b** with achiral **2a**, two compounds both

CD inactive, which gave rise to a Cotton effect. Two molecules **1b** act as chiral end-groups of the helix formed by **2a**, and express their chirality in the helix.

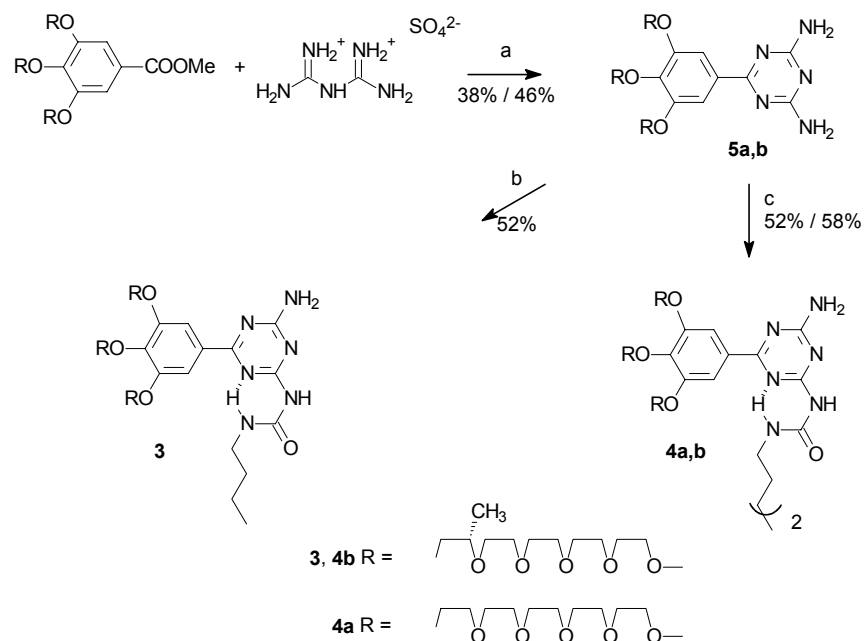
The creation of similar helical columnar architectures in water requires the presence of a hydrophobic microenvironment that shields the hydrogen bonding from the competitive solvent and makes them operative, similar to the way inter-strand hydrogen bonding occurs in DNA¹ and intramolecular hydrogen bonding occurs in the interior of proteins.^{29,30} It was anticipated that the solvophobic interactions between the aromatic surfaces would allow for the creation of such a hydrophobic microenvironment and that by providing the bifunctional monomers with penta(ethylene oxide) monomethyl ether side chains, solubility in water would be ensured. Compounds **3** and **4** were accordingly designed and synthesized in an enantiomerically pure form and subsequently studied in aqueous solutions.



5.2 Helical columns in water

5.2.1 Synthesis and characterization

The synthesis of the mono- and bifunctional molecules **3** and **4** is based upon the monoacylation of the corresponding diamino-*s*-triazines (**5a,b**) with *n*-butylisocyanate and hexane-1,6-diisocyanate, respectively. The purification was difficult, because of the polar character of the molecules and a combination of column chromatography and preparative size exclusion chromatography in THF needed to be employed.



Scheme 5.1: Synthesis of mono- and bifunctional **3** and **4a,b** respectively. a) Na, CH_3OH , $65\text{ }^\circ\text{C}$; b) BuNCO, pyridine, $80\text{ }^\circ\text{C}$; c) $\text{OCNC}_6\text{H}_{12}\text{NCO}$, pyridine, $80\text{ }^\circ\text{C}$.

All compounds exist as single molecules in DMSO resulting in $^1\text{H-NMR}$ spectra featuring the signals of the non-dimerized species. $^1\text{H-NMR}$ spectra recorded in deuterated chloroform, however, gave the characteristic resonances at $\delta = 10.3$, 9.7 and 9.3 ppm, indicative of four-fold intermolecular hydrogen bonding and intramolecular hydrogen bonding.²⁷ Compound **3** was obtained as a colorless oil, whereas compounds **4a, b** were obtained as waxy white solids that showed birefringence in polarized optical microscopy. Heating of the samples resulted in loss of birefringence at 115 and $73\text{ }^\circ\text{C}$, respectively. Above the clearing temperature compound **4a** became fluid, whereas **4b** initially formed an isotropic highly viscous liquid, in accordance with its supramolecular polymeric character. The formation of flower-like patterns for **4a** indicated the formation of a columnar liquid crystalline mesophase. However, cooling the isotropic melt of compound **4b** did not result in the quick reappearance of birefringence, most probably due to difficult reorientation of the molecules in the polymer melt with high viscosity.

5.2.2 Self-assembly in solution

The self-assembly of compounds **3** and **4** in solution was investigated by $^1\text{H-NMR}$ spectroscopy. When dissolved in deuterated chloroform, monofunctional **3** gave typical $^1\text{H-NMR}$ spectra for molecules dimerized via self-complementary hydrogen bonding; the three hydrogen bonded protons are visible between 9 and 10.5 ppm, whereas the non-hydrogen bonded amine proton can be found at $\delta = 5.8$ ppm (Figure 5.1, top spectrum). Monofunctional **3** dissolved readily in water

and the spectra between 11 and 5.3 ppm at different temperatures are given in Figure 5.1. At 80 °C, only the two aromatic protons and the two coinciding protons of the urea unit are visible. The amine protons exchange rapidly with the water hydrogens at this temperature and are, by consequence, not visible. Lowering of the temperature reveals the presence of two unequal urea protons and the appearance of the two amine protons as broad signals. At low temperatures (< 10 °C) broadening of the urea and aromatic signals occurs, suggesting stacking of the molecules via arene-arene interactions. The spectra thus indicate that at high temperatures in water the molecules are molecularly dissolved and upon lowering of the temperature aggregation takes place via stacking of the aromatic units, however, without occurrence of intermolecular hydrogen bonding.

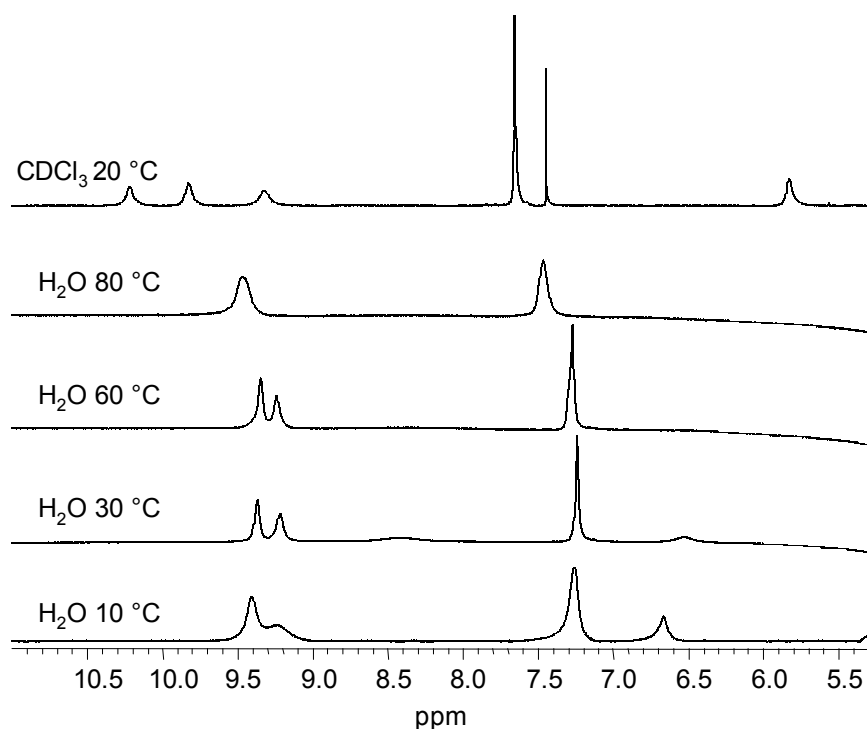


Figure 5.1: $^1\text{H-NMR}$ (500 MHz) spectra between 11.0 and 5.3 ppm of **3** in CDCl_3 and in $\text{H}_2\text{O}/\text{D}_2\text{O}$ 9/1 (~ 10 mg/ml; 10 mM) at different temperatures.

Similar to monofunctional **3**, bifunctional **4b** smoothly dissolved in chloroform wherein it dimerized via self-complementary four-fold hydrogen bonding (Figure 5.2, bottom spectrum), affording a random coil supramolecular polymer. In both methanol at room temperature as in water at higher temperatures, the amine protons of **4b** are in rapid exchange with the solvent and thus invisible (Figure 5.2). This indicates that the molecules dissolve molecularly in methanol as well as in water at high temperatures. Compound **4b**, however, did not dissolve readily in water of room temperature and heating and sonication for approximately 15 minutes needed to be employed to dissolve the compound. Lowering the temperature of the aqueous sample resulted in changes in the proton NMR spectrum suggestive for aggregation. A broadening of the signals occurred pointing to arene-arene

stacking and, more importantly, signals at positions typical for hydrogen bonded protons appeared between 9 and 10.5 ppm (Figure 5.3). Initially, only broadening of the signals can be observed, similar as for **3** in water at low temperatures. However, at temperatures below 50 °C the additional signals, expected in case of hydrogen bonding, come up. Due to the concomitant occurrence of both stacking and hydrogen bonding, the signals become broad.

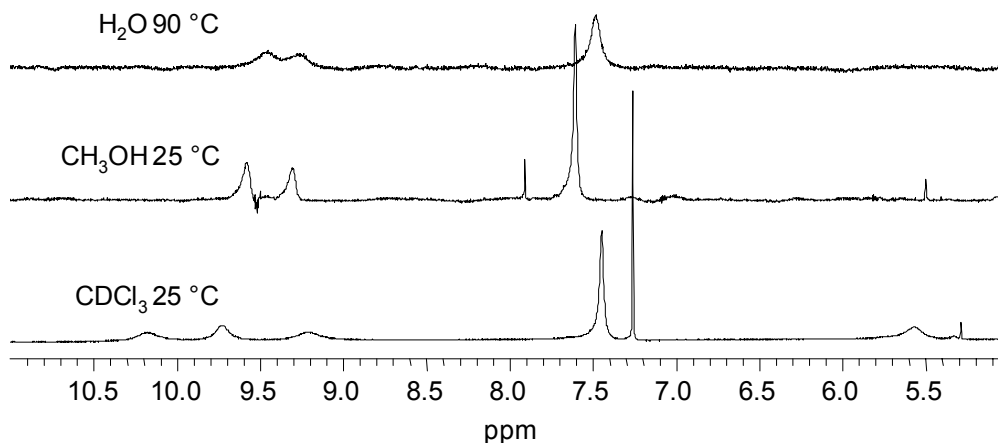


Figure 5.2: $^1\text{H-NMR}$ (500 MHz) spectra between 11.0 and 5.0 ppm of **4b** in CDCl_3 and $\text{CH}_3\text{OH}/\text{CD}_3\text{OD}$ 9/1 at room temperature and in $\text{H}_2\text{O}/\text{D}_2\text{O}$ 9/1 at 90 °C (~ 10 mg/ml; 5 mM).

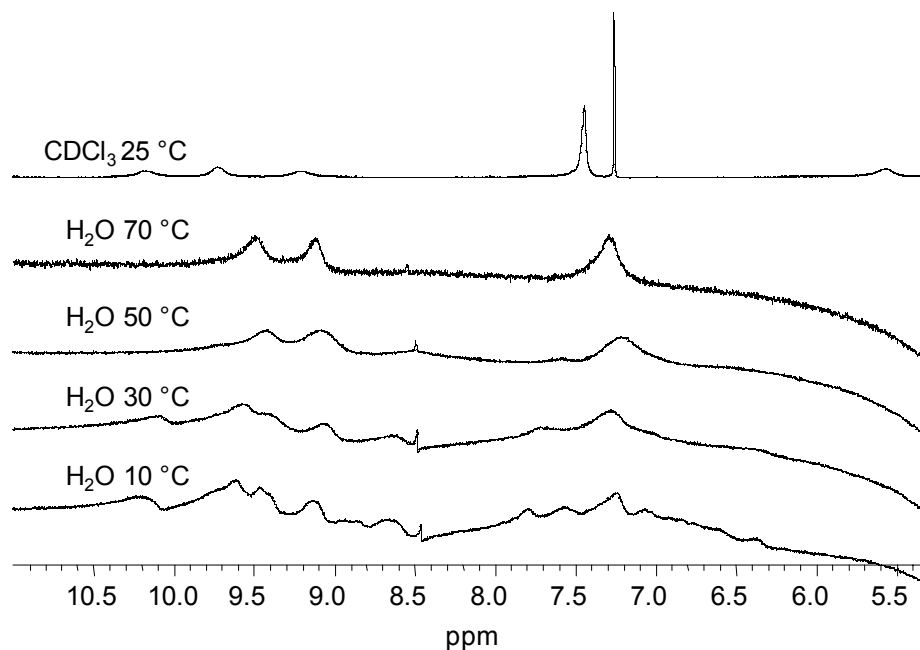


Figure 5.3: $^1\text{H-NMR}$ (500 MHz) spectra of **4b** in CDCl_3 at room temperature and in $\text{H}_2\text{O}/\text{D}_2\text{O}$ 9/1 (~ 10 mg/ml; 5 mM) at different temperatures in the regime of 5.3 to 11.0 ppm. The baseline of the water samples is curved near 5 ppm due to the measurement technique used (JUMPRET).

To investigate the self-assembly of **3** and **4** in solution, UV-Vis and CD spectroscopy measurements were performed in various solvents. The UV-Vis spectra of **4b** are depicted in Figure

5.4 (left). An absorption band around 290 nm is present in dilute (10^{-4} M) solutions. The absorption maximum in methanol, acetone and acetonitrile (not shown) lies around 288 nm whereas in water and chloroform a small, but significant, red-shift to 292 nm occurs. The absorption maximum in water and chloroform is at the same position as the maximum observed in the solid state (not shown) and of that of its apolar analog **2b** in chloroform and dodecane,³¹ thus indicating that a red-shifted maximum around 292 nm refers to a hydrogen bonded form of the molecules and the maximum around 288 nm corresponds to molecularly dissolved not hydrogen-bonded dimerized molecules. When the same solutions are monitored with CD spectroscopy, no Cotton effect is observed for the methanol and chloroform solutions, but surprisingly a Cotton effect is observed in water, at the position of the UV maximum (Figure 5.4, right). In methanol, but also in acetone and acetonitrile, the molecules are molecularly dispersed and are thus not present in a preferred supramolecular chiral conformation. In chloroform, the molecules do dimerize via quadruple hydrogen bonding and form supramolecular random coil polymers, in analogy with their ureidopyrimidinone counterparts.⁴ However, the aromatic units do not stack in chloroform, resulting in a disordered polymer as reflected in the absence of a Cotton effect. Apparently, only in water the molecules both dimerize via quadruple hydrogen bonding and stack, as was also observed with ¹H-NMR spectroscopy (Figure 5.3). The occurrence of both these interactions accounts for the formation of a columnar superstructure in which the chiral side-chains can transfer their chirality to the helical arranged aromatic core, reflected in the presence of a Cotton effect. It is proposed that, in analogy to the achiral counterparts **2a** and **b**,²⁶ the superstructure is a helical column of stacked hydrogen bonded pairs (Figure 5.5). The CD spectrum of **4b** features the same bandshape characteristics as that of **2b** in alkane solvents indicating that a similar helical structure is formed (see also Figure 5.6 (right)).²⁶ The opposite sign of the Cotton effect of **4b** in water with respect to **2b** in alkanes, shows the formation of helices with a preferred helicity opposite to the one in alkanes, despite their identical configuration; presumably due to the different positioning of the stereocenters.

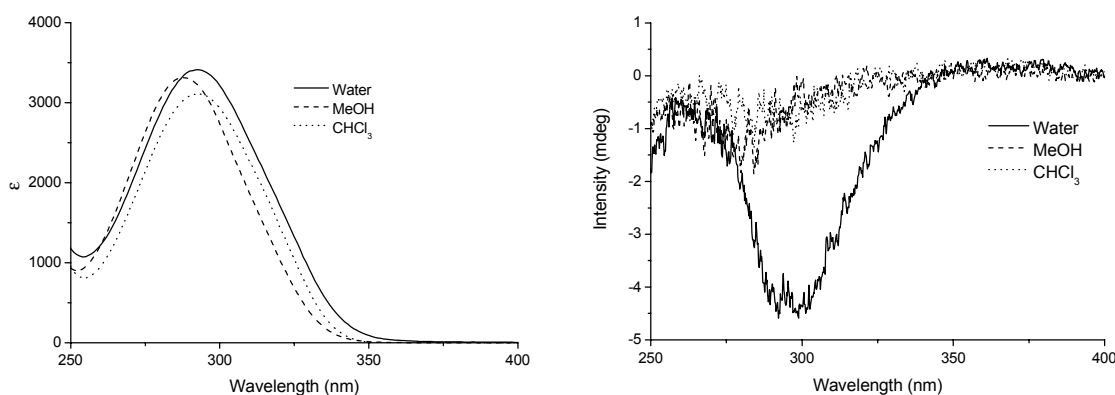


Figure 5.4: UV-Vis (left) and CD spectra (right) of **4b** in three different solvents at room temperature (10^{-4} M, 1 mm cuvette).

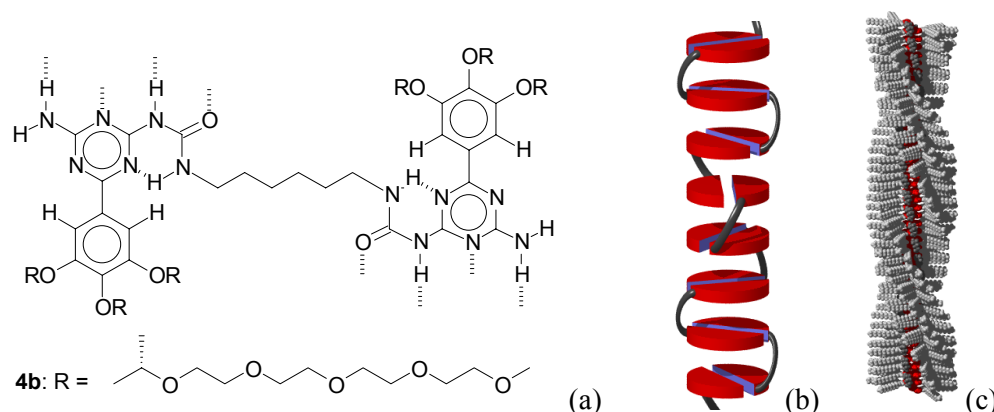


Figure 5.5: Proposed mode of association of bifunctional **4b** in water into helical columns, cartoonwise (b) and in a space filling model (c).

5.2.3 Self-assembly in chiral columns in water via stacking of hydrogen bonded pairs

The self-assembly of **4b** in water was investigated with temperature dependent UV-Vis and CD spectroscopy. An increase of the temperature results in a gradual blue shift of the absorption maximum from 292 to 288 nm (Figure 5.6, left). Simultaneously, the Cotton effect gradually decreases upon increase of the temperature and has disappeared around 90 °C (Figure 5.6, right).³² The changes observed upon increase of the temperature indicate the coincidental loss of positional order of the molecules within the columns (CD) and loss of intermolecular hydrogen bonding (UV-Vis and ¹H-NMR), thus showing that increased temperatures denature the hydrogen bonded and stacked pairs. At temperatures above 80 °C at $2 \cdot 10^{-4}$ M the aqueous solutions become turbid. This is ascribed to the phase-separation of the oligo(ethylene oxide) side-chains with the water.³³ In contrast to previously studied discotics,³⁴ however, the temperature induced aggregation does not result in the reappearance of a Cotton effect, affirming the loss of structuring interactions at high temperatures.

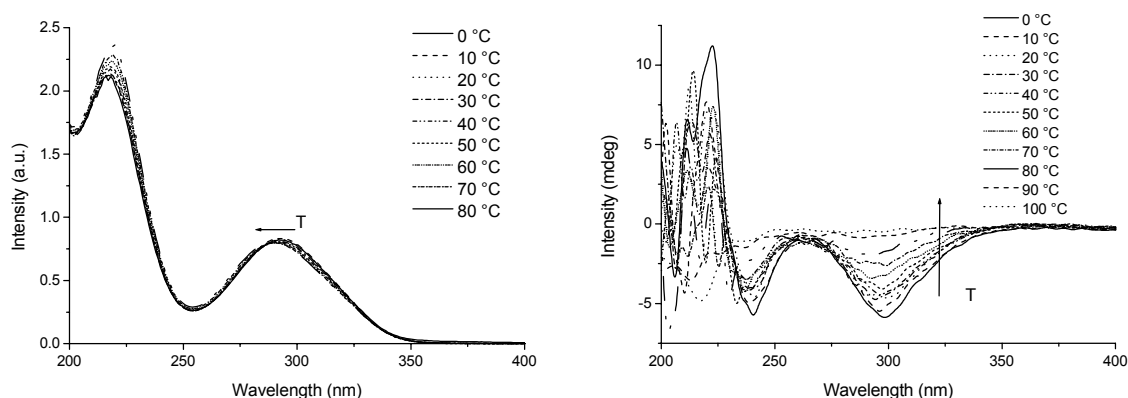


Figure 5.6: UV-Vis (left) and CD spectra (right) of **4b** in water ($2.4 \cdot 10^{-4}$ M) at different temperatures. The Cotton effects are stable in time and reversible and independent of cooling or heating rate.

To investigate the necessity for a supramolecular backbone, *i.e.* bifunctional molecules, UV-Vis and CD spectra of chiral monofunctional **3** in water were recorded at different concentrations. At 10^{-4} M the UV-Vis spectrum displays an absorption maximum around 288 nm and no Cotton effect is observed with CD spectroscopy (Figure 5.7). This shows that, in analogy with its apolar analog **1b** in dodecane and in contrast to bifunctional **4b** in water, chiral monofunctional water-soluble **3** does not form chiral supramolecular architectures in water at the applied low concentrations. In line with the $^1\text{H-NMR}$ experiments performed for **3** (Figure 5.1), the UV-Vis spectra indicate that intermolecular hydrogen bonding is not occurring in water. A red-shifted absorption maximum in the UV-Vis spectra only becomes visible at high concentration and concomitantly, also a small Cotton effect appears. Apparently, at low concentrations the monofunctional molecules are molecularly dispersed, but a strong increase of the concentration accounts for enhanced stacking probability and hence intermolecular hydrogen bonding and this allows the side-chain chirality to be transferred to the aromatic system. The fact that bifunctional **4b** forms helical columns at low concentrations in water, probably finds its origin in a high local concentration of hydrophobic units due to the hexamethylene linker, allowing for stronger stacking. The analogy might be made here to nucleic acid oligomers; whereas single mononucleotides do not form a hydrogen bonded supramolecular structure in water, oligomeric nucleotides of sufficient length do.¹ Thus, a (supramolecular) polymer backbone is necessary to form stable, well-defined helical columns. The polymer backbone allows the formation of hydrophobic micro-domains even at low concentrations due to the high local concentration of hydrophobic units. The induced arene-arene interactions then allow for cooperative hydrogen bonding and transfer of the peripheral chirality into the helix.

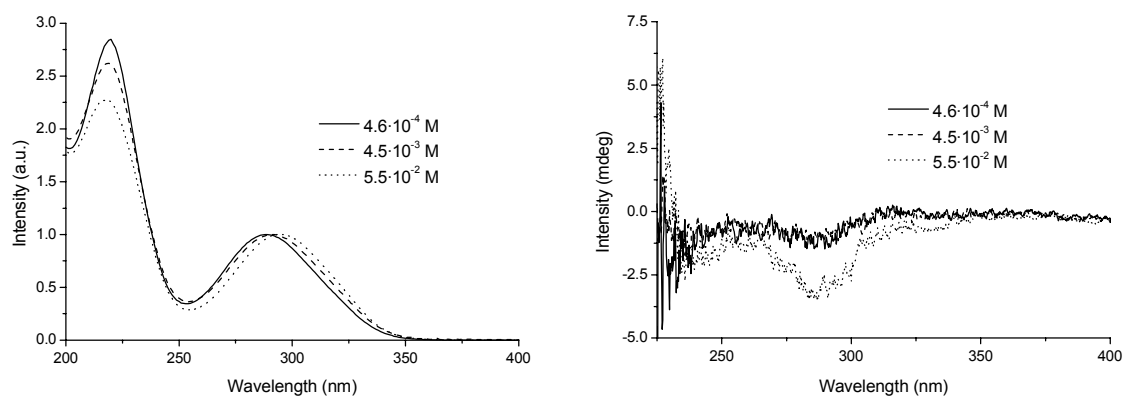


Figure 5.7: Normalized UV-Vis (left) and CD spectra (right) of **3** in water at different concentrations. The spectra were recorded in 1, 0.1 and 0.01 mm cuvettes, respectively.

In order to further explore the differences in aggregation behavior between **4** and **3**, fluorescence measurements in water and chloroform were undertaken. In water, the fluorescence of compounds **4a** and **4b** is highly quenched when compared to **3** in water or **4** in chloroform, acetone,

methanol or acetonitrile. The fluorescence of **4b** in chloroform is rather temperature independent (Figure 5.8 (a)), even though increase of the temperature initially results in a small increase of the fluorescence intensity. Further increase of the temperature ($> 30\text{ }^{\circ}\text{C}$), results in a normal small decrease of the fluorescence intensity, supporting the molecularly dissolved nature of the molecules at this low concentration. A similar behavior was found for monofunctional **3** in water; an increase of the temperature from 0 to $100\text{ }^{\circ}\text{C}$ resulted in a gradual decrease of the fluorescence intensity (Figure 5.8 (b)). The fluorescence maximum is somewhat red-shifted in water with respect to chloroform, which is most probably due to the difference in solvent polarity.

The fluorescence spectra of **4a** and **4b** in water show a totally different behavior upon changing the temperature. The aqueous solutions of **4a** and **4b** feature a strong increase of the fluorescence intensity with increased temperature (Figure 5.8 (c), (d)). This behavior is different from the usual decrease of the fluorescence intensity of molecularly dissolved molecules with increasing temperature. Generally, a temperature increase favors non-radiative decay processes and the opposite behavior for **4** suggests other processes occur, most probably because the molecules are not molecularly dispersed. For the quenched fluorescence of **4** in water the analogy might be made to *e.g.* the *m*-phenylene ethynylene oligomers as studied by Moore.³⁵ These oligomers feature a strong quenching of the fluorescence intensity when they fold from a random coil, in which there are no backbone-backbone interactions, into a helix that features strong stacking interactions of the aromatic backbone. These stacking interactions account for the formation of an 'excimer-like' structure that shows a low fluorescence intensity.³⁶ Similarly, the bifunctional molecules **4** are capable of stacking interactions between the two aromatic units. This stacking presumably causes the strong quenching of the fluorescence and this also explains why the fluorescence of **3** in water is not quenched.³⁷ UV-Vis and CD measurements have shown that an increase of the temperature accounts for increased motion of the molecules and concomitant decrease of stacking interactions. Accordingly, the increase of the fluorescence of **4** at higher temperatures results from a reduction of the stacking interactions.

The hexamethylene linker of **4** enables the stacking of two units in water, whereas the absence of this linker in compound **3**, renders the molecules already molecularly dissolved with concomitant expression of fluorescence. In chloroform, the driving force for stacking of the aromatic units of **4** is small and consequently the fluorescence is not quenched. The fluorescence experiments confirm that bifunctional **4** has a much stronger tendency for hydrophobic stacking of the units due to a high local concentration of functional groups, rationalizing why self-assembled architectures will form at lower concentrations than **3**.

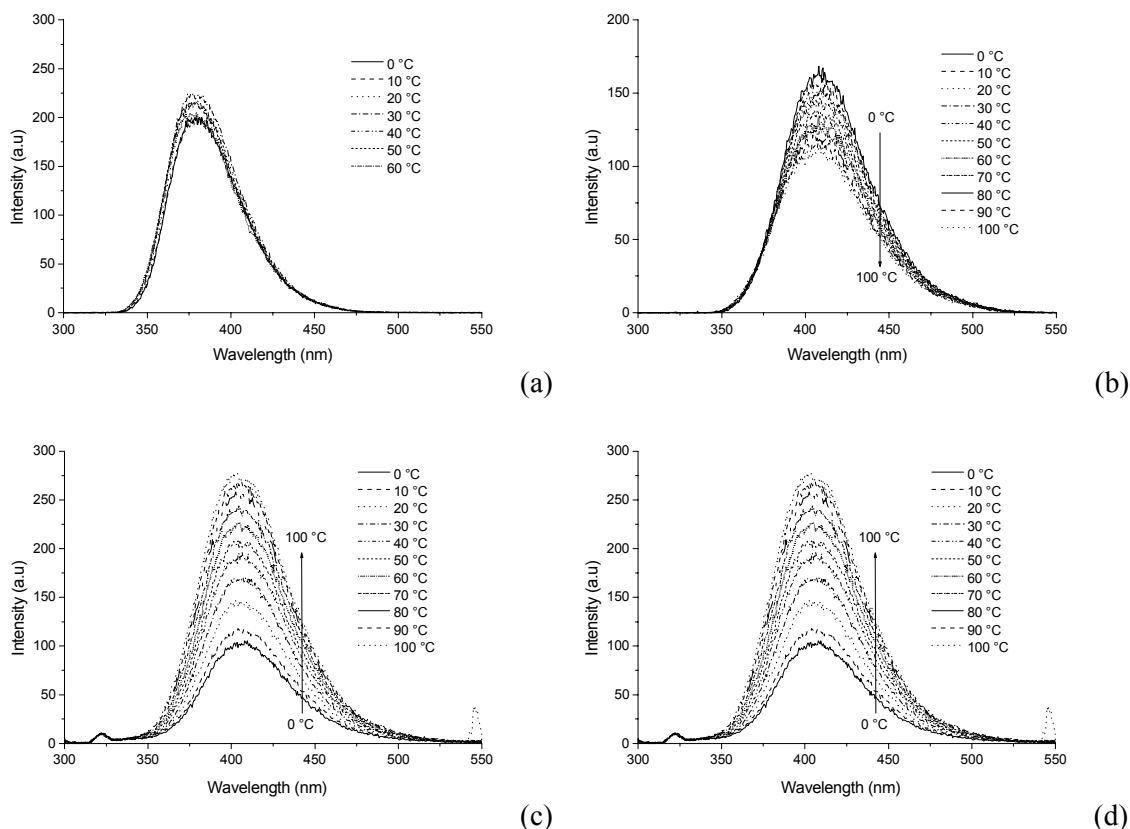


Figure 5.8: Fluorescence spectra of (a) bifunctional **4b** in chloroform; (b) monofunctional **3** in water; (c) bifunctional achiral **4a** in water (d) bifunctional chiral **4b** in water, recorded at $\sim 5 \cdot 10^{-6}$ M with λ_{exc} at 290 nm. It should be noted that, due to normalization, the approximately 20-fold stronger fluorescence of **4b** in chloroform (a) and **3** in water (b) is not reflected in the depicted intensities.

5.2.4 Cooperativity within the columns

In water the bifunctional molecules **4a** and **4b** aggregate at low concentrations in helical columns, whereas this aggregation does not occur for monofunctional **3** unless the concentrations is high. In principle these helical columns are well-matched for the transfer of chiral information from one molecule to the other. The stacking of a molecule with achiral side chains on top of a molecule with chiral side chains would possibly result in the amplification of chirality from the chiral to the achiral molecule. In order to investigate the cooperativity in the stacking of the molecules, ‘Sergeant and Soldiers’¹³ experiments were performed on mixtures of achiral bifunctional **4a** (soldiers) and chiral **3** or chiral **4b** (sergeants). In analogy with previously studied discotics,³⁴ the Cotton effect of the mixtures was studied as a function of their composition.

When solutions of varying amounts chiral **3** and achiral **4a** –keeping the total concentration of chromophores constant– were prepared at 10^{-4} M in water, no Cotton effect was observed for any of the mixtures. The maximum of the absorbance spectrum shifts linearly from 288 nm to 292 nm upon going from 100% **3** to 100% **4a**. Apparently, at this concentration the achiral bifunctional molecules

4a are aggregating, but their helicity is not biased, because the monofunctional chiral molecules **3** are not aggregating, in line with previous observations (Figure 5.7) and thus cannot express their side-chain chirality at a supramolecular level. The incapability of **3** to stack and form hydrogen bonds at this concentrations, prevents the transfer of chirality from **3** into the columns of **4**. When the measurements are performed at higher concentration ($5 \cdot 10^{-3}$ M) and low temperature (5°C), however, monofunctional **3** does aggregate to some extent. At these high concentrations, the UV-Vis spectra of both compounds superimpose, with their maximum around 292 nm. When the mixtures are then examined by CD spectroscopy, Cotton effects are observed, indeed. A non-linear increase of the g_{abs} can be observed upon addition of small amounts of **3** to **4a** (Figure 5.9 (a)). This positive deviation from linearity shows that the chirality is being transferred from the chiral monofunctional **3** to the achiral bifunctional **4a**. In Figure 5.9 (b) the proposed mode of the action of this chirality transfer is visualized in a picture.

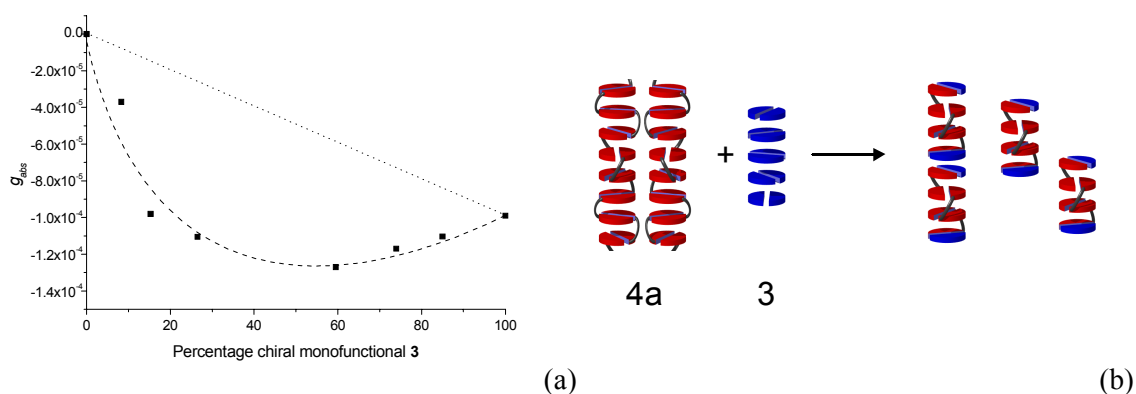


Figure 5.9: (a) Dependence of the overall chirality on the mole fraction of chiral **3** in mixtures of **3** and achiral **4a** in water at 5°C , expressed in terms of the g -value and measured at the maximum of the Cotton effect at 287 - 293 nm. Measurements were recorded at a constant total concentration of functional groups of 5×10^{-3} M in a 0.1 mm cell. (b) Proposed mode of amplification of chirality in mixtures of **3** and **4a**. Achiral **4a** forms non-biased helical columns, mixing with monofunctional chiral **3** results in the bias of the columns of **4a**.

The bias of the helical columns of **4a** should also be possible by addition of chiral bifunctional **4b**. The UV-Vis spectra of different mixtures of **4a** and **4b** in water superimpose, indicating that similar helical structures are being formed by all mixtures. Surprisingly, however, the intensity of the Cotton effect was found to be linearly dependent on the amount of chiral **4b**, showing that amplification of chirality does not occur for these mixtures. Two explanations can be thought of; either there is no cooperative order in the helix, or the molecules do not mix. The first explanation seems very unlikely since an amplification of chirality was observed for mixtures of **4a** and **3**. Although the second explanation might at first glance seem unlikely, a strong difference in solubility between **4a** and **4b** in water exists. Whereas achiral **4a** dissolved readily in water at room temperature

after several minutes, chiral **4b** could only be dissolved upon sonication at elevated temperatures for 15 minutes. This difference in solubility most probably prevents an exchange of the molecules between the aggregates. Heating of the solution and subsequent cooling did not result in an increase of the Cotton effect either. Moreover, because **4a** and **4b** have different transition temperatures, **4b** aggregates much sooner than **4a**.

5.3 Conclusions

The creation of columnar architectures in water by **3** and **4** using hydrogen bonded pairs requires the presence of a hydrophobic microenvironment that shields the hydrogen bonding from the solvent to make them operative. Whereas monofunctional **3** does not stack via hydrogen bonded pairs in water unless elevated concentrations and low temperatures are applied, bifunctional **4** does form in water at low concentrations a helical column, of which the helicity can be biased by peripheral chiral moieties. The supramolecular polymer backbone created by **4** is necessary to form stable, well-defined helices and induces stacking, even at low concentrations, due to a high local concentration of units. Within the columns a certain degree of cooperativity exists, as chiral monofunctional **3** is capable of biasing the helicity of columns formed by achiral bifunctional **4a**. However due to the low tendency of **3** to aggregate, this only occurs at elevated concentrations.

The findings presented in this chapter show that for the creation of well-defined chiral architectures in water, both specific, polar interactions and hydrophobic interactions are required. The implementation of these design criteria will allow the generation of a variety of ordered supramolecular architectures in water. The use of even stronger hydrogen bonding units, such as the 2-ureido-pyrimidin-4-one unit, might allow the creation of random coil supramolecular polymers in water, without the need for a hydrophobic microenvironment.

5.4 Towards water-soluble random coil supramolecular polymers

Water-soluble random coil supramolecular polymers are highly attractive systems to study, both from a theoretical as practical point of view, as they would combine the advantages of supramolecular systems such as reversibility,³⁸ with solubility in water as the solvent for tailored personal products. The creation of such water-soluble supramolecular polymers requires the utilization of a strong and specific interaction. Structures **3** and **4** use four-fold intermolecular hydrogen bonding and on top of that hydrophobic interactions. This results, however, in columnar polymers. In order to allow four-fold hydrogen bonding to be operative in water as the single driving force for self-assembly, a stronger unit is required. It has previously been shown that the 2-ureido-pyrimidin-4-one unit is an easy accessible and very strong self-complementary unit in organic solvents (DDAA),³⁹ affording supramolecular random coil polymers in chloroform solutions with very high virtual molecular weights.⁴ This unit was selected as a promising tool to create water-soluble supramolecular polymers. By functionalization with an oligo(ethylene oxide) side-chain and linkage to another unit, water-soluble bifunctional molecule **6** was obtained (Figure 5.10).⁴⁰ In chloroform **6** dimerizes via four-fold hydrogen bonding as reflected in the typical N-H absorptions around $\delta = 13, 12$ and 10 ppm in the ¹H-NMR spectra. In polar solvents like DMSO (a strong hydrogen bond breaking solvent) **6** is molecularly dispersed, giving rise to signals around $\delta = 11.5, 9.8$ and 7.4 ppm. Compound **6** dissolves in water after some heating and sonication, indicative of polymer properties. Surprisingly, the ¹H-NMR spectra of **6** in water at

room temperature show the N-H absorptions at positions typical for the hydrogen bonded form ($\delta = 12.8, 11.2$ and 10.0 ppm) (Figure 5.10). This indicates that in water, **6** forms supramolecular polymers via four-fold hydrogen bonding. Increase of the temperature results in broadening and shifting of the signal, indications that the molecules become molecularly dissolved. At low temperatures no new signals or strong broadening of the signals can be observed, in contrast to the behavior of **4b** at low temperatures (Figure 5.3). Actually, the N-H signals sharpen upon lowering the temperature, in line with slower exchange of the N-H protons with the solvent. Apparently, hydrophobic stacking of the units is not occurring significantly. Further investigations are necessary to qualify the strength and type (keto – enol)⁵⁹ of the hydrogen bonding. However, modification of other water-soluble systems with this functional unit brings intriguing applications in sight.

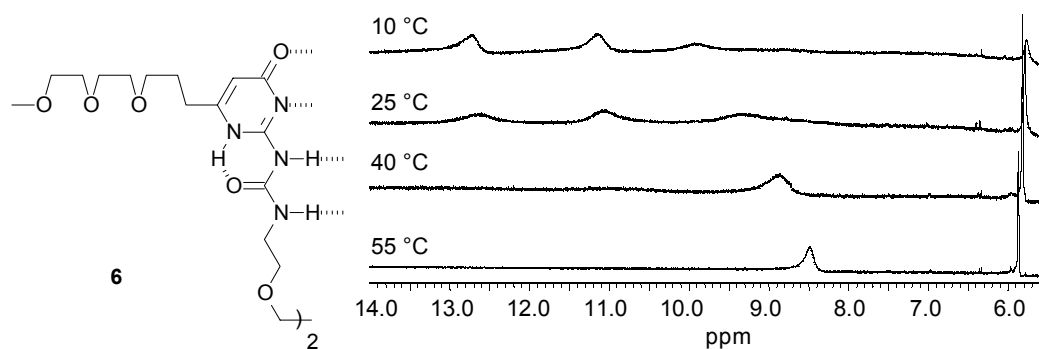


Figure 5.10: Water-soluble bifunctional 2-ureido-pyrimidin-4-one **6** and its NMR spectra (14.0 - 5.5 ppm) in water (H_2O / D_2O , 9/1) at different temperatures. At low temperatures the three hydrogen bonded protons at $\delta \sim 13, 11$ and 10 ppm are visible, as well as the alkylidene proton around 6 ppm. Due to the suppression of the water signal around 5 ppm, the intensity of the 6 ppm signal is too small.

5.5 Experimental section

General.⁴¹ Pyridine was dried over molesieves.

2-Amino-4-butylureido-6-(3,4,5-tris[(2*S*)-2-(2-{2-[2-(2-methoxyethoxy)-ethoxy]-ethoxy}-ethoxy)-propyloxy]-phenyl)-s-triazine (3). Butyl isocyanate (0.076 mL, 0.67 mmol) and 2,4-diamino-6-(3,4,5-tri[(2*S*)-2-(2-{2-[2-(2-methoxyethoxy)-ethoxy]-ethoxy}-ethoxy)-propyloxy]-phenyl)-s-triazine (**5b**) (0.33 g, 0.34 mmol) were heated under reflux in pyridine (2 mL) for 2 h. Subsequently the solvent was removed *in vacuo* and the residue was coevaporated with toluene (2*10 mL). The solid residue was purified by preparative size exclusion chromatography (Bio Beads S-X1, CH₂Cl₂) and column chromatography (silica gel, CHCl₃/EtOH 95/5) to yield the title compound as a colorless oil (0.19 g, 0.18 mmol, 52%). ¹H-NMR (CDCl₃): δ 10.20 (s, 1H), 9.78 (s, 1H), 9.26 (s, 1H), 7.50 (s, 2H), 5.58 (s, 1H), 4.18-4.08 (m, 3H), 3.98-3.84 (m, 6H), 3.81-3.42 (m, 48H), 3.40 (m, 2H), 3.35 (s, 9H), 1.66 (m, 2H), 1.43 (m, 2H), 1.32 (m, 9H), 0.95 (m, 3H). MALDI-TOF [C₅₀H₉₀N₆O₁₉+Na⁺] = Calcd. 1102.6 Da. Obsd. 1102.2 Da.

N⁰,N^{0'}[1,6-Hexanediyl]-bis-[4-ureido-2-amino-6-(3,4,5-tris[2-(2-{2-[2-(2-methoxyethoxy)-ethoxy]-ethoxy}-ethoxy)-propyloxy]-phenyl)-s-triazine] (4a). A solution of 2,4-diamino-6-(3,4,5-tri[(2*S*)-2-(2-{2-[2-(2-methoxyethoxy)-ethoxy]-ethoxy}-ethoxy)-propyloxy]-phenyl)-s-triazine (**5b**) (0.50 g, 0.53 mmol) and 1,6-diisocyanatohexane (0.043 mL, 0.26 mmol) in dry pyridine (4 mL) was stirred at reflux temperature for 3 days. The solvent was removed *in vacuo* and coevaporated twice with toluene (2*10 mL) giving an off-white waxy solid. Purification by column chromatography (silica gel, CHCl₃/MeOH 95/5), (silica gel, CH₃OCH₂CH₂OCH₃) and preparative size exclusion chromatography (Bio Beads S-X1, CH₂Cl₂) yielded the pure title compound as a white solid (0.27 g, 0.13 mmol, 52%). T_{cl} = 115 °C. ¹H-NMR (CDCl₃): δ 10.17 (s, 2H), 9.72 (s, 2H), 9.18 (s, 2H), 7.44 (s, 4H), 5.61 (s, 2H), 4.21 (m, 18H), 3.87 (t, 12H), 3.82 (t, 6H), 3.78-3.52 (m, 84H), 3.37 (s, 18H), 3.30 (m, 4H), 1.62 (m, 4H), 1.44 (m, 4H). ¹³C-NMR (CDCl₃): δ 170.2 (C-2), 167.1 (C-6), 163.7 (C-4), 155.7 (CO), 152.4 (gall. C-3,5), 142.0 (gall. C-4), 130.9 (gall. C-1), 108.0 (gall. C-2,6), 72.4, 71.9, 71.8, 70.7, 70.6-70.4, 69.7, 68.9, 58.9, 39.5, 29.0, 25.9.

N⁰,N^{0'}[1,6-Hexanediyl]-bis-[4-ureido-2-amino-6-(3,4,5-tris[(2*S*)-2-(2-{2-[2-(2-methoxyethoxy)-ethoxy]-ethoxy}-ethoxy)-propyloxy]-phenyl)-s-triazine] (4b). A solution of 2,4-diamino-6-(3,4,5-tri[(2*S*)-2-(2-{2-[2-(2-methoxyethoxy)-ethoxy]-ethoxy}-ethoxy)-propyloxy]-phenyl)-s-triazine (**5b**) (0.28 g, 0.29 mmol) and 1,6-diisocyanatohexane (0.014 mL, 0.085 mmol) in dry pyridine (2 mL) was stirred at reflux temperature for 2 days. The solvent was removed *in vacuo* and coevaporated twice with toluene (2*10 mL) giving an off-white waxy solid. Purification by column chromatography (silica gel, CHCl₃/MeOH 95/5) (silica gel, CH₃OCH₂CH₂OCH₃) yielded the pure title compound as a white waxy solid (0.11 g, 0.049 mmol, 58%). T_{cl} = 73 °C. ¹H-NMR (CDCl₃): δ 10.19 (s, 2H), 9.77 (s, 2H), 9.22 (s, 2H), 7.44 (s, 4H), 5.58 (s, 2H), 4.14-4.08 (m, 6H), 3.97-3.86 (m, 12H), 3.83-3.45 (m, 96H), 3.38 (m, 4H), 3.37 (s, 6H), 3.35 (s, 12H), 1.62 (m, 4H), 1.44 (m, 4H), 1.31 (m, 18H). ¹³C-NMR (CDCl₃): δ 170.1 (C-2), 167.2 (C-6), 163.7 (C-4), 155.7 (CO), 152.4 (gall. C-3,5), 141.6 (gall. C-4), 130.8 (gall. C-1), 107.3 (gall. C-2,6), 76.3, 75.0, 74.4, 72.8, 71.9, 71.8, 70.8-70.4, 68.8, 68.5, 59.0, 39.5, 29.4, 26.1, 17.7. MALDI-TOF [C₉₈H₁₇₄N₁₂O₃₈+Na⁺] = Calcd. 2151.2 Da. Obsd. 2151.2 Da.

2,4-Diamino-6-(3,4,5-tris[2-(2-{2-[2-(2-methoxyethoxy)-ethoxy]-ethoxy}-ethoxy)-ethoxy]-phenyl)-s-triazine (5a). Biguanide sulfate (1.40 g, 7.05 mmol) and sodium (0.34 g, 15 mmol) were added to dry methanol (35 mL) and the solution was stirred under reflux for 2 h. Subsequently methyl 3,4,5-tri[2-(2-{2-[2-(2-methoxyethoxy)-ethoxy]-ethoxy}-ethoxy)-ethoxy]-benzoate (2.50 g, 2.82 mmol) was added and reflux was continued overnight. After removal of the solvent *in vacuo*, the residue was purified by column chromatography (alumina, CHCl₃/MeOH 97/3), to yield the pure product as a colorless oil (1.00 g, 1.07 mmol, 38%). ¹H-NMR (CDCl₃): δ 7.62 (s, 2H), 5.56 (s, 4H), 4.22 (t, 6H), 4.20 (t, 3H), 3.85 (t, 6H), 3.80 (t, 3H), 3.76-3.65 (m, 48H), 3.37 (s, 9H). ¹³C-NMR (CDCl₃): δ 171.2 (C-2,4), 167.5 (C-6), 152.2 (gall. C-3,5), 141.3 (gall. C-4), 131.7 (gall. C-1), 107.8 (gall. C-2,6), 72.2, 71.8, 71.8, 70.6, 70.5, 70.5-70.3, 69.7, 58.9.

2,4-Diamino-6-(3,4,5-tris[(2*S*)-2-(2-{2-[2-(2-methoxyethoxy)-ethoxy]-ethoxy}-ethoxy)-propyloxy]-phenyl)-s-triazine (5b). Biguanide sulfate (1.34 g, 6.73 mmol) and sodium (0.34 g, 14 mmol) were added to dry methanol (30 mL) and the solution was stirred under reflux for 2 h. Subsequently methyl 3,4,5-tri[(2*S*)-2-(2-{2-[2-(2-methoxyethoxy)-ethoxy]-ethoxy}-ethoxy)-propyloxy]-benzoate (2.50 g, 2.69 mmol) was added and reflux was continued overnight. After removal of the solvent *in vacuo*, the residue was purified by column chromatography (alumina, CHCl₃/MeOH 96/4) (silica gel, CHCl₃/EtOH 85/15), to yield the pure product as a colorless oil (1.20 g, 1.22 mmol, 46%). ¹H-NMR (CDCl₃): δ 7.62 (s, 2H), 5.43 (s, 4H), 4.20-4.08 (m, 3H), 3.98-

3.85 (m, 6H), 3.81-3.53 (m, 48H), 3.38 (s, 6H), 3.37 (s, 3H), 1.30 (m). ^{13}C -NMR (CDCl_3): δ 171.1 (C-2,4), 167.4 (C-6), 152.0 (gall. C-3,5), 140.8 (gall. C-4), 131.5 (gall. C-1), 107.1 (gall. C-2,6), 76.3, 75.0, 74.4-70.3, 68.7, 59.0, 17.8.

$\text{N}^{\omega},\text{N}^{\omega}$ [1,8(3,5-Dioxaoctanediy)]-bis-[2-ureido-6-(3-{2-[2-methoxyethoxy]-ethoxy}-propyl)-4[1H]-pyrimidinone] (6).⁴⁰ Thoroughly dried 6-(3-[2-{2-methoxyethoxy}-ethoxy]-propyl)-isocytosine⁴² (4.01g, 14.8 mmol) and 3,6-dioxaoctyl diisocyanate (1.3 g, 6.5 mmol) were stirred at 100 °C for 3 h in pyridine (125 ml). Subsequently the solvent was evaporated *in vacuo* and the product was purified by column chromatography (silica gel, $\text{CH}_2\text{Cl}_2/\text{MeOH}$ 95/5), yielding pure **1**. ^1H -NMR (CDCl_3+TFA): δ 6.12 (s, 2H), 3.73-3.45 (m, 32H), 3.38 (s, 6H), 2.65 (t, 4H), 1.83 (q, 4H).

5.6 References and notes

- ¹ Saenger, W. *Principles of nucleic acid structure* New York: Springer-Verlag **1984**.
- ² Whitesides, G.M.; Mathias, J.P.; Seto, C.T. *Science* **1991**, *254*, 1312-1319.
- ³ G.-Krzywicki, F.; Fouguey, C.; Lehn, J.-M. *Proc. Natl. Acad. Sci. USA* **1993**, *90*, 163-167.
- ⁴ Sijbesma, R.P.; Beijer, F.H.; Brunsveld, L.; Folmer, B.J.B.; Hirschberg, J.H.K.K.; Lange, R.F.M.; Lowe, J.K.L.; Meijer, E.W. *Science* **1997**, *278*, 1601-1604.
- ⁵ Castellano, R.K.; Rudkevich, D.M.; Rebek, J. *Proc. Natl. Acad. Sci. USA* **1997**, *94*, 7132-7137.
- ⁶ Seebach, D.; Matthews, J.L. *Chem. Commun.* **1997**, 2015-2022.
- ⁷ Gellman, S.H. *Acc. Chem. Res.* **1998**, *31*, 172-180.
- ⁸ Palmans, A.R.A.; Vekemans, J.A.J.M.; Havinga, E.E.; Meijer, E.W. *Angew. Chem., Int. Ed. Engl.* **1997**, *36*, 2648-2651.
- ⁹ Prins, L.J.; Huskens, J.; de Jong, F.; Timmerman, P.; Reinhoudt, D.N. *Nature* **1999**, *398*, 498-502.
- ¹⁰ Brunsveld, L.; Schenning, A.P.H.J.; Broeren, M.A.C.; Janssen, H.M.; Vekemans, J.A.J.M.; Meijer, E.W. *Chem. Lett.* **2000**, 292-293.
- ¹¹ Brunsveld, L.; Zhang, H.; Glasbeek, M.; Vekemans, J.A.J.M.; Meijer, E.W. *J. Am. Chem. Soc.* **2000**, *122*, 6175-6182.
- ¹² Farina, M. *Topics in Stereochemistry* Eds. Eliel, E.L.; Wilen, S.H. New York: John Wiley & Sons **1987**, *17*, 1-111.
- ¹³ Green, M.M.; Reidy, M.P.; Johnson, R.D.; Darling, G.; O'Leary, D.J.; Willson, G. *J. Am. Chem. Soc.* **1989**, *111*, 6452-6454.
- ¹⁴ Moore, J.S.; Gorman, C.B.; Grubbs, R.H. *J. Am. Chem. Soc.* **1991**, *113*, 1704-1712.
- ¹⁵ Okamoto, Y.; Nakano, T. *Chem. Rev.* **1994**, *94*, 349-372.
- ¹⁶ Green, M.M.; Peterson, N.C.; Sato, T.; Teramoto, A.; Lifson, S. *Science* **1995**, *268*, 1860-1866.
- ¹⁷ Fujiki, M. *Polym. Prepr.* **1996**, *37(2)*, 454-455.
- ¹⁸ Schlitzer, D.S.; Novak, B.M. *J. Am. Chem. Soc.* **1998**, *120*, 2196-2197.
- ¹⁹ Yashima, E.; Maeda, K.; Okamoto, Y. *Nature* **1999**, *399*, 449-451.
- ²⁰ Prince, R.B.; Brunsveld, L.; Meijer, E.W.; Moore, J.S. *Angew. Chem. Int. Ed.* **2000**, *39*, 228-230.
- ²¹ Kunitake, T. *Angew. Chem. Int. Ed. Engl.* **1992**, *31*, 709-726.
- ²² Blokzijl, W.; Engberts, J.B.F.N. *Angew. Chem. Int. Ed. Engl.* **1993**, *32*, 1545-1579.
- ²³ Gottarelli, G.; Mezzina, E.; Spada, G.P.; Carsughi, F.; Di Nicola, G.; Mariani, P.; Sabatucci, A.; Bonazzi, S. *Helv. Chim. Acta* **1996**, *79*, 220-234.
- ²⁴ Appella, D.H.; Barchi Jr., J.J.; Durell, S.R.; Gellman, S.H. *J. Am. Chem. Soc.* **1999**, *121*, 2309-2310.
- ²⁵ Hirschberg, J.H.K.K.; Brunsveld, L.; Ramzi, A.; Vekemans, J.A.J.M.; Sijbesma, R.P.; Meijer, E.W. *Nature* **2000**, *407*, 167-170.
- ²⁶ Hirschberg, J.H.K.K. *Ph.D. thesis*, Eindhoven University of Technology, in preparation.
- ²⁷ Beijer, F.H.; Kooijman, H.; Spek, A.L.; Sijbesma, R.P.; Meijer, E.W. *Angew. Chem. Int. Ed.* **1998**, *37*, 75-78.
- ²⁸ Lydon, J. *Curr. Opin. Colloid Interface Sci.* **1998**, *3*, 458-466.
- ²⁹ Creighton, T.E. *Proteins, structures and molecular properties*; W.H. Freeman and Company: New York, **1984**.
- ³⁰ *Prediction of protein structure and the principles of protein conformation*; Fasman, G.D. Eds.; Plenum Press: New York, **1990**.
- ³¹ Hirschberg, J.H.K.K.; Marcos Ramos, A. *unpublished results*.
- ³² Similar experiments were performed on bifunctional **4a**. Obviously, no Cotton effect was detected in aqueous solutions, but a red-shift to 292 nm in the UV-Vis spectra was observed, suggesting similar structure formation in water by achiral **4a**.
- ³³ Bailey, F. Jr.; Koleske, J. *Poly (Ethylene Oxide)* Academic Press Inc., New York, **1976**.
- ³⁴ Brunsveld, L.; Lohmeijer, B.G.G.; Vekemans, J.A.J.M.; Meijer, E.W. *Chem. Commun.* **2000**, 2305-2306.
- ³⁵ Prince, R.B.; Saven, J.G.; Wolynes, P.G.; Moore, J.S. *J. Am. Chem. Soc.* **1999**, *121*, 3114-3121.
- ³⁶ It should be noted that for these oligomers, the decrease in fluorescence intensity is accompanied by a red-shift of the emission maximum, which is not observed for **4**.
- ³⁷ The decrease in luminescence for **4** upon stacking greatly contrasts with the increase of the luminescence upon stacking of the discotics discussed in Chapter 3. The reason lies in the difference of the luminescent chromophore. In the discotics the proton transferred 2,2'-bipyridine-3,3'-diamine unit is a single luminescent unit and its luminescence increases upon increasing rigidity. For **4** the luminescent *s*-triazine unit apparently interacts with another unit rendering a quenching of the luminescence.

- ³⁸ Brunsveld, L.; Folmer, B.J.B.; Meijer, E.W. *MRS Bulletin* **2000**, 25, 49-53.
- ³⁹ Beijer, F.H.; Sijbesma, R.P.; Kooijman, H.; Spek, A.L.; Meijer, E.W. *J. Am. Chem. Soc.* **1998**, 120, 6761-6769.
- ⁴⁰ For a full account on the synthesis of **6** see: van Buijtenen J. *Water soluble hydrogen bonded polymers*, **2000**, research report Eindhoven University of Technology.
- ⁴¹ For a description of the general procedures see also chapter 2, section 2.5 Experimental section and chapter 3, section 3.7 Experimental section.
- ⁴² Folmer, B.J.B. *Ph.D. thesis*, Eindhoven University of Technology, **2000**.

Chapter 6

Cooperative and hierarchical folding of chiral *m*-phenylene ethynylene oligomers and their self-assembly in columns[†]

Abstract: *A series of m-phenylene ethynylene oligomers containing chiral polar (2S)-methyl-3,6,9-trioxadecyloxy side chains has been synthesized and studied. The oligomers are present in a random coil conformation in chloroform, and fold in a stepwise process via helical conformations in acetonitrile/chloroform mixtures into chiral helices in acetonitrile. The hierarchical folding was unraveled using a combination of UV-Vis and CD spectroscopy. Oligomers containing both chiral and achiral side-chains revealed intramolecular cooperative interactions, but also showed that a 100 % helicity bias could not be achieved in acetonitrile. The helix could, however, be stabilized by the addition of water and in addition this resulted in the formation of helical columns via intermolecular stacking of the helices. Within these columnar aggregates chirality can be amplified from a chiral oligomer to an achiral oligomer owing to cooperative stacking interactions. A series of m-phenylene ethynylene oligomers containing chiral apolar (S)-3,7-dimethyl-1-octyloxy side chains was also synthesized and studied. These oligomers fold into helical conformations in apolar solvents (alkanes). In contrast to the polar oligomers, the formation of a chiral helix coincided with the formation of columnar aggregates. These aggregates are highly stable with a concomitant strong time-dependence for the expression of the side-chain chirality within the supramolecular helices.*

[†] This work has been performed in collaboration with Professor J.S. Moore and dr. R.B. Prince at the University of Illinois at Urbana-Champaign.

6.1 Introduction

The folding of non-biological oligomers into well-defined conformations in solution is an area of active study, and recent advances have provided ordered structures,^{1,2} both in apolar³⁻⁷ and polar^{6,8-16} solvents and in water.^{6,7,17-23} As an example, the architectures formed by β -amino acid peptides have been shown to possess increased stability with respect to their natural analogues.²⁴ However, the creation of larger, multimolecular architectures by these non-biological oligomers has not been investigated in great detail.^{4,5} This contrasts with discotic molecules which have been shown to self-assemble in columns in solution.²⁵⁻³⁵ Via specific assembly, well-defined long columns can be formed allowing for control over their chirality and their isodesmic or cooperative formation has been elucidated.³⁶⁻³⁹ Using electron microscopy, the presence of intertwined helices based on such columns and other chiral architectures has been clarified and indicated the occurrence of aggregation at a higher level, of the well-defined supramolecular columnar self-assemblies.⁴⁰⁻⁴⁶

Moore and coworkers have shown that random coil *m*-phenylene ethynylene oligomers (**1**) fold via a cooperative transition into helical conformations due to solvophobic forces.^{15,16} The folding was determined to be chain-length dependent and could be directed by programmed design elements in the oligomer.⁴⁷ In addition, they have demonstrated that the helical twist sense of these oligomers can be biased by the incorporation of a single chiral binaphthyl unit into the backbone or via complexation of a chiral guest molecule in the cavity.^{48,49} Here, it is demonstrated that a small, chiral perturbation to the side chains causes a bias to the helical twist sense without disrupting the conformational stability of oligomer series **2** (eq. 6.1). Moreover, solvent and thermal denaturation studies monitored by absorption and circular dichroism spectroscopies reveal insight into the cooperative nature of the folding process and the manner in which this conformational order develops. Specifically, these studies show that there is a significant hierarchical progression in conformational order following the initial helical state. Intramolecular 'Sergeants-and-Soldiers' experiments reveal a nonlinear dependence of the circular dichroism (CD) signal on the amount of chiral side chains indicating that there are cooperative interactions among the side chains. To further elucidate the nature of the folding and chirality transfer and for the creation of multi-molecular architectures, experiments in aqueous media have been performed. The helices stack under these conditions to form columnar architectures in which the chirality of a chiral oligomer can be amplified to achiral helical oligomers. By the attachment of chiral, apolar side chains to the *m*-phenylene ethynylene oligomers (oligomer series **3**) chiral helices in apolar solvents were generated, showing the generality of the folding principle for this type of oligomers. In apolar solvents, intermolecular aggregation was found to play an important role in the occurrence of a twist sense bias.

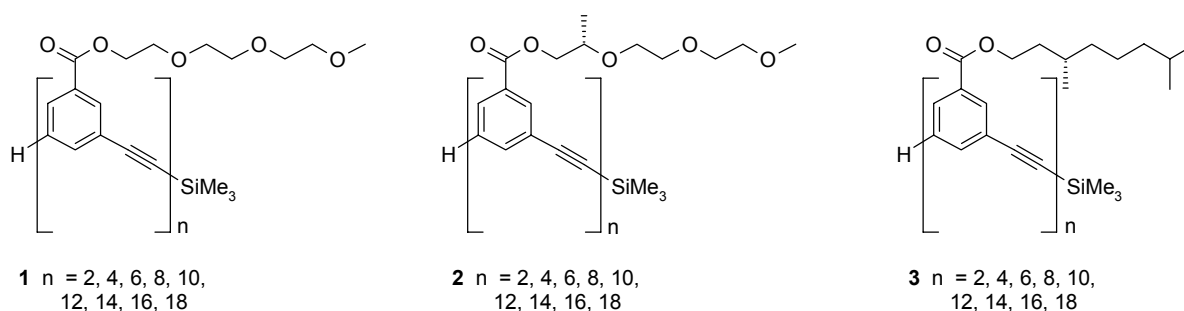


Figure 6.1: Chemical structures of oligomers series **1**, **2** and **3**.

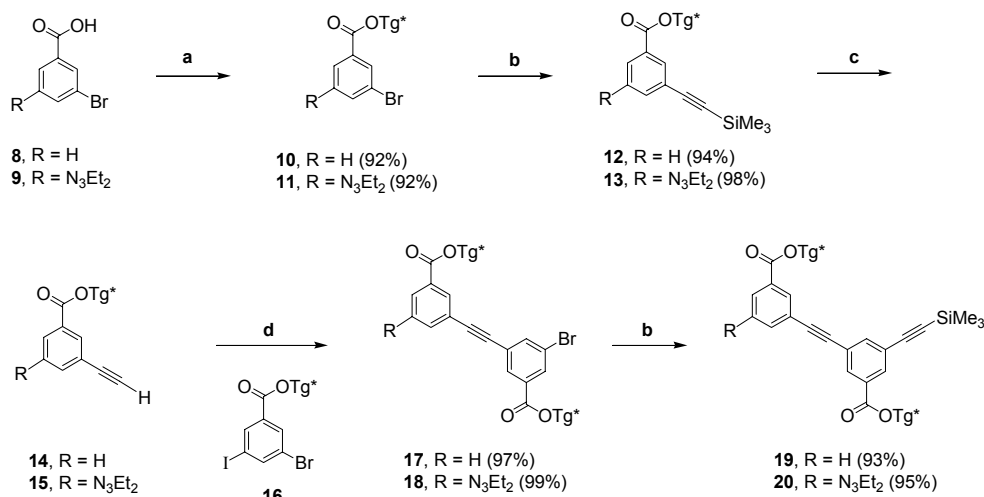


6.2 Conformational ordering of polar, chiral *m*-phenylene ethynylene oligomers

6.2.1 Synthesis

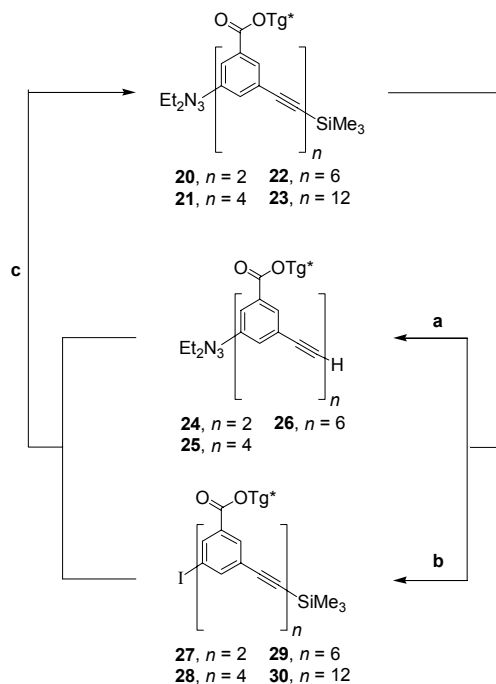
To study the folding into chiral helices, a series of *m*-phenylene ethynylene oligomers decorated with chiral side chains (**2**) was prepared. These oligomers are analogous to the previously reported achiral series **1**,¹⁶ except for the introduction of a methyl group at the second carbon of each of the side chains. This places the stereochemical information in reasonably close proximity to the aromatic backbone. The synthesis of the chiral side chain precursor **7** ((*2S*)-2-[2-(2-methoxy-ethoxy)-ethoxy]-propan-1-ol) is based on the chain elongation of (*2S*)-1-benzyloxy-propan-2-ol **4** by reaction with the tosylate of diethyleneglycol monomethyl ether (**5**) to afford the benzyl protected chiral triethyleneglycol (**6**). Deprotection afforded the chiral side chain **7**, the synthesis has been discussed in detail in chapter 2.

The convergent synthesis of the oligomer series required the preparation of orthogonally protected dimer **20** and capping dimer **19** (Scheme 6.1). The dimers **19** and **20** were synthesized in five steps from commercially available 3-bromobenzoic acid (**8**) and 3-bromo-5-[3,3-diethyl-triazenyl] benzoic acid (**9**). Attachment of the side chain was accomplished in high yields by a DCC-mediated esterification of chiral alcohol **7** with acids **8** and **9**, respectively. Subsequent palladium-catalyzed coupling of trimethylsilylacetylene afforded monomers **12** and **13**. Removal of the trimethylsilyl group, selective coupling with the iodo carbon of **16** and the coupling of trimethylsilylacetylene afforded dimers **19** and **20**. All compounds were characterized and proven to be pure by ¹H-NMR, ¹³C-NMR, mass spectrometry, HPLC (**19** and **20**) and elemental analysis (Section 6.7).



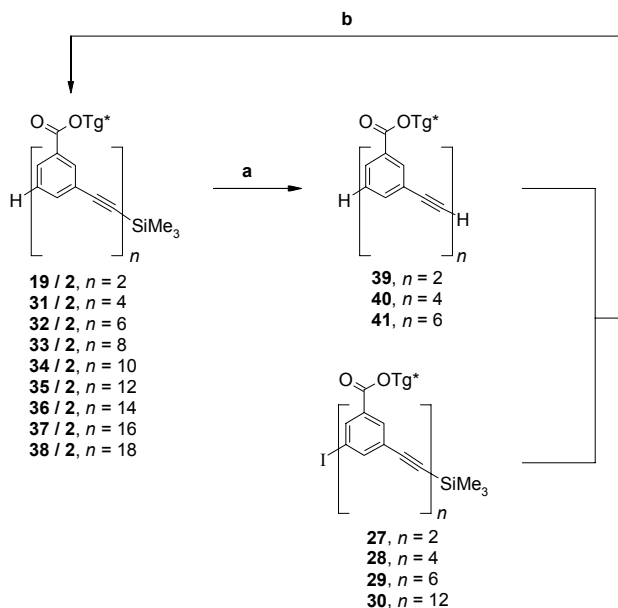
Scheme 6.1: (a) **7** (1.05 equiv), DCC, 4-DMAP, CH₂Cl₂, 0 °C; (b) Trimethylsilylacetylene, Pd₂(dba)₃, CuI, PPh₃, Et₃N, 70 °C; (c) TBAF, THF, r.t.; (d) Pd₂(dba)₃, CuI, PPh₃, Et₃N, 55 °C. Tg* = -(S)-CH₂CH(CH₃)-O-(CH₂CH₂O)₂CH₃.

Orthogonally protected dimer **20** was used to construct longer oligomer lengths via an iterative procedure. A portion of dimer **20** was deprotected to afford acetylene **24** and the remainder was converted to iodide **27**. Coupling of dimer acetylene **24** and dimer iodide **27** gave tetramer **21**. The synthesis of the remaining orthogonally protected oligomers was completed in a similar fashion in good yields and high chemical purity (Scheme 6.2). All compounds were characterized and shown to be pure by ¹H-NMR, mass spectrometry, HPLC and SEC (Section 6.7).



Scheme 6.2: (a) TBAF, THF, r.t.; (b) MeI, 110 °C; (c) Pd₂(dba)₃, CuI, PPh₃, Et₃N, CH₃CN, 70 °C. Tg* = -(S)-CH₂CH(CH₃)-O-(CH₂CH₂O)₂CH₃.

The synthesis of the capped oligomer series **2** is depicted in Scheme 6.3. This approach maximizes the amount of common intermediates which are used in the oligomer synthesis. In addition, it allowed for the facile purification of the desired oligomers by silica gel column chromatography. Beginning with capped dimer **19** / **2** ($n = 2$), the trimethylsilyl group was deprotected to afford free acetylene **39** which was coupled to dimer iodide **27** to afford capped tetramer **31** / **2** ($n = 4$). Continuing the synthesis in a similar fashion allowed all of the oligomers in the target series to be made in good yields and high chemical purity.



Scheme 6.3: (a) TBAF, THF, *r.t.*; (b) $\text{Pd}_2(\text{dba})_3$, CuI, PPh₃, Et₃N, 70 °C. Tg* = -(S)-CH₂CH(CH₃)-O-(CH₂CH₂O)₂CH₃.

The determination of the chemical purity and characterization of the final compounds was accomplished by several techniques. Proton NMR allowed for an easy determination of the purity (>95%) and identity of the desired products since it shows the characteristic signals of the terminal disubstituted aromatic ring as well as the trimethylsilyl group and the absence of signals corresponding to the terminal alkynyl protons or the aryl iodide. Conclusive evidence for the identity of the compounds was provided by mass spectrometry measurements (FAB: **2** ($n = 2-6$); MALDI: **2** ($n = 8-18$)). For the MALDI-MS measurements in each case the $[\text{M} + \text{Na}]^+$ adduct was observed. The purity of the compounds was determined by high performance liquid chromatography (HPLC) and size exclusion chromatography (SEC). All oligomers were >99% pure by HPLC as evidenced by the appearance of a single peak. Additional evidence for the purity of the compounds was provided by the SEC measurements. Each of the oligomers exhibits a single, symmetrical peak which indicates the absence of starting materials or byproducts of different length.

6.2.2 Hierarchical folding from random coils into chiral helices

UV absorption measurements established the conditions that caused oligomers **2** to adopt cisoidal or transoidal conformations. This is revealed from the ratio of absorbances at 287 and 303 nm as previously reported.¹⁶ In the random coil conformation, mainly transoidal conformations persist resulting in a high A_{303}/A_{287} ratio, whereas cisoidal conformations account for the formation helices and a significantly lower A_{303}/A_{287} ratio. It was found that, within experimental error, the conformational transitions of the chiral oligomers displayed the same chain-length and solvent dependence as their achiral counterparts (**1**).^{15,16} Thus, the introduction of a methyl group in the side chain did not destabilize the helical state.

Circular dichroism (CD) measurements were performed in order to study the twist sense bias.⁵⁰ In chloroform, chiral oligomers **2** showed no ellipticity in the backbone chromophore (250–400 nm), regardless of chain-length and temperature studied. This is not surprising, because in chloroform the oligomers are expected to be in a random coil conformation; hence, there is little possibility for transferring chiral information from the side chains to the unordered backbone. In sharp contrast to the behavior in chloroform, a remarkable Cotton effect was observed for oligomers **2** in dilute solutions of acetonitrile at room temperature. The ellipticity was found to be chain-length dependent and was zero only for oligomers not long enough to adopt a helical conformation ($n < 10$). As shown in Figure 6.2, the UV spectrum of **2** ($n = 8$) in acetonitrile exhibits a bandshape characteristic of the random coil conformation and a CD spectrum that displays no ellipticity. However, the UV spectrum of **2** ($n = 18$) in acetonitrile exhibits the bandshape indicative of the helical conformation and a CD spectrum that displays a bisignate Cotton effect. These results suggest that the transfer of chiral information from the side chains to the main chain can only occur once order is present in the backbone. The putative helical conformation likely places the side chains in close proximity thereby heightening their ability to cooperatively interact, giving rise to the diastereomeric preference of one twist sense over the other.

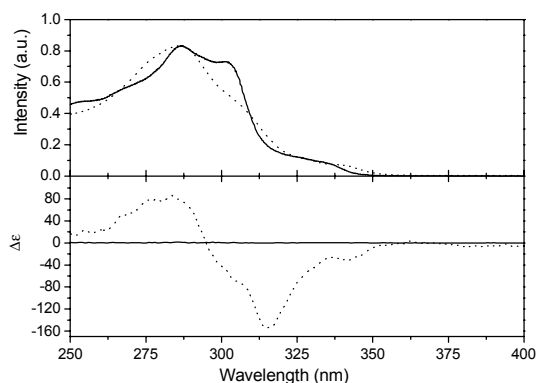


Figure 6.2: Normalized absorption and CD spectra of **2** ($n = 8$, solid line and $n = 18$, dashed line) in acetonitrile.

A measure of chiral induction is given by the anisotropy factor $g = \Delta\epsilon/\epsilon$ at 316 nm. Figure 6.3 shows how g varies with chain length in dilute acetonitrile solutions of **2** at several temperatures. It is evident from this plot that there is a critical chain length below which no chiral induction is observed (i.e., $n < 10$). This coincides with the length needed to form a stable helical conformation for **1**.¹⁶ It is also apparent that beyond the critical size, the chiral induction grows steadily as the chain lengthens (Figure 6.3). Also, the chiral induction decreases when the samples are heated. It is important to note that mixtures of **1** and **2** ($n = 18$) showed a linear relationship between ellipticity and mole percent of **2** (see also section 6.4). This, together with vapor pressure osmometry experiments,¹⁵ confirm that primarily unimolecular phenomena are involved.

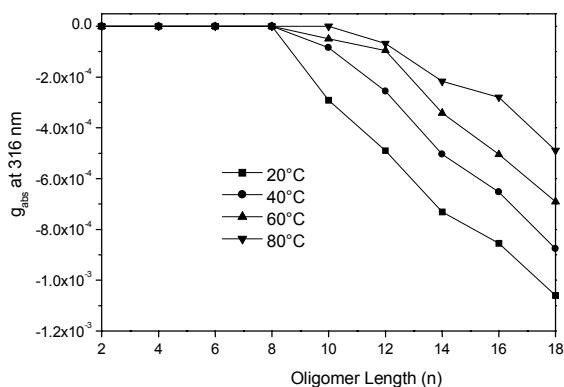


Figure 6.3: Plot of the chiral induction, expressed in terms of the anisotropy factor $g = \Delta\epsilon/\epsilon$, as a function of chain length at different temperatures for solutions of **2** in acetonitrile. The data were recorded at 316 nm.

Previous studies have shown that the helix-coil transition can be driven by changes in solvent or temperature.^{15,16} The effect of solvent on oligomers that display a preferential twist sense was monitored by absorption and CD spectroscopies. Typical solvent denaturation curves are shown in Figure 6.4. The addition of chloroform to dilute solutions of **2** in acetonitrile resulted in an increase in the ratio of absorbances at 303 and 287 nm (Figure 6.4, left).⁵¹ This increase is associated with the loss of cisoidal conformations as was previously shown.^{15,16} When the same solvent denaturation is monitored by CD spectroscopy, it is only at high acetonitrile contents that a Cotton effect is observed (Figure 6.4, right). The sudden onset and rapid growth in molar ellipticity at high acetonitrile concentrations is indicative of cooperative interactions.

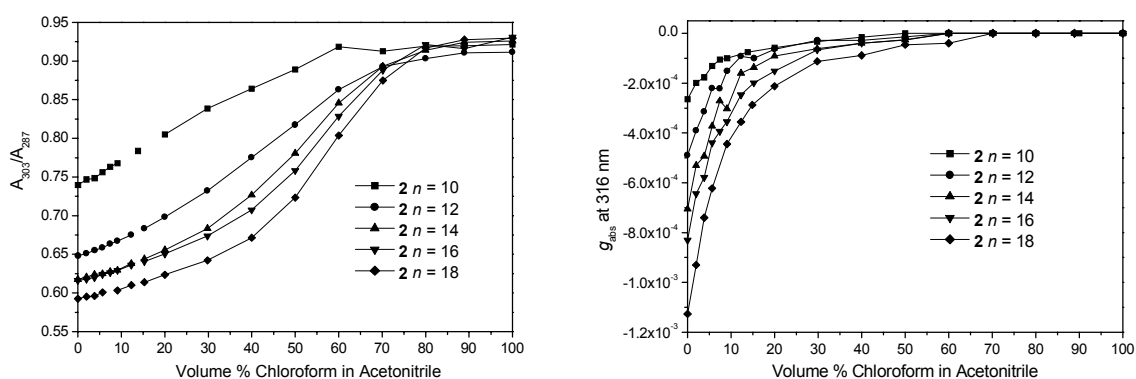


Figure 6.4: Solvent denaturation curves of **2** measured by UV absorbance ratio (A_{303}/A_{287}) (left) and circular dichroism (g_{abs} at 316 nm) (right).

It should be emphasized that the onset of the twist sense bias occurs at a solvent composition that is well beyond the helix-coil transition as monitored by UV-Vis spectroscopy. These different transition behaviors are intriguing and may reveal important aspects about the nature of this solvophobicity-induced organization. It is important to remember that UV-Vis spectroscopy detects the presence of a helical conformation, while CD spectroscopy detects the presence of diastereomeric excess. The solvophobicity of the hydrocarbon backbone, presumably being much larger than that of the polar side chains, could explain why the backbone adopts helical order well before bias is imparted to the helix twist sense. From the CD data it is deduced that diastereomeric excess appears at approximately the same chloroform composition regardless of chain length (Figure 6.4, right). Based on this observation it is plausible that ordering of the solvated side chains, a process that lags behind helix formation, is the mechanism by which chirality is transferred to the backbone. The analogy might be made to the "molten globular state" of proteins, a state in which the peptide backbone possesses a nature-like conformation while having disordered side chains.^{52,53}

An alternative way to explain the observed transition behavior is to consider the dynamics and conformational uniqueness of the backbone. At high chloroform compositions (but still helical as judged by UV) there are possibly a large number of energetically similar, helical-like backbone conformations that interconvert rapidly. Here the analogy might be made to the "compact denatured state" of proteins, a collapsed form in which there is a broad ensemble of backbone and side chain conformations even though there is extensive hydrophobic clustering.⁵⁴ The UV spectrum simply fails to provide the needed resolution to distinguish between a well ordered, conformationally unique backbone and a mixture of helical-like conformers. The dynamics and structural diversity available to the backbone in this conformational state may preclude cooperative interactions among the side chains that give rise to the twist sense bias. Upon increasing the amount of acetonitrile, a smaller set of backbone helical conformations becomes populated allowing the side chains to order and transfer

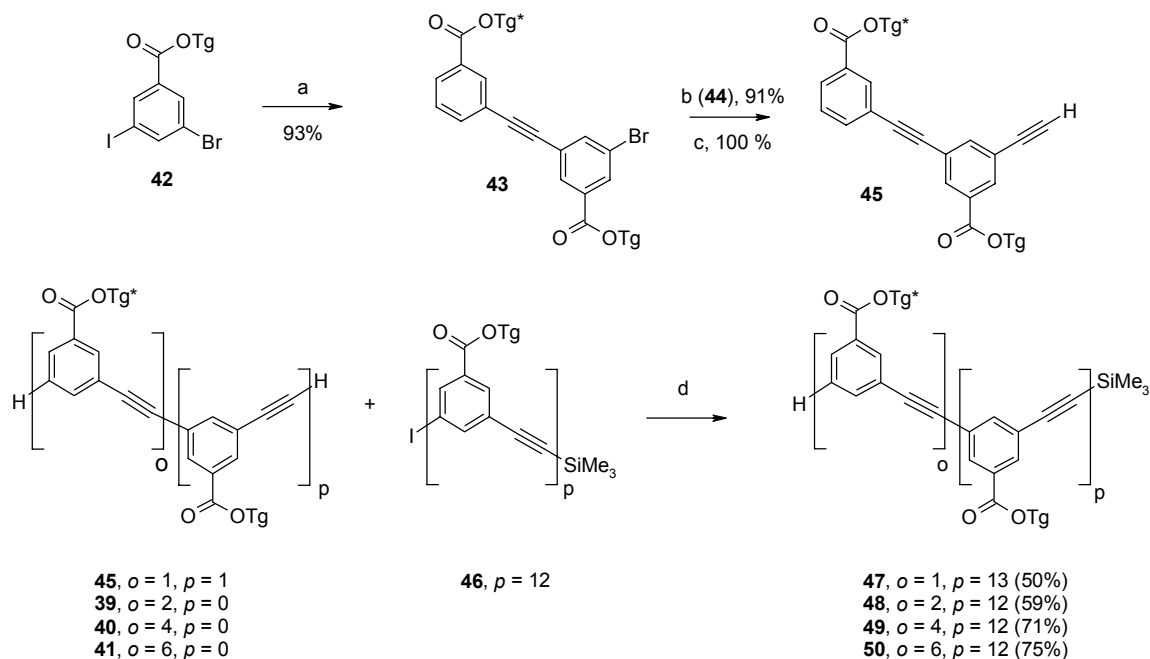
their chirality to the main chain. Regardless of which of these explanations is correct, the transfer of chirality appears to be a highly cooperative process that requires a progression of conformational order beyond the initially formed helical state.

6.3 Cooperativity in the folding of helical *m*-phenylene ethynylene oligomers based upon the 'Sergeant and Soldiers' principle

Cooperative interactions in polymeric chains is an active area of research that has provided a window to investigate weak interactions that cannot be deduced by standard methods.⁵⁵⁻⁶² The work of Green and co-workers on polyisocyanates has been pioneering in this field, demonstrating the 'Sergeant and Soldiers' and 'Majority Rules' principles as experimental approaches to reveal cooperativity through the amplification of chirality.⁶³⁻⁶⁷ The cooperative effects among side chains via the backbone may result in a non-linear relationship between the number of chiral side chains and the specific optical rotation in an intrinsically helical polymer. This phenomenon is referred to as the 'Sergeants and Soldiers' experiment,⁶³ where the few chiral units (sergeants) are controlling the overall chirality of the structure mediated through numerous achiral units (soldiers). More recently, this behavior has been extended to the intermolecular association of discotic molecules in solution^{36,37,68} and in well-defined self-assemblies.⁶⁹⁻⁷¹ In these situations, the overall chirality is due to an intrinsically chiral / helical packing of the molecules in the self-assembled architecture. The observation of a twist sense bias in the helically folded conformation of *m*-phenylene ethynylene oligomers series **2** has suggested the presence of cooperative interactions among the chiral side chains.⁷² For oligomer series **2**, all members were fully substituted with chiral side chains, not allowing for the cooperativity to be determined. In order accomplish this task, oligomers containing varying numbers of chiral side chains were synthesized and studied using UV-Vis and CD spectroscopy.

6.3.1 Synthesis

The synthesis was based on coupling of previously produced fragments containing achiral and chiral side chains (Scheme 6.4).^{16,72,73} The chemical purity and identity of the oligomers was determined by ¹H-NMR, mass spectrometry, HPLC and SEC. Four oligomers with both chiral and achiral side-chains were synthesized; two tetradecamers with either one or two chiral side-chains, a hexadecamer with 4 chiral side-chains and an octadecamer provided with 6 chiral side-chains. For all of the oligomers the chiral side-chains were placed at the beginning of the oligomer.



Scheme 6.4: (a) **14**, $\text{Pd}_2(\text{dba})_3$, CuI , PPh_3 , Et_3N , 55°C . (b) Trimethylsilylacetylene, $\text{Pd}_2(\text{dba})_3$, CuI , PPh_3 , 70°C ; (c) TBAF, THF, *r.t.*; (d) $\text{Pd}_2(\text{dba})_3$, CuI , PPh_3 , Et_3N , 70°C . $\text{Tg} = -(\text{CH}_2\text{CH}_2\text{O})_3\text{CH}_3$. $\text{Tg}^* = -(\text{S})\text{-CH}_2\text{CH}(\text{CH}_3)\text{-O}-(\text{CH}_2\text{CH}_2\text{O})_2\text{CH}_3$.

6.3.2 Cooperative transfer of side chain chirality

By analogy to the fully chiral (**2**)⁷² and achiral (**1**)¹⁶ oligomers, the mixed side-chain oligomers existed as a random coil in chloroform and formed a helical conformation in acetonitrile as determined with UV-Vis spectroscopy. Circular dichroism measurements were performed in order to determine the extent of cooperative interactions between the side chains. Depicted in Figure 6.5 are the CD spectra of the four tetradecamers (**1** ($m = 14$), **47**, **48** and **2** ($n = 14$)) with varying amounts of chiral side chains. As expected, oligomer **1** ($m = 14$) without chiral side chains is optically inactive and tetradecamer **2** ($n = 14$) with all chiral side chains shows the strongest Cotton effect. Surprisingly, the oligomer with one out of fourteen chiral side chains **47** displays a fairly strong Cotton effect, larger than expected on the basis of linearity. Furthermore, comparing the spectra of **2** ($n = 14$), **47** and **48** reveals the presence of an isodichroic point at 295 nm, suggesting a similar helical conformation to be adopted by all oligomers. Importantly, these results also indicate that overall, the helical conformation is highly ordered and there does not appear to be any “fraying” at the sides, since in oligomer **8** the only chiral side chain is located at the beginning of the helix.

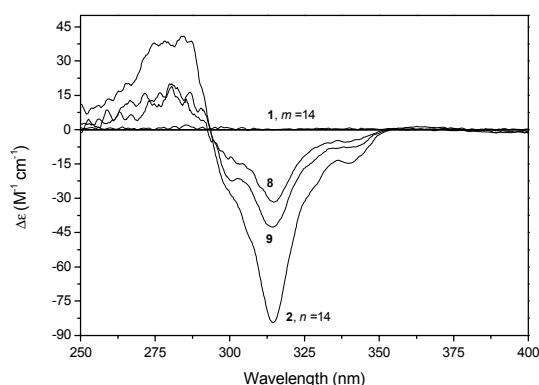


Figure 6.5: Plots of $\Delta\epsilon$ vs λ in acetonitrile for tetradecamers with varying numbers of chiral side chains.

The ability of one chiral side chain to transfer its chirality to the helical backbone was examined further by performing variable temperature experiments (Figure 6.6, left). It can be seen that in acetonitrile a modest twist sense bias is observed even at 70 °C and that the CD signal continues to increase as the temperature is lowered. The temperature denaturation of **47** (Figure 6.6, right) shows a similar transition shape as for the fully chiral oligomer **2** ($n = 14$), (Figure 6.3).⁷² The parallel temperature denaturation of the chiral helical conformations of **2** ($n = 14$) and **47** shows that the helix stability is not affected by the number of chiral side-chains at any temperature.

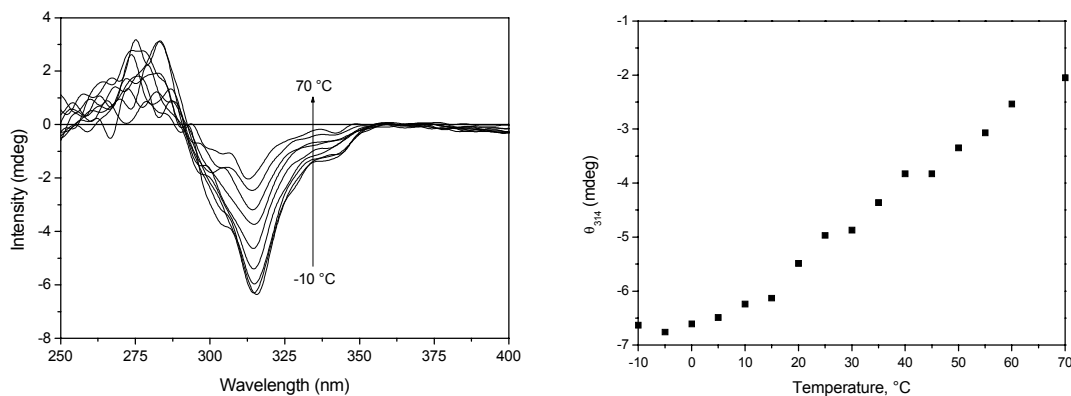


Figure 6.6: Variable temperature CD spectra of tetradecamer **47** at various temperatures (70 → -10 °C) in acetonitrile (left). Plot of CD intensity at 314 nm vs temperature for tetradecamer **47** in acetonitrile (right).

The intramolecular transfer of chirality was determined for the tetradecamer through octadecamer length oligomers. Shown in Figure 6.7 is a plot of the normalized Cotton effect (g_{abs} / g_{max}) vs the percent chiral side chains. It can be seen that regardless of overall oligomer length, a

positive nonlinear dependence of the optical activity on the percentage of chiral side chain is observed. This positive nonlinear effect strongly supports the cooperative nature of the folding process. The results further indicate that the twist sense bias is equally strong for every oligomer length, as the normalized Cotton effect versus percentage of chiral side chains seems to be independent on the oligomers length. The cooperativity as observed using the 'Sergeant and Soldiers' measurements is, however, not very strong. Around 15 % chiral side-chains is needed for obtaining half the intensity of the Cotton effect of the homochiral oligomers. This result contrasts with the cooperativity as observed for polyisocyanates⁶³⁻⁶⁷ and for helical columns of discotic molecules, which have been shown to become homochiral after addition of a small percentage of chiral seed molecules.^{36,37,68} In addition, the induced Cotton effect does not reach an asymptotic value at higher percentages of chiral side chains, but increases up to 100 % chiral side chains as can be seen from the dotted line in Figure 6.7. This indicates that even for the oligomers fully substituted with chiral side chains, a 100 percent bias of the helicity is not reached. Apparently, the chiral side-chains do not account for a sufficient energy difference to move the equilibrium between M and P helices (Eq. 1) to one side only.

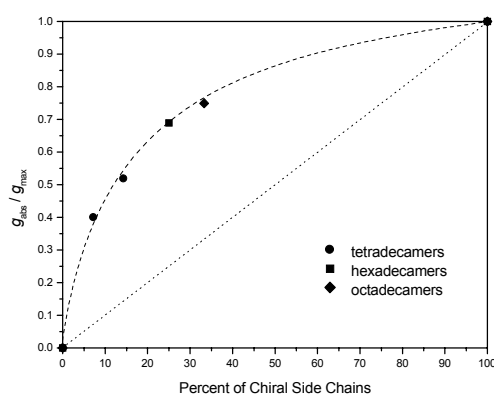


Figure 6.7: Plot of normalized g_{abs}/g_{max} at 315 nm vs percent of chiral side chains for the mixed tetradecamers (**1** ($n = 14$), **47**, **48** and **2** ($n = 14$)), hexadecamers (**1** ($n = 16$), **49** and **2** ($n = 16$)) and octadecamers (**1** ($n = 18$), **50** and **2** ($n = 18$)) in acetonitrile at 20 °C. The dotted lines are meant to guide the eye, but do indicate that an asymptotic value is not reached.

6.4 Self-assembly of folded *m*-phenylene ethynylene oligomers into helical columns

The formation of a well-defined helical conformation by oligomers series **2** is accompanied by structuring side-chain interactions and transfer of chirality to the backbone. The stability of the helical conformation of the oligomers should be increased by additional solvophobic interactions in a more polar environment. Furthermore, it can be expected that the single helices may show intermolecular interactions upon an increase in the polarity of the solvent.^{74,75} In such a way, the self-assembly process can be extended to a higher level by the formation of supramolecular columns via

stacking of the chiral helical oligomers upon the addition of the more polar solvent water. Intermolecular ‘Sergeant and Soldiers’⁶³ experiments were performed in order to elucidate the cooperativity of the different processes and the hierarchical growth.

6.4.1 Aggregation in aqueous acetonitrile

In order to promote backbone interactions for stabilization of the helix and to investigate whether multi-molecular architectures are created, studies were performed on aqueous acetonitrile solutions. The optical characteristics of the oligomers were monitored with UV-Vis and CD spectroscopy in order to visualize the stacking of the apolar backbone (UV-Vis) and the order and helicity within the self-assemblies (CD). Shown in Figure 6.8 are the CD spectra of dodecamer **2** ($n = 12$) and octadecamer **2** ($n = 18$) in water-acetonitrile mixtures of varying composition. The Cotton effect observed for the dodecamer increases upon increase of the water content from 0 to 40 % (v/v) (Figure 6.8, left). The presence of an isodichroic point at 295 nm indicates that the oligomer is adopting a similar conformation in each of the solvent mixtures. A similar behavior (increase of θ_{\max}) was observed for the shorter octamer **2** ($n = 8$) and decamer **2** ($n = 10$). In contrast, the longer octadecamer shows dramatically different behavior as it is placed into an aqueous environment (Figure 6.8, right). The increase of the volume % of water initially results in a decrease of the Cotton effect, followed by an increase at higher water content. Important is the lack of an isodichroic point, which demonstrates that the oligomer is adopting several conformations or aggregation states in aqueous solutions. The tetradecamer **2** ($n = 14$) and hexadecamer **2** ($n = 16$) show a behavior in between that of the dodecamer and octadecamer, but are both also characterized by a decrease of the Cotton effect, followed by an increase upon increase of the water content. Hypochromicity is observed in the absorbance spectra of all oligomers as the fraction of water is increased, as well as a decrease in intensity. Even though these data provide little information concerning the conformation of the oligomers, they do indicate stacking of the folded oligomers with increasing water content.⁷³ Furthermore, a similar hypochromicity has been observed for apolar oligomers upon aggregation of the helices in apolar solvent.⁷⁶ Thus, these results indicate that the oligomers stack in helical columns in aqueous solutions (*vide infra* Eq. 6.2). This stacking, upon addition of water, accounts for an increased stability of the helical conformation for the shorter oligomers, from the octamer through to the dodecamer. The longer oligomers already have a stable helical conformation in acetonitrile and the stacking induced by the addition of water results in little additional stability of the helical conformation. The stacks formed by the longer oligomers result in an alternative (helical) conformation or mode of aggregation –with respect to the situation in pure acetonitrile– as evidenced by the lack of an isodichroic point. This suggests that intermolecular aggregation may stabilize the helical conformations and that additionally aggregation into differently structured multimolecular architectures may occur.

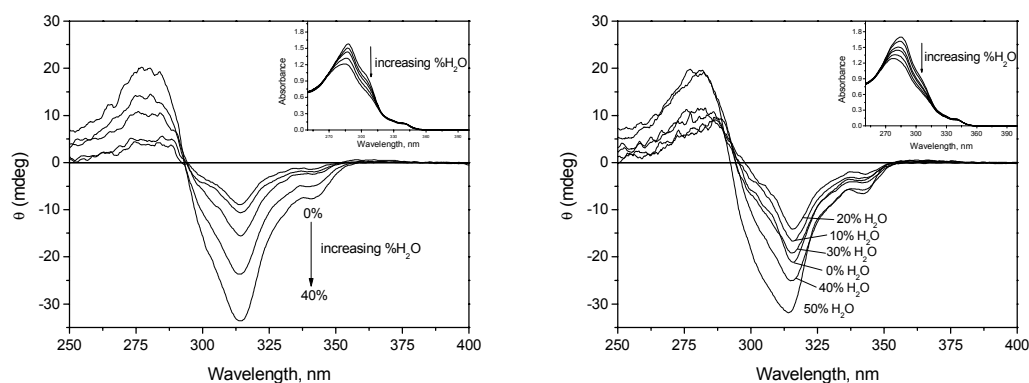


Figure 6.8: CD spectra of dodecamer 2 ($n = 12$) (left) and octadecamer 2 ($n = 18$) (right) in increasing amounts of water/acetonitrile (v/v). Insets show the accompanying absorbance spectra of the solutions. All measurements were recorded after equilibrating the samples at 20 °C for 10 minutes.

In order to further elucidate the intermolecular aggregation of the helices in columns, the temperature dependent behavior of their aqueous solutions was examined. Previous results have shown that an increase of temperature results in a decrease in the stability of the helical conformation.¹⁶ Depicted in Figure 6.9 is a plot of the CD signals at 315 and 295 nm against temperature for a solution of the dodecamer 2 ($n = 12$) in 20 % water/acetonitrile. The decrease of the temperature of the solution results in an increase of the CD signal at 315 nm in a sigmoidal fashion. A similar plot of the CD signal at 295 nm (isodichroic point) shows no change as the temperature is decreased. For the longer octadecamer 2 ($n = 18$), a different behavior is observed (Figure 6.10). A plot of the θ_{\max} at 315 nm against temperature shows an initial increase as the temperature is lowered from 80 to 55 °C. However, as the temperature is decreased further, the CD signal decreases and finally shows a positive CD signal. A plot of the intensity of the 295 nm band is nearly constant from 80 to 55 °C, but increases as the temperature is lowered further. The loss of the isodichroic point at 295 nm coincides with the decrease of the CD maximum at 315 nm. The accompanying CD spectra show the initial increase in CD signal and the subsequent change to the opposite sign (Figure 6.10). Although the two extreme CD spectra (80 and -10 °C) are not exactly their mirror images, the inversion of the Cotton effect indicates that there is a temperature dependent inversion in the overall chirality of the supramolecular structure. Most probably the occurrence of lateral intercolumnar interactions results in multicolumnar architectures with a different overall chirality.

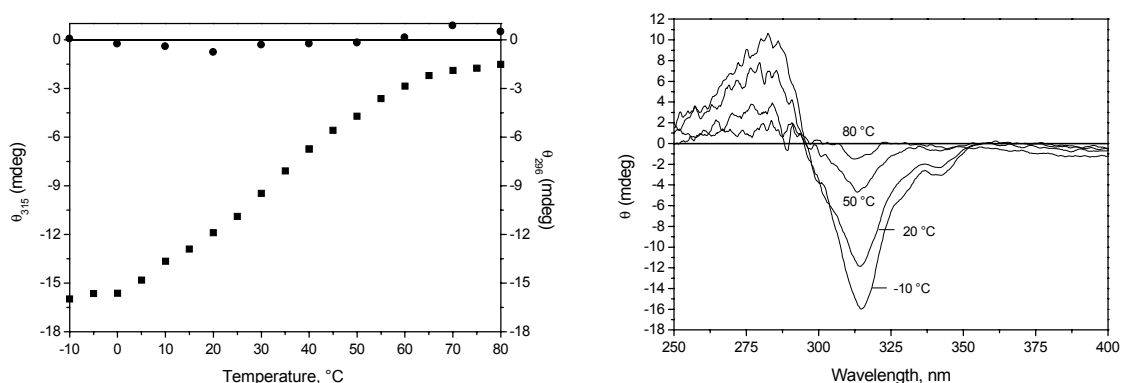


Figure 6.9: Plot of θ_{315} (squares) and θ_{296} (circles) vs temperature for a solution of dodecamer 2 ($n = 12$) as it was cooled from $80 \rightarrow -10$ °C (left). CD spectra recorded during the temperature run for the dodecamer (right). The measurements were recorded in 20 volume percent water in acetonitrile with an oligomer concentration of $5.5 \mu\text{M}$.

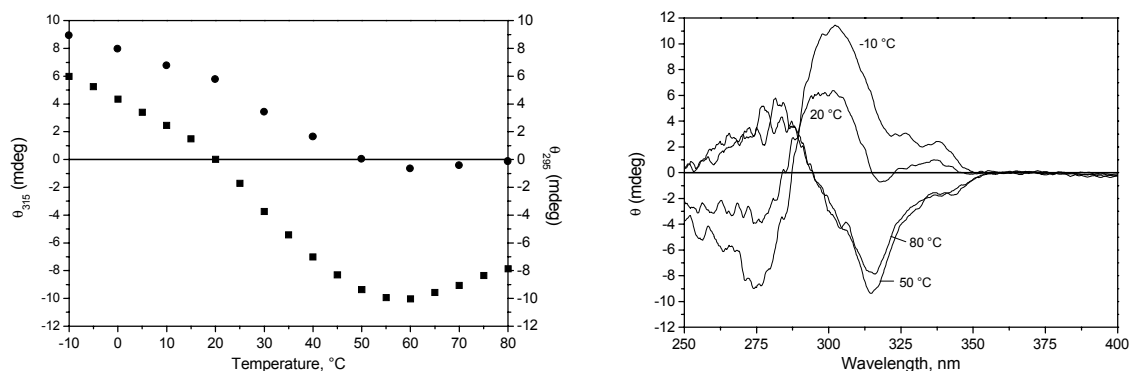


Figure 6.10: Plot of θ_{315} (squares) and θ_{295} (circles) vs temperature for a solution of octadecamer 2 ($n = 18$) as it was cooled from $80 \rightarrow -10$ °C (left). CD spectra recorded during the temperature run for the octadecamer (right). The measurements were recorded in 20 volume percent water in acetonitrile with an oligomer concentration of $3.8 \mu\text{M}$.

The temperature dependence of the Cotton effect was examined for all of the oligomers in several aqueous acetonitrile solutions (Figure 6.11).⁷⁷ For the shortest oligomer, the octamer, previous measurements in acetonitrile showed no evidence of any optical activity. However, a Cotton effect could be observed in the aqueous solutions. For a 20 % water solution, no CD signal is observed until 20 °C, but at lower temperatures, the Cotton effect increases rapidly. The addition of more water allows for a stable helix at even higher temperatures. The temperature denaturations for the octamer all show a sigmoidal curve. These results indicate that the addition of water stabilizes the helical conformation and the UV spectra show that this is caused by stacking of the helical oligomers. From the other graphs in Figure 6.11 it can be seen that the increase of the oligomer length is responsible

for a deviation from the sigmoidal behavior of the temperature denaturations in solvent with a high water content. It can be seen that as the oligomer length or volume % water is increased, the plot begins to show an initial increase followed by a decrease of the θ_{\max} , similar to the octadecamer discussed above.

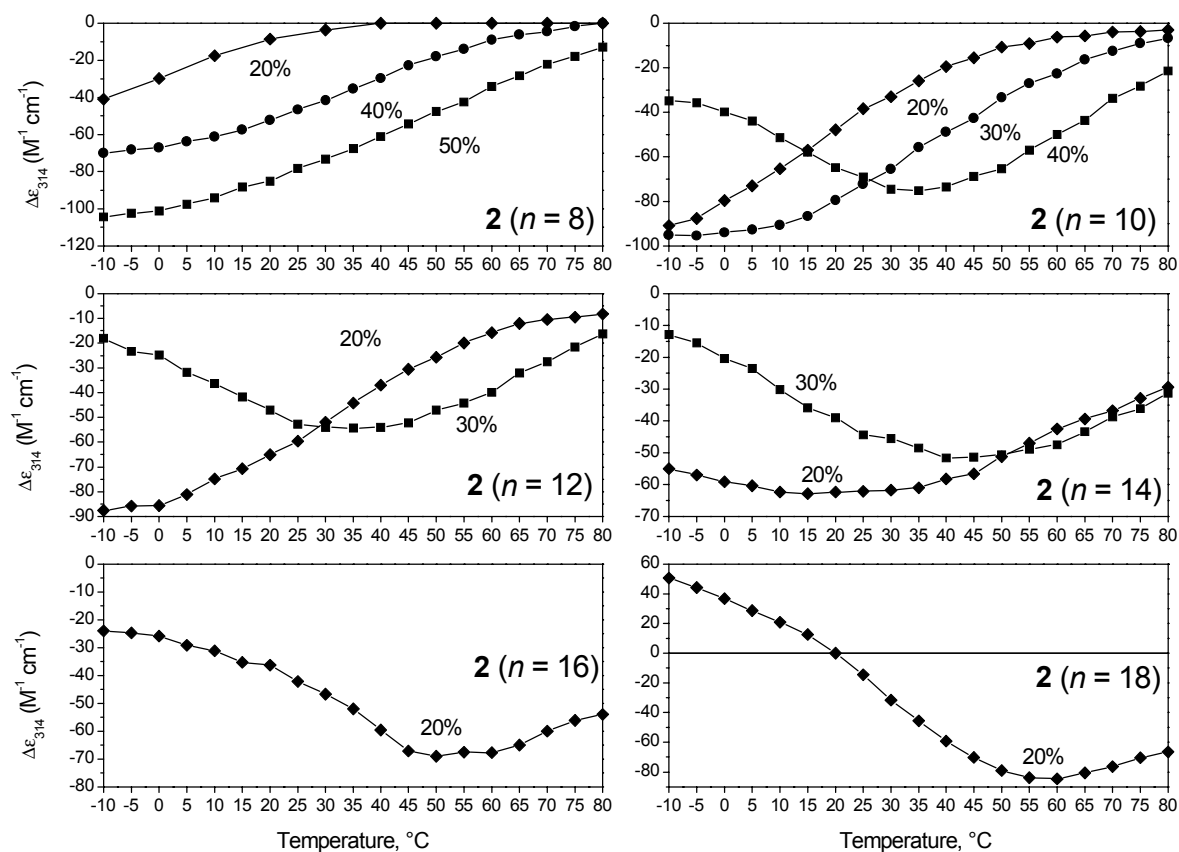


Figure 6.11: Plots of $\Delta\epsilon_{314}$ vs temperature for octamer 2 ($n = 8$) through octadecamer 2 ($n = 18$) in varying water/acetonitrile mixtures (v/v). All solutions were cooled from 80 \rightarrow -10 $^{\circ}C$.

A comparison of all oligomers in 20 % water/acetonitrile is depicted in Figure 6.12. The results indicate that the aggregation properties of the oligomers are clearly chain-length dependent. For the shorter oligomers (octamer - dodecamer) sigmoidal curves are seen; the decrease in temperature is accompanied by an increase in the CD signal at 314 nm. The longer oligomers (tetradecamer - octadecamer) no longer show sigmoidal transitions, but there is a steady growth in the positive direction of the CD signal at low temperatures. These results suggest that column formation can be attributed to the presence of helical oligomers and superstructure formation, with concomitant inversion of optical activity, results from lateral interactions between these columns.

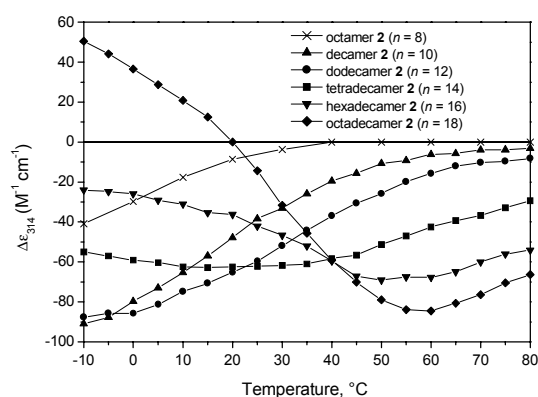
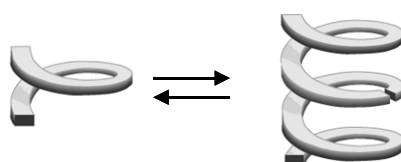


Figure 6.12: Plots of $\Delta\epsilon_{314}$ vs temperature for octamer **2** ($n = 8$) through octadecamer **2** ($n = 18$) in 20 volume percent water in acetonitrile. All solutions were cooled from 80 \rightarrow -10 $^{\circ}\text{C}$.

6.4.2 Intermolecular cooperative transfer of chirality

The results presented in the previous section pointed towards the aggregation of the oligomers in aqueous acetonitrile solutions in a fashion that requires the presence of a stable helical conformation. It is hypothesized that the aggregation occurs via the formation of columns of stacked helices (Eq. 6.2), later on followed by lateral interactions between the columns. Such a chiral supramolecular column is well-matched for the transfer of chiral information from one oligomer to the other. The stacking of a helix with no twist sense bias (i.e., one with achiral side chains) on top of a helix whose twist sense is biased (i.e., one with chiral side chains) would possibly impart a twist sense bias to the initially unbiased helix. To investigate this hypothesis, intermolecular ‘Sergeant and Soldiers’⁶³ experiments were performed on mixtures of achiral oligomers series **1** (soldiers) and chiral oligomers series **2** (sergeants).



(Eq. 6.2)

When solutions of varying amounts of chiral octamer **2** ($n = 8$) and achiral octamer **1** ($n = 8$) were prepared in 50 % water/acetonitrile (v/v) –keeping the total concentration of chromophores constant–, the absorbance spectra superimpose and no conclusions can be drawn about intermolecular association, although the results do indicate the formation of similar helical conformations by both oligomers. However, when the same solutions are examined by CD spectroscopy, deviations from linearity are observed. A plot of CD signal intensity at 314 nm against mole percent chiral octamer features a small positive deviation from linearity (Figure 6.13 (circles)). When an experiment is performed without the addition of achiral oligomer, but just diluting chiral octamer **2** ($n = 8$) a linear

dependence of the CD signal on mole percent chiral octamer **2** ($n = 8$) is observed (Figure 6.13 (boxes)). The positive deviation from linearity and lack of concentration dependent CD clearly shows that the chirality is being transferred from the chiral to the achiral octamers.⁷⁸

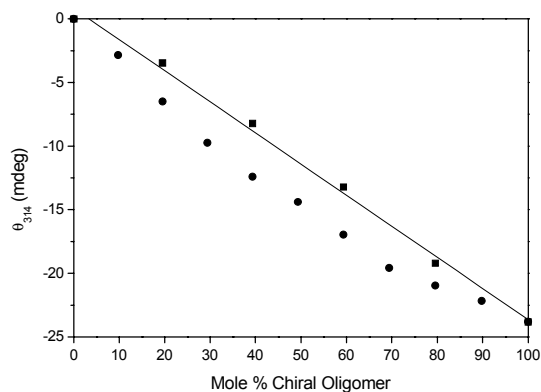


Figure 6.13: Plot of θ_{314} vs mole % chiral octamer **2** ($n = 8$) for solutions of varying relative amounts of chiral and achiral **1** ($n = 8$) octamers (circles). The squares show the θ_{314} as the chiral octamer is diluted without the addition of achiral oligomer. The solid line is the least squares linear fit of the chiral octamer dilution data (correlation coefficient = 0.998). All spectra were recorded in 50 % acetonitrile/water (v/v). The experiments containing both achiral and chiral octamer were recorded with a total oligomer concentration of 7.0 μM .

To examine the intermolecular transfer of chirality in greater detail, the aggregation behavior of chiral **2** ($n = 18$) and achiral **1** ($n = 18$) octadecamers was studied in several water-acetonitrile mixtures. In 100 % acetonitrile, the CD signal was found to be linearly dependent on the mole percent of chiral octadecamer (Figure 6.14, top left). This indicates that if intermolecular aggregation is occurring there is no transfer of chirality in 100 % acetonitrile. More importantly, this shows that the CD signals observed for the longer oligomers in 100 % acetonitrile (see above) can be attributed to a purely intramolecular effect. Examination of solutions containing increasing fractions of water showed a positive deviation from linearity, meaning that the magnitude of the CD signal is larger than expected for an ideal mixture (Figure 6.14). Intriguing is the observation that the maximum CD signal of certain mixtures of chiral and achiral oligomers is greater than that of the purely chiral octadecamer. A rationale for this behavior is that there is a more efficient packing between achiral molecules than between the chiral molecules, since in the former no branching methyl group is present.⁷⁹ The transfer of chirality to achiral oligomers appears to be dependent on the presence and intermolecular aggregation of a helical conformation, which is supported by the larger transfer of chirality, observed for the longer octadecamers. These observations led to the proposed mode for the transfer of chirality, shown in equation 6.2. The stacking is promoted due to the highly polar, aqueous

environment and efficient intermolecular stacking would allow for the chirality to be transferred to the achiral helices.

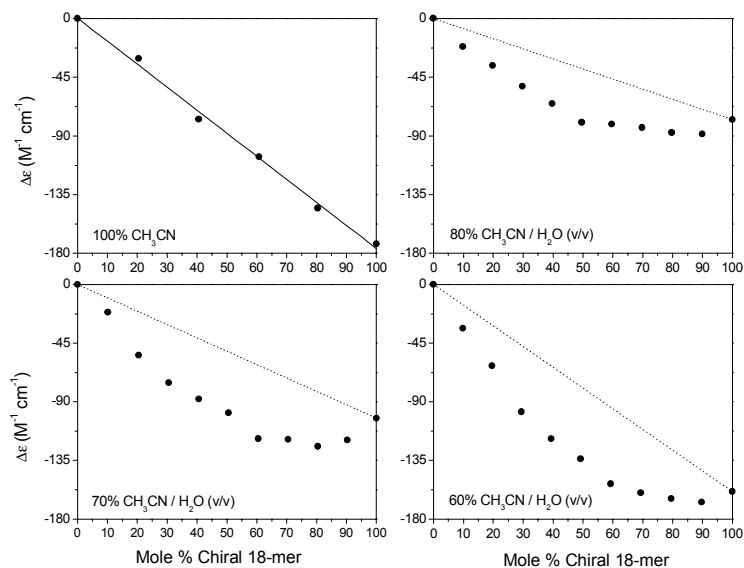


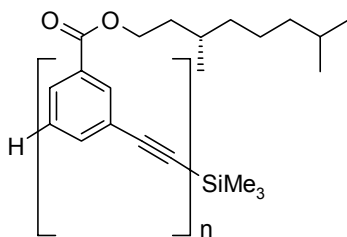
Figure 6.14: Plot of $\Delta\epsilon_{314}$ vs mole % chiral octadecamer **2** ($n = 18$) for solutions of varying relative amounts chiral and achiral **1** ($n = 18$) octadecamers in different water/acetonitrile compositions (v/v). All spectra were recorded from solutions with a total oligomer concentration of $3.3 \mu\text{M}$. The dotted lines represent the expected signals that should arise upon dilution of a sample only containing chiral octadecamer. The solid line is the least squares linear fit of the chiral octadecamer dilution data (top left, correlation coefficient = 0.998).

The transfer of chirality as observed applying the 'Sergeant and Soldiers' measurements is not very large. For the octadecamer it seems that on average 50 % chiral oligomer **2** ($n = 18$) is needed for a full bias of the helicity of the achiral oligomers **1** ($n = 18$). This result is in contrast to the amplification of chirality as observed for helical columns of discotic molecules for which a strong cooperativity has been found.^{36,37,68} Three explanations can be thought of that explain a small amplification of chirality. First of all the size of the aggregates is determining. Aggregates consisting of only 2 or 3 molecules can only give a small amplification of chirality. The aggregate size should, however, strongly depend on the amount of water present, as increase of the water content induces stronger aggregation. In fact at high water contents (> 60 %) the solutions become turbid evidencing large aggregates. No evidence for an influence of this type can be observed in Figure 6.14. It should be noted, however, that the chirality of the aggregates, annex shape, at higher amounts of water changes, which might counteract the influence of increasing aggregate size (Figure 6.10). As a second option it should be considered that the stacking interactions between the oligomers, though being strong, are not very specific. In such a situation, the chirality of the helix would not be strongly recognized as such by the folded achiral oligomers. In other words, the cooperativity length of

chirality amplification is very small. Such results have also been found for the aggregation of polythiophenes,⁸⁰ for which the intermolecular interactions are also only of the generic solvophobic type, in contrast to specific interactions such as hydrogen bonding.^{36,37,68} Finally, from the results presented in section 6.2 and those presented in this section it is not possible to quantify the diastereomeric excess of the chiral helix. If for oligomers **2** the side-chains do not account for a homochiral situation, but rather for a small diastereomeric excess, the amplification of chirality will be small as well. In such a situation also the 'majority rules' principle⁶⁵ would not apply to these supramolecular assemblies and only small effects will be found. The results concerning intramolecular amplification of chirality (section 6.3), obtained for the oligomers containing both chiral as achiral side-chains, have indicated the intramolecular induction of chirality to be cooperative, but not as impressive as observed in conventional polymers and possibly not complete. The most plausible explanations of the small amplification of chirality thus lie in the small directing power of the generic solvophobic effect and absence of full diastereomeric purity of the chiral helices. The use of more specific interactions would possibly induce a stronger amplification.

6.5 Conformational ordering of apolar, chiral *m*-phenylene ethynylene oligomers

In the *m*-phenylene ethynylene oligomers series **2**, an amphiphilic-type of heterogeneity is present in that polar side chains are attached to an all-carbon backbone. In order to explore the possibility of broadening the scope of this effect, an oligomer series (**3**) was designed in which the heterogeneity results from the attachment of lipophilic side chains. The addition of apolar side-chains renders the aromatic backbone polar with respect to the side-chains. The ability to induce conformational order in such an oligomer is intriguing for at least two reasons. First, since both the side chain and backbone are hydrocarbon segments, the heterogeneity in this system is intuitively less pronounced. Second, the promotion of helical order in a lipophilic solvent would bode well for the possibility of forming helical channels in bilayer membranes.



3 $n = 2, 4, 6, 8, 10,$
 $12, 14, 16, 18$

6.5.1 Synthesis

The synthesis of oligomer series **3** was performed in solution using a divergent/convergent growth strategy, analogous to oligomer series **2**.⁸¹ (*S*)-3,7-Dimethyl-1-octanol was selected as the

starting material of the side chain since it is easily obtained in high enantiomeric purity.⁸² Due to the apolar character of the oligomers column chromatography using apolar solvent mixtures was used. However, purification for some of the oligomers was extended with preparative size exclusion chromatography to separate the product from contaminants with similar R_f values, but different chain-lengths. All oligomers were characterized by $^1\text{H-NMR}$ spectroscopy, mass spectrometry, HPLC and size-exclusion chromatography (SEC) and shown to be > 99 % pure. Each of the oligomers **3** exhibited a single, symmetrical peak by SEC indicating the absence of starting materials or undesired oligomers. For the MALDI-MS measurements, only the $[\text{M} + \text{Na}]^+$ adduct was observed.

6.5.2 Hierarchical folding from random coils into chiral helices

UV absorption measurements were performed on oligomers **3** in order to establish the conditions that guarantee helical conformations. The ratio of the absorbance bands at 287 and 303 nm was monitored as previously reported for **2** (the helical conformation has a significantly lower A_{303}/A_{287} ratio than the random conformation).⁷² In chloroform the 303 and 287 nm bands are present in the same relative intensity regardless of chain length, indicating that these oligomers are in a random coil conformation (Figure 6.15, right).⁸³ In heptane, however, strongly contrasting observations were made (Figure 6.15, left). The octamer (**3**, $n = 8$) and decamer (**3**, $n = 10$) display absorbance spectra similar to that observed in chloroform, whereas the longer oligomers (**3**, $n = 12$, 14, 16, and 18) in heptane exhibit a decrease in the intensity of the 303 nm band and a broadening of the absorbance maximum (most pronounced for the longest oligomers).⁸⁴ For the previously studied oligomers **1** and **2** the decrease in the 303 nm band has been attributed to the collapse of the oligomer to a helical conformation, which can only occur once the oligomer is long enough to fold back on itself.^{16,72} These results suggest that the use of selective solvation to drive conformational order can be extended to non-polar solvents through the judicious choice of side chains.

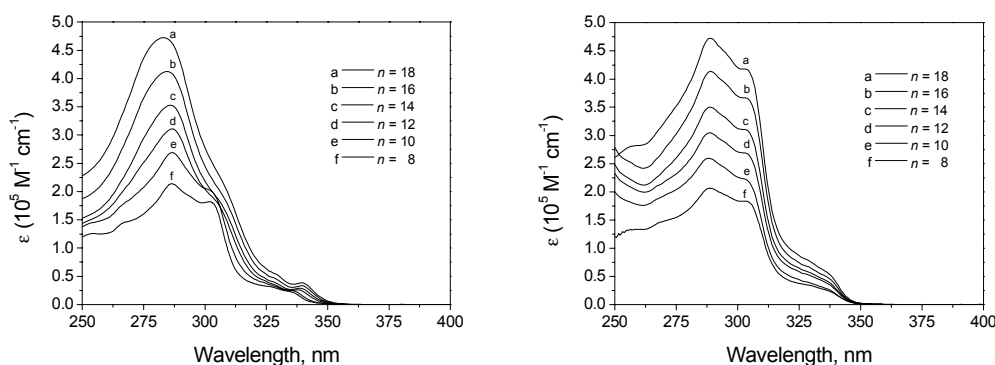


Figure 6.15: Plots of ϵ vs λ for chiral octamer **3** ($n = 8$) through octadecamer **3** ($n = 18$) in heptane (left) and chloroform (right). Note the decrease in the intensity of the 303 nm band in heptane as the oligomer length is increased beyond **3** ($n = 10$).

Circular dichroism measurements were performed in order to study the twist sense bias of the helical conformation. In chloroform, none of the oligomers showed a Cotton effect attributable to the backbone chromophore. This is not surprising given that in chloroform the "molecularly dissolved" oligomers were found to be in a random coil conformation; hence, there is little opportunity for transferring the chiral information from the side chains to the unordered backbone. In sharp contrast to the behavior in chloroform, a remarkable Cotton effect was observed for the chiral oligomers in dilute solutions in heptane (Figure 6.16). As shown in Figure 6.16, the ellipticity was found to be chain-length dependent and was observed for oligomers long enough to adopt a helical conformation as determined by UV-Vis spectroscopy (**3**, $n > 10$). The presence of an isodichroic point at 292 nm suggests that all of the oligomers adopt a similar collapsed conformation whose twist sense bias increases as a function of chain length.⁸⁵ In combination with the UV data it is justified to state that the transfer of chirality from the side chain to the backbone can only occur once order is already present in the backbone. It is likely that the helical conformation places the side chains in close proximity thereby heightening their ability to interact in a cooperative manner and hence giving rise to the diastereomeric preference of one twist sense.

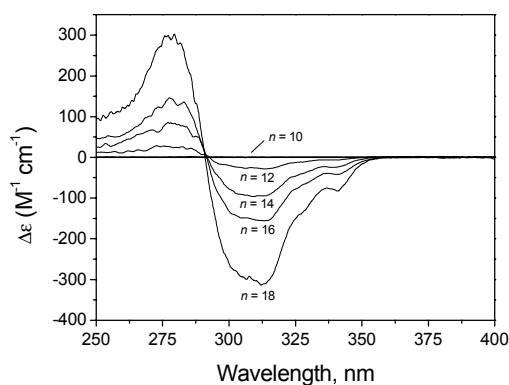


Figure 6.16: Plots of $\Delta\epsilon$ vs λ for chiral decamer **3** ($n = 10$) through octadecamer **3** ($n = 18$) in heptane at 20 °C. Note the presence of an isodichroic point at 292 nm.

The conformational transition of the apolar oligomers **3** was studied by changes in solvent composition to distinguish between cooperative and non-cooperative processes. For these experiments, chloroform was used as the "good" solvent and heptane was employed as the "poor" solvent.⁸⁶ Depicted in Figure 6.17 is a plot of the absorbance ratios (A_{303}/A_{287} , left) and $\Delta\epsilon$ at 316 nm (right) as a function of the volume percent chloroform in heptane. The addition of chloroform to dilute solutions of oligomers in heptane resulted in an increase in the ratio of absorbances at 303 and 287 nm. This increase is associated with the loss of helical order as previously shown. For the 18-mer (and less pronounced for the shorter oligomers) the change is clearly sigmoidal. When monitoring the same

solutions by CD spectroscopy, it is only at very high volume percent heptane (>90%) that a Cotton effect is observed. In a similar fashion as observed for the polar oligomers **2**, the onset of the twist sense bias occurs abruptly at a solvent composition that is well beyond the conformational transition as monitored by UV spectroscopy. Although the underlying phenomena responsible for this behavior are not well understood, it is apparent that the transfer of chirality is a highly cooperative process that requires a progression of conformational order beyond the initially formed helical state. It is noteworthy that for the apolar oligomers **3**, the Cotton effect disappears at much smaller volume % chloroform than for the polar oligomers.⁸⁷ This is most likely due to the greater rate at which solvent polarity changes upon addition of chloroform to heptane, compared to the smaller change upon addition of chloroform to acetonitrile.

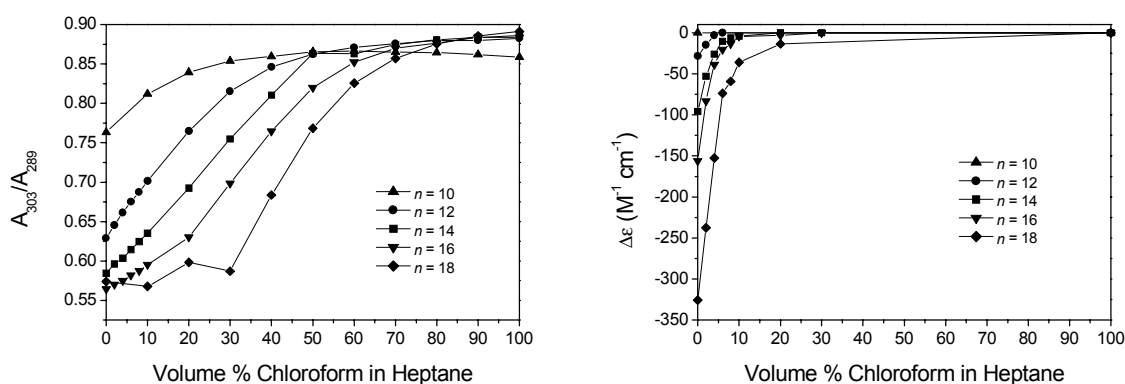


Figure 6.17: Plot of UV absorbance ratio (A_{303}/A_{287} , left) and CD signal ($\Delta\epsilon$ at 316 nm, right) for decamer **3** ($n = 10$) through octadecamer **3** ($n = 18$) vs the volume % chloroform in heptane.

The conformational transition of apolar oligomers **3** was further studied by changing the temperature. Temperature dependent UV and CD measurements in heptane demonstrated that decreasing the temperature of a solution of **3** ($n = 18$) from 80 °C to 30 °C gives rise to stabilization of the helical conformation as evidenced by a decreasing A_{303}/A_{287} ratio. However, the twist sense of the helices is not biased at temperatures above 30 °C, since no Cotton effect was observed. Below 30 °C a Cotton effect appears and the absorbance maximum decreases with a concomitant blue shift, similar to the spectral changes that occur at increased concentrations.⁸⁸ Therefore, the temperature dependent folding into a helical conformation below 30 °C is explained by aggregation that coincides with the expression of chirality. It is easy to imagine that the *m*-phenylene ethynylene oligomers **3** form a large aromatic scaffold that promotes aggregation into columnar architectures at higher concentrations and low temperatures.⁸⁹ These columns stabilize the helical states of the oligomers by imposing a restriction of motion onto the oligomers, resulting in a twist sense bias as expressed by an increase of the CD-effect. The variable temperature CD data are consistent with a behavior where intermolecular aggregation contributes to twist sense bias. In contrast to oligomer series **2** in aqueous acetonitrile, no

indications for lateral intercolumnar aggregation were found. Apparently, the apolar side-chains of oligomers series **3** allow for a good solubility of the columns in heptane in contrast to the short oligo(ethylene oxide) side chains of **2** in water.

6.5.3 Time dependent folding

Variable temperature measurements performed on oligomer series **3** were determined to be highly time dependent. This sharply contrasts with the behavior of the oligomers **2**, which were found to reach equilibrium within a few minutes. To investigate the origin of this strong time dependency, several variable temperature and time-dependent studies were performed on solutions of **3** ($n=18$) in dodecane using absorbance and CD spectroscopy. In order to reach an optically inactive state the solution was heated to 60 °C for 20 minutes. The sample was then placed into a thermostated 20 °C cuvette and absorbance and CD spectra were recorded as a function of time. As shown in Figure 6.18 (right), no optical activity was observed in the backbone chromophore at 60 °C. The oligomer, however, was present mainly in its helical form as could be detected by UV spectroscopy (left). At 20 °C, a plot of the CD signal against time shows that in dodecane it takes approximately 4 hours for the CD signal to reach equilibrium (right, inset). The presence of an isodichroic point at 292 nm indicates that the oligomer maintains the same conformation with time. The UV spectra recorded over this same period indicate a small decrease of the molar absorptivity and a small blue shift of the band at 284 nm. This suggests that in time, the oligomers are gaining order, presumably due to a more regular packing into columns; similarly, optically active polythiophenes show a strong time-dependence due to intermolecular aggregation, evidenced as well by small spectral changes in the UV spectra and an increasing CD intensity.⁹⁰ Upon addition of heptane to the chloroform solution, the oligomers first collapse into a helical state and then begin to aggregate intermolecularly. Since the twist sense of the oligomers is not biased yet, left- and right-handed columns are formed in equal amounts initially. In pure heptane the chiral side chains are capable of biasing the chirality of the helices, but due to the stable aggregates, the bias is only fully imparted after long equilibrium times.⁹¹ It remains still a question however, whether aggregation is necessary for the bias of the twist sense or if it is just coinciding with the twist sense bias under these highly apolar conditions.

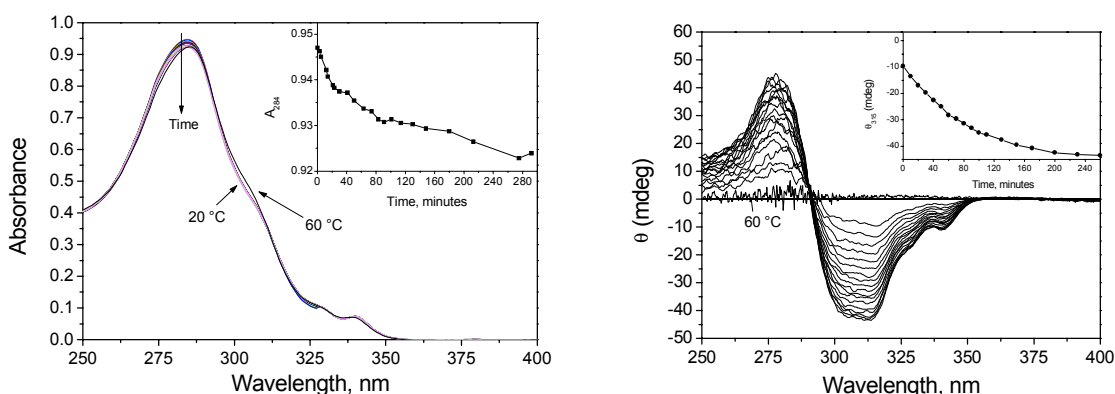


Figure 6.18: Overlay of the absorbance (left) and circular dichroism (right) spectra collected over time for a solution of octadecamer **3** ($n = 18$) that was heated to 60 °C for 20 minutes and then placed in a thermostatted 20 °C cuvette. The insets show the plots of the absorbance intensity at 284 nm and CD intensity at 315 nm as a function of time. All spectra were recorded on the same 3.9 μM solution in dodecane.

6.6 Conclusions

Circular dichroism has proven to be an extremely valuable tool for studying the collapsed conformations of chiral *m*-phenylene ethynylene oligomers. It was demonstrated that it is possible to bias the twist sense of a solvophobic driven helical conformation by the attachment of chiral side chains. The diastereomeric bias only appears after the backbone acquires a conformationally ordered state. Solvent denaturation studies showed that a helical conformation is a necessary, but not a sufficient condition for inducing a diastereomeric bias. In particular, the onset of the twist sense bias was shown to lag significantly behind the appearance of helical conformations, possibly because a large ensemble of "collapsed" conformations is initially formed. Intramolecular 'Sergeants-and-Soldiers' experiments have indicated a nonlinear dependence of the CD signal on the amount of chiral side chains indicating that there are cooperative interactions among the side chains and that they allow the chirality to be transferred to the backbone, illustrating that the side chains play more than just an ancillary role in the conformationally ordered oligomers. On the other hand, the experiments indicate that in acetonitrile a full bias of the helicity cannot be accomplished by chiral side-chains alone. Nevertheless, the folded oligomers are ordered since only one chiral side chain positioned at the beginning of an oligomer is capable of introducing a strong twist sense bias.

Examination of the oligo(ethylene oxide) decorated oligomers in aqueous solutions revealed a chain length dependent aggregation. Apparently, oligomers that adopt stable helical conformations easily aggregate into columns when the polarity of the solvent is increased by the addition of water. The formation of these columns ultimately results in the reversal of the CD signal, most probably

because of a reversal in twist sense bias due to lateral intercolumnar interactions. Mixtures of chiral and achiral oligomers in an aqueous environment showed a nonlinear dependence of θ_{\max} on the mole fraction of chiral oligomer, strongly supporting an intermolecular transfer of chirality. This transfer of chirality is hypothesized to occur through the intermolecular stacking of helical conformations and has been shown to be slightly cooperative.

The attachment of chiral, apolar side chains to *m*-phenylene ethynylene oligomers **3** allows for a twist sense bias in the helically folded conformation driven through the selective solvation with a nonpolar solvent. Intermolecular aggregation into columns of stacked helices was found to play an important role in the expression of the twist sense bias and is subject to hysteresis.

The results have shown the generality of the design principle and proved that generic interactions can be used for controlling the conformational ordering of nonbiological oligomers. The work represents a study at the mesoscopic level to understand the stepwise formation of large chiral aggregates. Previously, control over the formation of multi-molecular architectures in the micrometer scale has been achieved and impressive helical structures have been observed by scanning and transmission electron microscopy (SEM / TEM).^{4,40-46,92-100} However, the hierarchical formation of these architectures by the individual molecules is a less explored area and offers a challenging subject of investigation to elucidate the structural requirements and processes at hand. Given that biological architectures are sized in the nano to micrometer scale regime underscores the importance of the fundamental understanding of these complex assembly processes. In order to understand the formation of such structures, let alone to mimic them, a detailed knowledge of their hierarchical formation is important. The stepwise and reversible hierarchical growth of the chiral assemblies presented here reveal valuable information to better understanding the folding and assembly of proteins and polynucleotides and should, eventually, lead to the formation of functional non-biological multimolecular species. The combinations of monomer units from oligomer series **2** and **3** in a single chain or in a multi-molecular assembly eventually allow for the development of such systems with even higher degrees of conformational order through sequence heterogeneity.

6.7 Experimental section

General.¹⁰¹ Dry acetonitrile was obtained by vacuum transfer from calcium hydride. Low-resolution mass spectra were obtained on either a Hewlett-Packard GC-MS equipped with a 30 m HP-1 capillary column operating at 70 eV or a Finnigan-MAT CH5 spectrometer operating at 70 eV. High-resolution electron impact mass spectra were obtained on a Finnigan-MAT 731 spectrometer operating at 70 eV. Low and high-resolution fast atom bombardment (FAB) mass spectra were obtained on VG ZAB-SE and VG 70-SE-4F spectrometers. Low resolution matrix assisted laser desorption ionization (MALDI) mass spectra were obtained using 4-HMBN (4-hydroxybenzylidenemalononitrile) as the matrix. Elemental analyses were performed by the University of Illinois Micro Analytical Service Laboratory. Preparative size exclusion chromatography was performed using Bio-Beads S-XI Beads (200-400 mesh) from Bio-Rad laboratories using toluene as the eluent. Size exclusion chromatography (SEC) analysis was performed using a Waters 510 HPLC Pump, Waters 996 photodiode array, and a series of three Waters styragel HR 4E (7.8 x 300 mm) columns which were calibrated with narrow molecular weight polystyrene standards. High performance liquid chromatography (HPLC) analysis was performed on a Rainin binary gradient system equipped with two SD-200 pumps, a Si 80-125-C5 analytical column (4.6 x 250 mm), and a UV detector operating at 275 nm. The synthesis of compounds **4-7** is described in chapter 2 (**8**, **9**, **11** and **14**). Compounds **8** and **9** were obtained from commercial suppliers.

Nomenclature of oligomers. All oligomers of dimer length and longer are named using an abbreviated nomenclature system. The naming of the oligomers has the following generic naming pattern: **X-A_n-Y**. The **X** represents either a hydrogen (H), triazene (Et₂N₃) or an iodide group (I). The **Y** represents either a trimethylsilyl-protected acetylene (TMS), a deprotected acetylene (H), or a bromide group (Br). **A** corresponds to an aromatic ring with a (2*S*)-2-[2-(2-methoxyethoxy)-ethoxy] propanoxy side chain; **B** corresponds to an aromatic ring with a triethyleneglycol monomethyl ether side chain and **C** corresponds to an aromatic ring with a (S)-3,7-dimethyl-1-octyloxy side chain. Compounds **51-81** are only mentioned in the experimental.

(2*S*)-2-[2-(2-Methoxyethoxy)-ethoxy]-propyl 3-bromobenzoate (10). To an oven-dried 500 mL round bottom flask was added **8** (5.00 g, 24.9 mmol), **7** (4.03 g, 22.61 mmol), *N,N'*-dimethylaminopyridine (0.82 g, 6.80 mmol) and dry CH₂Cl₂ (150 mL). The homogeneous, yellow solution was placed under a N₂ atmosphere and cooled in a 0 °C bath. Dicyclohexylcarbodiimide (9.28 g, 45.0 mmol) was added in one portion and the solution was stirred for 1 h at 0 °C, warmed to room temperature and stirred 12 h. The solution was cooled in a 0 °C ice bath, gravity filtered to remove the DCU and then concentrated in vacuo resulting in a yellow oil. The crude product was purified by silica gel column chromatography (5/4, heptane/EtOAc) to afford 6.50 g (18.0 mmol, 92%) of analytically pure **10** as a colorless oil: ¹H NMR (400 MHz, CDCl₃) δ 8.18 (ddd, *J* = 1.84, 1.70, 0.39 Hz, 1H), 7.97 (ddd, *J* = 7.83, 1.65, 1.09 Hz, 1H), 7.69 (ddd, *J* = 8.02, 2.05, 1.10 Hz, 1H), 7.32 (ddd, *J* = 8.24, 7.97, 0.35 Hz, 1H), 4.31 (ABX, *J*_{ab} = 11.5, *J*_{ax} = 4.70 Hz, 1H), 4.29 (ABX, *J*_{bx} = 6.32 Hz, 1H), 3.85 (quind, *J* = 6.32, 4.35 Hz, 1H), 3.78-3.68 (m, 2H), 3.67-3.62 (m, 4H), 3.55-3.51 (m, 2H), 3.35 (s, 3H), 1.26 (d, *J* = 6.46 Hz, 3H); ¹³C NMR (100 MHz, CDCl₃) δ 165.0, 135.9, 132.5, 132.0, 129.7, 128.2, 122.4, 71.9, 70.8, 70.5, 68.7, 68.0, 58.8, 17.0; MS (FAB) *m/z* 363.0 (20), 361.0 (21); TLC R_f = 0.30 (heptane/EtOAc, 5/4); Anal. Calcd for C₁₅H₂₁O₅Br (361.24): C, 49.88; H, 5.86; Found: C, 49.99; H, 5.97.

(2*S*)-2-[2-(2-Methoxyethoxy)-ethoxy]-propyl 3-bromo-5-(3,3-diethyltriazenyl)-benzoate (11). To an oven-dried 50 mL round bottom flask was added **9** (1.00 g, 3.32 mmol), **7** (0.63 g, 3.51 mmol), *N,N'*-dimethylaminopyridine (0.13 g, 1.02 mmol) and dry CH₂Cl₂ (22 mL). The homogeneous, yellow solution was placed under a N₂ atmosphere and cooled in a 0 °C bath. Dicyclohexylcarbodiimide (1.35 g, 6.66 mmol) was added in one portion and the solution was stirred for 1 h at 0 °C, warmed to room temperature and stirred 12 h. The solution was cooled in a 0 °C bath, gravity filtered to remove the DCU and then concentrated in vacuo resulting in a yellow oil. The crude product was purified by silica gel column chromatography (hexanes/EtOAc, 2/1) to afford 1.40 g (3.04 mmol, 92%) of analytically pure **11** as a light yellow oil: ¹H NMR (400 MHz, CDCl₃) δ 7.98 (dd, *J* = 1.81, 1.55 Hz, 1H), 7.88 (dd, *J* = 1.92, 1.48 Hz, 1H), 7.75 (t, *J* = 1.89 Hz, 1H), 4.27-4.32 (m, 2H), 3.82-3.89 (m, 1H), 3.67-3.81 (m, 6H), 3.62-3.66 (m, 4H), 3.49-3.52 (m, 2H), 3.36 (s, 3H), 1.15-1.40 (m, 6H), 1.26 (d, *J* = 6.29 Hz, 3H); ¹³C NMR (100 MHz, CDCl₃) δ 165.2, 152.5, 132.1, 128.1, 126.8, 122.4, 121.0, 73.7, 71.8, 70.7, 70.4, 68.6, 67.9, 58.9, 17.0; MS (FAB) *m/z* 460.1 (100), 462.1 (96.7); TLC R_f = 0.24 (hexanes/EtOAc, 2/1); Anal. Calcd for C₁₉H₃₀N₃O₅Br (460.37): C, 49.57; H, 6.57; N, 9.13. Found: C, 49.60; H, 6.60; N, 9.13.

(2*S*)-2-[2-(2-Methoxyethoxy)-ethoxy]-propyl 3-trimethylsilylethynyl-benzoate (12). To a sealed tube fitted with a magnetic stirrer was added **10** (3.10 g, 8.57 mmol), Pd₂(dba)₃ (240 mg, 0.26 mmol), CuI (103 mg, 0.54 mmol), PPh₃ (564 mg, 2.14 mmol), and dry triethylamine (35 mL). The mixture was evacuated and back-filled

with nitrogen three times and dry, degassed trimethylsilylacetylene (2.8 mL, 20 mmol) was added. The tube was sealed and stirred at 75 °C for 31 h (during which time a white salt precipitate formed). The solution was diluted with Et₂O (100 mL), filtered to remove the precipitate and concentrated in vacuo leaving a brown oil. The residue was purified by silica gel column chromatography (hexanes/EtOAc, 2/1) to give 3.04 g (8.04 mmol, 94%) of analytically pure **12** as a colorless oil: ¹H NMR (400 MHz, CDCl₃) δ 8.12 (t, *J* = 1.73 Hz, 1H), 7.98 (dt, *J* = 7.78, 1.73 Hz, 1H), 7.63 (dt, *J* = 7.77, 1.73 Hz, 1H), 7.37 (t, *J* = 7.68 Hz, 1H), 4.30 (ABX, *J*_{ab} = 11.5, *J*_{ax} = 4.12 Hz, 1H), 4.28 (ABX, *J*_{bx} = 6.4 Hz, 1H), 3.89-3.80 (quin d, *J* = 6.25, 4.88 Hz, 1H), 3.77-3.67 (m, 2H), 3.66-3.61 (m, 4H), 3.52-3.48 (m, 2H), 3.35 (s, 3H), 1.26 (d, *J* = 6.38 Hz, 3H), 0.25 (s, 9H); ¹³C NMR (100 MHz, CDCl₃) δ 165.5, 136.0, 132.8, 130.1, 129.4, 128.2, 123.4, 103.7, 95.2, 73.7, 71.7, 70.7, 70.4, 68.6, 67.7, 58.8, 17.0, -0.3; MS (EI) *m/z* 379.2 (30), 259.1 (83), 201 (100); TLC *R*_f = 0.22 (hexanes/EtOAc, 2/1); Anal. Calcd for C₂₀H₃₀O₅Si (378.54): C, 63.46; H, 7.99; Found: C, 63.56; H, 7.97.

(2S)-2-[2-(2-Methoxyethoxy)-ethoxy]-propyl 3-(3,3-diethyltriazenyl)-5-trimethylsilylethynyl-benzoate (13). To a sealed tube fitted with a magnetic stirrer was added **11** (2.50 g, 5.43 mmol), Pd₂(dba)₃ (0.20 g, 0.22 mmol), copper iodide (0.08 g, 0.44 mmol), PPh₃ (0.45 g, 1.7 mmol) and dry triethylamine (30 mL). The mixture was evacuated and back-filled with nitrogen three times and dry, degassed trimethylsilylacetylene (2.5 mL, 14.2 mmol) was added. The tube was sealed and stirred at 70 °C for 23 h (during which time a white precipitate formed). After being cooled to rt, the contents of the flask were added to diethyl ether (100 mL). The insoluble amine salts were filtered off and the resulting solution was concentrated in vacuo to provide an orange oil. The crude product was purified by silica gel column chromatography (hexanes/EtOAc, 5/2) to afford 2.54 g (5.32 mmol, 98%) of analytically pure **13** as a light yellow oil: ¹H NMR (400 MHz, CDCl₃) δ 8.01 (dd, *J* = 2.02, 1.60 Hz, 1H), 7.87 (t, *J* = 1.56 Hz, 1H), 7.69 (dd, *J* = 1.97, 1.57 Hz, 1H), 4.27-4.32 (m, 2H), 3.82-3.89 (m, 1H), 3.67-3.81 (m, 6H), 3.62-3.66 (m, 4H), 3.49-3.52 (m, 2H), 3.35 (s, 3H), 1.15-1.40 (m, 6H), 1.26 (d, *J* = 6.29, 3H), 0.25 (s, 9H) ¹³C NMR (100 MHz, CDCl₃) δ 165.8, 151.2, 130.7, 129.1, 127.6, 123.6, 121.4, 104.2, 94.4, 73.7, 71.8, 70.7, 70.4, 68.6, 67.7, 58.8, 17.0, -0.21; MS (FAB) *m/z* 478.3 (100), 300.1 (87); TLC *R*_f = 0.26 (hexanes/EtOAc, 2/1); Anal. Calcd for C₂₄H₃₉N₃O₅Si (477.68): C, 60.35, H, 8.23, N, 8.80. Found: C, 60.59; H, 8.05; N, 8.74.

(2S)-2-[2-(2-Methoxyethoxy)-ethoxy]-propyl 3-ethynyl-benzoate (14). To a solution of **12** (2.76 g, 7.30 mmol) and THF (50 mL) was added a solution of tetrabutylammonium fluoride in wet THF (9.5 mL, 1.0 M). The solution was stirred for 1 minute, filtered through silica (eluting with hexanes/EtOAc, 1/1), and the solvent was removed in vacuo to leave an orange oil. The crude acetylene was used without further purification.

(2S)-2-[2-(2-Methoxyethoxy)-ethoxy]-propyl 3-(3,3-diethyltriazenyl)-5-ethynyl-benzoate (15). To a solution of **13** (2.11 g, 4.41 mmol) and THF (30 mL) was added a solution of tetrabutylammonium fluoride in wet THF (5.8 mL, 1.0 M). The solution was stirred for 1 minute, filtered through silica (eluting with hexanes/EtOAc, 1/1), and the solvent was removed in vacuo to leave a brown oil. The crude acetylene was used without further purification.

(2S)-2-[2-(2-Methoxyethoxy)-ethoxy]-propyl 5-bromo-3-iodobenzoate (16). To an oven-dried 500 mL round bottom flask was added 3-bromo-5-iodobenzoic acid (12.0 g, 36.7 mmol), **7** (6.79 g, 38.1 mmol), *N,N'*-dimethylaminopyridine (1.35 g, 11.0 mmol) and dry CH₂Cl₂ (200 mL). The heterogeneous, yellow solution was placed under a N₂ atmosphere and cooled in a 0 °C bath. Dicyclohexylcarbodiimide (15.0 g, 72.0 mmol) was added in small portions and the solution was stirred for 1 h at 0 °C, warmed to room temperature and stirred 12 h. The solution was cooled in a 0 °C ice bath, gravity filtered to remove the DCU and then concentrated in vacuo resulting in a yellow oil. The crude product was purified by silica gel column chromatography (heptane/EtOAc, 5/4) to afford 14.2 g (29.2 mmol, 80%) of analytically pure **16** as a colorless oil: ¹H NMR (400 MHz, CDCl₃) δ 8.29 (t, *J* = 1.6 Hz, 1H), 8.12 (dd, *J* = 1.81, 1.5 Hz, 1H), 8.04 (t, *J* = 1.4 Hz, 1H), 4.31 (ABX, *J*_{ab} = 11.5, *J*_{ax} = 4.20 Hz, 1H), 4.29 (ABX, *J*_{bx} = 6.29 Hz, 1H), 3.85 (quin d, *J* = 6.41, 4.38 Hz, 1H), 3.77-3.68 (m, 2H), 3.67-3.62 (m, 4H), 3.54-3.50 (m, 2H), 3.36 (s, 3H), 1.26 (d, *J* = 6.42 Hz, 3H); ¹³C NMR (100 MHz, CDCl₃) δ 163.7, 143.8, 137.1, 133.3, 132.0, 123.0, 94.0, 73.9, 71.9, 70.8, 70.6, 68.7, 68.3, 59.0, 17.0; MS (FAB) *m/z* 488.9 (67), 486.9 (70), 368.8 (99), 366.8 (100); TLC *R*_f = 0.25 (heptane/EtOAc, 5/4); Anal. Calcd for C₁₅H₂₀O₅BrI (487.13): C, 36.99; H, 4.14; Found: C, 37.03; H, 4.21.

H-[A]₂-Br (17). To a sealed tube fitted with a magnetic stirrer was added **14** (2.14 g, 7.00 mmol), **16** (4.91 g, 10.1 mmol), Pd₂(dba)₃ (130 mg, 0.14 mmol), CuI (60 mg, 0.31 mmol), PPh₃ (304 mg, 1.16 mmol), and dry triethylamine (35 mL). The mixture was evacuated and back-filled with nitrogen three times and heated at 55 °C for 14 h (during which time a white salt precipitate formed). The solution was diluted with EtOAc (125 mL), filtered to remove the precipitate and concentrated in vacuo leaving a brown residue. The residue was purified

by silica gel column chromatography (hexanes/EtOAc, 1/1, 1/2) to give 4.49 g (6.75 mmol, 97%) of analytically pure **17** as a light yellow oil: ^1H NMR (400 MHz, CDCl_3) δ 8.21 (td, $J = 1.69, 0.58$ Hz, 1H), 8.14 (dd, $J = 1.88, 1.56$ Hz, 1H), 8.13 (t, $J = 1.48$ Hz, 1H), 8.05 (ddd, $J = 7.83, 1.74, 1.19$ Hz, 1H), 7.86 (dd, $J = 1.90, 1.49$ Hz, 1H), 7.71 (ddd, $J = 7.72, 1.60, 1.28$ Hz, 1H), 7.45 (td, $J = 7.78, 0.62$ Hz, 1H), 4.38-4.24 (m, 4H), 3.90-3.81 (m, 2H), 3.80-3.68 (m, 4H), 3.67-3.63 (m, 8H), 3.53-3.48 (m, 4H), 3.36 (s, 3H), 3.35 (s, 3H), 1.29 (d, $J = 6.41$ Hz, 3H), 1.28 (d, $J = 6.40$ Hz, 3H); ^{13}C NMR (100 MHz, CDCl_3) δ 165.4, 164.3, 138.2, 135.8, 132.7, 132.4, 132.0, 131.2, 130.5, 129.8, 128.6, 125.0, 122.7, 122.2, 90.4, 87.6, 73.8, 73.6, 71.8, 70.7, 70.5, 68.7, 68.6, 68.1, 67.9, 58.9, 17.0, 16.9; MS (FAB) m/z 667.2 (15), 665.2 (15), 154.1 (100), 136 (69); TLC $R_f = 0.30$ (hexanes/EtOAc, 4/1); Anal. Calcd for $\text{C}_{32}\text{H}_{41}\text{O}_{10}\text{Br}$ (665.58): C, 57.75; H, 6.21; Found: C, 57.52; H, 6.22.

$\text{Et}_2\text{N}_3\text{-[A]}_2\text{-Br}$ (18**).** To a sealed tube fitted with a magnetic stirrer was added **15** (1.79 g, 4.41 mmol), **16** (2.80 g, 5.75 mmol), $\text{Pd}_2(\text{dba})_3$ (110 mg, 0.12 mmol), CuI (51 mg, 0.27 mmol), PPh_3 (256 mg, 0.97 mmol), and dry triethylamine (22 mL). The mixture was evacuated and back-filled with nitrogen three times and heated at 55 °C for 10 h (during which time a white salt precipitate formed). The solution was diluted with EtOAc (125 mL), filtered to remove the precipitate and concentrated in vacuo leaving a brown residue. The residue was purified by silica gel column chromatography (hexanes/EtOAc, 1/1) to give 3.34 g (0.99 mmol, 99%) of analytically pure **18** as a yellow oil: ^1H NMR (400 MHz, CDCl_3) δ 8.13 (t, $J = 1.6$ Hz, 1H), 8.12 (t, $J = 1.4$ Hz, 1H), 8.06 (dd, $J = 1.9, 1.67$ Hz, 1H), 7.94 (t, $J = 1.5$ Hz, 1H), 7.86 (t, $J = 1.5$ Hz, 1H), 7.76 (t, $J = 1.5$ Hz, 1H), 4.36-4.28 (m, 4H), 3.92-3.82 (m, 2H), 3.79 (q, $J = 7$ Hz, 4H), 3.79-3.68 (m, 4H), 3.67-3.61 (m, 8H), 3.53-3.48 (m, 4H), 3.35 (s, 3H), 3.35 (s, 3H), 1.29 (d, $J = 6.38, 3\text{H}$), 1.29 (br s, 6H), 1.28 (d, $J = 6.28, 3\text{H}$); ^{13}C NMR (100 MHz, CDCl_3) δ 165.6, 164.3, 151.5, 138.1, 132.1, 132.0, 131.2, 131.0, 128.7, 127.2, 125.2, 122.7, 122.4, 122.1, 91.0, 86.9, 73.7, 73.6, 70.7, 70.4, 68.7, 68.6, 68.1, 67.8, 58.9, 17.1, 16.9; MS (FAB) m/z 766.3 (100), 764.3 (96); TLC $R_f = 0.11$ (hexanes/EtOAc, 1/1); Anal. Calcd for $\text{C}_{36}\text{H}_{50}\text{O}_{10}\text{N}_3\text{Br}$ (764.71): C, 56.54; H, 6.59; N, 5.49; Found: C, 56.58; H, 6.60; N, 5.56.

$\text{H-[A]}_2\text{-SiMe}_3$ (19**, [**2** ($n = 2$))].** To a sealed tube fitted with a magnetic stirrer was added **17** (4.14 g, 6.22 mmol), $\text{Pd}_2(\text{dba})_3$ (170 mg, 0.18 mmol), CuI (73 mg, 0.39 mmol), PPh_3 (430 mg, 1.64 mmol), and dry triethylamine (30 mL). The mixture was evacuated and back-filled with nitrogen three times and dry, degassed trimethylsilylacetylene (3.0 mL, 21 mmol) was added. The tube was sealed and stirred at 70 °C for 18 h (during which time a white precipitate formed). The solution was diluted with ethyl acetate (500 mL), filtered to remove the precipitate and concentrated in vacuo leaving a yellow residue. The residue was purified by silica gel column chromatography (hexanes/EtOAc, 1/2) to give 3.97 g (5.81 mmol, 93%) of analytically pure **19** as a colorless oil: ^1H NMR (400 MHz, CDCl_3) δ 8.18 (td, $J = 1.65, 0.5$ Hz, 1H), 8.11 (t, $J = 1.6$ Hz, 1H), 8.06 (t, $J = 1.61$ Hz, 1H), 8.02 (ddd, $J = 7.9, 1.7, 1.2$ Hz, 1H), 7.8 (t, $J = 1.6$ Hz, 1H), 7.69 (ddd, $J = 7.7, 1.5, 1.2$ Hz, 1H), 7.44 (td, $J = 7.9, 0.6$ Hz, 1H), 4.31-4.29 (m, 4H), 3.89-3.81 (m, 2H), 3.78-3.65 (m, 4H), 3.65-3.60 (m, 8H), 3.36 (s, 3H), 3.35 (s, 3H), 1.20 (d, $J = 6.41$ Hz, 3H), 1.28 (d, $J = 6.40$ Hz, 3H), 0.25 (s, 9H); ^{13}C NMR (100 MHz, CDCl_3) δ 165.4, 164.8, 138.6, 135.7, 132.6, 132.5, 132.2, 130.6, 130.4, 129.6, 128.5, 123.9, 123.4, 122.9, 102.7, 96.2, 89.6, 88.2, 73.7, 73.6, 71.1, 70.7, 70.4, 68.6, 68.5, 67.9, 67.8, 58.8, 17.0, 16.9, -0.3; MS (FAB) m/z 683 (40), 563 (100); TLC $R_f = 0.32$ (hexanes/EtOAc, 1/2); Anal. Calcd for $\text{C}_{37}\text{H}_{50}\text{O}_{10}\text{Si}$: C, 65.08; H, 7.38; Found: C, 64.71; H, 7.34; GPC 1175 (M_n), 1.03 (M_w/M_n), 100%.

$\text{Et}_2\text{N}_3\text{-[A]}_2\text{-SiMe}_3$ (20**).** To a sealed tube fitted with a magnetic stirrer was added **18** (4.05 g, 5.29 mmol), $\text{Pd}_2(\text{dba})_3$ (152 mg, 0.17 mmol), CuI (62 mg, 0.33 mmol), PPh_3 (366 mg, 0.39 mmol), and dry triethylamine (27 mL). The mixture was evacuated and back-filled with nitrogen three times and dry, degassed trimethylsilylacetylene (2.5 mL, 17.7 mmol) was added. The tube was sealed and stirred at 75 °C for 24 h (during which time a white salt precipitate formed). The solution was diluted with EtOAc (125 mL), filtered to remove the precipitate and concentrated in vacuo leaving an orange oil. The crude product was purified by silica gel column chromatography (hexanes/EtOAc, 2/1, 3/2) to give 3.93 g (5.03 mmol, 95%) of analytically pure **20** as a light yellow oil: ^1H NMR (400 MHz, CDCl_3) δ 8.12 (t, $J = 1.6$ Hz, 1H), 8.07 (t, $J = 1.6$ Hz, 1H), 8.05 (dd, $J = 2.0, 1.6$ Hz, 1H), 7.93 (t, $J = 1.6$ Hz, 1H), 7.81 (t, $J = 1.6$ Hz, 1H), 7.76 (dd, $J = 2.1, 1.5$ Hz, 1H), 4.36-4.24 (m, 4H), 3.92-3.84 (m, 4H), 3.80 (q, $J = 7.2$ Hz, 4H), 3.76-3.68 (m, 4H), 3.68-3.62 (m, 8H), 3.52-3.48 (m, 4H), 3.36 (s, 3H), 3.35 (s, 3H), 1.30 (d, $J = 6.38$ Hz, 3H), 1.29 (br s, 6H), 1.28 (d, $J = 6.35$ Hz, 3H), 0.26 (s, 9H); ^{13}C NMR (100 MHz, CDCl_3) δ 165.8, 165.0, 151.5, 138.7, 132.5, 132.3, 131.0, 130.6, 128.8, 127.2, 124.0, 123.8, 123.1, 122.3, 102.8, 96.2, 90.2, 87.6, 73.8, 73.7, 71.8, 70.8, 70.5, 68.7, 68.6, 67.9, 67.8, 58.9, 17.7, 17.0, -0.3; MS (FAB) m/z 782.4 (100); TLC $R_f = 0.31$ (hexanes/EtOAc, 1/2); Anal. Calcd for $\text{C}_{41}\text{H}_{59}\text{N}_3\text{O}_{10}\text{Si}$: C, 62.96; H, 7.61; N, 5.38; Found: C, 63.29; H, 7.77; N, 5.44.

Et₂N₃-[A]₄-SiMe₃ (21). To a sealed tube fitted with a magnetic stirrer was added **27** (2.05 g, 2.55 mmol), **24** (1.70 g, 2.40 mmol) Pd₂(dba)₃ (47 mg, 0.05 mmol), CuI (20 mg, 0.11 mmol), PPh₃ (114 mg, 0.43 mmol), and dry triethylamine (27 mL). The mixture was evacuated and back-filled with nitrogen three times. The tube was sealed and stirred at 75 °C for 15 h (during which time a white salt precipitate formed). The solution was diluted with EtOAc (60 mL), filtered to remove the precipitate and concentrated in vacuo leaving a yellow oil. The crude product was purified by silica gel column chromatography (CHCl₃/acetone, 7/1, 5/1) to give 3.30 g (2.31 mmol, 99%) of **21** as a light yellow oil: ¹H NMR (400 MHz, CDCl₃) δ 8.19 (t, *J* = 1.6 Hz, 1H), 8.18 (t, *J* = 1.7 Hz, 1H), 8.17 (t, *J* = 1.6 Hz, 2H), 8.14 (t, *J* = 1.5 Hz, 1H), 8.09 (t, *J* = 1.6 Hz, 1H), 8.07 (dd, *J* = 1.75, 1.67 Hz, 1H), 7.96 (t, *J* = 1.6 Hz, 1H), 7.90 (t, *J* = 1.6 Hz, 1H), 7.88 (t, *J* = 1.7 Hz, 1H), 7.83 (t, *J* = 1.6 Hz, 1H), 7.78 (dd, *J* = 1.9, 1.7 Hz, 1H), 4.40-4.28 (m, 8H), 3.92-3.84 (m, 4H), 3.81 (q, *J* = 7.2 Hz, 4H), 3.78-3.64 (m, 8H), 3.68-3.62 (m, 16H), 3.54-3.48 (m, 8H), 3.35 (s, 3H), 3.34 (s, 6H), 3.34 (s, 3H), 1.32-1.28 (m, 12H), 1.29 (br s, 6H), 0.27 (s, 9H); ¹³C NMR (100 MHz, CDCl₃) δ 165.6, 164.7, 164.6, 151.4, 138.6, 138.2, 132.7, 132.4, 132.3, 132.2, 132.1, 130.9, 130.88, 130.8, 130.7, 128.7, 127.1, 124.0, 123.8, 123.4, 123.2, 123.1, 122.9, 122.2, 102.6, 96.3, 90.3, 88.95, 88.91, 88.7, 88.6, 87.3, 73.6, 73.5, 71.7, 70.6, 70.4, 68.6, 68.5, 67.9, 67.8, 67.7, 58.8, 17.0, 16.9, 16.8, -0.4; MS (FAB) *m/z* 1390.6 (19), 391.3 (14); TLC R_f = 0.20 (hexanes/acetone, 2/1).

Et₂N₃-[A]₆-SiMe₃ (22). To a sealed tube fitted with a magnetic stirrer was added **27** (1.50 g, 1.85 mmol), **25** (2.31 g, 1.75 mmol), Pd₂(dba)₃ (25 mg, 0.03 mmol), CuI (11 mg, 0.06 mmol), PPh₃ (60 mg, 0.23 mmol), dry triethylamine (2 mL) and dry acetonitrile (10 mL). The mixture was evacuated and back-filled with nitrogen three times. The tube was sealed and stirred at 65 °C for 15 h. The solution was concentrated in vacuo leaving a yellow oil. The crude product was purified by silica gel column chromatography (CHCl₃/acetone, 1/0, 8/1, 6/1, 5/1) to give 3.08 g (1.54 mmol, 88%) of **22** as a light yellow oil: ¹H NMR (400 MHz, CDCl₃) δ 8.20-8.15 (m, 7H), 8.12 (t, *J* = 1.5 Hz, 1H), 8.08 (t, *J* = 1.5 Hz, 1H), 8.05 (dd, *J* = 2.0, 1.68 Hz, 1H), 7.94 (t, *J* = 1.5 Hz, 1H), 7.90 (t, *J* = 1.6 Hz, 2H), 7.89 (t, *J* = 1.6 Hz, 2H), 7.88 (t, *J* = 1.6 Hz, 1H), 7.81 (t, *J* = 1.6 Hz, 1H), 7.77 (dd, *J* = 2.0, 1.6 Hz, 1H), 4.44-4.29 (m, 12H), 3.92-3.82 (m, 6H), 3.80 (q, *J* = 7.2 Hz, 4H), 3.76-3.68 (m, 12H), 3.68-3.60 (m, 24H), 3.52-3.48 (m, 12H), 3.33 (s, 3H), 3.32 (bs, 12H), 3.32 (s, 3H), 1.32-1.26 (m, 18H), 1.29 (br s, 6H), 0.25 (s, 9H); MS (FAB) *m/z* 2000.3 (100); TLC R_f = 0.33 (CHCl₃/acetone, 5/1).

Et₂N₃-[A]₁₂-SiMe₃ (23). To a sealed tube fitted with a magnetic stirrer was added **29** (702 mg, 0.35 mmol), **26** (639 mg, 0.33 mmol), Pd₂(dba)₃ (15 mg, 0.02 mmol), CuI (6.5 mg, 0.03 mmol), PPh₃ (41 mg, 0.16 mmol), dry triethylamine (2 mL) and dry acetonitrile (10 mL). The mixture was evacuated and back-filled with nitrogen three times. The tube was sealed and stirred at 65 °C for 15 h. The solution was concentrated in vacuo leaving a brown oil. The crude product was purified by silica gel column chromatography (CHCl₃/acetone, 1/0, 4/1, 3/1, 2/1) to give 881 mg (0.23 mmol, 70%) of **23** as an off-white wax: ¹H NMR (400 MHz, CDCl₃) δ 8.20-8.15 (m, 20H), 8.12 (t, *J* = 1.5 Hz, 1H), 8.08 (t, *J* = 1.5 Hz, 1H), 8.05 (dd, *J* = 2.0, 1.7 Hz, 1H), 7.94 (t, *J* = 1.5 Hz, 1H), 7.90 (m, 9H), 7.89 (t, *J* = 1.6 Hz, 1H), 7.82 (t, *J* = 1.6 Hz, 1H), 7.78 (dd, *J* = 2.0, 1.6 Hz, 1H), 4.44-4.29 (m, 24H), 3.92-3.82 (m, 12H), 3.80 (q, *J* = 7.2 Hz, 4H), 3.76-3.68 (m, 24H), 3.68-3.60 (m, 48H), 3.52-3.48 (m, 24H), 3.33 (s, 3H), 3.32 (bs, 33H), 1.33-1.27 (m, 36H), 1.29 (br s, 6H), 0.25 (s, 9H); MS (MALDI) *m/z* 3847.3 (calcd [M + Na]⁺ = 3847.7); TLC R_f = 0.29 (CHCl₃/acetone, 3/1).

Et₂N₃-[A]₂-H (24). To a solution of **20** (1.87 g, 2.39 mmol) and THF (16 mL) was added a solution of tetrabutylammonium fluoride in wet THF (3.1 mL, 1.0 M). The solution was stirred for 1 minute, filtered through silica (eluting with hexanes/EtOAc, 1/2), and the solvent was removed in vacuo to leave a yellow oil. The crude product was used without further purification.

Et₂N₃-[A]₄-H (25). To a solution of **21** (2.67 g, 1.92 mmol) and THF (15 mL) was added a solution of tetrabutylammonium fluoride in wet THF (2.5 mL, 1.0 M). The solution was stirred for 1 minute, filtered through silica (eluting with hexanes/acetone, 1/1), and the solvent was removed in vacuo to leave a yellow oil. The crude product was used without further purification.

Et₂N₃-[A]₆-H (26). To a solution of **22** (813 mg, 0.40 mmol) and THF (10 mL) was added a solution of tetrabutylammonium fluoride in wet THF (0.70 mL, 1.0 M). The solution was stirred for 1 minute, filtered through silica (eluting with CHCl₃/acetone, 1/1), and the solvent was removed in vacuo to leave a yellow oil. The crude product was used without further purification.

I-[A]₂-SiMe₃ (27). To a 55 mL sealed tube was added **20** (3.61 g, 4.63 mmol), and iodomethane (25 mL). The mixture was degassed three times by evacuation, sealed and stirred at 110 °C for 13 h. The iodomethane was removed in vacuo to give a dark brown oil. The crude product was purified by silica gel column chromatography (hexanes/EtOAc, 1/2) to give 3.44 g (4.26 mmol, 92%) of analytically pure **27** as a light yellow

oil: ^1H NMR (400 MHz, CDCl_3) δ 8.34 (t, $J = 1.6$ Hz, 1H), 8.13 (t, $J = 1.5$ Hz, 1H), 8.11 (t, $J = 1.6$ Hz, 1H), 8.09 (t, $J = 1.6$ Hz, 1H), 8.05 (t, $J = 1.6$ Hz, 1H), 7.80 (t, $J = 1.6$ Hz, 1H), 4.36-4.28 (m, 4H), 3.92-3.82 (m, 2H), 3.78-3.68 (m, 4H), 3.68-3.62 (m, 8H), 3.52-3.48 (m, 4H), 3.35 (s, 3H), 3.34 (s, 3H), 1.29 (d, $J = 6.38$ Hz, 3H), 1.27 (d, $J = 6.34$ Hz, 3H), 0.26 (s, 9H); ^{13}C NMR (100 MHz, CDCl_3) δ 164.8, 164.1, 144.0, 138.7, 138.4, 132.9, 132.3, 132.0, 131.8, 130.7, 124.8, 124.0, 102.6, 96.5, 93.3, 89.5, 88.0, 73.7, 73.6, 71.8, 70.8, 70.5, 68.6, 68.1, 68.0, 59.0, 17.0, 17.0, -0.2; MS (FAB) m/z 809.2 (50), 689.1 (98); TLC $R_f = 0.30$ (hexanes/EtOAc, 1/2); Anal. Calcd for $\text{C}_{37}\text{H}_{49}\text{O}_{10}\text{Si}$: C, 54.95; H, 6.11; Found: C, 54.79; H, 5.99.

I-[A]₄-SiMe₃ (28). To a 15 mL sealed tube was added **21** (824 mg, 0.59 mmol), and iodomethane (5 mL). The mixture was degassed three times by evacuation, sealed and stirred at 110 °C for 14 h. The iodomethane was removed in vacuo to give a dark brown oil. The crude product was purified by silica gel column chromatography (CHCl_3 /acetone, 1/0, 7/1) to give 764 mg (0.54 mmol, 91%) of **28** as a light yellow oil: ^1H NMR (400 MHz, CDCl_3) δ 8.35 (t, $J = 1.7$ Hz, 1H), 8.19-8.15 (m, 5H), 8.13 (t, $J = 1.6$ Hz, 1H), 8.10 (t, $J = 1.6$ Hz, 1H), 8.08 (t, $J = 1.6$ Hz, 1H), 7.89 (t, $J = 1.6$ Hz, 1H), 7.88 (t, $J = 1.6$ Hz, 1H), 7.83 (t, $J = 1.6$ Hz, 1H), 4.38-4.28 (m, 8H), 3.92-3.84 (m, 4H), 3.80-3.68 (m, 8H), 3.68-3.62 (m, 16H), 3.52-3.48 (m, 8H), 3.36 (s, 3H), 3.36 (s, 3H), 3.35 (s, 3H), 3.35 (s, 3H), 1.32-1.26 (m, 12H), 0.26 (s, 9H); MS (FAB) m/z 1417.4 (25), 1297.4 (100); TLC $R_f = 0.45$ (CHCl_3 /acetone, 5/1).

I-[A]₆-SiMe₃ (29). To a 15 mL sealed tube was added **22** (1.07 g, 0.53 mmol), and iodomethane (7 mL). The mixture was degassed three times by evacuation, sealed and stirred at 110 °C for 13 h. The iodomethane was removed in vacuo to give a dark brown oil. The crude product was purified by silica gel column chromatography (CHCl_3 /acetone, 1/0, 5/1, 3/1) to give 664 mg (0.43 mmol, 91%) of **29** as a yellow oil: ^1H NMR (400 MHz, CDCl_3) δ 8.35 (t, $J = 1.6$ Hz, 1H), 8.19-8.15 (m, 9H), 8.13 (t, $J = 1.7$ Hz, 1H), 8.09 (t, $J = 1.6$ Hz, 1H), 8.08 (t, $J = 1.6$ Hz, 1H), 7.91 (t, $J = 1.6$ Hz, 2H), 7.89 (t, $J = 1.6$ Hz, 1H), 7.88 (t, $J = 1.6$ Hz, 1H), 7.82 (t, $J = 1.6$ Hz, 1H), 4.38-4.28 (m, 12H), 3.92-3.84 (m, 6H), 3.80-3.68 (m, 12H), 3.68-3.62 (m, 24H), 3.52-3.48 (m, 12H), 3.35 (s, 3H), 3.34 (s, 3H), 3.33 (s, 12H), 1.32-1.26 (m, 18H), 0.26 (s, 9H); MS (FAB) m/z 2026.51 (50), 1906.51 (100); TLC $R_f = 0.35$ (CHCl_3 /acetone, 5/1).

I-[A]₁₂-SiMe₃ (30). To a 25 mL sealed tube was added **23** (702 mg, 0.18 mmol), and iodomethane (12 mL). The mixture was degassed three times by evacuation, sealed and stirred at 110 °C for 14 h. The iodomethane was removed in vacuo to give a dark brown oil. The crude product was purified by silica gel column chromatography (CHCl_3 /acetone, 1/0, 1/3) to give 627 mg (0.16 mmol, 89%) of **30** as a white wax: ^1H NMR (400 MHz, CDCl_3) δ 8.35 (t, $J = 1.6$ Hz, 1H), 8.19-8.15 (m, 21H), 8.13 (t, $J = 1.7$ Hz, 1H), 8.09 (t, $J = 1.6$ Hz, 1H), 8.08 (t, $J = 1.6$ Hz, 1H), 7.91 (m, 8H), 7.89 (m, 2H), 7.82 (t, $J = 1.6$ Hz, 1H), 4.38-4.28 (m, 24H), 3.92-3.84 (m, 12H), 3.80-3.68 (m, 24H), 3.68-3.62 (m, 48H), 3.52-3.48 (m, 24H), 3.35 (s, 3H), 3.34 (s, 3H), 3.33 (s, 30H), 1.32-1.26 (m, 36H), 0.26 (s, 9H); MS (MALDI) m/z 3874.6 (calcd $[\text{M} + \text{Na}]^+ = 3874.5$); TLC $R_f = 0.30$ (CHCl_3 /acetone, 3/1).

H-[A]₄-SiMe₃ (31, [2 ($n = 4$))]. To a sealed tube fitted with a magnetic stirrer was added **27** (645 mg, 0.80 mmol), **39** (460 mg, 0.75 mmol), $\text{Pd}_2(\text{dba})_3$ (14 mg, 0.02 mmol), CuI (6.4 mg, 0.03 mmol), PPh_3 (33 mg, 0.12 mmol), and dry triethylamine (10 mL). The mixture was evacuated and back-filled with nitrogen three times. The tube was sealed and stirred at 75 °C for 15 h (during which time a white salt precipitate formed). The solution was diluted with EtOAc (60 mL), filtered to remove the precipitate and concentrated in vacuo leaving a yellow oil. The crude product was purified by silica gel column chromatography (CHCl_3 /acetone, 7/1, 5/1) to give 0.86 g (0.67 mmol, 89%) of **31** as a light yellow oil: ^1H NMR (400 MHz, CDCl_3) δ 8.22 (td, $J = 1.7, 0.48$ Hz, 1H), 8.19-8.16 (m, 4H), 8.13 (t, $J = 1.6$ Hz, 1H), 8.10 (t, $J = 1.6$ Hz, 1H), 8.05 (ddd, $J = 7.8, 1.7, 1.2$ Hz, 1H), 7.90 (t, $J = 1.6$ Hz, 1H), 7.88 (t, $J = 1.6$ Hz, 1H), 7.83 (t, $J = 1.6$ Hz, 1H), 7.73 (ddd, $J = 7.7, 1.6, 1.3$ Hz, 1H), 7.47 (td, $J = 7.7, 0.55$ Hz, 1H), 4.37-4.30 (m, 8H), 3.93-3.83 (m, 4H), 3.80-3.69 (m, 8H), 3.69-3.62 (m, 16H), 3.53-3.49 (m, 8H), 3.36 (s, 3H), 3.350 (s, 3H), 3.346 (s, 3H), 3.344 (s, 3H), 1.32-1.28 (m, 12H), 0.27 (s, 9H); ^{13}C NMR (100 MHz, CDCl_3) δ 165.4, 164.8, 164.7, 138.7, 138.3, 135.8, 132.7, 132.5, 132.3, 132.2, 130.94, 130.9, 130.7, 130.4, 129.7, 128.5, 124.0, 123.7, 123.5, 123.4, 123.3, 123.1, 122.9, 102.6, 96.4, 89.8, 89.0, 88.9, 88.8, 88.6, 88.1, 73.7, 73.6, 73.5, 71.8, 70.7, 70.5, 68.6, 68.5, 68.0, 67.9, 67.8, 58.9, 17.0, 16.9, -0.3; MS (FAB) m/z 1291.5 (5), 1171.5 (9); TLC $R_f = 0.35$ (hexanes/acetone, 2/1); GPC 2152 (M_n), 1.04 (M_w/M_n), 99.1%.

H-[A]₆-SiMe₃ (32, [2 ($n = 6$))]. To a sealed tube fitted with a magnetic stirrer was added **39** (340 mg, 0.56 mmol), **28** (738 mg, 0.52 mmol), $\text{Pd}_2(\text{dba})_3$ (15.5 mg, 0.02 mmol), CuI (8.3 mg, 0.04 mmol), PPh_3 (43.0 mg, 0.16 mmol), dry triethylamine (1.5 mL) and dry acetonitrile (7.5 mL). The mixture was evacuated and back-filled with nitrogen three times. The tube was sealed and stirred at 65 °C for 17 h. The solution was

concentrated in vacuo leaving a brown oil. The crude product was purified by silica gel column chromatography (CHCl₃/acetone, 1/0, 5/1) to give 773 mg (0.41 mmol, 78%) of **32** as a light yellow oil: ¹H NMR (400 MHz, CDCl₃) δ 8.22 (td, *J* = 1.68, 0.47 Hz, 1H), 8.21-8.16 (m, 7H), 8.13 (t, *J* = 1.7 Hz, 1H), 8.09 (t, *J* = 1.7 Hz, 1H), 8.04 (ddd, *J* = 7.76, 1.64, 1.14 Hz, 1H), 7.92-7.90 (m, 4H), 7.88 (t, *J* = 1.6 Hz, 1H), 7.82 (t, *J* = 1.6 Hz, 1H), 7.73 (ddd, *J* = 7.71, 1.58, 1.26 Hz, 1H), 7.45 (td, *J* = 7.83, 0.55 Hz, 1H), 4.38-4.32 (m, 12H), 3.92-3.84 (m, 6H), 3.80-3.68 (m, 12H), 3.68-3.62 (m, 24H), 3.52-3.48 (m, 12H), 3.34 (s, 3H), 3.33 (s, 3H), 3.33 (bs, 12H), 1.32-1.26 (m, 18H), 0.26 (s, 9H); MS (FAB) *m/z* 1899.6 (39), 1780.7 (100); TLC *R_f* = 0.35 (hexanes/acetone, 2/1); GPC 2952 (M_n), 1.05 (M_w/M_n), 100%.

H-[A]₈-SiMe₃ (33, [2 (n = 8)]). To a sealed tube fitted with a magnetic stirrer was **39** (83 mg, 0.14 mmol), **29** (187 mg, 0.09 mmol), Pd₂(dba)₃ (6.5 mg, 0.01 mmol), CuI (2.3 mg, 0.01 mmol), PPh₃ (15 mg, 0.06 mmol), dry triethylamine (0.5 mL) and dry acetonitrile (2.5 mL). The mixture was evacuated and back-filled with nitrogen three times. The tube was sealed and stirred at 65 °C for 16 h. The solution was concentrated in vacuo leaving a brown oil. The crude product was purified by silica gel column chromatography (CHCl₃/acetone, 1/0, 5/1, 4/1, 3/1) to give 106 mg (0.04 mmol, 47%) of **33** as an off-white wax: ¹H NMR (400 MHz, CDCl₃) δ 8.22 (td, *J* = 1.8, 0.5 Hz, 1H), 8.21-8.16 (m, 11H), 8.13 (t, *J* = 1.7 Hz, 1H), 8.09 (t, *J* = 1.7 Hz, 1H), 8.04 (ddd, *J* = 7.8, 1.6, 1.1 Hz, 1H), 7.92-7.90 (m, 6H), 7.88 (t, *J* = 1.6 Hz, 1H), 7.82 (t, *J* = 1.6 Hz, 1H), 7.73 (ddd, *J* = 7.7, 1.6, 1.3 Hz, 1H), 7.45 (td, *J* = 7.8, 0.6 Hz, 1H), 4.38-4.32 (m, 16H), 3.92-3.84 (m, 8H), 3.80-3.68 (m, 16H), 3.68-3.62 (m, 32H), 3.52-3.48 (m, 16H), 3.34 (bs, 6H), 3.33 (bs, 18H), 1.32-1.26 (m, 24H), 0.27 (s, 9H); MS (MALDI) *m/z* 2531.5 (calcd [M + Na]⁺ = 2531.10); TLC *R_f* = 0.18 (CHCl₃/acetone, 5/1); GPC 3853 (M_n), 1.04 (M_w/M_n), 99.1%.

H-[A]₁₀-SiMe₃ (34, [2 (n = 10)]). To a sealed tube fitted with a magnetic stirrer was added **29** (186 mg, 0.09 mmol), **40** (152 mg, 0.13 mmol), Pd₂(dba)₃ (12 mg, 0.01 mmol), CuI (4.9 mg, 0.03 mmol), PPh₃ (26 mg, 0.10 mmol), dry triethylamine (1 mL) and dry acetonitrile (5 mL). The mixture was evacuated and back-filled with nitrogen three times. The tube was sealed and stirred at 65 °C for 13 h. The solution was concentrated in vacuo leaving a brown oil. The crude product was purified by silica gel column chromatography (CHCl₃/acetone, 1/0, 4/1, 3/1, 1/1, 2/5) to give 207 mg (0.07 mmol, 73%) of **34** as an off-white wax: ¹H NMR (400 MHz, CDCl₃) δ 8.22 (td, *J* = 1.7, 0.4 Hz, 1H), 8.21-8.16 (m, 15H), 8.13 (t, *J* = 1.8 Hz, 1H), 8.09 (t, *J* = 1.6 Hz, 1H), 8.05 (ddd, *J* = 7.7, 1.7, 1.2 Hz, 1H), 7.92-7.90 (m, 8H), 7.88 (t, *J* = 1.6 Hz, 1H), 7.82 (t, *J* = 1.6 Hz, 1H), 7.73 (ddd, *J* = 7.7, 1.6, 1.3 Hz, 1H), 7.45 (td, *J* = 7.8, 0.6 Hz, 1H), 4.38-4.32 (m, 20H), 3.92-3.84 (m, 10H), 3.80-3.68 (m, 20H), 3.68-3.62 (m, 40H), 3.52-3.48 (m, 20H), 3.34 (s, 3H), 3.33 (s, 3H), 3.33 (bs, 24H), 1.32-1.26 (m, 30H), 0.27 (s, 9H); MS (MALDI) *m/z* 3139.6 (calcd [M + Na]⁺ = 3140.4); TLC *R_f* = 0.08 (CHCl₃/acetone, 5/1); GPC 4426 (M_n), 1.05 (M_w/M_n), 100%.

H-[A]₁₂-SiMe₃ (35, [2 (n = 12)]). To a sealed tube fitted with a magnetic stirrer was added **29** (201 mg, 0.10 mmol), **41** (192 mg, 0.11 mmol), Pd₂(dba)₃ (11 mg, 0.01 mmol), CuI (7 mg, 0.04 mmol), PPh₃ (30 mg, 0.11 mmol), dry triethylamine (1 mL) and dry acetonitrile (5 mL). The mixture was evacuated and back-filled with nitrogen three times. The tube was sealed and stirred at 65 °C for 24 h. The solution was concentrated in vacuo leaving a brown oil. The crude product was purified by silica gel column chromatography (CHCl₃/acetone, 1/0, 5/1, 4/1, 5/2, 2/1) to give 254 mg (0.07 mmol, 69%) of **35** as an off-white wax: ¹H NMR (400 MHz, CDCl₃) δ 8.22 (td, *J* = 1.7, 0.4 Hz, 1H), 8.21-8.16 (m, 19H), 8.13 (t, *J* = 1.8 Hz, 1H), 8.09 (t, *J* = 1.6 Hz, 1H), 8.05 (ddd, *J* = 7.7, 1.7, 1.2 Hz, 1H), 7.92-7.90 (m, 10H), 7.88 (t, *J* = 1.6 Hz, 1H), 7.82 (t, *J* = 1.6 Hz, 1H), 7.73 (ddd, *J* = 7.7, 1.6, 1.3 Hz, 1H), 7.45 (td, *J* = 7.8, 0.6 Hz, 1H), 4.38-4.32 (m, 24H), 3.92-3.84 (m, 12H), 3.80-3.68 (m, 24H), 3.68-3.62 (m, 48H), 3.52-3.48 (m, 24H), 3.34 (s, 3H), 3.33 (s, 3H), 3.33 (bs, 30H), 1.32-1.26 (m, 36H), 0.27 (s, 9H); MS (MALDI) *m/z* 3748.6 (calcd [M + Na]⁺ = 3748.7); TLC *R_f* = 0.36 (CHCl₃/acetone, 2/1); GPC 5536 (M_n), 1.06 (M_w/M_n), 99%.

H-[A]₁₄-SiMe₃ (36, [2 (n = 14)]). To a sealed tube fitted with a magnetic stirrer was **39** (82 mg, 0.13 mmol), **30** (220 mg, 0.06 mmol), Pd₂(dba)₃ (9 mg, 0.01 mmol), CuI (4 mg, 0.02 mmol), PPh₃ (23 mg, 0.09 mmol), dry triethylamine (0.5 mL) and dry acetonitrile (3 mL). The mixture was evacuated and back-filled with nitrogen three times. The tube was sealed and stirred at 65 °C for 19 h. The solution was concentrated in vacuo leaving a brown oil. The crude product was purified by silica gel column chromatography (CHCl₃/acetone, 1/0, 5/1, 4/1, 3/1, 2/1, 1/1) to give 200 mg (0.05 mmol, 81%) of **36** as an off-white wax: ¹H NMR (400 MHz, CDCl₃) δ 8.22 (td, *J* = 1.7, 0.4 Hz, 1H), 8.21-8.16 (m, 24H), 8.13 (t, *J* = 1.8 Hz, 1H), 8.09 (t, *J* = 1.6 Hz, 1H), 8.05 (ddd, *J* = 7.7, 1.7, 1.2 Hz, 1H), 7.92-7.90 (m, 11H), 7.88 (t, *J* = 1.6 Hz, 1H), 7.82 (t, *J* = 1.6 Hz, 1H), 7.73 (ddd, *J* = 7.7, 1.6, 1.3 Hz, 1H), 7.45 (td, *J* = 7.8, 0.6 Hz, 1H), 4.38-4.32 (m, 28H), 3.92-3.84 (m, 14H), 3.80-3.68 (m, 28H), 3.68-3.62 (m, 56H), 3.52-3.48 (m, 28H), 3.34 (s, 3H), 3.33 (s, 3H), 3.33 (bs, 36H), 1.32-1.26 (m, 42H), 0.27 (s,

9H); MS (MALDI) m/z 4358.4 (calcd $[M + Na]^+ = 4357.9$); TLC $R_f = 0.28$ ($CHCl_3$ /acetone, 2/1); GPC 5877 (M_n), 1.07 (M_w/M_n), 99.1%.

H-[A]₁₆-SiMe₃ (37, [2 (*n* = 16))]. To a sealed tube fitted with a magnetic stirrer was added **40** (89 mg, 0.07 mmol), **30** (159 mg, 0.04 mmol), Pd₂(dba)₃ (11 mg, 0.01 mmol), CuI (5 mg, 0.03 mmol), PPh₃ (27 mg, 0.10 mmol), dry triethylamine (0.5 mL) and dry acetonitrile (3.5 mL). The mixture was evacuated and back-filled with nitrogen three times. The tube was sealed and stirred at 65 °C for 17 h. The solution was concentrated in vacuo leaving a brown oil. The crude product was purified by silica gel column chromatography ($CHCl_3$ /acetone, 1/0, 5/1, 4/1, 3/1, 2/1, 1/1) to give 122 mg (0.03 mmol, 69%) of **37** as an off-white wax: ¹H NMR (400 MHz, CDCl₃) δ 8.22 (td, $J = 1.7, 0.4$ Hz, 1H), 8.21-8.16 (m, 28H), 8.13 (t, $J = 1.8$ Hz, 1H), 8.09 (t, $J = 1.6$ Hz, 1H), 8.05 (ddd, $J = 7.7, 1.7, 1.2$ Hz, 1H), 7.92-7.90 (m, 13H), 7.88 (t, $J = 1.6$ Hz, 1H), 7.82 (t, $J = 1.6$ Hz, 1H), 7.73 (ddd, $J = 7.7, 1.6, 1.3$ Hz, 1H), 7.45 (td, $J = 7.8, 0.6$ Hz, 1H), 4.38-4.32 (m, 32H), 3.92-3.84 (m, 16H), 3.80-3.68 (m, 32H), 3.68-3.62 (m, 64H), 3.52-3.48 (m, 32H), 3.34 (s, 3H), 3.33 (s, 3H), 3.33 (bs, 42H), 1.32-1.26 (m, 48H), 0.27 (s, 9H); MS (MALDI) m/z 4967.6 (calcd $[M + Na]^+ = 4966.6$); TLC $R_f = 0.26$ ($CHCl_3$ /acetone, 2/1); GPC 6972 (M_n), 1.05 (M_w/M_n), 100%.

H-[A]₁₈-SiMe₃ (38, [2 (*n* = 18))]. To a sealed tube fitted with a magnetic stirrer was added **41** (130 mg, 0.07 mmol), **30** (193 mg, 0.05 mmol), Pd₂(dba)₃ (15 mg, 0.02 mmol), CuI (8.2 mg, 0.04 mmol), PPh₃ (34 mg, 0.13 mmol), dry triethylamine (0.5 mL) and dry acetonitrile (3.5 mL). The mixture was evacuated and back-filled with nitrogen three times. The tube was sealed and stirred at 65 °C for 14 h. The solution was concentrated in vacuo leaving a brown oil. The crude product was purified by silica gel column chromatography ($CHCl_3$ /acetone, 1/0, 5/1, 3/2) to give 193 mg (0.03 mmol, 69%) of **38** as an off-white wax: ¹H NMR (400 MHz, CDCl₃) δ 8.22 (td, $J = 1.7, 0.4$ Hz, 1H), 8.21-8.16 (m, 32H), 8.13 (t, $J = 1.8$ Hz, 1H), 8.09 (t, $J = 1.6$ Hz, 1H), 8.05 (ddd, $J = 7.7, 1.7, 1.2$ Hz, 1H), 7.92-7.90 (m, 15H), 7.88 (t, $J = 1.6$ Hz, 1H), 7.82 (t, $J = 1.6$ Hz, 1H), 7.73 (ddd, $J = 7.7, 1.6, 1.3$ Hz, 1H), 7.45 (td, $J = 7.8, 0.6$ Hz, 1H), 4.38-4.32 (m, 36H), 3.92-3.84 (m, 18H), 3.80-3.68 (m, 36H), 3.68-3.62 (m, 72H), 3.52-3.48 (m, 36H), 3.34 (s, 3H), 3.33 (s, 3H), 3.33 (bs, 48H), 1.32-1.26 (m, 54H), 0.27 (s, 9H); MS (MALDI) m/z 5574.8 (calcd $[M + Na]^+ = 5575.4$); TLC $R_f = 0.25$ ($CHCl_3$ /acetone, 2/1); GPC 7902 (M_n), 1.07 (M_w/M_n), 99.1%.

H-[A]₂-H (39). To a solution of **19** (0.60 g, 0.88 mmol) and THF (6 mL) was added a solution of tetrabutylammonium fluoride in wet THF (1.1 mL, 1.0 M). The solution was stirred for 1 minute, filtered through silica (eluting with hexanes/EtOAc, 1/2), and the solvent was removed in vacuo to leave a yellow oil. The crude product was used without further purification.

H-[A]₄-H (40). To a solution of **31** (0.60 g, 0.46 mmol) and THF (3 mL) was added a solution of tetrabutylammonium fluoride in wet THF (0.6 mL, 1.0 M). The solution was stirred for 1 minute, filtered through silica (eluting with CH_2Cl_2 /acetone, 1/3), and the solvent was removed in vacuo to leave a yellow oil. The crude product was used without further purification.

H-[A]₆-H (41). To a solution of **32** (516 mg, 0.27 mmol) and THF (8 mL) was added a solution of tetrabutylammonium fluoride in wet THF (0.4 mL, 1.0 M). The solution was stirred for 1 minute, filtered through silica (eluting with $CHCl_3$ /acetone, 2/1), and the solvent was removed in vacuo to leave a yellow oil. The crude product was used without further purification.

2-[2-(2-Methoxyethoxy)-ethoxy]-ethyl 5-bromo-3-iodobenzoate (42). The synthesis of this compound has been described previously.¹⁶

H-[A]₁-[B]₁-Br (43). To a solution of **12** (274 mg, 7.23 mmol) and THF (5 mL) was added a solution of tetrabutylammonium fluoride in wet THF (1.0 mL, 1.0 M). The solution was stirred for 1 minute, filtered through silica (eluting with hexanes/EtOAc, 1/1), and the solvent was removed in vacuo to leave an orange oil. The crude acetylene was used without further purification. To a sealed tube fitted with a magnetic stirrer was added **14** (213 mg, 0.695 mmol), **42** (449 mg, 0.950 mmol), Pd₂(dba)₃ (14 mg, 0.02 mmol), CuI (8.0 mg, 0.04 mmol), PPh₃ (38 mg, 0.14 mmol), and dry triethylamine (5 mL). The mixture was evacuated and back-filled with nitrogen three times and heated at 55 °C for 16 h (during which time a white salt precipitate formed). The solution was diluted with EtOAc (20 mL), filtered to remove the precipitate and concentrated in vacuo leaving a brown residue. The crude product was purified by silica gel column chromatography (hexanes/EtOAc, 1/1, 1/2) to give 425 mg (0.652 mmol, 93%) of analytically pure **43** as a light yellow oil: ¹H NMR (400 MHz, CDCl₃) δ 8.20 (td, $J = 1.69, 0.58$ Hz, 1H), 8.15 (dd, $J = 1.88, 1.56$ Hz, 1H), 8.14 (t, $J = 1.63$ Hz, 1H), 8.04 (ddd, $J = 7.73, 1.74, 1.19$ Hz, 1H), 7.86 (dd, $J = 1.87, 1.47$ Hz, 1H), 7.71 (ddd, $J = 7.80, 1.64, 1.32$ Hz, 1H), 7.46 (td, $J = 7.77,$

0.77 Hz, 1H), 4.38-4.24 (m, 4H), 3.90-3.81 (m, 2H), 3.80-3.68 (m, 4H), 3.67-3.63 (m, 8H), 3.53-3.48 (m, 4H), 3.36 (s, 3H), 3.35 (s, 3H), 1.28 (d, $J = 6.49$ Hz, 3H); ^{13}C NMR (100 MHz, CDCl_3) δ 165.4, 164.5, 138.2, 135.8, 132.7, 132.4, 132.0, 131.3, 130.5, 129.8, 128.6, 125.0, 122.7, 122.2, 90.4, 87.6, 73.8, 71.8, 70.7, 70.5, 68.7, 68.6, 68.1, 67.9, 58.9, 17.0; MS (FAB) m/z 653.2 (50), 651.2 (48), 154.1 (100), 136 (69); TLC $R_f = 0.10$ (hexanes/EtOAc, 1/1); Anal. Calcd for $\text{C}_{31}\text{H}_{39}\text{O}_{10}\text{Br}$ (651.55): C, 57.15; H, 6.03; Found: C, 56.91; H, 5.99.

H-[A]₁-[B]₁-SiMe₃ (44). To a sealed tube fitted with a magnetic stirrer was added **43** (293 mg, 0.450 mmol), $\text{Pd}_2(\text{dba})_3$ (12 mg, 0.01 mmol), CuI (5.0 mg, 0.03 mmol), PPh_3 (31 mg, 0.12 mmol), and dry triethylamine (5 mL). The mixture was evacuated and back-filled with nitrogen three times and dry, degassed trimethylsilylacetylene (1.0 mL, 7.1 mmol) was added. The tube was sealed and stirred at 70 °C for 18 h (during which time a white precipitate formed). The solution was diluted with ethyl acetate (50 mL), filtered to remove the precipitate and concentrated in vacuo leaving a yellow residue. The crude product was purified by silica gel column chromatography (hexanes/EtOAc, 2/3, 2/5) to give 275 mg (0.411 mmol, 91%) of analytically pure **44** as a colorless oil: ^1H NMR (400 MHz, CDCl_3) δ 8.20 (td, $J = 1.70, 0.6$ Hz, 1H), 8.14 (t, $J = 1.6$ Hz, 1H), 8.10 (t, $J = 1.6$ Hz, 1H), 8.04 (ddd, $J = 8.0, 1.8, 1.2$ Hz, 1H), 7.81 (t, $J = 1.6$ Hz, 1H), 7.71 (ddd, $J = 7.77, 1.62, 1.34$ Hz, 1H), 7.45 (td, $J = 7.73, 0.75$ Hz, 1H), 4.52-4.48 (m, 2H), 4.35-4.32 (m, 2H), 3.89-3.81 (m, 3H), 3.78-3.63 (m, 12H), 3.56-3.48 (m, 4H), 3.36 (s, 3H), 3.35 (s, 3H), 1.30 (d, $J = 6.50$ Hz, 3H), 0.26 (s, 9H); ^{13}C NMR (100 MHz, CDCl_3) δ 165.4, 165.0, 138.6, 135.7, 132.6, 132.5, 132.3, 130.6, 130.4, 129.6, 128.5, 123.9, 122.9, 102.7, 96.2, 89.5, 88.2, 73.7, 71.8, 70.7, 70.5, 70.48, 70.47, 70.45, 68.9, 68.6, 67.8, 64.3, 58.8, 17.0, -0.3; MS (FAB) m/z 669 (50), 154.1 (100); TLC $R_f = 0.24$ (hexanes/EtOAc, 1/2); Anal. Calcd for $\text{C}_{36}\text{H}_{48}\text{O}_{10}\text{Si}$ (668.86): C, 64.65; H, 7.23; Found: C, 64.97; H, 7.13.

H-[A]₁-[B]₁-H (45). To a solution of **44** (84 mg, 0.13 mmol) and THF (5 mL) was added a solution of tetrabutylammonium fluoride in wet THF (200 μL , 1.0 M). The solution was stirred for 1 minute, filtered through silica (eluting with hexanes/EtOAc, 1/2), and the solvent was removed in vacuo to leave an orange oil. The crude acetylene was used without further purification.

I-[B]₁₂-SiMe₃ (46). The synthesis of this compound has been described previously.¹⁶

H-[A]₁-[B]₁₃-SiMe₃ (47). To a sealed tube fitted with a magnetic stirrer was added **45** (75 mg, 0.13 mmol), **46** (82 mg, 0.02 mmol), $\text{Pd}_2(\text{dba})_3$ (10 mg, 0.01 mmol), CuI (4.1 mg, 0.02 mmol), PPh_3 (21 mg, 0.08 mmol), dry triethylamine (1 mL) and dry acetonitrile (3 mL). The mixture was evacuated and back-filled with nitrogen three times and heated at 70 °C for 19 h. The solution was concentrated in vacuo leaving a brown residue. The crude product was purified by silica gel column chromatography (CHCl_3 /acetone, 1/0, 1/1) followed by (CHCl_3 /*i*-PrOH, 95/5, 94/6, 93/7, 91/9) to give 46 mg (0.01 mmol, 50%) of **47** as an off-white wax: ^1H NMR (400 MHz, CDCl_3) δ 8.23-8.17 (m, 25H), 8.14 (t, $J = 1.8$ Hz, 1H), 8.11 (t, $J = 1.6$ Hz, 1H), 8.05 (ddd, $J = 7.7, 1.7, 1.2$ Hz, 1H), 7.92-7.90 (m, 11H), 7.88 (t, $J = 1.6$ Hz, 1H), 7.82 (t, $J = 1.6$ Hz, 1H), 7.73 (ddd, $J = 7.7, 1.6, 1.3$ Hz, 1H), 7.45 (td, $J = 7.8, 0.6$ Hz, 1H), 4.56-4.48 (m, 26H), 4.35-4.32 (m, 2H), 3.92-3.84 (m, 28H), 3.76-3.68 (m, 84H), 3.54-3.48 (m, 28H), 3.34 (s, 3H), 3.33 (s, 39H), 1.30 (d, $J = 6.43$ Hz, 1H), 0.27 (s, 9H); MS (MALDI) m/z 4174.72 (calcd $[\text{M} + \text{Na}]^+ = 4175.69$); TLC $R_f = 0.28$ (CHCl_3 /acetone, 2/1); GPC 3642 (M_n), 1.08 (M_w/M_n), 98.2%.

H-[A]₂-[B]₁₂-SiMe₃ (48). To a solution of **19** (0.60 g, 0.88 mmol) and THF (6 mL) was added a solution of tetrabutylammonium fluoride in wet THF (1.1 mL, 1.0 M). The solution was stirred for 1 minute, filtered through silica (eluting with hexanes/EtOAc, 1/2), and the solvent was removed in vacuo to leave a yellow oil. The crude product was used without further purification. To a sealed tube fitted with a magnetic stirrer was added **39** (38 mg, 0.06 mmol), **46** (70 mg, 0.02 mmol), $\text{Pd}_2(\text{dba})_3$ (9.3 mg, 0.01 mmol), CuI (3.7 mg, 0.02 mmol), PPh_3 (22 mg, 0.08 mmol), dry triethylamine (0.2 mL) and dry acetonitrile (2 mL). The mixture was evacuated and back-filled with nitrogen three times and heated at 70 °C for 35 h. The solution was concentrated in vacuo leaving a brown residue. The crude product was purified by silica gel column chromatography (CHCl_3 /acetone, 1/0, 2/1) followed by (CHCl_3 /*i*-PrOH, 95/5, 92/8) to give 47 mg (0.01 mmol, 59%) of **48** as an off-white wax: ^1H NMR (400 MHz, CDCl_3) δ 8.23-8.17 (m, 25H), 8.14 (t, $J = 1.8$ Hz, 1H), 8.11 (t, $J = 1.6$ Hz, 1H), 8.05 (ddd, $J = 7.7, 1.7, 1.2$ Hz, 1H), 7.92-7.90 (m, 11H), 7.88 (t, $J = 1.6$ Hz, 1H), 7.82 (t, $J = 1.6$ Hz, 1H), 7.73 (ddd, $J = 7.7, 1.6, 1.3$ Hz, 1H), 7.45 (td, $J = 7.8, 0.6$ Hz, 1H), 4.56-4.48 (m, 24H), 4.35-4.32 (m, 4H), 3.92-3.84 (m, 26H), 3.76-3.68 (m, 84H), 3.54-3.48 (m, 28H), 3.34 (s, 3H), 3.33 (s, 39H), 1.30 (d, $J = 6.5$ Hz, 1H), 1.28 (d, $J = 6.4$ Hz, 1H), 0.27 (s, 9H); MS (MALDI) m/z 4188.8 (calcd $[\text{M} + \text{Na}]^+ = 4186.7$); TLC $R_f = 0.28$ (CHCl_3 /acetone, 2/1); GPC 4210 (M_n), 1.15 (M_w/M_n), 95%.

H-[A]₄-[B]₁₂-SiMe₃ (49). To a solution of **31** (0.60 g, 0.88 mmol) and THF (6 mL) was added a solution of tetrabutylammonium fluoride in wet THF (1.1 mL, 1.0 M). The solution was stirred for 1 minute, filtered through silica (eluting with hexanes/EtOAc, 1/2), and the solvent was removed in vacuo to leave a yellow oil. The crude product was used without further purification. To a sealed tube fitted with a magnetic stirrer was added **40** (44 mg, 0.04 mmol), **46** (76 mg, 0.02 mmol), Pd₂(dba)₃ (7.0 mg, 0.01 mmol), CuI (3.4 mg, 0.18 mmol), PPh₃ (19 mg, 0.07 mmol), dry triethylamine (1 mL) and dry acetonitrile (6 mL). The mixture was evacuated and back-filled with nitrogen three times and heated at 70 °C for 19 h. The solution was concentrated in vacuo leaving a brown residue. The crude product was purified by silica gel column chromatography (CHCl₃/acetone, 1/0, 1/1, 1/2) followed by (CHCl₃/*i*-PrOH, 95/5, 94/6, 93/7, 91/9) to give 70 mg (0.02 mmol, 71%) of **49** as an off-white wax: ¹H NMR (400 MHz, CDCl₃) δ 8.23-8.197 (m, 29H), 8.14 (t, *J* = 1.8 Hz, 1H), 8.11 (t, *J* = 1.6 Hz, 1H), 8.05 (ddd, *J* = 7.7, 1.7, 1.2 Hz, 1H), 7.92-7.90 (m, 13H), 7.88 (t, *J* = 1.6 Hz, 1H), 7.82 (t, *J* = 1.6 Hz, 1H), 7.73 (ddd, *J* = 7.7, 1.6, 1.3 Hz, 1H), 7.45 (td, *J* = 7.8, 0.6 Hz, 1H), 4.56-4.48 (m, 24H), 4.35-4.32 (m, 8H), 3.92-3.84 (m, 28H), 3.76-3.68 (m, 96H), 3.54-3.48 (m, 32H), 3.34 (s, 3H), 3.33 (s, 45H), 1.33-1.27 (m, 12H), 0.27 (s, 9H); MS (MALDI) *m/z* 4795.55 (calcd [M + Na]⁺ = 4799.97); TLC R_f = 0.25 (CHCl₃/*i*-PrOH, 93/7); GPC 5603 (M_n), 1.15 (M_w/M_n), 97.5%.

H-[A]₆-[B]₁₂-SiMe₃ (50). To a solution of **32** (516 mg, 0.27 mmol) and THF (8 mL) was added a solution of tetrabutylammonium fluoride in wet THF (0.4 mL, 1.0 M). The solution was stirred for 1 minute, filtered through silica (eluting with CHCl₃/acetone, 2/1), and the solvent was removed in vacuo to leave a yellow oil. The crude product was used without further purification. To a sealed tube fitted with a magnetic stirrer was added **41** (51 mg, 0.03 mmol), **46** (70 mg, 0.02 mmol), Pd₂(dba)₃ (8.0 mg, 0.01 mmol), CuI (3.6 mg, 0.02 mmol), PPh₃ (21 mg, 0.08 mmol), dry triethylamine (1 mL) and dry acetonitrile (3 mL). The mixture was evacuated and back-filled with nitrogen three times and heated at 70 °C for 10 h. The solution was concentrated in vacuo leaving a brown residue. The crude product was purified by silica gel column chromatography (CHCl₃/acetone, 1/0, 1/1) followed by (CHCl₃/*i*-PrOH, 95/5, 94/6, 93/7, 92/8) to give 76 mg (0.01 mmol, 75%) of **50** as an off-white wax: ¹H NMR (400 MHz, CDCl₃) δ 8.23-8.197 (m, 33H), 8.14 (t, *J* = 1.8 Hz, 1H), 8.11 (t, *J* = 1.6 Hz, 1H), 8.05 (ddd, *J* = 7.7, 1.7, 1.2 Hz, 1H), 7.92-7.90 (m, 15H), 7.88 (t, *J* = 1.6 Hz, 1H), 7.82 (t, *J* = 1.6 Hz, 1H), 7.73 (ddd, *J* = 7.7, 1.6, 1.3 Hz, 1H), 7.45 (td, *J* = 7.8, 0.6 Hz, 1H), 4.56-4.48 (m, 24H), 4.35-4.32 (m, 30H), 3.92-3.84 (m, 28H), 3.76-3.68 (m, 108H), 3.54-3.48 (m, 36H), 3.34 (s, 3H), 3.33 (s, 51H), 1.33-1.27 (m, 18H), 0.27 (s, 9H); MS (MALDI) *m/z* 5407.1 (calcd [M + Na]⁺ = 5406.2); TLC R_f = 0.25 (CHCl₃/*i*-PrOH, 93/7); GPC 5931 (M_n), 1.16 (M_w/M_n), 100%.

(S)-3,7-Dimethyloctyl 3-bromobenzoate (51). To an oven-dried 500 mL round bottom flask was added **8** (6.05 g, 31.6 mmol), (*S*)-3,7-dimethyl-1-octanol (5.00 g, 31.6 mmol), *N,N'*-dimethylaminopyridine (1.22 g, 1.00 mmol) and dry CH₂Cl₂ (150 mL). The homogeneous, yellow solution was placed under a N₂ atmosphere and cooled in a 0 °C bath. Dicyclohexylcarbodiimide (12.4 g, 60.0 mmol) was added in portions and the solution was stirred for 1 h at 0 °C, warmed to room temperature and stirred 12 h. The solution was cooled in a 0 °C ice bath, gravity filtered to remove the DCU and then concentrated in vacuo resulting in a yellow oil. The crude product was purified by silica gel column chromatography (heptane/CH₂Cl₂, 1/0, 2/3) to afford 9.70 g (28.4 mmol, 94%) of analytically pure **51** as a colorless oil: ¹H NMR (400 MHz, CDCl₃) δ 8.16 (ddd, *J* = 1.86, 1.70, 0.39 Hz, 1H), 7.96 (ddd, *J* = 7.83, 1.65, 1.09 Hz, 1H), 7.66 (ddd, *J* = 8.02, 2.05, 1.10 Hz, 1H), 7.30 (ddd, *J* = 8.24, 7.97, 0.35 Hz, 1H), 4.38-4.32 (m, 2H), 1.82-1.78 (m, 1H), 1.61-1.50 (m, 3H), 1.36-1.13 (m, 6H), 0.95 (d, *J* = 6.5 Hz, 3H), 0.87 (d, *J* = 6.5 Hz, 3H), 0.87 (d, *J* = 6.5 Hz, 3H); ¹³C NMR (100 MHz, CDCl₃) δ 165.2, 135.7, 132.5, 132.4, 129.6, 128.1, 122.4, 64.0, 39.1, 37.1, 35.5, 29.7, 27.9, 24.6, 22.6, 22.6, 19.6; MS (FAB) *m/z* 343.1 (40), 341.1 (47), 185.0 (74), 183.0 (76); Anal. Calcd for C₁₇H₂₅O₂Br (341.29): C, 59.83; H, 7.38; Found: C, 60.11; H, 7.57.

(S)-3,7-Dimethyloctyl 3-bromo-5-(3,3-diethyltriazenyl)-benzoate (52). To an oven-dried 50 mL round bottom flask was added **9** (2.01 g, 6.71 mmol), (*S*)-3,7-dimethyl-1-octanol (1.13 g, 7.16 mmol), *N,N'*-dimethylaminopyridine (0.25 g, 2.07 mmol) and dry CH₂Cl₂ (40 mL). The homogeneous, yellow solution was placed under a N₂ atmosphere and cooled in a 0 °C bath. Dicyclohexylcarbodiimide (2.82 g, 13.7 mmol) was added in one portion and the solution was stirred for 1 h at 0 °C, warmed to room temperature and stirred 15 h. The solution was cooled in a 0 °C ice bath, gravity filtered to remove the DCU and then concentrated in vacuo resulting in a yellow oil. The crude product was purified by silica gel column chromatography (hexanes/CH₂Cl₂, 2/1) to afford 2.77 g (6.33 mmol, 94%) of analytically pure **52** as a light yellow oil: ¹H NMR (400 MHz, CDCl₃) δ 7.97 (dd, *J* = 1.89, 1.52 Hz, 1H), 7.88 (dd, *J* = 1.93, 1.46 Hz, 1H), 7.75 (t, *J* = 1.87 Hz, 1H), 4.30-4.40 (m, 2H), 3.76-3.82 (m, 4H), 1.76-1.85 (m, 1H), 1.50-1.68 (m, 4H), 1.10-1.37 (m, 13H), 0.95 (d, *J* = 6.49 Hz, 3H), 0.86 (d, *J* = 6.54, 6H); ¹³C NMR (100 MHz, CDCl₃) δ 165.6, 152.6, 132.5, 128.3, 126.7, 122.5, 121.0, 63.9, 39.1, 37.1, 35.5, 29.9, 27.9, 24.6, 22.6, 22.5, 19.6; MS (FAB) *m/z* 440.2 (100), 442.2 (94.6); TLC R_f = 0.41

(hexanes/CH₂Cl₂, 2/1); Anal. Calcd for C₂₁H₃₄N₃O₂Br (440.42): C, 57.27; H, 7.78; N, 9.54. Found: C, 57.27; H, 7.80; N, 9.50.

(S)-3,7-Dimethyloctyl-3-trimethylsilylethynyl-benzoate (53). To a sealed tube fitted with a magnetic stirrer was added **51** (5.00 g, 14.65 mmol), Pd₂(dba)₃ (400 mg, 0.44 mmol), CuI (170 mg, 0.88 mmol), PPh₃ (1.0 g, 3.81 mmol), and dry triethylamine (50 mL). The mixture was evacuated and back-filled with nitrogen three times and dry, degassed trimethylsilylacetylene (12.9 mL, 77 mmol) was added. The tube was sealed and stirred at 75 °C for 60 h (during which time a white salt precipitate formed). The solution was diluted with hexanes (300 mL), filtered to remove the precipitate and concentrated in vacuo leaving a brown oil. The residue was purified by silica gel column chromatography (hexanes/CH₂Cl₂, 1/0, 4/1) to give 2.55 g (7.11 mmol, 49%) of analytically pure **53** as a colorless oil: ¹H NMR (400 MHz, CDCl₃) δ 8.12 (t, *J* = 1.73 Hz, 1H), 7.98 (dt, *J* = 7.78, 1.73 Hz, 1H), 7.63 (dt, *J* = 7.77, 1.73 Hz, 1H), 7.37 (t, *J* = 7.68 Hz, 1H), 4.40-4.30 (m, 2H), 1.82-1.78 (m, 1H), 1.61-1.50 (m, 3H), 1.36-1.13 (m, 6H), 0.95 (d, *J* = 6.5 Hz, 3H), 0.87 (d, *J* = 6.5 Hz, 3H), 0.87 (d, *J* = 6.5 Hz, 3H), 0.27 (s, 9H); ¹³C NMR (100 MHz, CDCl₃) δ 165.9, 136.0, 132.9, 130.6, 129.4, 128.2, 123.5, 103.9, 95.2, 39.1, 37.1, 35.5, 29.9, 27.9, 24.6, 22.7, 19.6, -0.2; MS (FAB) *m/z* 359.2 (30), 219.1 (33), 201.1 (100); TLC *R_f* = 0.07 (hexanes/CH₂Cl₂, 9/1); Anal. Calcd for C₂₂H₃₄O₂Si (358.60): C, 73.69; H, 9.56; Found: C, 73.54; H, 9.48.

(S)-3,7-Dimethyloctyl 3-(3,3-diethyltriazenyl)-5-trimethylsilylethynyl-benzoate (54). To a sealed tube fitted with a magnetic stirrer was added **52** (3.51 g, 7.97 mmol), Pd₂(dba)₃ (0.23 g, 0.25 mmol), copper iodide (0.09 g, 0.48 mmol), PPh₃ (0.54 g, 2.1 mmol) and dry triethylamine (40 mL). The mixture was evacuated and back-filled with nitrogen three times and dry, degassed trimethylsilylacetylene (2.5 mL, 14.2 mmol) was added. The tube was sealed and stirred at 70 °C for 22 h. After being cooled to rt, the contents of the flask were added to diethyl ether (100 mL). The insoluble amine salts were filtered off and the resulting solution was concentrated in vacuo to provide an orange oil. The crude product was purified by silica gel column chromatography (hexanes/CH₂Cl₂, 5/2) to afford 3.58 g (7.82 mmol, 98%) of analytically pure **54** as a light yellow oil: ¹H NMR (400 MHz, CDCl₃) δ 8.00 (dd, *J* = 1.89, 1.52 Hz, 1H), 7.87 (t, *J* = 1.87 Hz, 1H), 7.68 (dd, *J* = 1.93, 1.46 Hz, 1H), 4.30-4.40 (m, 2H), 3.76-3.82 (m, 4H), 1.76-1.85 (m, 1H), 1.50-1.68 (m, 4H), 1.10-1.37 (m, 13H), 0.95 (d, *J* = 6.51 Hz, 3H), 0.86 (d, *J* = 6.63 Hz, 6H), 0.25 (s, 3H); ¹³C NMR (100 MHz, CDCl₃) δ 166.1, 151.3, 131.2, 129.1, 127.5, 123.6, 122.0, 104.4, 94.2, 63.7, 39.1, 37.1, 35.5, 29.9, 27.9, 24.6, 22.7, 22.6, 19.6, -0.1; MS (FAB) *m/z* 458.3 (49), 318.2 (19); TLC *R_f* = 0.20 (hexanes/CH₂Cl₂, 2/1); Anal. Calcd for C₂₆H₄₃N₃O₂Si (457.73): C, 68.22; H, 9.47; N, 9.18. Found: C, 68.11; H, 9.53; N, 9.22.

(S)-3,7-Dimethyloctyl 3-ethynyl-benzoate (55). To a solution of **53** (2.32 g, 6.47 mmol) and THF (50 mL) was added a solution of tetrabutylammonium fluoride in wet THF (8.4 mL, 1.0 M). The solution was stirred for 1 minute, filtered through silica (eluting with hexanes/CH₂Cl₂, 1/1), and the solvent was removed in vacuo to leave a yellow oil. The crude acetylene was used without further purification.

(S)-3,7-Dimethyloctyl 3-(3,3-diethyltriazenyl)-5-ethynyl-benzoate (56). To a solution of **54** (2.58 g, 5.64 mmol) and THF (35 mL) was added a solution of tetrabutylammonium fluoride in wet THF (7.3 mL, 1.0 M). The solution was stirred for 1 minute, filtered through silica (eluting with hexanes/CH₂Cl₂, 1/1), and the solvent was removed in vacuo to leave a brown oil. The crude acetylene was used without further purification.

(S)-3,7-Dimethyloctyl 5-bromo-3-iodobenzoate (57). To an oven-dried 500 mL round bottom flask was added 3-bromo-5-iodobenzoic acid (12.0 g, 36.7 mmol), (*S*)-1-hydroxy-3,7-dimethyloctane (6.1 g, 39 mmol), *N,N'*-dimethylaminopyridine (1.35 g, 11.0 mmol) and dry CH₂Cl₂ (200 mL). The heterogeneous, yellow solution was placed under a N₂ atmosphere and cooled in a 0 °C bath. Dicyclohexylcarbodiimide (15.2 g, 73.4 mmol) was added in small portions and the solution was stirred for 1 h at 0 °C, warmed to room temperature and stirred 12 h. The solution was cooled in a 0 °C ice bath, gravity filtered to remove the DCU and then concentrated in vacuo resulting in a yellow oil. The crude product was purified by silica gel column chromatography (heptane/CH₂Cl₂, 1/0, 2/3) to afford 13.7 g (29.3 mmol, 80%) of analytically pure **57** as a colorless oil: ¹H NMR (400 MHz, CDCl₃) δ 8.29 (t, *J* = 1.5 Hz, 1H), 8.11 (dd, *J* = 1.8, 1.5 Hz, 1H), 8.03 (t, *J* = 1.8 Hz, 1H), 4.38-4.32 (m, 2H), 1.82-1.78 (m, 1H), 1.61-1.50 (m, 3H), 1.36-1.13 (m, 6H), 0.95 (d, *J* = 6.5 Hz, 3H), 0.87 (d, *J* = 6.5 Hz, 3H), 0.87 (d, *J* = 6.5 Hz, 3H); ¹³C NMR (100 MHz, CDCl₃) δ 163.9, 143.6, 137.1, 133.6, 131.9, 123.0, 94.0, 64.5, 39.1, 37.1, 35.4, 29.9, 27.9, 24.6, 22.7, 22.6, 19.6; MS (FAB) *m/z* 469.0 (29), 467.0 (33), 310.8 (41), 308.8 (41); TLC *R_f* = 0.30 (heptane/CH₂Cl₂, 2/3); Anal. Calcd for C₁₇H₂₄O₂BrI (467.19): C, 43.71; H, 5.18; Found: C, 43.80; H, 5.28.

H-[C]₂-Br (58). To a sealed tube fitted with a magnetic stirrer was added **55** (1.80 g, 6.3 mmol), **57** (4.2 g, 9.0 mmol), Pd₂(dba)₃ (127 mg, 0.13 mmol), CuI (50 mg, 0.26 mmol), PPh₃ (300 mg, 1.15 mmol), and dry triethylamine (30 mL). The mixture was evacuated and back-filled with nitrogen three times and heated at 55 °C for 36 h (during which time a white salt precipitate formed). The solution was diluted with hexanes (300 mL), filtered to remove the precipitate and concentrated in vacuo leaving a yellow residue. The residue was purified by silica gel column chromatography (hexanes/EtOAc, 1/0, 10/1) to give 3.81 g (6.09 mmol, 97%) of analytically pure **58** as a light yellow oil: ¹H NMR (400 MHz, CDCl₃) δ 8.21 (td, *J* = 1.69, 0.58 Hz, 1H), 8.14 (dd, *J* = 1.88, 1.56 Hz, 1H), 8.13 (t, *J* = 1.48 Hz, 1H), 8.05 (ddd, *J* = 7.83, 1.74, 1.19 Hz, 1H), 7.86 (dd, *J* = 1.90, 1.49 Hz, 1H), 7.71 (ddd, *J* = 7.72, 1.60, 1.28 Hz, 1H), 7.45 (td, *J* = 7.78, 0.62 Hz, 1H), 4.43-4.32 (m, 4H), 1.85-1.78 (m, 2H), 1.68-1.47 (m, 6H), 1.39-1.11 (m, 12H), 0.97 (d, *J* = 6.5 Hz, 3H), 0.95 (d, *J* = 6.5 Hz, 3H), 0.87 (m, 12H); ¹³C NMR (100 MHz, CDCl₃) δ 165.8, 164.7, 138.1, 135.7, 132.7, 132.5, 132.4, 131.2, 130.9, 129.8, 128.6, 125.1, 122.7, 122.2, 90.4, 87.6, 64.3, 63.9, 39.1, 37.1, 37.1, 35.5, 35.4, 29.9, 29.9, 27.9, 24.6, 22.7, 22.6, 19.6, 19.6; MS (FAB) *m/z* 626.2 (76), 624.2 (66); TLC R_f = 0.35 (hexanes/EtOAc, 20/1); Anal. Calcd for C₃₆H₄₉O₄Br (625.69): C, 69.11; H, 7.89; Found: C, 68.71; H, 7.87.

Et₂N₃-[C]₂-Br (59). To a sealed tube fitted with a magnetic stirrer was added **56** (2.16 g, 5.60 mmol), **57** (3.40 g, 7.28 mmol), Pd₂(dba)₃ (103 mg, 0.11 mmol), CuI (43 mg, 0.23 mmol), PPh₃ (265 mg, 1.00 mmol), and dry triethylamine (30 mL). The mixture was evacuated and back-filled with nitrogen three times and heated at 55 °C for 14 h (during which time a white salt precipitate formed). The solution was diluted with hexanes (250 mL), filtered to remove the precipitate and concentrated in vacuo leaving a brown residue. The residue was purified by silica gel column chromatography (hexanes/EtOAc, 1/0, 20/1) to give 2.57 g (3.55 mmol, 63%) of analytically pure **59** as a colorless oil: ¹H NMR (400 MHz, CDCl₃) δ 8.13 (t, *J* = 1.6 Hz, 1H), 8.12 (t, *J* = 1.4 Hz, 1H), 8.06 (dd, *J* = 1.9, 1.7 Hz, 1H), 7.93 (t, *J* = 1.5 Hz, 1H), 7.85 (t, *J* = 1.5 Hz, 1H), 7.76 (dd, *J* = 1.9, 1.6 Hz, 1H), 4.41-4.32 (m, 4H), 3.84-3.76 (q, 4H), 1.87-1.78 (m, 2H), 1.68-1.48 (m, 6H), 1.37-1.10 (m, 18H), 0.95 (d, *J* = 6.5 Hz, 3H), 0.95 (d, *J* = 6.5 Hz, 3H), 0.86 (d, *J* = 6.6 Hz, 6H); ¹³C NMR (100 MHz, CDCl₃) δ 166.1, 164.7, 151.5, 138.1, 132.4, 132.2, 131.5, 131.2, 128.9, 127.2, 125.3, 122.9, 122.5, 122.2, 91.1, 86.9, 64.3, 63.8, 39.1, 37.1, 37.0, 35.5, 35.4, 29.9, 29.9, 27.9, 24.6, 24.5, 22.7, 22.6, 19.6, 19.6; MS (FAB) *m/z* 726.3 (96), 724.3 (100); TLC R_f = 0.15 (hexanes/EtOAc, 33/1); Anal. Calcd for C₄₀H₅₈O₄N₃Br (724.83): C, 66.28; H, 8.07; N, 5.80; Found: C, 65.95; H, 8.16; N, 5.64.

H-[C]₂-SiMe₃ (60, [3 (*n* = 2)]). To a sealed tube fitted with a magnetic stirrer was added **58** (3.41 g, 5.45 mmol), Pd₂(dba)₃ (100 mg, 0.11 mmol), CuI (62 mg, 0.33 mmol), PPh₃ (373 mg, 1.42 mmol), and dry triethylamine (18 mL). The mixture was evacuated and back-filled with nitrogen three times and dry, degassed trimethylsilylacetylene (2.6 mL, 18.5 mmol) was added. The tube was sealed and stirred at 75 °C for 36 h (during which time a white precipitate formed). The solution was diluted with hexanes (300 mL), filtered to remove the precipitate and concentrated in vacuo leaving a yellow residue. The residue was purified by silica gel column chromatography (hexanes/CH₂Cl₂, 1/0, 1/1) to give 3.34 g (5.18 mmol, 95%) of analytically pure **60** as a colorless oil: ¹H NMR (400 MHz, CDCl₃) δ 8.18 (td, *J* = 1.65, 0.5 Hz, 1H), 8.12 (t, *J* = 1.6 Hz, 1H), 8.07 (t, *J* = 1.6 Hz, 1H), 8.03 (ddd, *J* = 7.9, 1.7, 1.2 Hz, 1H), 7.8 (t, *J* = 1.6 Hz, 1H), 7.70 (ddd, *J* = 7.7, 1.5, 1.2 Hz, 1H), 7.45 (td, *J* = 7.8, 0.6 Hz, 1H), 4.42-4.35 (m, 4H), 1.86-1.78 (m, 2H), 1.68-1.47 (m, 6H), 1.40-1.12 (m, 12H), 0.98 (d, *J* = 6.48 Hz, 3H), 0.97 (d, *J* = 6.47 Hz, 3H), 0.86 (m, 12H), 0.27 (s, 9H); ¹³C NMR (100 MHz, CDCl₃) δ 165.8, 165.2, 138.6, 135.6, 132.7, 132.6, 132.3, 131.1, 130.9, 129.6, 128.5, 124.0, 123.66, 123.0, 102.9, 96.2, 89.7, 88.3, 64.1, 63.9, 39.17, 39.15, 37.10, 37.09, 35.50, 35.48, 29.91, 29.87, 27.93, 24.59, 24.58, 22.68, 22.59, 19.62, 19.60, -0.2; MS (FAB) *m/z* 642 (53), 345 (68); TLC R_f = 0.05 (hexanes/CH₂Cl₂, 7/1); Anal. Calcd for C₄₁H₅₈O₄Si: C, 76.59; H, 9.09; Found: C, 76.27; H, 9.29.

Et₂N₃-[C]₂-SiMe₃ (61). To a sealed tube fitted with a magnetic stirrer was added **59** (8.40 g, 11.59 mmol), Pd₂(dba)₃ (176 mg, 0.19 mmol), CuI (132 mg, 0.70 mmol), PPh₃ (793 mg, 3.0 mmol), and dry triethylamine (70 mL). The mixture was evacuated and back-filled with nitrogen three times and dry, degassed trimethylsilylacetylene (12 mL, 84 mmol) was added. The tube was sealed and stirred at 75 °C for 72 h (during which time a white salt precipitate formed). The solution was diluted with hexanes (400 mL), filtered to remove the precipitate and concentrated in vacuo leaving a brown oil. The crude product was purified by silica gel column chromatography (hexanes/CH₂Cl₂, 1/0, 1/1) to give 6.45 g (8.69 mmol, 75%) of analytically pure **61** as a light brown oil: ¹H NMR (400 MHz, CDCl₃) δ 8.12 (t, *J* = 1.6 Hz, 1H), 8.06 (t, *J* = 1.6 Hz, 1H), 8.05 (dd, *J* = 2.0, 1.6 Hz, 1H), 7.93 (t, *J* = 1.6 Hz, 1H), 7.80 (t, *J* = 1.6 Hz, 1H), 7.75 (dd, *J* = 2.1, 1.5 Hz, 1H), 4.41-4.35 (m, 4H), 3.80 (q, *J* = 7.2 Hz, 4H), 1.87-1.78 (m, 2H), 1.69-1.45 (m, 6H), 1.42-1.11 (m, 18H), 0.98 (d, *J* = 6.5 Hz, 3H), 0.97 (d, *J* = 6.5 Hz, 3H), 0.85 (m, 12H) 0.26 (s, 9H); ¹³C NMR (100 MHz, CDCl₃) δ 166.1, 165.2, 151.5, 138.6, 132.4, 132.3, 131.4, 131.0, 128.8, 127.1, 123.9, 123.8, 123.1, 122.3, 103.0, 96.1, 90.3, 87.6, 64.1, 63.8,

39.16, 39.14, 37.12, 37.07, 35.52, 35.46, 29.90, 29.85, 27.9, 24.59, 24.56, 22.67, 22.58, 19.62, 19.60, -0.2; MS (FAB) m/z 742.4 (100); TLC R_f = 0.35 (hexanes/ CH_2Cl_2 , 1/1); Anal. Calcd for $\text{C}_{45}\text{H}_{67}\text{N}_3\text{O}_4\text{Si}$ (742.14): C, 72.83; H, 9.10; N, 5.66; Found: C, 72.62; H, 9.10; N, 5.46.

$\text{Et}_2\text{N}_3\text{-[C]}_4\text{-SiMe}_3$ (62). To a sealed tube fitted with a magnetic stirrer was added **68** (1.50 g, 1.95 mmol), **65** (1.30 g, 1.85 mmol), $\text{Pd}_2(\text{dba})_3$ (34 mg, 0.037 mmol), CuI (16 mg, 0.083 mmol), PPh_3 (80 mg, 0.31 mmol), and dry triethylamine (10 mL). The mixture was evacuated and back-filled with nitrogen three times. The tube was sealed and stirred at 65 °C for 15 h (during which time a white salt precipitate formed). The solution was diluted with hexanes (100 mL), filtered to remove the precipitate and concentrated in vacuo leaving a yellow oil. The crude product was purified by silica gel column chromatography (hexanes/EtOAc, 1/0, 20/1) to give 2.26 g (1.72 mmol, 93%) of **62** as a colorless oil: ^1H NMR (400 MHz, CDCl_3) δ 8.19 (t, J = 1.6 Hz, 1H), 8.18 (t, J = 1.7 Hz, 1H), 8.17 (t, J = 1.6 Hz, 2H), 8.14 (t, J = 1.5 Hz, 1H), 8.09 (t, J = 1.6 Hz, 1H), 8.06 (dd, J = 1.75, 1.67 Hz, 1H), 7.95 (t, J = 1.6 Hz, 1H), 7.88 (t, J = 1.6 Hz, 1H), 7.87 (t, J = 1.7 Hz, 1H), 7.81 (t, J = 1.6 Hz, 1H), 7.78 (dd, J = 1.9, 1.7 Hz, 1H), 4.44-4.35 (m, 8H), 3.81 (q, J = 7.2 Hz, 4H), 1.86-1.78 (m, 4H), 1.68-1.47 (m, 12H), 1.40-1.12 (m, 30H), 0.99-0.96 (m, 12H), 0.86 (m, 24H), 0.26 (s, 9H); ^{13}C NMR (100 MHz, CDCl_3) δ 166.1, 165.2, 165.1, 165.0, 151.5, 138.6, 138.2, 132.7, 132.5, 132.4, 132.3, 132.2, 131.4, 131.3, 131.2, 131.0, 128.9, 127.2, 124.1, 124.0, 123.6, 123.6, 123.4, 123.2, 123.1, 122.3, 102.9, 96.3, 90.6, 89.1, 89.1, 88.8, 88.7, 87.5, 64.21, 64.17, 64.12, 63.80, 39.17, 39.14, 37.12, 37.08, 35.56, 35.49, 31.55, 29.93, 29.91, 29.88, 27.91, 24.59, 24.56, 22.66, 22.62, 22.57, 22.47, 19.63, 19.59, 14.08, -0.3; MS (MALDI) m/z 1311.8 (calcd $[\text{M} + \text{H}]^+ = 1311.9$); TLC R_f = 0.10 (hexanes/ CH_2Cl_2 , 2/1); GPC 2884 (M_n), 1.04 (M_w/M_n), 96.4%.

$\text{Et}_2\text{N}_3\text{-[C]}_6\text{-SiMe}_3$ (63). To a sealed tube fitted with a magnetic stirrer was added **68** (1.25 g, 1.63 mmol), **66** (1.90 g, 1.54 mmol), $\text{Pd}_2(\text{dba})_3$ (28 mg, 0.03 mmol), CuI (13 mg, 0.07 mmol), PPh_3 (67 mg, 0.25 mmol), and dry triethylamine (12 mL). The mixture was evacuated and back-filled with nitrogen three times. The tube was sealed and stirred at 65 °C for 15 h. The solution was diluted with hexanes (150 mL), filtered to remove the precipitate and concentrated in vacuo leaving a yellow oil. The crude product was purified by silica gel column chromatography (hexanes/EtOAc, 1/0, 20/1) to give 2.71 g (1.44 mmol, 94%) of **63** as a colorless oil: ^1H NMR (400 MHz, CDCl_3) δ 8.20-8.15 (m, 8H), 8.12 (t, J = 1.6 Hz, 1H), 8.08 (t, J = 1.5 Hz, 1H), 8.06 (t, J = 1.6 Hz, 1H), 7.95 (t, J = 1.5 Hz, 1H), 7.90-7.85 (m, 4H), 7.81 (t, J = 1.6 Hz, 1H), 7.77 (t, J = 1.6 Hz, 1H), 4.46-4.35 (m, 12H), 3.80 (q, J = 7.2 Hz, 4H), 1.86-1.78 (m, 6H), 1.68-1.47 (m, 18H), 1.40-1.12 (m, 42H), 0.99-0.96 (m, 18H), 0.86 (m, 36H), 0.26 (s, 9H); MS (MALDI) m/z 1879.15 (calcd $[\text{M}]^+ = 1879.20$); TLC R_f = 0.20 (hexanes/ CH_2Cl_2 , 1/1); GPC 3786 (M_n), 1.04 (M_w/M_n), 97%.

$\text{Et}_2\text{N}_3\text{-[C]}_{12}\text{-SiMe}_3$ (64). To a sealed tube fitted with a magnetic stirrer was added **69** (750 mg, 0.39 mmol), **67** (677 mg, 0.38 mmol), $\text{Pd}_2(\text{dba})_3$ (7 mg, 0.008 mmol), CuI (3.2 mg, 0.017 mmol), PPh_3 (16 mg, 0.06 mmol), and dry triethylamine (8 mL). The mixture was evacuated and back-filled with nitrogen three times. The tube was sealed and stirred at 65 °C for 15 h. The solution was diluted with hexanes (100 mL), filtered to remove the precipitate and concentrated in vacuo leaving a yellow solid. The crude product was purified by silica gel column chromatography (hexanes/ CH_2Cl_2 , 1/0, 1/4) to give 960 mg (0.27 mmol, 71%) of **64** as an off-white solid: ^1H NMR (400 MHz, CDCl_3) δ 8.20-8.15 (m, 20H), 8.12 (t, J = 1.5 Hz, 1H), 8.08 (t, J = 1.5 Hz, 1H), 8.05 (t, J = 1.8 Hz, 1H), 7.95 (t, J = 1.5 Hz, 1H), 7.90-7.87 (m, 9H), 7.86 (t, J = 1.6 Hz, 1H), 7.81 (t, J = 1.6 Hz, 1H), 7.78 (dd, J = 2.0, 1.6 Hz, 1H), 4.46-4.33 (m, 24H), 3.80 (q, J = 7.2 Hz, 4H), 1.86-1.78 (m, 12H), 1.68-1.47 (m, 36H), 1.40-1.12 (m, 78H), 0.99-0.96 (m, 36H), 0.88-0.84 (m, 72H), 0.26 (s, 9H); MS (MALDI) m/z 3588.9 (calcd $[\text{M} + \text{H}]^+ = 3586.3$); TLC R_f = 0.15 (hexanes/ CH_2Cl_2 , 1/4); GPC 6092 (M_n), 1.04 (M_w/M_n), 100%.

$\text{Et}_2\text{N}_3\text{-[A]}_2\text{-H}$ (65). To a solution of **61** (1.37 g, 1.85 mmol) and THF (13 mL) was added a solution of tetrabutylammonium fluoride in wet THF (2.5 mL, 1.0 M). The solution was stirred for 1 minute, filtered through silica (eluting with CH_2Cl_2), and the solvent was removed in vacuo to leave a yellow oil. The crude product was used without further purification.

$\text{Et}_2\text{N}_3\text{-[A]}_4\text{-H}$ (66). To a solution of **62** (2.02 g, 1.54 mmol) and THF (10 mL) was added a solution of tetrabutylammonium fluoride in wet THF (2.0 mL, 1.0 M). The solution was stirred for 1 minute, filtered through silica (eluting with CH_2Cl_2), and the solvent was removed in vacuo to leave a yellow oil. The crude product was used without further purification.

$\text{Et}_2\text{N}_3\text{-[A]}_6\text{-H}$ (67). To a solution of **63** (800 mg, 0.43 mmol) and THF (5 mL) was added a solution of tetrabutylammonium fluoride in wet THF (0.55 mL, 1.0 M). The solution was stirred for 1 minute, filtered through silica (eluting with CH_2Cl_2), and the solvent was removed in vacuo to leave a yellow oil. The crude product was used without further purification.

I-[C]₂-SiMe₃ (68). To a 25 mL sealed tube was added **63** (2.00 g, 2.69 mmol), and iodomethane (15 mL). The mixture was degassed three times by evacuation, sealed and stirred at 110 °C for 14 h. The iodomethane was removed in vacuo to give a dark brown oil. The crude product was purified by silica gel column chromatography (hexanes/CH₂Cl₂, 1/0, 1/2) to give 1.86 g (2.42 mmol, 90%) of analytically pure **68** as a colorless oil: ¹H NMR (400 MHz, CDCl₃) δ 8.34 (t, *J* = 1.6 Hz, 1H), 8.13 (t, *J* = 1.5 Hz, 1H), 8.11 (t, *J* = 1.6 Hz, 1H), 8.09 (t, *J* = 1.6 Hz, 1H), 8.05 (t, *J* = 1.6 Hz, 1H), 7.80 (t, *J* = 1.6 Hz, 1H), 4.41-4.35 (m, 4H), 1.86-1.78 (m, 2H), 1.68-1.47 (m, 6H), 1.40-1.12 (m, 12H), 0.97 (d, *J* = 6.5 Hz, 3H), 0.96 (d, *J* = 6.5 Hz, 3H), 0.86 (m, 12H), 0.27 (s, 9H); ¹³C NMR (100 MHz, CDCl₃) δ 165.1, 164.4, 143.9, 138.7, 138.4, 132.9, 132.3, 132.2, 131.8, 131.1, 124.8, 124.0, 123.1, 102.8, 96.5, 93.3, 89.6, 88.0, 64.23, 64.18, 39.15, 37.09, 35.47, 35.44, 29.89, 29.87, 27.93, 24.58, 22.69, 22.60, 19.60, -0.2; MS (FAB) *m/z* 769.2 (6), 307.0 (15); TLC R_f = 0.45 (hexanes/CH₂Cl₂, 1/2); Anal. Calcd for C₄₁H₅₇O₄Si (768.40): C, 64.05; H, 7.47; Found: C, 63.81; H, 7.52.

I-[C]₆-SiMe₃ (69). To a 15 mL sealed tube was added **63** (1.00 g, 0.53 mmol), and iodomethane (4 mL). The mixture was degassed three times by evacuation, sealed and stirred at 110 °C for 14 h. The iodomethane was removed in vacuo to give a dark brown oil. The crude product was purified by silica gel column chromatography (hexanes EtOAc, 1/0, 33/1) to give 922 mg (0.484 mmol, 91%) of **69** as a waxy, white solid: ¹H NMR (400 MHz, CDCl₃) δ 8.35 (t, *J* = 1.5 Hz, 1H), 8.19-8.15 (m, 9H), 8.13 (t, *J* = 1.4 Hz, 1H), 8.09 (t, *J* = 1.4 Hz, 1H), 8.08 (t, *J* = 1.4 Hz, 1H), 7.91 (t, *J* = 1.6 Hz, 2H), 7.89-7.87 (m, 2H), 7.81 (t, *J* = 1.5 Hz, 1H), 4.44-4.35 (m, 12H), 1.86-1.78 (m, 6H), 1.68-1.47 (m, 18H), 1.40-1.12 (m, 36H), 0.99-0.96 (m, 18H), 0.86 (m, 36H), 0.27 (s, 9H); MS (FAB) *m/z* 1906.3 (28); TLC R_f = 0.25 (hexanes/CH₂Cl₂, 1/1); GPC 3689 (M_n), 1.04 (M_w/M_n), 100%.

I-[C]₁₂-SiMe₃ (70). To a 25 mL sealed tube was added **64** (900 mg, 0.25 mmol), and iodomethane (8 mL). The mixture was degassed three times by evacuation, sealed and stirred at 110 °C for 14 h. The iodomethane was removed in vacuo to give a dark brown oil. The crude product was purified by silica gel column chromatography (hexanes/CH₂Cl₂, 9/1, 1/2) to give 819 mg (0.23 mmol, 90%) of **70** as a white solid: ¹H NMR (400 MHz, CDCl₃) δ 8.34 (t, *J* = 1.6 Hz, 1H), 8.20-8.14 (m, 21H), 8.12 (t, *J* = 1.6 Hz, 1H), 8.08 (t, *J* = 1.6 Hz, 1H), 8.06 (t, *J* = 1.6 Hz, 1H), 7.91-7.88 (m, 8H), 7.86 (m, 2H), 7.81 (t, *J* = 1.6 Hz, 1H), 4.46-4.33 (m, 24H), 1.90-1.78 (m, 12H), 1.70-1.47 (m, 36H), 1.40-1.12 (m, 72H), 0.99-0.96 (m, 36H), 0.88-0.84 (m, 72H), 0.27 (s, 9H); MS (MALDI) *m/z* 3636.5 (calcd [M + Na]⁺ = 3636.1); TLC R_f = 0.15 (hexanes/CH₂Cl₂, 1/1); GPC 6004 (M_n), 1.04 (M_w/M_n), 100%.

H-[C]₄-SiMe₃ (71, [3 (*n* = 4)]). To a sealed tube fitted with a magnetic stirrer was added **68** (875 mg, 1.14 mmol), **79** (620 mg, 1.08 mmol), Pd₂(dba)₃ (20 mg, 0.02 mmol), CuI (9.2 mg, 0.05 mmol), PPh₃ (47 mg, 0.18 mmol), and dry triethylamine (6 mL). The mixture was evacuated and back-filled with nitrogen three times. The tube was sealed and stirred at 65 °C for 36 h (during which time a white salt precipitate formed). The solution was diluted with hexanes (50 mL), filtered to remove the precipitate and concentrated in vacuo leaving a yellow oil. The crude product was purified by silica gel column chromatography (hexanes/CH₂Cl₂, 2/1, 1/1) to give 1.07 g (0.88 mmol, 82%) of **71** as a colorless oil: ¹H NMR (400 MHz, CDCl₃) δ 8.22 (td, *J* = 1.6, 0.48 Hz, 1H), 8.19-8.16 (m, 4H), 8.12 (t, *J* = 1.6 Hz, 1H), 8.09 (t, *J* = 1.6 Hz, 1H), 8.03 (ddd, *J* = 7.8, 1.7, 1.2 Hz, 1H), 7.88 (t, *J* = 1.6 Hz, 1H), 7.86 (t, *J* = 1.6 Hz, 1H), 7.81 (t, *J* = 1.6 Hz, 1H), 7.72 (ddd, *J* = 7.7, 1.6, 1.3 Hz, 1H), 7.46 (td, *J* = 7.7, 0.55 Hz, 1H), 4.44-4.35 (m, 8H), 1.86-1.78 (m, 4H), 1.68-1.47 (m, 12H), 1.40-1.12 (m, 24H), 0.99-0.96 (m, 12H), 0.86 (m, 24H), 0.27 (s, 9H); ¹³C NMR (100 MHz, CDCl₃) δ 165.7, 165.1, 165.0, 165.0, 138.7, 138.2, 138.2, 135.7, 135.7, 132.8, 132.7, 132.6, 132.5, 132.4, 132.3, 132.3, 131.4, 131.3, 131.2, 130.9, 129.7, 129.7, 128.6, 128.5, 124.1, 123.9, 123.7, 123.6, 123.5, 123.2, 122.9, 102.9, 96.4, 89.9, 89.2, 89.1, 88.9, 88.8, 88.3, 64.23, 64.24, 64.15, 63.90, 39.19, 39.17, 37.13, 37.11, 35.54, 35.52, 31.61, 29.94, 29.91, 29.89, 29.87, 27.95, 24.62, 22.71, 22.67, 22.62, 22.49, 19.66, 19.64, 14.14, -0.2; MS (FAB) *m/z* 1211.7 (2), 1053.5 (2); TLC R_f = 0.15 (hexanes/CH₂Cl₂, 2/1). Anal. Calcd for C₇₉H₁₀₆O₈Si: C, 78.30; H, 8.82; Found: C, 78.28; H, 8.75; GPC 2782 (M_n), 1.04 (M_w/M_n), 99.4%.

H-[C]₆-SiMe₃ (72, [3 (*n* = 6)]). To a sealed tube fitted with a magnetic stirrer was added **68** (312 mg, 0.41 mmol), **80** (440 mg, 0.39 mmol), Pd₂(dba)₃ (7.0 mg, 0.008 mmol), CuI (3.4 mg, 0.017 mmol), PPh₃ (17 mg, 0.064 mmol), and dry triethylamine (4 mL). The mixture was evacuated and back-filled with nitrogen three times. The tube was sealed and stirred at 65 °C for 14 h (during which time a white salt precipitate formed). The solution was diluted with hexanes (30 mL), filtered to remove the precipitate and concentrated in vacuo leaving a yellow oil. The crude product was purified by silica gel column chromatography (hexanes/CH₂Cl₂, 1/0, 1/2) to give 657 mg (0.37 mmol, 96%) of **72** as a light yellow oil: ¹H NMR (400 MHz, CDCl₃) δ 8.21 (td, *J* = 1.68, 0.47 Hz, 1H), 8.20-8.15 (m, 7H), 8.12 (t, *J* = 1.7 Hz, 1H), 8.08 (t, *J* = 1.7 Hz, 1H), 8.03 (ddd, *J* = 7.8,

1.64, 1.14 Hz, 1H), 7.90-7.88 (m, 4H), 7.88 (t, $J = 1.6$ Hz, 1H), 7.81 (t, $J = 1.6$ Hz, 1H), 7.72 (ddd, $J = 7.7, 1.58, 1.26$ Hz, 1H), 7.46 (td, $J = 7.83, 0.55$ Hz, 1H), 4.44-4.35 (m, 12H), 1.86-1.78 (m, 6H), 1.68-1.47 (m, 18H), 1.40-1.12 (m, 36H), 0.99-0.96 (m, 18H), 0.86 (m, 36H), 0.27 (s, 9H); MS (MALDI) m/z 1781.3 (calcd $[M + H]^+ = 1781.1$); TLC $R_f = 0.25$ (hexanes/ CH_2Cl_2 , 1/1); GPC 3728 (M_n), 1.03 (M_w/M_n), 98.7%.

H-[C]₈-SiMe₃ (73, [3 ($n = 8$))). To a sealed tube fitted with a magnetic stirrer was added **79** (92 mg, 0.16 mmol), **69** (213 mg, 0.11 mmol), Pd₂(dba)₃ (11 mg, 0.012 mmol), CuI (6 mg, 0.034 mmol), PPh₃ (36 mg, 0.098 mmol) and dry triethylamine (6 mL). The mixture was evacuated and back-filled with nitrogen three times. The tube was sealed and stirred at 70 °C for 18 h. The solution was diluted with hexanes (50 mL), filtered to remove the precipitate and concentrated in vacuo leaving a yellow solid. The crude product was purified by silica gel column chromatography (hexanes/ CH_2Cl_2 , 1/0, 1/1) and size exclusion chromatography (toluene) to give 152 mg (0.065 mmol, 58%) of **73** as a white solid: ¹H NMR (400 MHz, CDCl₃) δ 8.21 (td, $J = 1.6, 0.5$ Hz, 1H), 8.20-8.15 (m, 11H), 8.13 (t, $J = 1.7$ Hz, 1H), 8.09 (t, $J = 1.7$ Hz, 1H), 8.04 (ddd, $J = 7.8, 1.6, 1.1$ Hz, 1H), 7.91-7.88 (m, 6H), 7.87 (t, $J = 1.6$ Hz, 1H), 7.82 (t, $J = 1.6$ Hz, 1H), 7.72 (ddd, $J = 7.7, 1.6, 1.3$ Hz, 1H), 7.46 (td, $J = 7.8, 0.6$ Hz, 1H), 4.46-4.34 (m, 16H), 1.86-1.78 (m, 8H), 1.68-1.47 (m, 24H), 1.40-1.12 (m, 48H), 0.99-0.96 (m, 24H), 0.86 (m, 48H), 0.27 (s, 9H); MS (MALDI) m/z 2371.78 (calcd $[M + Na]^+ = 2371.42$); TLC $R_f = 0.20$ (hexanes/ CH_2Cl_2 , 1/1); GPC 4552 (M_n), 1.03 (M_w/M_n), 100%.

H-[C]₁₀-SiMe₃ (74, [3 ($n = 10$))). To a sealed tube fitted with a magnetic stirrer was added **69** (180 mg, 0.094 mmol), **80** (129 mg, 0.113 mmol), Pd₂(dba)₃ (8.6 mg, 0.009 mmol), CuI (4.3 mg, 0.02 mmol), PPh₃ (21 mg, 0.08 mmol), and dry triethylamine (4 mL). The mixture was evacuated and back-filled with nitrogen three times. The tube was sealed and stirred at 65 °C for 15 h. The solution was diluted with hexanes (50 mL), filtered to remove the precipitate and concentrated in vacuo leaving a yellow solid. The crude product was purified by silica gel column chromatography (hexanes/ CH_2Cl_2 , 1/0, 1/1) and size exclusion chromatography (toluene) to give 244 mg (0.085 mmol, 90%) of **74** as a white wax: ¹H NMR (400 MHz, CDCl₃) δ 8.21 (td, $J = 1.6, 0.4$ Hz, 1H), 8.21-8.16 (m, 15H), 8.12 (t, $J = 1.7$ Hz, 1H), 8.08 (t, $J = 1.6$ Hz, 1H), 8.03 (ddd, $J = 7.9, 1.7, 1.2$ Hz, 1H), 7.91-7.88 (m, 8H), 7.86 (t, $J = 1.6$ Hz, 1H), 7.81 (t, $J = 1.6$ Hz, 1H), 7.71 (ddd, $J = 7.7, 1.6, 1.3$ Hz, 1H), 7.45 (td, $J = 7.8, 0.6$ Hz, 1H), 4.46-4.34 (m, 20H), 1.88-1.78 (m, 10H), 1.68-1.47 (m, 30H), 1.40-1.12 (m, 60H), 0.99-0.96 (m, 30H), 0.88-0.84 (m, 60H), 0.27 (s, 9H); MS (MALDI) m/z 2940.9 (calcd $[M + Na]^+ = 2940.8$); TLC $R_f = 0.15$ (hexanes/ CH_2Cl_2 , 1/1); GPC 5298 (M_n), 1.03 (M_w/M_n), 100%.

H-[C]₁₂-SiMe₃ (75, [3 ($n = 12$))). To a sealed tube fitted with a magnetic stirrer was added **69** (186 mg, 0.098 mmol), **81** (204 mg, 0.119 mmol), Pd₂(dba)₃ (8.6 mg, 0.01 mmol), CuI (4.2 mg, 0.02 mmol), PPh₃ (21 mg, 0.08 mmol), and dry triethylamine (5 mL). The mixture was evacuated and back-filled with nitrogen three times. The tube was sealed and stirred at 65 °C for 18 h. The solution was diluted with hexanes (80 mL), filtered to remove the precipitate and concentrated in vacuo leaving a yellow solid. The crude product was purified by silica gel column chromatography (hexanes/ CH_2Cl_2 , 2/1, 2/3) and size exclusion chromatography (toluene) to give 217 mg (0.062 mmol, 64%) of **75** as a white solid: ¹H NMR (400 MHz, CDCl₃) δ 8.21 (td, $J = 1.7, 0.4$ Hz, 1H), 8.21-8.16 (m, 19H), 8.12 (t, $J = 1.8$ Hz, 1H), 8.08 (t, $J = 1.6$ Hz, 1H), 8.03 (ddd, $J = 7.7, 1.7, 1.2$ Hz, 1H), 7.91-7.88 (m, 10H), 7.86 (t, $J = 1.6$ Hz, 1H), 7.81 (t, $J = 1.6$ Hz, 1H), 7.72 (ddd, $J = 7.7, 1.6, 1.3$ Hz, 1H), 7.45 (td, $J = 7.8, 0.6$ Hz, 1H), 4.46-4.34 (m, 24H), 1.90-1.78 (m, 12H), 1.68-1.47 (m, 36H), 1.40-1.12 (m, 72H), 0.99-0.96 (m, 36H), 0.88-0.84 (m, 72H), 0.27 (s, 9H); MS (MALDI) m/z 3510.56 (calcd $[M + Na]^+ = 3510.18$); TLC $R_f = 0.15$ (hexanes/ CH_2Cl_2 , 1/1); GPC 6075 (M_n), 1.04 (M_w/M_n), 100%.

H-[C]₁₄-SiMe₃ (76, [3 ($n = 14$))). To a sealed tube fitted with a magnetic stirrer was added **79** (58 mg, 0.10 mmol), **70** (212 mg, 0.06 mmol), Pd₂(dba)₃ (6.5 mg, 0.007 mmol), CuI (2.9 mg, 0.015 mmol), PPh₃ (21 mg, 0.08 mmol) and dry triethylamine (7 mL). The mixture was evacuated and back-filled with nitrogen three times. The tube was sealed and stirred at 70 °C for 23 h. The solution was diluted with hexanes (100 mL), filtered to remove the precipitate and concentrated in vacuo leaving a yellow solid. The crude product was purified by silica gel column chromatography (hexanes/ CH_2Cl_2 , 2/1, 2/3) and size exclusion chromatography (toluene) to give 179 mg (0.044 mmol, 75%) of **76** as a white solid: ¹H NMR (400 MHz, CDCl₃) δ 8.21 (td, $J = 1.7, 0.4$ Hz, 1H), 8.20-8.15 (m, 24H), 8.12 (t, $J = 1.8$ Hz, 1H), 8.08 (t, $J = 1.6$ Hz, 1H), 8.03 (ddd, $J = 7.7, 1.7, 1.2$ Hz, 1H), 7.90-7.88 (m, 11H), 7.86 (t, $J = 1.6$ Hz, 1H), 7.81 (t, $J = 1.6$ Hz, 1H), 7.71 (ddd, $J = 7.7, 1.6, 1.3$ Hz, 1H), 7.45 (td, $J = 7.8, 0.6$ Hz, 1H), 4.46-4.33 (m, 28H), 1.90-1.78 (m, 14H), 1.70-1.47 (m, 42H), 1.40-1.12 (m, 84H), 0.99-0.96 (m, 42H), 0.88-0.84 (m, 84H), 0.27 (s, 9H); MS (MALDI) m/z 4077.87 (calcd $[M + Na]^+ = 4078.54$); TLC $R_f = 0.20$ (hexanes/ CH_2Cl_2 , 1/2); GPC 6807 (M_n), 1.04 (M_w/M_n), 100%.

H-[C]₁₆-SiMe₃ (77, [3 ($n = 16$))). To a sealed tube fitted with a magnetic stirrer was added **80** (89 mg, 0.08 mmol), **70** (199 mg, 0.055 mmol), Pd₂(dba)₃ (9.3 mg, 0.01 mmol), CuI (3.6 mg, 0.02 mmol), PPh₃ (27 mg, 0.10

mmol) and dry triethylamine (7 mL). The mixture was evacuated and back-filled with nitrogen three times. The tube was sealed and stirred at 70 °C for 21 h. The solution was diluted with hexanes (80 mL), filtered to remove the precipitate and concentrated in vacuo leaving a yellow solid. The crude product was purified by silica gel column chromatography (hexanes/CH₂Cl₂, 2/1, 2/3) and size exclusion chromatography (toluene) to give 159 mg (0.034 mmol, 62%) of **77** as a white solid: ¹H NMR (400 MHz, CDCl₃) δ 8.21 (td, *J* = 1.7, 0.4 Hz, 1H), 8.20-8.15 (m, 28H), 8.13 (t, *J* = 1.8 Hz, 1H), 8.08 (t, *J* = 1.6 Hz, 1H), 8.04 (ddd, *J* = 7.7, 1.7, 1.2 Hz, 1H), 7.90-7.88 (m, 13H), 7.86 (t, *J* = 1.6 Hz, 1H), 7.81 (t, *J* = 1.6 Hz, 1H), 7.71 (ddd, *J* = 7.7, 1.6, 1.3 Hz, 1H), 7.45 (td, *J* = 7.8, 0.6 Hz, 1H), 4.46-4.33 (m, 32H), 1.90-1.78 (m, 16H), 1.70-1.47 (m, 48H), 1.40-1.12 (m, 96H), 0.99-0.96 (m, 48H), 0.88-0.84 (m, 96H), 0.27 (s, 9H); MS (MALDI) *m/z* 4644.2 (calcd [M + Na]⁺ = 4646.90); TLC R_f = 0.25 (hexanes/CH₂Cl₂, 1/2); GPC 7493 (M_n), 1.03 (M_w/M_n), 99.8%.

H-[C]₁₈-SiMe₃ (78, [3 (n = 18)]). To a sealed tube fitted with a magnetic stirrer was added **81** (126 mg, 0.074 mmol), **70** (196 mg, 0.054 mmol), Pd₂(dba)₃ (2.9 mg, 0.003 mmol), CuI (1.1 mg, 0.006 mmol), PPh₃ (69 mg, 0.026 mmol) and dry triethylamine (8 mL). The mixture was evacuated and back-filled with nitrogen three times. The tube was sealed and stirred at 70 °C for 18 h. The solution was diluted with hexanes (90 mL), filtered to remove the precipitate and concentrated in vacuo leaving a yellow solid. The crude product was purified by silica gel column chromatography (hexanes/CH₂Cl₂, 2/1, 2/3) and size exclusion chromatography (toluene) to give 192 mg (0.037 mmol, 68%) of **78** as a white solid: ¹H NMR (400 MHz, CDCl₃) δ 8.22 (td, *J* = 1.7, 0.4 Hz, 1H), 8.21-8.16 (m, 32H), 8.13 (t, *J* = 1.8 Hz, 1H), 8.09 (t, *J* = 1.6 Hz, 1H), 8.05 (ddd, *J* = 7.7, 1.7, 1.2 Hz, 1H), 7.92-7.90 (m, 15H), 7.88 (t, *J* = 1.6 Hz, 1H), 7.82 (t, *J* = 1.6 Hz, 1H), 7.73 (ddd, *J* = 7.7, 1.6, 1.3 Hz, 1H), 7.45 (td, *J* = 7.8, 0.6 Hz, 1H), 4.46-4.33 (m, 36H), 1.90-1.78 (m, 18H), 1.70-1.47 (m, 54H), 1.40-1.12 (m, 108H), 0.99-0.96 (m, 54H), 0.88-0.84 (m, 108H), 0.27 (s, 9H); MS (MALDI) *m/z* 5214.6 (calcd [M + Na]⁺ = 5216.26); TLC R_f = 0.30 (hexanes/CH₂Cl₂, 1/2); GPC 8207 (M_n), 1.03 (M_w/M_n), 100%.

H-[A]₂-H (79). To a solution of **60** (0.71 g, 1.10 mmol) and THF (7 mL) was added a solution of tetrabutylammonium fluoride in wet THF (1.4 mL, 1.0 M). The solution was stirred for 1 minute, filtered through silica (eluting with hexanes/CH₂Cl₂, 1/1), and the solvent was removed in vacuo to leave a yellow oil. The crude product was used without further purification.

H-[A]₄-H (80). To a solution of **71** (0.35 g, 0.29 mmol) and THF (4 mL) was added a solution of tetrabutylammonium fluoride in wet THF (0.38 mL, 1.0 M). The solution was stirred for 1 minute, filtered through silica (eluting with CH₂Cl₂), and the solvent was removed in vacuo to leave a yellow oil. The crude product was used without further purification.

H-[A]₆-H (81). To a solution of **72** (414 mg, 0.23 mmol) and THF (10 mL) was added a solution of tetrabutylammonium fluoride in wet THF (0.4 mL, 1.0 M). The solution was stirred for 1 minute, filtered through silica (eluting with CH₂Cl₂), and the solvent was removed in vacuo to leave a light yellow oil. The crude product was used without further purification.

6.8 References and notes

- ¹ Gellman, S. H. *Acc. Chem. Res.* **1998**, *31*, 173-180.
- ² Kirshenbaum, K.; Zuckermann, R.N.; Dill, K.A. *Curr. Opin. Struct. Biol.* **1999**, *9*, 530-535.
- ³ Berl, V.; Krische, M.J.; Huc, I.; Lehn, J.-M.; Schmutz, M. *Chem. Eur. J.* **2000**, *6*, 1938-1946.
- ⁴ Cuccia, L.A.; Lehn, J.-M.; Homo, J.-C.; Schmutz, M. *Angew. Chem. Int. Ed.* **2000**, *39*, 233-237.
- ⁵ Huck, B.R.; Fisk, J.D.; Gellman, S.H. *Org. Lett.* **2000**, *2*, 2607-2610.
- ⁶ Sifferlen, T.; Rueping, M.; Gademann, K.; Jaun, B.; Seebach, D. *Helv. Chim. Acta* **1999**, *82*, 2067-2093.
- ⁷ Hirschberg, J.H.K.K.; Brunsveld, L.; Ramzi, A.; Vekemans, J.A.J.M.; Sijbesma, R.P.; Meijer, E.W. *Nature* **2000**, *407*, 167-170.
- ⁸ Appella, D.H.; Christianson, L.A.; Karle, I.L.; Powell, D.R.; Gellman, S.H. *J. Am. Chem. Soc.* **1999**, *121*, 6206-6212.
- ⁹ Armand, P.; Kirshenbaum, K.; Goldsmith, R.A.; Farr-Jones, S.; Barron, A.E.; Truong, K.T.V.; Dill, K.A.; Mierke, D.F.; Cohen, F.E.; Zuckermann, R.N.; Bradley, E.K. *Proc. Natl. Acad. Sci. U. S. A.* **1998**, *95*, 4309-4314.
- ¹⁰ Gademann, K.; Jaun, B.; Seebach, D.; Perozzo, R.; Scapozza, L.; Folkers, G. *Helv. Chim. Acta* **1999**, *82*, 1-11.
- ¹¹ Seebach, D.; Sifferlen, T.; Mathieu, P.A.; Hane, A.M.; Krell, C.M.; Bierbaum, D.J.; Abele, S. *Helv. Chim. Acta* **2000**, *83*, 2849-2864.
- ¹² Schreiber, J.V.; Seebach, D. *Helv. Chim. Acta* **2000**, *83*, 3139-3152.
- ¹³ Barchi, J.J., Jr.; Huang, X.; Appella, D.H.; Christianson, L.A.; Durell, S.R.; Gellman, S.H. *J. Am. Chem. Soc.* **2000**, *122*, 2711-2718.
- ¹⁴ Seebach, D.; Abele, S.; Gademann, K.; Jaun, B. *Angew. Chem., Int. Ed.* **1999**, *38*, 1595-1597.
- ¹⁵ Nelson, J. C.; Saven, J. G.; Moore, J. S.; Wolynes, P. G. *Science* **1997**, *277*, 1793-1796.
- ¹⁶ Prince, R. B.; Saven, J. G.; Wolynes, P. G.; Moore, J. S. *J. Am. Chem. Soc.* **1999**, *121*, 3114-3121.
- ¹⁷ Appella, D.H.; Barchi, J.J., Jr.; Durell, S.R.; Gellman, S.H. *J. Am. Chem. Soc.* **1999**, *121*, 2309-2310.
- ¹⁸ Lokey, R.S.; Iverson, B.L. *Nature* **1995**, *375*, 303-305.
- ¹⁹ Lokey, R.S.; Kwok, Y.; Guelev, V.; Pursel, C.J.; Hurley, L.H.; Iverson, B.L. *J. Am. Chem. Soc.* **1997**, *119*, 7202-7210.
- ²⁰ Kirshenbaum, K.; Barron, A.E.; Goldsmith, R.A.; Armand, P.; Bradley, E.K.; Truong, K.T.V.; Dill, K.A.; Cohen, F.E.; Zuckermann, R.N. *Proc. Natl. Acad. Sci. U. S. A.* **1998**, *95*, 4303-4308.
- ²¹ Seebach, D.; Jacobi, A.; Rueping, M.; Gademann, K.; Ernst, M.; Jaun, B. *Helv. Chim. Acta* **2000**, *83*, 2115-2140.
- ²² Wang, X.; Espinosa, J.F.; Gellman, S.H. *J. Am. Chem. Soc.* **2000**, *122*, 4821-4822.
- ²³ Fisk, J.D.; Gellman, S.H. *J. Am. Chem. Soc.* **2001**, *123*, 343-344.
- ²⁴ Seebach, D.; Matthews, J.L. *Chem. Commun.* **1997**, 2015-2022.
- ²⁵ Sheu, E.Y.; Liang, K.S.; Chiang, L.Y. *J. Phys. France* **1989**, *50*, 1279-1295.
- ²⁶ Bonazzi, S.; Capobianco, M.; DeMorais, M.M.; Garbesi, A.; Gottarelli, G.; Mariani, P.; Ponzi Bossi, M.G.; Spada, G.P.; Tondelli, L. *J. Am. Chem. Soc.* **1991**, *113*, 5809-5816.
- ²⁷ Markovitsi, D.; Bengs, H.; Pfeffer, N.; Charra, F.; Nunzi, J.-M.; Ringsdorf, H. *J. Chem. Soc. Faraday Trans.* **1993**, *89*, 37-42.
- ²⁸ Bonazzi, S.; DeMorais, M.M.; Gottarelli, G.; Mariani, P.; Spada, G.P. *Angew. Chem. Int. Ed. Engl.* **1993**, *32*, 248-250.
- ²⁹ Gallivan, J.P.; Schuster, G.B. *J. Org. Chem.* **1995**, *60*, 2423-2429.
- ³⁰ Boden, N.; Bushby, R.J.; Clements, J.; Movaghar, B.; Donovan, K.J.; Kreozis, T. *Phys. Rev. B* **1995**, *52*, 13274-13280.
- ³¹ van Nostrum, C.F.; Nolte, R.J.M. *Chem. Commun.* **1996**, 2385-2392.
- ³² Shetty, A.S.; Zhang, J.; Moore, J.S. *J. Am. Chem. Soc.* **1996**, *118*, 1019-1027.
- ³³ Proni, G.; Spada, G.P.; Gottarelli, G.; Ciuchi, F.; Mariani, P. *Chirality* **1998**, *10*, 734-741.
- ³⁴ Kraft, A.; Osterod, F.; Fröhlich, R. *J. Org. Chem.* **1999**, *64*, 6425-6433.
- ³⁵ Forman, S.L.; Fettinger, J.C.; Pieraccini, S.; Gottarelli, G.; Davis, J.T. *J. Am. Chem. Soc.* **2000**, *122*, 4060-4067.
- ³⁶ Palmans, A.R.A.; Vekemans, J.A.J.M.; Havinga, E.E.; Meijer, E.W. *Angew. Chem. Int. Ed. Engl.* **1997**, *36*, 2648-2651.
- ³⁷ Brunsveld, L.; Schenning, A.P.H.J.; Broeren, M.A.C.; Janssen, H.M.; Vekemans, J.A.J.M.; Meijer, E.W. *Chem. Lett.* **2000**, 292-293.

- 38 Brunsveld, L.; Zhang, H.; Glasbeek, M.; Vekemans, J.A.J.M.; Meijer, E.W. *J. Am. Chem. Soc.* **2000**, *122*, 6175-6182.
- 39 van der Schoot, P.; Michels, M.A.J.; Brunsveld, L.; Sijbesma, R.P.; Ramzi, A. *Langmuir* **2000**, *16*, 10076-10083.
- 40 van Nostrum, D.F.; Picken, S.J.; Nolte, R.J.M. *Angew. Chem. Int. Ed. Engl.* **1994**, *33*, 2173-2175.
- 41 Yasuda, Y.; Iishi, E.; Inada, H.; Shirota, Y. *Chem. Lett.* **1996**, 575-576.
- 42 Osburn, E.J.; Schmidt, A.; Chau, L.-K.; Chen, S.Y.; Smolenyak, P.; Armstrong, N.R.; O'Brien, D.F. *Adv. Mater.* **1996**, *8*, 926-928.
- 43 Yasuda, Y.; Takebe, Y.; Fukumoto, M.; Inada, H.; Shirota, Y. *Adv. Mater.* **1996**, *8*, 740-741.
- 44 Hanabusa, K.; Kawakami, A.; Kimura, M.; Shirai, H. *Chem. Lett.* **1997**, 191-192.
- 45 Hanabusa, K.; Koto, C.; Kimura, M.; Shirai, H.; Kakehi, A. *Chem. Lett.* **1997**, 429-430.
- 46 Engelkamp, H.; Middelbeek, S.; Nolte, R.J.M. *Science* **1999**, *284*, 785-788.
- 47 Prince, R.B.; Okada, T.; Moore, J.S. *Angew. Chem., Int. Ed.* **1999**, *38*, 233-236.
- 48 Gin, M. S.; Yokozawa, T.; Prince, R. B.; Moore, J. S. *J. Am. Chem. Soc.* **1999**, *121*, 2643-2644.
- 49 Prince, R.B.; Barnes, S.A.; Moore, J.S. *J. Am. Chem. Soc.* **2000**, *122*, 2758-2762.
- 50 Of course, no ellipticity could be detected for any of the achiral oligomers of series **1** under conditions where it has been previously shown that the helical conformation is stable, due to the equal presence of left and right handed helices.
- 51 All measurements were determined to be independent of time.
- 52 Shakhnovich, E.I.; Finkelstein, A.V. *Biopolymers* **1989**, *28*, 1667-1680.
- 53 Finkelstein, A.V.; Shakhnovich, E.I. *Biopolymers* **1989**, *28*, 1681-1694.
- 54 Dill, K.A.; Stigter, D. *Advances in Protein Chemistry* **1995**, *46*, 59-104.
- 55 Pino, P.; Ciardelli, F.; Montagnoli, G.; Pieroni, O. *Pol. Lett.* **1967**, *5*, 307-311.
- 56 Carlini, C.; Ciardelli, F.; Pino, P. *Makromol. Chem.* **1968**, *119*, 244-248.
- 57 Farina, M. *Top. Stereochem.* Eds. Eliel, E.L.; Wilen, S.H. New York: John Wiley & Sons **1987**, *17*, 1-111.
- 58 Moore, J.S.; Gorman, C.B.; Grubbs, R.H. *J. Am. Chem. Soc.* **1991**, *113*, 1704-1712.
- 59 Okamoto, Y.; Nakano, T. *Chem. Rev.* **1994**, *94*, 349-372.
- 60 Fujiki, M. *Polym. Prepr.* **1996**, *37(2)*, 454-455.
- 61 Schlitzer, D.S.; Novak, B.M. *J. Am. Chem. Soc.* **1998**, *120*, 2196-2197.
- 62 Yashima, E.; Maeda, K.; Okamoto, Y. *Nature* **1999**, *399*, 449-451.
- 63 Green, M.M.; Reidy, M.P.; Johnson, R.D.; Darling, G.; O'Leary, D.J.; Willson, G. *J. Am. Chem. Soc.* **1989**, *111*, 6452-6454.
- 64 Green, M.M.; Peterson, N.C.; Sato, T.; Teramoto, A.; Lifson, S. *Science* **1995**, *268*, 1860-1866.
- 65 Green, M.M.; Garetz, B.A.; Munoz, B.; Chang, H.; Hoke, S.; Cooks, R.G. *J. Am. Chem. Soc.* **1995**, *117*, 4181-4182.
- 66 Green, M.M.; Park, J.-W.; Sato, T.; Teramoto, A.; Lifson, S.; Selinger, R.L.B.; Selinger, J.V. *Angew. Chem. Int. Ed.* **1999**, *38*, 3138-3154.
- 67 Li, J.; Schuster, G.B.; Cheon, K.-S.; Green, M.M.; Selinger, J.V. *J. Am. Chem. Soc.* **2000**, *122*, 2603-2612.
- 68 Brunsveld, L.; Lohmeijer, B.G.G.; Vekemans, J.A.J.M.; Meijer, E.W. *Chem. Commun.* **2000**, 2305-2306.
- 69 Castellano, R.K.; Nuckolls, C.; Rebek, Jr. J. *J. Am. Chem. Soc.* **1999**, *121*, 11156-11163.
- 70 Prins, L.J.; Huskens, J.; de Jong, F.; Timmerman, P.; Reinhoudt, D.N. *Nature* **1999**, *398*, 498-502.
- 71 See section 6.4
- 72 Prince, R.B.; Brunsveld, L.; Meijer, E.W.; Moore, J.S. *Angew. Chem. Int. Ed.* **2000**, *39*, 228-230. See also section 6.2.
- 73 Prince, R.B. *Ph. D. Thesis*, University of Illinois at Urbana-Champaign, 2000.
- 74 Nuckolls, C.; Katz, T.J. *J. Am. Chem. Soc.* **1998**, *120*, 9541-9544.
- 75 Nuckolls, C.; Katz, T.J.; Katz, G.; Collings, P.J.; Castellanos, L. *J. Am. Chem. Soc.* **1999**, *121*, 79-88.
- 76 Brunsveld, L.; Prince, R.B.; Meijer, E.W.; Moore, J.S. *Org. Lett.* **2000**, *2*, 1525-1528. See also section 6.5.
- 77 All variable temperature data was determined to be at equilibrium and independent of time since a spectrum recorded at 20 °C during the run and a spectrum measured at 20 °C at the end of the run (after heating the solution up from -10 °C and equilibrating for 10 minutes) were identical.
- 78 All measurements were assumed to be at equilibrium since the observations were independent of time (spectra were measured 10 minutes after preparation, then again 24 hours later).
- 79 Similar results were obtained for the association of a discotic molecules into helical columns, see refs: 36, 68.

- ⁸⁰ Langeveld-Voss, B.M.W.; Waterval, R.J.M.; Janssen, R.A.J.; Meijer, E.W. *Macromolecules* **1999**, *32*, 227-230.
- ⁸¹ Zhang, J.; Pesak, D.J.; Ludwick, J.J.; Moore, J.S. *J. Am. Chem. Soc.* **1994**, *116*, 4227-4239.
- ⁸² Schouten, P.G.; van der Pol, J.F.; Zwikker, J.W.; Drenth, W.; Picken, S.J. *Mol. Cryst. Liq. Cryst.* **1991**, *195*, 291-305.
- ⁸³ The shorter oligomers (**1**, $n = 2, 4$, and 6) have been studied and show no solvent dependent conformational transitions. They are present in a random coil conformation under all conditions.
- ⁸⁴ It was determined that for **1** ($n = 18$) in heptane at concentrations above $1 \mu\text{M}$, Beer's law was not followed anymore and a decrease of the molar ellipticity and broadening with concomitant blue-shift of the absorbance maximum could be observed.
- ⁸⁵ The $\Delta\epsilon$ of **1** ($n = 18$) is constant up to concentrations of ca. $1 \mu\text{M}$, but significantly increases at higher concentrations.
- ⁸⁶ The terms "poor solvent" and "good solvent" are used in the usual polymer chemistry sense. See: Flory, P. J. *Principles of Polymer Chemistry*; Cornell University Press: Ithaca, 1953; p 424.
- ⁸⁷ The onset of the twist sense bias for the polar oligomers **2** lies at a solvent composition of at least 50% acetonitrile in chloroform (dodecamer), whereas this is approximately 10% heptane in chloroform for the apolar oligomers. The folding of the polar oligomers also occurs at solvent compositions that consist of a higher chloroform percentage (70%) than for the apolar oligomers ($\sim 50\%$).
- ⁸⁸ The broadening and blue shift of absorbance maximum at increasing concentration or lower temperatures are typical for an intermolecular aggregation process. See: Cornelissen, J.J.L.M.; Peeters, E.; Janssen, R.A.J.; Meijer, E.W. *Acta Polym.* **1998**, *49*, 471-476.
- ⁸⁹ Aggregation via π - π stacking is highly favorable in alkanes, for an example see ref. 36.
- ⁹⁰ Langeveld-Voss, B.M.W. Ph. D. Thesis, Eindhoven University of Technology, **1999**; Pieterse, K.; Meijer, E.W. Eindhoven University of Technology, unpublished results.
- ⁹¹ The polar oligomers **2** do not show this time dependence, consistent with its behavior being a purely intramolecular phenomenon.
- ⁹² Eyre, D.R. *Science* **1980**, *207*, 1315-1322.
- ⁹³ Fuhrhop, J.-H. *Compr. Supramol. Chem.* **1996**, *9*, 407-450.
- ⁹⁴ Gulik-Krzywicki, T.; Fouquey, C.; Lehn, J.-M. *Proc. Natl. Acad. Sci. U. S. A.* **1993**, *90*, 163-167.
- ⁹⁵ Kimizuka, N.; Fujikawa, S.; Kuwahara, H.; Kunitake, T.; Marsh, A.; Lehn, J.-M. *J. Chem. Soc., Chem. Commun.* **1995**, 2103-2104.
- ⁹⁶ Rowan, A.E.; Nolte, R.J.M.; *Angew. Chem. Int. Ed.* **1998**, *37*, 63-68.
- ⁹⁷ Rogalska, E.; Rogalski, M.; Gulik-Krzywicki, T.; Gulik, A.; Chipot, C. *Proc. Natl. Acad. Sci. U. S. A.* **1999**, *96*, 6577-6580.
- ⁹⁸ Lindsell, W.E.; Preston, P.N.; Seddon, J.M.; Rosair, G.M.; Woodman, T.A.J. *Chem. Mater.* **2000**, *12*, 1572-1576.
- ⁹⁹ Boettcher, C.; Schade, B.; Fuhrhop, J.-H. *Langmuir* **2001**, *17*, 873-877.
- ¹⁰⁰ Jung, J.H.; Ono, Y.; Shinkai, S. *Chem. Eur. J.* **2000**, *6*, 4552-4557.
- ¹⁰¹ For a description of the general procedures see also chapter 2, section 2.5 Experimental section and chapter 3, section 3.7 Experimental section.

Summary

Biopolymers derive their unique conformation in solution from the cooperative action of weak interactions like π - π stacking, hydrogen bonding and hydrophobicity. The combined use of these interactions as design elements for well-defined synthetic multimolecular systems in water is not often pursued. The control over the structure of such ordered, chiral architectures in polar, protic media via cooperativity is challenging.

The research described in this thesis deals with the formation of well-defined, chiral, multimolecular architectures in polar solvents, including the investigation of their hierarchical formation and supramolecular conformation (Figure 1). A number of supramolecular interactions has been used to achieve a controlled architecture. The presence or absence of these interactions at the supramolecular level strongly depends on the environment, like type of solvent and temperature. As a result, the different interactions arise in a stepwise fashion. Supramolecular chirality, controlled *via* chiral side chains, has been applied for the recognition of the degree of order in the supramolecular architectures. By combining circular dichroism spectroscopy for the detection of helical order with other characterization techniques that demonstrate the assembly, a detailed insight has been obtained into the hierarchical formation of the architectures. Solvophobic / hydrophobic interactions occur first in polar solvents and subsequently allow other interactions to be active in the created hydrophobic microenvironment.

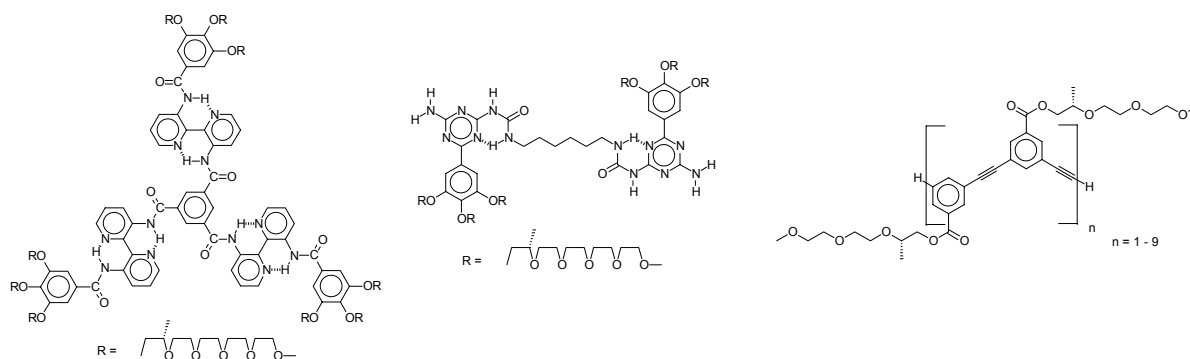


Figure 1: Three structures investigated; all giving rise to helical architectures in water.

To allow for solubility of the supramolecular assemblies in polar solvents, side-chains based upon oligo(ethylene oxide)s were designed and applied. These side-chains proved to ensure water-solubility and to effect chirality transfer to the backbone of the assembly. Additionally, they were easily adjusted with respect to length and presence or absence of a stereocenter.

As a first approach to generate well-defined chiral architectures in polar media, a C_3 -symmetrical discotic molecule was provided with nine achiral or chiral oligo(ethylene oxide) side

chains at the periphery. These molecules assemble reversibly and in a stepwise fashion in columns. Specific, solvent-sensitive interactions account for an extraordinarily strong stabilization of a chiral helix within the created hydrophobic environment. The presence of helicity at the supramolecular level and the length of the columns can be directed with temperature or solvent. Analogous compounds lacking a hydrophobic core and having only the possibility for intermolecular hydrogen bond formation do not form well-defined architectures.

The double helix of DNA is one of the most inspiring natural systems. Important design criteria for the chiral double helix are 1) hydrophobic interactions 2) intermolecular hydrogen bonding and 3) a chiral polymeric backbone. A resembling system could be created based on simple organic molecules. The implementation of both hydrophobic groups and hydrogen bonding units in one bifunctional molecule allows for such a self-assembled architecture in water. The design implies the polymerization of the molecules via four-fold intermolecular hydrogen bonding, which in turn is enabled by the stacking of the hydrophobic groups. In this way hydrogen bond formation is made possible in a hydrophobic environment. The chiral side-chains bias the helicity of the columnar polymer. Analogous structures lacking the possibility for the formation of a supramolecular polymeric backbone, like the corresponding monofunctional molecules, do not form such a chiral helix.

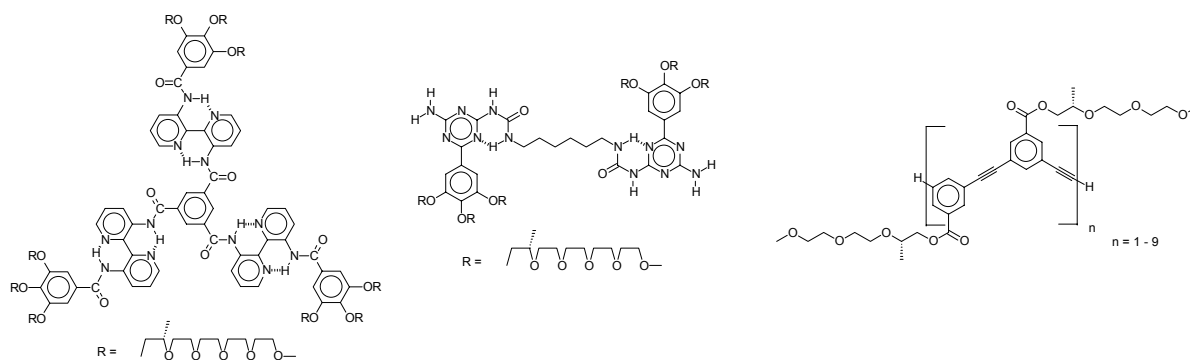
With the α -helix as a source of inspiration, a series of *m*-phenylene ethynylene oligomers has been provided with chiral side chains. These oligomers were found to fold from a random coil into a chiral helix. However, first the main chain collapses to a compact 'denatured' state before forming a well-defined helix, which chirality is directed by the chiral side chains. The folding of the helices can lead to a higher level of organization by addition of water. This increases the stability of the chiral helix and on top of that initiates intermolecular interactions between the oligomers. As a result the helices stack and form chiral columns. In these columns the folded oligomers can amplify their chirality. Ultimately the columns cluster laterally and form even larger architectures with opposite optical activity.

All the molecules studied feature a hierarchical self-assembly process showing great similarity to the way biomacromolecules adopt their structure in solution. The combined and subtle action of various secondary interactions leads to a cooperative formation of ordered supramolecular polymeric structures. The knowledge acquired from the study of the architectures created as well as the insight into the required design elements to achieve ordered structures, will aid in bridging the gap between artificial simple architectures and complex biomacromolecules. Furthermore, the properties of these artificial systems clarify the differences between self-assembly in apolar and polar media. The usage of these kinds of well-defined chiral architectures in water for the creation of functional catalytic systems should allow the formation of water-soluble supramolecular polymeric architectures having functionality comparable to that present in biomacromolecules.

Samenvatting

Biopolymeren ontleen hun unieke structuur in oplossing aan de coöperativiteit van zwakke interacties zoals van der Waals en hydrofobe interacties, π - π stapeling en waterstofbruggen. Het gecombineerd gebruik van deze interacties als ontwerpregels voor goed geordende synthetische multimoleculaire systemen in water is echter zeldzaam. Controle over de structuur van dusdanig geordende, chirale architecturen in polaire, protische media via coöperativiteit is een uitdaging.

Het promotieonderzoek beschreven in dit proefschrift behandelt de vorming van goedgedefinieerde, chirale, multi-moleculaire architecturen in polaire oplosmiddelen, inclusief het onderzoek van hun hiërarchische opbouw en supramoleculaire conformatie (Figuur 1). Om tot een gecontroleerde opbouw van de architecturen te komen, is een aantal supramoleculaire interacties gebruikt. Het wel of niet voorkomen van deze interacties hangt erg af van de omgeving, zoals concentratie, oplosmiddeltype en temperatuur en de verschillende interacties treden daardoor stapsgewijs op. Supramoleculaire chiraliteit, gecontroleerd via chirale zijketens, is gebruikt voor de herkenning van de mate van ordening in de supramoleculaire polymeerarchitecturen. Door de combinatie van circulair dichroïsme spectroscopie voor de detectie van ordening, met andere karakterisatietechnieken die de assemblage laten zien, is gedetailleerd inzicht verkregen in de stapsgewijze vorming van de architecturen. Solvofobe / hydrofobe interacties moeten eerst optreden in de polaire oplosmiddelen, om daarna de meer oplosmiddelgevoelige interacties toe te staan in een gecreëerde hydrofobe micro-omgeving.



Figuur 1: Drie bestudeerde structuren die in water goedgeordende helische structuren vormen.

Als eerste aanpak om tot goed gedefinieerde chirale structuren in water te komen, werd een C₃-symmetrisch discotisch molecuul gekozen met negen achirale of chirale oligo(ethyleenoxide) staarten aan de buitenkant. Deze moleculen assembleren reversibel in kolommen. De assemblage gebeurt stapsgewijs en specifieke en oplosmiddelgevoelige interacties zorgen in een gecreëerde hydrofobe omgeving voor een uitermate sterke stabilisatie van een chirale helix. De aanwezigheid van

heliceiteit op het supramoleculaire niveau en de lengte van de kolom kan gestuurd worden met temperatuur of oplosmiddel. Analoge verbindingen zonder hydrofobe kern en met alleen de mogelijkheid tot intermoleculaire waterstofbrugvorming, vormen geen goed gedefinieerde structuren in water.

De dubbelhelix van DNA is één van de meest inspirerende natuurlijke structuren. Door combinatie van hydrofobe interacties, waterstofbruggen en een chirale polymere ruggengraat vormt het biopolymeer zijn chirale dubbelhelix. Het is gelukt een gelijkaardig systeem te creëren op basis van eenvoudige bifunctionele organische moleculen. Door in het molecuul zowel hydrofobe groepen als waterstofbrugvormende eenheden in te bouwen is het mogelijk gebleken zo'n structuur in water te creëren. Het ontwerp impliceert dat het molecuul polymeriseert door middel van viervoudige waterstofbruggen, wat weer mogelijk wordt gemaakt doordat de hydrofobe gedeelten eerst associëren en op die manier waterstofbrugvorming toestaan in een hydrofobe omgeving. Analoge structuren die niet de mogelijkheid hebben tot vorming van een supramoleculaire polymere ruggengraat, zoals de overeenkomstige monofunctionele moleculen, bleken deze dubbelhelix niet te vormen.

Geïnspireerd door de α -helix is een serie *m*-fenyleen ethynyleen oligomeren voorzien van chirale staarten. Deze oligomeren bleken op te vouwen van een random coil tot een chirale helix. Echter, eerst vouwt de hoofdketen tot een compacte 'gedenatureerde' toestand, waarna pas een goed gedefinieerde helix ontstaat waarvan de chiraliteit gedirigeerd wordt door de chirale staarten. De aggregatie kan naar een hoger niveau worden getild door toevoeging van water aan de helices. Hierdoor wordt de stabiliteit van de chirale helix verhoogd en worden bovendien intermoleculaire interacties tussen de oligomeren geïnitieerd. De helices stapelen daardoor in chirale kolommen. In de ontstane kolom kunnen de moleculen hun chiraliteit aan elkaar overdragen. Uiteindelijk clusteren deze kolommen lateraal samen en vormen nog grotere structuren.

De bestudeerde architecturen ondergaan een hiërarchisch proces van zelfassemblage dat grote gelijkenis vertoont met de manier waarop biomacromoleculen hun structuur in oplossing verkrijgen. Subtiel samenspel van verscheidene secundaire interacties leidt tot een coöperatieve opbouw van geordende supramoleculaire polymeerstructuren. De kennis die is verkregen uit de studie van de gevormde architecturen en de noodzakelijke designelementen die eraan ten grondslag liggen, zullen de kloof tussen kunstmatige simpele structuren en complexe biomacromoleculen helpen overbruggen. De eigenschappen van deze kunstmatige structuren verhelderden tevens de verschillen tussen zelfassemblage in apolaire en polaire media. Door dit type van goed gedefinieerde chirale architecturen in water te gebruiken voor de vorming van functionele, katalytische systemen moet het mogelijk zijn in water supramoleculaire polymeerarchitecturen te vormen die een functionaliteit bezitten vergelijkbaar met deze van biomacromoleculen.

Curriculum Vitae



Luc Brunsveld werd geboren op 24 augustus 1975 te Culemborg. Na de VWO-opleiding aan het Koningin Wilhelmina College te Culemborg werd in 1993 begonnen aan de studie Scheikundige Technologie aan de Technische Universiteit Eindhoven. Na een kort verblijf aan de Universiteit van Osaka (Prof. Dr. A. Harada) in de zomer van 1996, werd in augustus 1997 het afstudeerproject binnen de vakgroep Organische Chemie (Prof. Dr. E.W. Meijer) afgerond. Vanaf september 1997 was hij werkzaam binnen de NRSC-Katalyse als promovendus in de capaciteitsgroep Macromoleculaire en Organische Chemie aan de Technische Universiteit Eindhoven, onder leiding van Professor Dr. E.W. Meijer en Dr. J.A.J.M. Vekemans. De belangrijkste resultaten van dit onderzoek, waarvan een gedeelte is uitgevoerd aan de Universiteit van Illinois in Urbana-Champaign in samenwerking met Professor Dr. J.S. Moore en Dr. R.B. Prince in de herfst van 1998, staan beschreven in dit proefschrift.

Luc Brunsveld was born in Culemborg, the Netherlands on August 24th, 1975. He attended the Koningin Wilhelmina College where he obtained his VWO (pre-university education) degree. In 1993 he started the study of Chemical Engineering at the Eindhoven University of Technology. After a short stay at the Osaka University (Prof. A. Harada) in the summer of 1996, he graduated in August 1997 with the graduation project at the laboratory of Organic Chemistry (Prof. Dr. E.W. Meijer). In September 1997 he started as a Ph. D. student in the NRSC-Catalysis, in the laboratory of Macromolecular and Organic Chemistry at the Eindhoven University of Technology under the supervision of Professor Dr. E.W. Meijer and Dr. J.A.J.M. Vekemans. The most important results of the investigations, part of which is performed in the autumn of 1998 at the University of Illinois at Urbana-Champaign in cooperation with Professor Dr. J.S. Moore and Dr. R.B. Prince, are described in this thesis.

Dankwoord

De afgelopen vier jaar zijn de meest leerzame, uitdagende, interessante en leuke jaren van mijn scholing geweest. Hiervoor wil ik mijn onderzoeksbegeleiders Professor Bert Meijer en dr. Jef Vekemans oprecht bedanken. Hun positieve instelling en openheid, zowel ten opzichte van het onderzoek als mij persoonlijk, zijn een voortdurende stimulans geweest. Het vriendschappelijke contact en de interesse die zij toonden hebben ervoor gezorgd dat ik met volle teugen heb mogen genieten van mijn promotieonderzoek. Hun toewijding aan en enthousiasme voor de chemie en de wetenschap in het algemeen zijn voor mij een voorbeeld waaraan ik mij de rest van mijn wetenschappelijke carrière hoop te mogen spiegelen. De afgelopen jaren waren fantastisch en het was een eer om met hen te mogen werken en van hen te leren.

With sincere and utmost appreciation I would like to thank Professor J.S. Moore and Dr. Ryan B. Prince from the University of Illinois at Urbana-Champaign. Their inspiring involvement with science and hospitality has made our collaboration one of the most educational and interesting periods for me and is a goal to pursue during the rest of my scientific career. Bas Lohmeijer, Jeroen van Buijtenen, Richard Hoogenboom en Jochem Langeveld wil ik uitermate bedanken voor hun gemotiveerde inzet en prettige samenwerking tijdens hun afstuderen of researchstage met mij of samen met Henk Keizer. Aan hoofdstuk 2 hebben dr. Albert Schenning, dr. E.E. Havinga en Maarten Broeren bijgedragen, mijn dank hiervoor. De succesvolle en aangename samenwerking betreffende de tijdsopgeloste fluorescentie met Professor M. Glasbeek en dr. Hong Zhang heeft geleid tot belangrijke fundamentele inzichten en een belangrijk deel van hoofdstuk 3; mijn oprechte dank hiervoor. De enthousiasmerende gesprekken en samenwerking met dr. Paul van der Schoot en Professor M.A.J. Michels zijn van groot belang geweest voor mijn inzicht in moleculaire assemblage. De verkregen resultaten zijn vergeleken met de waardevolle experimenten gedaan in samenwerking met dr. Aissa Ramzi en staan gedeeltelijk beschreven in hoofdstuk 3; mijn erkentelijkheid hiervoor. Graag bedank ik ook dr. Anja Palmans en dr. Henk Janssen met wie het onderzoek beschreven in hoofdstuk 4 is geïnitieerd. Voor de plezierige samenwerking met dr. Rifat Hikmet en dr. Hartmut Fischer, betreffende de iongeleiding en X-ray metingen van hoofdstuk 4, wil ik ook hun graag bedanken. Graag wil ik ook dr. Rint Sijbesma en Ky Hirschberg bedanken. Zij hebben in grote mate bijgedragen aan de ideeën en uitvoering omtrent hoofdstuk 5.

Gedurende mijn promotie heb ik met veel mensen mogen discussiëren en samenwerken. Mijn dank gaat uit naar al deze geïnteresseerden. Zij hebben in belangrijke mate bijgedragen aan de resultaten hier beschreven en hebben mijn blikveld verruimd. De leden van de lees- en promotiecommissie ben ik bijzonder erkentelijk voor hun constructieve bijdrage aan dit proefschrift. Bijzondere dank gaat uit naar alle vroegere en huidige leden van de capaciteitsgroep

Macromoleculaire en Organische Chemie voor hun wetenschappelijke betrokkenheid en vriendschap. Met name wil ik Koen Pieterse bedanken, die menig artikel een aantrekkelijke verschijning heeft gegeven, en Joost van Dongen, voor belangrijke hulp met karakterisering. Graag bedank ik ook Hans Damen, Ingrid Dirx, Henk Eding, Hannie van der Lee en Hanneke Veldhoen. Gerne bedanke ich mich bei den Kollegen des Max Planck Instituts für Polymerforschung in Mainz für die NMR-Messungen und Diskussionen über Diskoten. Insbesondere gilt mein Dank Professor K. Müllen, Dr. Florian Dötz, Andreas Fechtenkötter, Dr. Manfred Wagner, Professor H. W. Spiess und Dr. Kay Saalwächter. I also would like to thank all the members of the Moore group at the University of Illinois at Urbana-Champaign who gave me such a pleasant and educational stay. De collega's van het laboratorium voor Fysisch Organische en Supramoleculaire Chemie van de Katholieke Universiteit Nijmegen wil ik graag bedanken voor menig overleg en hulp bij metingen.

Als laatste dank ik mijn ouders die mij altijd gestimuleerd hebben tot leren en studeren en natuurlijk Alicia, jij was op z'n minst het meest; En pocas palabras, tú lo eres todo.

Luc